

**Transition metal complexes of ONS and NNS donor  
thiosemicarbazones: Crystal structures and  
spectral studies**

*Thesis submitted to  
Cochin University of Science and Technology  
in partial fulfillment of the requirements  
for the award of the degree of  
Doctor of Philosophy  
Under the Faculty of Science*

*by*

**Nisha K.**



**Department of Applied Chemistry  
Cochin University of Science and Technology  
Kochi 682 022**

*February 2016*

**Transition metal complexes of ONS and NNS donor thiosemicarbazones:  
Crystal structures and spectral studies**

*Ph. D. Thesis under the Faculty of Science*

*Author:*

**Nisha K.**  
Research Fellow, Department of Applied Chemistry  
Cochin University of Science and Technology  
Kochi 682 022  
India  
Email: nichuanil@gmail.com

*Research Advisor:*

**Dr. M.R. Prathapachandra Kurup**  
Professor  
Department of Applied Chemistry  
Cochin University of Science and Technology  
Kochi 682 022  
India  
Email: mrp@cusat.ac.in

Department of Applied Chemistry  
Cochin University of Science and Technology  
Kochi 682 022  
India

February 2016

Front cover: Packing diagram of  $[\text{Zn}(\text{Hbpet})](\text{NO}_3)_2 \cdot \text{H}_2\text{O}$  viewed along  $c$  axis.

Back cover:  $\pi \cdots \pi$  interactions in  $[\text{Ni}(\text{bpet})\text{NCS}]$ .

---

*“Fix your mind on Me, be devoted to Me, offer service to Me,  
bow down to Me, and you shall certainly reach Me.  
I promise you because you are very dear to Me...”*

---

**(Bhagavat Gita)**





*To my most beloved Achan*





Phone Off. 0484-2862423  
Phone Res. 0484-2576904  
Telex: 885-5019 CUIIN  
Fax: 0484-2577595  
Email: mrp@cusat.ac.in  
mrp\_k@yahoo.com



Department of Applied Chemistry  
Cochin University of Science and Technology  
Kochi 682 022, India

**Dr. M.R. Prathapachandra Kurup**  
Professor

6<sup>th</sup> February 2016

## Certificate

*This is to certify that the thesis entitled “Transition metal complexes of ONS and NNS donor thiosemicarbazones: Crystal structures and spectral studies” submitted by Ms. Nisha K., in partial fulfillment of the requirements for the degree of Doctor of Philosophy, to the Cochin University of Science and Technology, Kochi-22, is an authentic record of the original research work carried out by her under my guidance and supervision. The results embodied in this thesis, in full or in part, have not been submitted for the award of any other degree. All the relevant corrections and modifications suggested by the audience during the pre-synopsis seminar and recommended by the Doctoral committee have been incorporated in the thesis.*

**M.R. Prathapachandra Kurup**  
(Supervisor)



## *Declaration*

*I hereby declare that the work presented in this thesis entitled “Transition metal complexes of ONS and NNS donor thiosemicarbazones: Crystal structures and spectral studies” is entirely original and was carried out independently under the supervision of Prof. M.R. Prathapachandra Kurup, Department of Applied Chemistry, Cochin University of Science and Technology and has not been included in any other thesis submitted previously for the award of any other degree.*

06-02-2016  
Kochi-22

**Nisha K.**



---

## *Acknowledgement*

At this turning point of my research it is my pleasure and privilege to remember each and everyone who helped me during this crucial period of my research work at the department of Applied Chemistry, CUSAT and I am really indebted to all those who have rendered timely help.

First and foremost let me bow my head before my **Almighty** for being my strength and source of wisdom

I would like to express my special appreciation and thanks to my advisor Prof. (Dr.) M.R. Prathapachandra Kurup, Department of Applied Chemistry, CUSAT. I consider it as a great privilege to work under his guidance. I owe sincere gratitude and thanks to him for his whole hearted support and inspiration throughout the study. Without his constructive criticisms, valuable suggestions and corrections, I would not have been able to successfully complete my work.

I express my sincere thanks to former Heads, Prof. K. Girish Kumar who is my doctoral committee member and Prof. K. Sreekumar for their encouragement and support. I am very much thankful to Dr. N. Manoj, Head, Department of Applied Chemistry, CUSAT for the support and cooperation during the period of this work. I am thankful for the support received from all the teaching and non-teaching staff of the Department of Applied Chemistry, CUSAT.

I sincerely thank the Council of Scientific and Industrial Research, New Delhi, India for financial support offered. I deeply acknowledge the heads of the institutions of SAIF Kochi, IIT Madras and IIT Bombay for the services rendered in sample analyses. I express my thanks to Dr. Shibu Eapen, Sophisticated Testing and Instrumentation Centre, SAIF, Kochi for doing single crystal XRD studies of the compounds.

My sincere thanks also goes to Dr. S. Muraleedharan Nair (Head of the Department, Department of Chemical Oceanography, School of

Marine Sciences), Dr. C.H. Sujatha (Former Head of the Department) and Prof. Chandrmohana Kumar for their special support towards the completion of my thesis. I thank my colleague Dr. Prashob, all my friends and my students of the Department of Chemical Oceanography for their love and support. I would like to thank Dr. Manju, who as a good friend, was always willing to help and give her best suggestions.

I remember all my seniors, Dr. Seena E.B., Dr. Sheeja S.R., Dr. Reena T.A., Dr. Neema Ani Mangalam and Dr. Renjusha S., who helped me a lot in the beginning years of my research. I thank from the depth of my heart the teacher fellows Dr. Jessy Emmanuel, Dr. Annie C.F., Dr. K. Jayakumar and Dr. Laly K. for their valuable care, help and attention. My thanks are due to Roji sir and Dr. M. Sithambaresan for their valuable advices and extensive discussions around my work. Dear Bibitha and Jinsa, the moments spent with you are so special and will remain in my heart forever. Thank you so much for your love, care and advices. I will surely cherish the beautiful moments spent with my dear friends, Reshma and Bhagyesh. I fondly remember my junior friends, Ambili, Aiswarya, Sreejith and Mridula for creating a fun filled environment in the lab and their whole-hearted support during the period.

My special thanks to my junior labmates, Vineetha, Nithya, Rakhi, Sajitha, Anila, Fousia, Daly, Lincy and Asha for their support during the period. I am also indebted to Asokan sir and Yamuna miss for their encouragement and support.

Words cannot express how grateful I am to my mother-in law, father-in-law and my amma, for all of the sacrifices that you've made on my behalf. I also express my deep sense of love to my dear husband Anil and to my little daughter Janu, who missed my care and attention during the course of this investigation. I dedicate this thesis before the fond memories of my most beloved Achan showering his blessings upon me from heaven.

*Nisha K.*



## ||| Preface |||

Thiosemicarbazones have emerged as an important class of ligands over a period of time, for a variety of reasons, such as variable donor properties, structural diversity, and biological applications. The structural diversity of thiosemicarbazide-based compounds is considerably increased not only due to the condensation of the different carbonyls but also due to the alkylation of the different parts of the thiosemicarbazide moiety. These ligands can therefore provide a non-reducing source of anionic sulfur and also due to residual multiple bonding between C and S, the tendency for the sulfur to bridge metal ions is substantially less compared to thiolate. The ability of this class of ligands to act a source of 'masked thiolate' is one of the contributing factors to their ability to act as highly versatile donors towards a range of metal ions. Interesting as the coordination chemistry may be, the driving force for the study of these ligands has undoubtedly been their biological properties and the majority of the 3000 or so publications on thiosemicarbazones since 2000 have alluded to this feature.

Coordination chemistry of a number of metals has been investigated, and a wide variety of complexes have been reported. Thiosemicarbazides first appeared in the literature in the late 1800s and thiosemicarbazones were reported as potential derivatisation agents for ketones and aldehydes in the 1900s. Thiosemicarbazone complexes have shown interesting biological properties such as anticancer, antibacterial, antifungal, and antiviral owing to their property to diffuse through the semipermeable membrane of the cell lines. Due to the tendency of thiosemicarbazone ligands to form complexes with metals, analytical applications have also been observed. The low cost of thiosemicarbazones as well as their easy preparative methods could provide a major attraction for the development of analytical reagents for a range of applications in future.

In order to pursue the interesting coordinating properties of thiosemicarbazones, complexes with different types of ligand environments are essential. So in the present work we chose two different ONS and NNS donor thiosemicarbazones as principal ligands. Introduction of heterocyclic bases like 1,10-phenanthroline, 2,2'-bipyridine, 4,4'-dimethyl-2,2'-bipyridine and 5,5'-dimethyl-2,2'-bipyridine and anions like azide, thiocyanate, chloride, iodide and thiocyanato, the classical N,N donor ligands leads to the syntheses of mixed ligand complexes which can cause different bonding, spectral properties and geometries in coordination compounds. The molecular structures of these thiosemicarbazones were established by single crystal X-ray diffraction studies. The metals selected for the preparation of the complexes are vanadium, nickel, copper, zinc and cadmium. The crystal structures of five of the complexes were studied through single crystal XRD.

The thesis is divided into seven chapters. Chapter 1 involves a brief overview to thiosemicarbazones and their metal complexes, bonding and coordination strategy of thiosemicarbazones and their various applications. The objectives of the present work and the various physicochemical methods adopted for the characterization of the thiosemicarbazones and their complexes are also discussed in this chapter. Chapter 2 describes the syntheses of two new aldehyde based ONS donor thiosemicarbazones and two ketone based NNS donor thiosemicarbazones, their characterization by elemental analyses, mass, FT-IR, UV-Vis and  $^1\text{H}$  NMR spectral studies. X-ray quality single crystals of all ligands were grown and their molecular structures were established by single crystal X-ray diffraction studies. Chapters 3-7 discuss the syntheses and characterization of oxido/dioxidovanadium (IV/V), nickel(II), copper(II), zinc(II) and cadmium(II) complexes derived from the thiosemicarbazones under study. A brief summary and conclusion of the work is also included in the last part of the thesis.

# Contents

## Chapter 1

### THIOSEMICARBAZONES AND THEIR METAL

#### COMPLEXES – A BRIEF OVERVIEW ..... 1-18

1.1	Introduction.....	1
1.2	Thiosemicarbazones .....	3
1.3	Bonding and coordination strategy of thiosemicarbazones .....	4
1.3.1	Bonding modes in neutral form.....	6
1.3.2	Bonding modes in anionic form.....	7
1.3.3	Bonding modes of bis-thiosemicarbazones.....	8
1.4	Importance of thiosemicarbazones.....	9
1.4.1	Biological applications .....	9
1.4.1a	<i>Antifungal and antibacterial properties</i> .....	9
1.4.1b	<i>Anticancer properties</i> .....	9
1.4.2	Analytical applications .....	10
1.5	Objectives of the present work.....	10
1.6	Physical measurements.....	13
1.6.1	Elemental analyses .....	13
1.6.2	Molar Conductivity measurements.....	14
1.6.3	Magnetic susceptibility measurements .....	14
1.6.4	Infrared spectroscopy .....	14
1.6.5	Ultraviolet-visible spectroscopy.....	15
1.6.6	Mass spectroscopy.....	15
1.6.7	NMR spectroscopy .....	15
1.6.8	EPR spectroscopy.....	16
1.6.9	Thermogravimetric studies .....	16
1.6.10	Single crystal X-ray diffraction studies .....	17

## Chapter 2

### SYNTHESES AND CHARACTERIZATION OF ONS

#### AND NNS DONOR THIOSEMICARBAZONES ..... 19-60

2.1	Introduction.....	19
2.2	Experimental .....	20
2.2.1	Materials .....	20
2.2.2	Syntheses of thiosemicarbazones .....	21
2.2.2.1	<i>4-Benzyloxysalicylaldehyde-N<sup>t</sup>-phenylthiosemicarbazone</i> <i>(H<sub>2</sub>bspt)</i> .....	21
2.2.2.2	<i>5-Bromosalicylaldehyde-N<sup>t</sup>-ethylthiosemicarbazone</i> <i>(H<sub>2</sub>brset)</i> .....	22

2.2.2.3	2-Benzoylpyridine- <i>N</i> <sup>4</sup> -ethylthiosemicarbazone ( <i>Hbpet</i> ).....	22
2.2.2.4	2-Benzoylpyridine- <i>N</i> <sup>4</sup> , <i>N</i> <sup>4</sup> -dimethyl-3-thiosemicarbazone ( <i>Hbpd</i> ).....	23
2.3	Characterization of thiosemicarbazones .....	24
2.3.1	Elemental analysis .....	24
2.3.2	Mass spectra .....	24
2.3.3	Infrared spectra .....	25
2.3.4	Electronic spectra .....	28
2.3.5	NMR spectra .....	29
2.3.5a.	<sup>1</sup> H NMR spectrum- <i>H</i> <sub>2</sub> <i>bspt</i> .....	29
2.3.5a.1	<sup>13</sup> C NMR spectrum.....	31
2.3.5b	<sup>1</sup> H NMR spectrum- <i>H</i> <sub>2</sub> <i>brset</i> .....	33
2.3.5c.	<sup>1</sup> H NMR spectrum- <i>Hbpet</i> .....	34
2.3.5d	<sup>1</sup> H NMR spectrum- <i>Hbpd</i> .....	36
2.3.6	X-ray Crystallography .....	37
2.3.6a	Crystal structure- <i>H</i> <sub>2</sub> <i>bspt</i> .....	37
2.3.6b	Crystal structure- <i>H</i> <sub>2</sub> <i>brset</i> .....	43
2.3.6c.	Crystal structure- <i>Hbpet</i> .....	50
2.3.6d	Crystal structure- <i>Hbpd</i> .....	54

## Chapter 3

### SYNTHESES, SPECTRAL AND STRUCTURAL CHARACTERIZATION OF OXIDO/DIOXIDO VANADIUM (IV/V) COMPLEXES OF ONS AND NNS DONOR THIOSEMICARBAZONES.....

		<b>61 - 85</b>
3.1	Introduction.....	61
3.2	Experimental .....	63
3.2.1	Materials .....	63
3.2.2	Syntheses of the thiosemicarbazones.....	63
3.2.3	Syntheses of the complexes .....	63
3.2.3.1	[VO( <i>bspt</i> )( <i>bipy</i> )] (1) .....	63
3.2.3.2	[VO( <i>bspt</i> )( <i>phen</i> )] (2) .....	63
3.2.3.3	[VO( <i>bspt</i> )(4,4'- <i>dmbipy</i> )] (3) .....	64
3.2.3.4	[VO( <i>bspt</i> )(5,5'- <i>dmbipy</i> )] (4).....	64
3.2.3.5	[VO <sub>2</sub> ( <i>bpdt</i> )] (5) .....	65
3.3	Results and discussion.....	65
3.3.1	Elemental analyses .....	66
3.3.2	Molar conductivity and magnetic susceptibility measurements.....	66
3.3.3	X-ray crystallography .....	67
3.3.3.1	Crystal structure of [VO <sub>2</sub> ( <i>bpdt</i> )] (5).....	68
3.3.4	Infrared spectra.....	73

3.3.5	Electronic spectra .....	76
3.3.6	EPR spectra .....	79

## Chapter 4

### SYNTHESES, SPECTRAL AND STRUCTURAL CHARACTERIZATION OF NICKEL(II) COMPLEXES OF ONS AND NNS DONOR

<b>THIOSEMICARBAZONES .....</b>	<b>87-110</b>	
4.1	Introduction .....	87
4.2	Experimental .....	90
4.2.1	Materials .....	90
4.2.2	Syntheses of thiosemicarbazones .....	90
4.2.3	Syntheses of nickel complexes .....	90
4.2.3.1	$[Ni_2(bspt)_2]$ (6) .....	90
4.2.3.2	$[Ni(bspt)(bipy)] \cdot H_2O$ (7) .....	91
4.2.3.3	$[Ni(bspt)(phen)] \cdot H_2O$ (8) .....	91
4.2.3.4	$[Ni(bspt)(4,4'-dmbipy)] \cdot CH_3OH$ (9) .....	91
4.2.3.5	$[Ni(bpet)(NCS)]$ (10) .....	92
4.2.3.6	$[Ni(bpet)(NCO)]$ (11) .....	92
4.3	Results and discussion .....	93
4.3.1	Elemental analyses .....	93
4.3.2	Molar conductivity and magnetic susceptibility measurements .....	93
4.3.3	X-ray crystallography .....	95
4.3.3.1	Crystal structure of $[Ni(bpet)(NCS)]$ (10) .....	97
4.3.4	Infrared spectra .....	103
4.3.5	Electronic spectra .....	106
4.3.6	Thermogravimetric studies .....	109

## Chapter 5

### SYNTHESES, SPECTRAL AND STRUCTURAL CHARACTERIZATION OF COPPER(II) COMPLEXES OF ONS AND NNS DONOR

<b>THIOSEMICARBAZONES .....</b>	<b>111-137</b>	
5.1	Introduction .....	111
5.2	Experimental .....	114
5.2.1	Materials .....	114
5.2.2	Syntheses of the thiosemicarbazones and complexes .....	114
5.2.3	Syntheses of copper complexes .....	115
5.2.3.1	$[Cu_2(bspt)_2]$ (12) .....	115

5.2.3.2	[Cu(bspt)(phen)] (13)	115
5.2.3.3	[Cu(bspt)(bipy)] (14)	115
5.2.3.4	[Cu(bspt)(4,4'-dmbipy)] (15)	116
5.2.3.5	[Cu(bspt)(5,5'-dmbipy)] (16)	116
5.2.3.6	[Cu <sub>2</sub> (brset) <sub>2</sub> ] (17)	116
5.2.3.7	[Cu(brset)(phen)] (18)	117
5.2.3.8	[Cu(bpet)(I)] (19)	117
5.2.3.9	[Cu(bpet)(N <sub>3</sub> )] (20)	117
5.3	Results and discussion	118
5.3.1	Elemental analyses	118
5.3.2	Molar conductivity and magnetic susceptibility measurements	119
5.3.3	Infrared spectra	119
5.3.4	Electronic spectra	123
5.3.5	EPR spectra	127

## Chapter 6

### SYNTHESES, SPECTRAL AND STRUCTURAL CHARACTERIZATION OF Zn(II) COMPLEXES OF ONS AND NNS DONOR THIOSEMICARBAZONES ..... 139-166

6.1	Introduction	139
6.2	Experimental	141
6.2.1	Materials	141
6.2.2	Syntheses of the thiosemicarbazones	141
6.2.3	Syntheses of the complexes	141
6.2.3.1	[Zn <sub>2</sub> (bspt) <sub>2</sub> ] (21)	141
6.2.3.2	[Zn(bspt)(phen)] (22)	142
6.2.3.3	[Zn(bspt)(bipy)] (23)	142
6.2.3.4	[Zn(bspt)(4,4'-dmbipy)] (24)	142
6.2.3.5	[Zn(bspt)(5,5'-dmbipy)] (25)	143
6.2.3.6	[Zn(bpet)(dca)] <sub>n</sub> (26)	143
6.2.3.7	[Zn(bpet)](NO <sub>3</sub> ) <sub>2</sub> ·H <sub>2</sub> O (27)	144
6.2.3.8	[Zn(bpet)(OAc)] (28)	144
6.3	Results and discussion	144
6.3.1	Elemental analyses	145
6.3.2	Molar conductivity measurements	145
6.3.3	Infrared spectra	146
6.3.4	Electronic spectra	149
6.3.5	<sup>1</sup> H NMR spectra	151
6.3.6	X-ray crystallography	153
6.3.6a.	Crystal structures of the compound [Zn(bpet)dca] <sub>n</sub> (26) and [Zn(bpet)](NO <sub>3</sub> ) <sub>2</sub> ·H <sub>2</sub> O (27)	154

## Chapter 7

### SYNTHESES, SPECTRAL AND STRUCTURAL CHARACTERIZATION OF Cd(II) COMPLEXES OF

### ONS AND NNS DONOR THIOSEMICARBAZONES ..... 167-185

7.1	Introduction.....	167
7.2	Experimental.....	169
7.2.1	Materials.....	169
7.2.2	Syntheses of thiosemicarbazones.....	169
7.2.3	Syntheses of cadmium complexes.....	170
7.2.3.1	[Cd <sub>2</sub> (bspt) <sub>2</sub> ] (29).....	170
7.2.3.2	[Cd(bspt)(phen)] (30).....	170
7.2.3.3	[Cd(bspt)(bipy)] (31).....	170
7.2.3.4	[Cd(bspt)(4,4'-dmbipy)] (32).....	171
7.2.3.5	[Cd(bspt)(5,5'-dmbipy)] (33).....	171
7.2.3.6	[Cd(bpet)(NCS)] (34).....	171
7.2.3.7	[Cd(bpet)(N <sub>3</sub> )] (35).....	172
7.2.3.8	[Cd <sub>2</sub> (bpet) <sub>2</sub> (Cl) <sub>2</sub> ] (36).....	172
7.3	Results and discussion.....	173
7.3.1	Elemental analyses.....	173
7.3.2	Molar conductivity measurements.....	173
7.3.3	X-ray crystallography.....	174
7.3.3.1	Crystal structure of [Cd <sub>2</sub> (bpet) <sub>2</sub> (Cl) <sub>2</sub> ] (36).....	175
7.3.4	Infrared spectra.....	180
7.3.5	Electronic spectra.....	183
7.3.6	<sup>1</sup> H NMR spectra.....	184

### SUMMARY AND CONCLUSION ..... 187

### REFERENCES..... 197





## List of Abbreviations

H <sub>2</sub> bspt	2-benzoyloxysalicylaldehyde- <i>N</i> <sup>4</sup> -phenylthiosemicarbazone
H <sub>2</sub> brset	5-bromosalicylaldehyde- <i>N</i> <sup>4</sup> -phenylthiosemicarbazone
Hbpet	2-benzoylpyridine- <i>N</i> <sup>4</sup> -ethylthiosemicarbazone
Hbpd	2-benzoylpyridine- <i>N</i> <sup>4</sup> , <i>N</i> <sup>4</sup> -dimethylthiosemicarbazone
phen	1,10-phenanthroline
bipy	2,2'-bipyridine
4,4'-dmbipy	4,4'-dimethyl-2,2'-bipyridine
5,5'-dmbipy	5,5'-dimethyl-2,2'-bipyridine
Complex 1	[VO(bspt)(bipy)]
Complex 2	[VO(bspt)(phen)]
Complex 3	[VO(bspt)(4,4'-dmbipy)]
Complex 4	[VO(bspt)(5,5'-dmbipy)]
Complex 5	[VO <sub>2</sub> (bpd)]
Complex 6	[Ni <sub>2</sub> (bspt) <sub>2</sub> ]
Complex 7	[Ni(bspt)(bipy)]·H <sub>2</sub> O
Complex 8	[Ni(bspt)(phen)]·H <sub>2</sub> O
Complex 9	[Ni(bspt)(4,4'-dmbipy)(H <sub>2</sub> O)]
Complex 10	[(Ni(bpet)(NCS)]
Complex 11	[(Ni(bpet)(NCO)]
Complex 12	[Cu <sub>2</sub> (bspt) <sub>2</sub> ]
Complex 13	[(Cu(bspt)(phen)]
Complex 14	[Cu(bspt)(bipy)]
Complex 15	[Cu(bspt)(4,4'-dmbipy)]
Complex 16	[Cu(bspt)(5,5'-dmbipy)]
Complex 17	[Cu <sub>2</sub> (brset) <sub>2</sub> ]
Complex 18	[(Cu(brset)(phen)]
Complex 19	[Cu(bpet)(I)]
Complex 20	[Cu(bpet)(N <sub>3</sub> )]
Complex 21	[Zn <sub>2</sub> (bspt) <sub>2</sub> ]

Complex 22	[Zn(bspt)(phen)]·H <sub>2</sub> O
Complex 23	[Zn(bspt)(bipy)]
Complex 24	[Zn(bspt)(4,4'-dmbipy)]
Complex 25	[Zn(bspt)(5,5'-dmbipy)]
Complex 26	[Zn(bpet)(dca)] <sub>n</sub>
Complex 27	[Zn(bpet)](NO <sub>3</sub> ) <sub>2</sub> ·H <sub>2</sub> O
Complex 28	[Zn(bpet)(OAc)]
Complex 29	[Cd <sub>2</sub> (bspt) <sub>2</sub> ]
Complex 30	[Cd(bspt)(phen)]
Complex 31	[Cd(bspt)(bipy)]
Complex 32	[Cd(bspt)(4,4'-dmbipy)]
Complex 33	[Cd(bspt)(5,5'-dmbipy)]
Complex 34	[Cd(bpet)(NCS)]
Complex 35	[Cd(bpet)(N <sub>3</sub> )]
Complex 36	[Cd <sub>2</sub> (bpet) <sub>2</sub> (Cl) <sub>2</sub> ]

---

---

## THIOSEMICARBAZONES AND THEIR METAL COMPLEXES – A BRIEF OVERVIEW

---

---

<i>Contents</i>	1.1 <i>Introduction</i>
	1.2 <i>Thiosemicarbazones</i>
	1.3 <i>Bonding and coordination nature of thiosemicarbazones</i>
	1.4 <i>Importance of thiosemicarbazones</i>
	1.5 <i>Objectives of the present work</i>
	1.6 <i>Physical measurements</i>

---

### 1.1 Introduction

The field of inorganic chemistry is very broad and diverse. By an old definition, inorganic chemistry was the chemistry of non-living things, as opposed to organic chemistry, which was assumed to deal with carbon-containing compounds which make up a large part of the living world. Nowadays areas as diverse as nanomaterials, metals in biological systems, compounds with interesting and useful magnetic and spectroscopic properties, precursors for electronic materials and others all fall within the designation of inorganic chemistry. In fact, our everyday life could not be thought of without large contributions from inorganic chemistry. Most catalysts utilized in organic chemistry are metal-based. Life on

earth would not be possible without the metals in biological systems, such as iron in haemoglobin which has a pivotal role in oxygen transport, and the metal ions at the center of enzymes which help to regulate several biological processes.

Coordination chemistry is a part of inorganic chemistry deals with the study of complexes. Coordination compounds are the backbone of modern inorganic and bio-inorganic chemistry and chemical industry. These compounds are very important in day to day life. The ligand attached to it, is important, and the geometry of the complexes are studied under inorganic chemistry. Inorganic compounds have been used in medicine for thousands of years, often without a known molecular basis for their mechanism of action, and with little attempt to design them. The design of coordination (metal) complexes is not an easy task.

Coordination compounds are a class of substances with chemical structures in which a central metal atom is surrounded by nonmetal atoms or groups of atoms, called ligands, joined to it by chemical bonds. Coordination compounds include such substances as vitamin B<sub>12</sub>, hemoglobin, and chlorophyll, dyes and pigments, and catalysts used in preparing organic substances. Coordination compounds are important for at least three reasons. First, most of the elements in the periodic table are metals, and almost all metals form complexes, so metal complexes are a feature of the chemistry of more than half the elements. Second, many industrial catalysts are metal complexes, and such catalysts are steadily becoming more important as a way to control reactivity. A technological and scientific development of major significance was the discovery in

1954 that certain complex metal catalysts namely, a combination of titanium trichloride,  $\text{TiCl}_3$  and triethylaluminum,  $\text{Al}(\text{C}_2\text{H}_5)_3$  bring about the polymerizations of organic compounds with carbon-carbon double bonds under mild conditions to form polymers of high molecular weight and highly ordered (stereoregular) structures. Some of these polymers are of great commercial importance because they are used to make many kinds of fibres, films, and plastics. Perhaps the earliest known coordination compound is the bright red alizarin dye first used in India and known to the ancient Persians and Egyptians. It is a calcium aluminum chelate complex of hydroxyanthraquinone. The first synthesis of a complex is ascribed to the German physicist and alchemist Andreas Libavius (1540-1615). Around the year 1600 he obtained blue  $[\text{Cu}(\text{NH}_3)_4]^{2+}$  from  $\text{NH}_4\text{Cl}$ ,  $\text{Ca}(\text{OH})_2$  and brass in water. The modern theory of coordination chemistry is based largely on the work of Alfred Werner (1866–1919; Nobel Prize in Chemistry in 1913) [1].

The applications of coordination compounds are of great importance. These compounds are widely present in the mineral, plant and animal worlds and are known to play many important functions in the area of analytical chemistry, metallurgy, biological function system, industry and medicine.

## **1.2 Thiosemicarbazones**

Thiosemicarbazones and their metal complexes are a broad class of biologically active compounds [2]. Mixed-ligand complexes of transition metals containing ligands with N, S and N, S, O donors are known to exhibit interesting stereochemical, electrochemical, and electronic

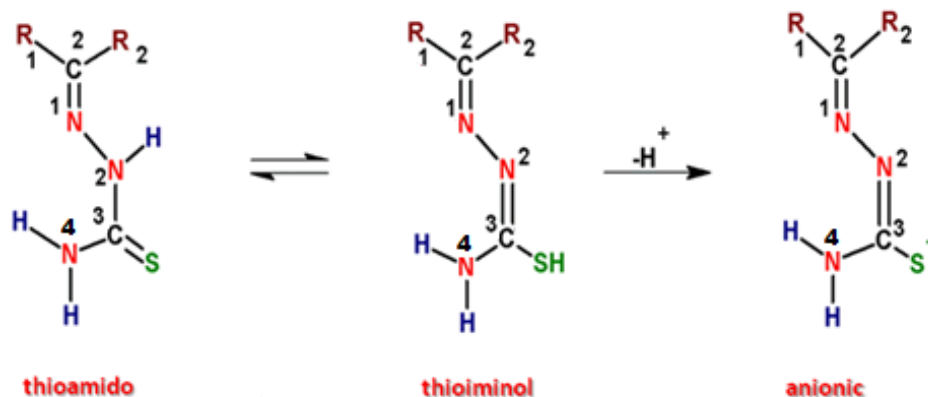
properties [3-5]. Thiosemicarbazones have emerged as an important class of sulfur ligands particularly for transition metal ions. The real impetus towards developing their coordination chemistry was due to their physicochemical properties [6,7] and significant biological activities [8,9].

Thiosemicarbazones are thiourea derivatives and the studies on their chemical and structural properties have received much attention due to the widespread application in the chemotherapeutic field. In view of fact that these compounds form complexes with many metals they are of special interest to coordination chemists. Thiosemicarbazones are prepared by the condensation of thiosemicarbazides with aldehydes or ketones in the presence of a few drops of glacial acetic acid.

Thiosemicarbazones with general formula  $R^1R^2C=N-NH-C(S)-NR^3R^4$  usually react as chelate with transition metal ions by bonding through the sulfur and hydrazinic nitrogen atoms in ligands. The group  $N-C=S$  is of considerable chemotherapeutic interest and is responsible for pharmacological activity. Thiosemicarbazones are versatile ligands in both neutral (HL) and anionic forms ( $L^-$ ). They are extensively delocalized systems, especially when aromatic radicals are bound to the azomethine carbon atom. The  $R^1$  and  $R^2$  groups may provide additional donor atoms and  $R^3$  and  $R^4$  are the  $N^4$  substituents.

### 1.3 Bonding and coordination strategy of thiosemicarbazones

Thiosemicarbazones exist in thioamido form in solid state and in solution, they tend to exist as an equilibrium mixture of thioamido and thioiminol forms.



Complexation usually takes place *via* dissociation of the acidic proton, resulting in the formation of a five-membered chelate ring. Thiosemicarbazones act as a neutral bidentate ligand, while the loss of the thiol proton from thioimino tautomer yields a singly charged bidentate ligand. Therefore, depending upon preparative conditions (especially pH), the complex unit can be cationic, neutral or anionic. However, most investigations of metal thiosemicarbazone complexes have involved ligands in the neutral form, while definitive data on the complexes containing thiosemicarbazone in the thioimino form are generally lacking. Furthermore, it is possible to isolate complexes containing both tautomeric forms of the ligand. Ablov and Gerbeleu [10] explained that formation of such mixed-ligand tautomeric complexes is promoted by the central metal ion and is generally accompanied by oxidation of the central metal ion. The thiosemicarbazide molecule itself exists in the *trans* configuration [11], and while complexing in this configuration, it behaves as a monodentate ligand, bonding only through the sulfur atom. In most of the complexes studied, the thiosemicarbazone

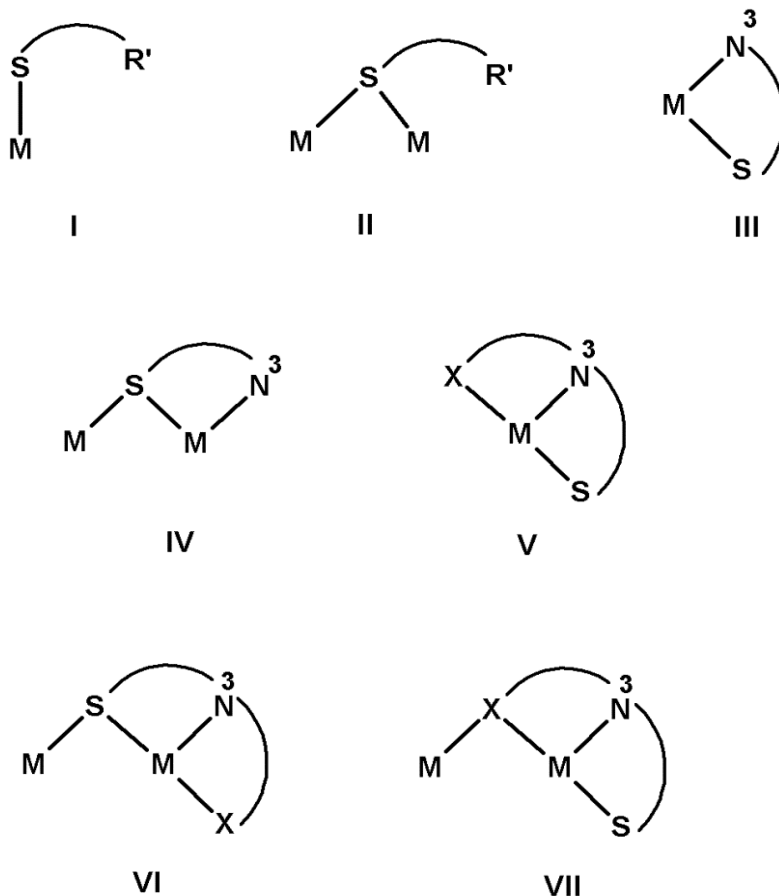
function coordinates to the metal ion in the *cis* configuration, as a bidentate ligand bonding both through the thioamide/thioiminol sulfur atom and the hydrazine nitrogen atom in a bidentate manner. When an additional coordinating functionality is present in the proximity of the SN donating centers, the ligands are found to act as tridentate species. The stereochemistry adopted by thiosemicarbazone ligands while interacting with transition metal ions depends essentially upon the presence of additional coordination centre in the ligand moiety and the charge on the ligand, which in turn is influenced by the thioamido-thioiminol equilibrium. Many thiosemicarbazones are crystalline solids used for identification of the corresponding aldehydes or ketones [12]. However, these small molecules (compared to peptides) have interesting biological activities.

A number of bonding modes have been observed for the thiosemicarbazones in their neutral or anionic forms.

### 1.3.1 Bonding modes in neutral form

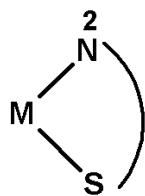
In neutral form, the binding occurs *via* only S atom in  $\eta^1$ -S (I),  $\mu^2$ -S (II),  $\eta^2$ -N<sup>3</sup>, S-chelation (III),  $\eta^2$ -N<sup>3</sup>, S-chelation and S-bridging (IV) modes. However, if the substituent at C<sup>2</sup> has a donor atom, and engages in bonding, the additional bonding modes observed are,  $\eta^3$ -X, N<sup>3</sup>, S-chelation (V),  $\eta^3$ -X, N<sup>3</sup>, S-chelation and S-bridging (VI) and  $\eta^3$ -X, N<sup>3</sup>, S-chelation and X-bridging (VII) (eg. X = N, O) [13-22].



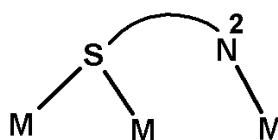


### 1.3.2 Bonding modes in anionic form

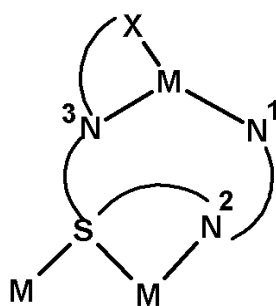
The modes (I-VII) shown by the neutral ligands are also exhibited by the anionic ligands, *viz.*  $\eta^1$ -S,  $\mu^2$ -S,  $\eta^2$ -N<sup>3</sup>, S-chelation,  $\eta^2$ -N<sup>3</sup>, S-chelation and S-bridging,  $\eta^3$ -X, N<sup>3</sup>, S-chelation,  $\eta^3$ -X, N<sup>3</sup>, S-chelation-cum-S-bridging and  $\eta^3$ -X, N<sup>3</sup>, S-chelation and X-bridging [23-29]. In addition,  $\eta^2$ -N<sup>2</sup>, S (VIII) and  $\eta^2$ -N<sup>2</sup>, S-bridging (IX) modes are identified [30,31]. A rare example of pentacoordination (X) by a thiosemicarbazone ligand has also been reported [32].



VIII



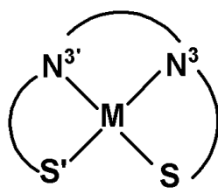
IX



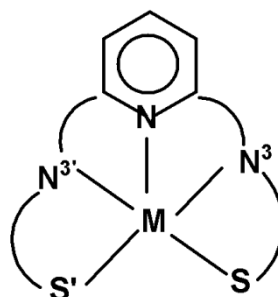
X

### 1.3.3 Bonding modes of bis-thiosemicarbazones

Bis-thiosemicarbazones can bind in neutral as well as anionic forms using their both arms. The common coordination modes are (XI) and (XII) depending on the participation of the central ring connecting the two arms [33-35].



XI



XII

## **1.4 Importance of thiosemicarbazones**

Thiosemicarbazones and their metal complexes present a wide range of applications that stretch from their use in analytical chemistry, through pharmacology to nuclear medicine [36-39]. The presence of amide, imine and thione groups makes them potential polydentate ligands [40] and it is not surprising that numerous thiosemicarbazone complexes have been prepared and characterized [41]. In addition, in the last few years, there has been a growing attention towards thiosemicarbazones related to their range of biological properties, specifically as antifungal, antiviral, antibacterial and anticancer agents [42-50].

### **1.4.1 Biological applications**

#### **1.4.1a *Antifungal and antibacterial properties***

Copper(II) complexes of 2-acetylpyridine-*N*<sup>4</sup>-substituted thiosemicarbazones are found to be more active in the growth inhibition of the fungus *Paecilomyces variolii* at higher concentrations than nickel(II) complexes [51]. The copper complexes of 2-furan carbaldehyde thiosemicarbazone were the most active against all strains, including dermatophytes and phytopathogenic fungi and presented good activity against *Haemophilus influenzae*, a very harmful bacterium to humans [52].

#### **1.4.1b *Anticancer properties***

The development of novel anticancer agents is an important field of current drug discovery. Novel ligands namely di-2-pyridyl ketone, 4-cyclohexyl-4-methyl-3-thiosemicarbazone and 2-benzoylpyridine

thiosemicarbazone show potent anticancer activity without mediating cardiotoxicity [53]. Copper complexes derived from a great variety of ligands, such as thiosemicarbazones, imidazoles, and phosphines, have been proposed as potential anticancer agents [54].

#### 1.4.2 Analytical applications

Only a few phenyl thiosemicarbazones have been synthesised and used as chromogenic reagents for the spectrophotometric determination of metal ions. Renewed interest in the synthesis of phenyl thiosemicarbazones is due to their sensitive reactions with metal ions and the easy extractability of metal - phenyl thiosemicarbazone complexes into organic solvents [55].

*N*-Ethyl-3-carbazolecarboxaldehyde-3-thiosemicarbazone is used as chelating agent for the simultaneous removal and trace determination of Cd(II) and Pb(II) in food and water samples [56]. The ligand 2,6-diacetylpyridine-bis(-4-phenyl-3-thiosemicarbazone) acts as complexing reagent for zinc in food and environmental samples [57]. Anisaldehyde-4-phenyl-3-thiosemicarbazone is used as an analytical reagent for the extractive spectrophotometric determination of gold [58].

### 1.5 Objectives of the present work

Thiosemicarbazides first appeared in the literature in the late 1800s and thiosemicarbazones were reported as potential derivatisation agents for ketones and aldehydes in the 1900s. In addition, thiosemicarbazones are well known compounds possessing N and S donor atoms, and their chemistry with transition metals has been extensively reviewed. The chemistry of thiosemicarbazone complexes of the transition metal ions

has been receiving significant current attention, primarily because of the bioinorganic relevance of the complexes [59]. A large majority of the thiosemicarbazone complexes have found wide medicinal applications owing to their potentially beneficial biological (viz. antibacterial, antimalarial, antiviral and antitumor) activities [60]. Systematic studies on the binding of thiosemicarbazones of selected types to different transition metal ions are of considerable importance in this respect. However, we have been exploring the chemistry of transition metal complexes of the thiosemicarbazones.

Various thiosemicarbazones and their heterocyclic thiadiazoline (TDZ) derivatives have been used in an array of drug categories such as antimicrobial, anti-HIV-1, anticancer and central nervous system (CNS) inhibitor activities and the literature concerning these subjects is steadily increasing. The synthesis of TSCs has been developed due to the facility to replace the substituent groups by alkyl, aryl, or heterocyclic derivative and thus leading to a broad spectrum of new multi-dentate ligands, capable of coordinating to metal centers through the imine nitrogen and sulfur atom [61].

Thiosemicarbazones and their transition metal complexes have been receiving considerable attention because of their biological relevance and applications in the field of analysis. Their structural diversity also attracted inorganic chemists. A good deal of work has been reported on the synthesis and structural investigation of thiosemicarbazones and their complexes. This is due to their capability of acting as multidentate, NNS and ONS donors with the formation of either mono, bi or polynuclear

complexes. Their chemistry and pharmacological applications have been extensively investigated.

Appreciable biological applications as well as diverse stereochemistry of their metal complexes prompted us to synthesize two new tridentate ONS donor  $N^4$ -phenyl thiosemicarbazones derived from 4-benzyloxysalicylaldehyde and 5-bromosalicylaldehyde and their transition metal complexes. These aldehydes were selected since they can provide a further binding site from phenolic  $-OH$  and can thus increase the denticity. Introduction of heterocyclic bases like 1,10-phenanthroline, 2,2'-bipyridine, 4,4'-dimethyl-2,2'-bipyridine and 5,5'-dimethyl-2,2'-bipyridine and some pseudohalides like azide and thiocyanate ion can result in mixed ligand metal chelates with different geometries in coordination compounds.

All the above said facts stimulated our interest in the study of transition metal complexes with ONS and NNS donor thiosemicarbazones and we undertook the present work with the following objectives.

- To synthesize some ONS donor thiosemicarbazones by the condensation of 4-benzyloxysalicylaldehyde and 5-bromosalicylaldehyde with  $N^4$ -phenylthiosemicarbazide.
- To synthesize some NNS donor thiosemicarbazones by the condensation of 2-benzoylpyridine with  $N^4$ -ethylthiosemicarbazide and  $N^4, N^4$ -dimethyl-3-thiosemicarbazide.
- To characterize the synthesized thiosemicarbazones by different physicochemical techniques.

- To synthesize different transition metal complexes using the synthesized thiosemicarbazones as principal ligands and some heterocyclic bases as coligands.
- To study the coordination modes of different thiosemicarbazones in metal complexes by using different physicochemical methods.
- To isolate single crystals of the synthesized compounds and establish its structure using single crystal X-ray diffraction studies.

## **1.6 Physical measurements**

The physicochemical methods adopted during the present study are discussed below.

### **1.6.1 Elemental analyses**

Elemental analysis is a process where a sample of a chemical compound is analyzed for its elemental and sometimes isotopic composition. Elemental analysis can be qualitative (determining what elements are present) and it can be quantitative (determining how much of each is present). This information is important to help to determine the purity of a synthesized compound. Elemental analyses of C, H, N and S present in all the compounds were done on a Vario EL III CHNS elemental analyzer at the Sophisticated Analytical Instrument Facility, Cochin University of Science and Technology, Kochi-22, Kerala, India.

### 1.6.2 Molar Conductivity measurements

The conductivity (or specific conductance) of an electrolyte solution is a measure of its ability to conduct electricity. The SI unit of conductivity is siemens per meter (S/m). Conductivity measurements are used as a fast, inexpensive and reliable way of measuring the ionic content in a solution. The molar conductivities of the complexes in DMF solutions ( $10^{-3}$  M) at room temperature were measured using a Systronic model 303 direct reading conductivity meter at the Department of Applied Chemistry, CUSAT, Kochi, India.

### 1.6.3 Magnetic susceptibility measurements

In electromagnetism, the magnetic susceptibility is a dimensionless proportionality constant that indicates the degree of magnetization of a material in response to an applied magnetic field. Magnetic susceptibility measurements of the complexes were carried out on a Vibrating Sample Magnetometer using  $\text{Hg}[\text{Co}(\text{SCN})_4]$  as a calibrant at the SAIF, Indian Institute of Technology, Madras.

### 1.6.4 Infrared spectroscopy

Infrared (IR) spectroscopy is one of the most common spectroscopic techniques used by inorganic chemists. The main goal of IR spectroscopic analysis is to determine the chemical functional groups in the sample. Different functional groups absorb characteristic frequencies of IR radiation. Thus, IR spectroscopy is an important and popular tool for structural elucidation and compound identification. Infrared spectra of some of the complexes were recorded on a JASCO FT-IR-5300



Spectrometer in the range 4000-400  $\text{cm}^{-1}$  using KBr pellets at the Department of Applied Chemistry, CUSAT, Kochi, India.

### **1.6.5 Ultraviolet-visible spectroscopy**

Ultraviolet-visible spectroscopy is a technique in which intensity of light passing through a sample ( $I$ ) is measured and is compared to the intensity of light before it passes through the sample ( $I_0$ ). The ratio ( $I/I_0$ ) is called the transmittance and is usually expressed as a percentage (%T). The electronic spectra of the compounds were taken on a Spectro UV-vis Double Beam UVD-3500 spectrometer in the 200-900 nm range at the Department of Applied Chemistry, CUSAT, Kochi, India.

### **1.6.6 Mass spectroscopy**

Mass spectrometry (MS) is an analytical technique that measures the mass-to-charge ratio of charged particles. It is used for determining masses of particles, for determining the elemental composition of a sample or molecule and for elucidating the chemical structures of molecules. MS works by ionizing chemical compounds to generate charged molecules or molecular fragments and measuring their mass-to-charge ratios. Mass spectra of the thiosemicarbazones were recorded by direct injection on WATERS 3100 Mass Detector using Electron Spray Ionization (ESI) technique designed for routine HPLC-MS analyses at the Department of Applied Chemistry, CUSAT, Kochi, India.

### **1.6.7 NMR spectroscopy**

Nuclear magnetic resonance spectroscopy, most commonly known as NMR spectroscopy, is a research technique that exploits the magnetic

properties of certain atomic nuclei to determine physical and chemical properties of atoms or the molecules in which they are contained. It relies on the phenomenon of nuclear magnetic resonance and can provide detailed information about the structure, dynamics, reaction state and chemical environment of molecules.  $^1\text{H}$  NMR spectra of thiosemicarbazones were recorded using Bruker AMX 400 FT-NMR Spectrometer with deuterated DMSO as the solvent and TMS as internal standard at the Sophisticated Analytical Instrument Facility, CUSAT, Kochi, India.

#### **1.6.8 EPR spectroscopy**

Electron paramagnetic resonance (EPR) or electron spin resonance (ESR) spectroscopy is a technique for studying materials with unpaired electrons. The basic concepts of EPR are analogous to those of nuclear magnetic resonance (NMR), but it is electron spins that are excited instead of the spins of atomic nuclei. Because most stable molecules have all their electrons paired, the EPR technique is less widely used than NMR. The EPR spectra of the complexes in the solid state at 298 K and in DMF/DMSO at 77 K were recorded on a Varian E-112 spectrometer using TCNE as the standard, with 100 kHz modulation frequency, 2 G modulation amplitude and 9.1 GHz microwave frequency at SAIF, IIT Bombay, India.

#### **1.6.9 Thermogravimetric analyses**

TG-DTG analyses of the complexes were carried out in a Perkin Elmer Pyris Diamond TG/DTA analyzer under nitrogen at a heating rate of  $10\text{ }^\circ\text{C min}^{-1}$  in the range 50-700  $^\circ\text{C}$  at Sophisticated Analytical Instrument Facility, CUSAT, Kochi, India

### **1.6.10 Single crystal X-ray diffraction studies**

Single crystal X-ray diffraction is a non-destructive analytical technique which provides detailed information about the internal lattice of crystalline substances, including unit cell dimensions, bond lengths, bond angles and details of site-ordering. Ideal crystals should be between  $1.5 \times 10^6$ - $2.5 \times 10^6$  Å in size. Samples are mounted on the tip of a thin glass fiber using an epoxy or cement. This fiber is attached to a brass mounting pin, usually by the use of modeling clay and the pin is then inserted into the goniometer head. The goniometer head and sample are then affixed to the diffractometer. Then data is collected and phase problem is solved to find the unique set of phases that can be combined with the structure factors to determine the electron density and therefore, the crystal structure. The trial structure is then solved and refined.

Single crystal X-ray diffraction studies of the compounds were carried out using a Bruker SMART APEXII CCD diffractometer at SAIF, Cochin University of Science and Technology, Kochi-22, Kerala, India. Bruker SMART software was used for data acquisition and Bruker SAINT software for data integration [62]. Absorption corrections were carried out using SADABS based on Laue symmetry using equivalent reflections [63]. The structure was solved by direct methods using SHELXS97 [64] and refined by full-matrix least-squares refinement on  $F^2$  using SHELXL97 [65]. The graphics tool used was DIAMOND version 3.2g [66].

.....*SC*.....



# Chapter 2

## SYNTHESES AND CHARACTERIZATION OF ONS AND NNS DONOR THIOSEMICARBAZONES

Contents

- 2.1 Introduction
- 2.2 Experimental
- 2.3 Characterization of thiosemicarbazones

### 2.1 Introduction

Thiosemicarbazones  $\{(R^1R^2C^2=N^3-N^2(H)-C^1(=S)N^1R^3R^4)\}$  are versatile N, S donor ligands with potential to bind to a metal *via* one or more donor atoms. The importance of thiosemicarbazones lies in their structural diversity [67-74], ion-sensing ability [75-78], metal extraction properties [79,80] and pharmacological properties [81-84]. Thiosemicarbazones and their metal complexes have become the subject of intensive study because of their wide ranging biological activities, analytical applications and interesting chemical and structural properties. The structural diversity of thiosemicarbazide-based compounds is considerably increased not only due to the condensation of the different carbonyls but also due to the alkylation of the different parts of the thiosemicarbazide moiety [85]. The biological activity and the medicinal properties of thiosemicarbazones depend upon the chemical nature of the

moiety attached to the C=S carbon atom. Thiosemicarbazones and their derivatives have antifungal activity.  $N^4$ -Tolyl-2-benzoylpyridine thiosemicarbazones and their copper(II) complexes were tested as antifungal on *Candida albicans* [86]. 5-Methyl-2-furfural thiosemicarbazone and its nickel and copper complexes were used as antifungal against on *Aspergillus fumigatus* and *C. albicans* [87].

Here, we have prepared four tridentate ligands out of which two are ONS and remaining are NNS ligands and are used for the preparation of metal complexes.

- 4-benzyloxysalicylaldehyde- $N^4$ -phenylthiosemicarbazone (H<sub>2</sub>bspt)
- 5-bromosalicylaldehyde- $N^4$ -ethylthiosemicarbazone (H<sub>2</sub>brset)
- 2-benzoylpyridine- $N^4$ -ethylthiosemicarbazone (Hbpet)
- 2-benzoylpyridine- $N^4,N^4$ -dimethylthiosemicarbazone (Hbpd)

The ligand Hbpd is reported [88]. This chapter discusses the syntheses, crystal structures and spectral aspects of these thiosemicarbazones.

## 2.2 Experimental

### 2.2.1 Materials

4-Benzyloxysalicylaldehyde (Alfa Aesar),  $N^4$ -phenylthiosemicarbazide (Sigma-Aldrich), 5-bromosalicylaldehyde (Alfa Aesar), 4-ethylthiosemicarbazide (Sigma-Aldrich), 2-benzoylpyridine (Sigma-Aldrich) and  $N^4,N^4$ -dimethyl-3-thiosemicarbazide (Sigma-Aldrich) were of Analar grade and were used as received. The solvent methanol (Spectrochem)

and dimethylformamide (Spectrochem) were used without further purification.

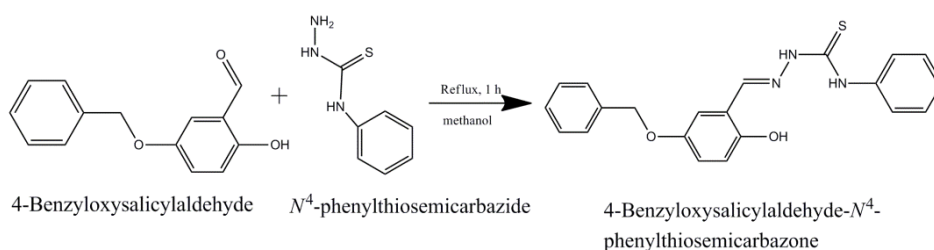
## 2.2.2 Syntheses of thiosemicarbazones

The thiosemicarbazones were synthesized by the condensation between appropriate aldehyde/ketone with the respective thiosemicarbazide as described below.

### 2.2.2.1 4-Benzyloxysalicylaldehyde-*N*<sup>4</sup>-phenylthiosemicarbazone (*H*<sub>2</sub>*bspt*)

4-Benzyloxysalicylaldehyde-*N*<sup>4</sup>-phenylthiosemicarbazone was prepared by the condensation of 4-benzyloxysalicylaldehyde and *N*<sup>4</sup>-phenylthiosemicarbazide in acid medium (Scheme 2.1). A methanolic solution (20 mL) of *N*<sup>4</sup>-phenylthiosemicarbazide (0.167 g, 1 mmol) was added to a solution of 4-benzyloxysalicylaldehyde (0.228 g, 1 mmol) in 20 ml methanol and the reaction mixture was refluxed for 1 hour. The product formed was filtered, washed with methanol and dried *in vacuo*.

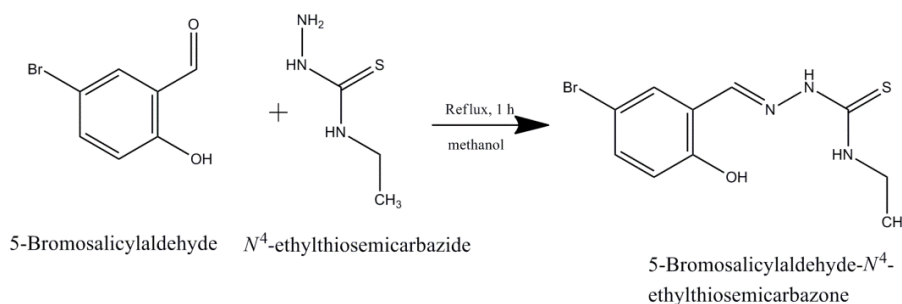
Yield: 65%, M.P.: 175 °C, Elemental Anal. Found (calcd) %: C, 66.18 (66.82); H, 5.24 (5.07); N, 10.90 (11.13); S, 8.59 (8.49)



Scheme 2.1

### 2.2.2.2 5-Bromosalicylaldehyde-*N*<sup>4</sup>-ethylthiosemicarbazone (*H<sub>2</sub>brset*)

5-Bromosalicylaldehyde-*N*<sup>4</sup>-ethylthiosemicarbazone was prepared by the condensation of 5-bromosalicylaldehyde and *N*<sup>4</sup>-ethylthiosemicarbazide (Scheme 2.2). A methanolic solution (20 mL) of *N*<sup>4</sup>-ethylthiosemicarbazide (0.119 g, 1 mmol) was added to a solution of 5-bromosalicylaldehyde (0.201 g, 1 mmol) in 20 mL methanol and the reaction mixture is refluxed for 1 hour in presence of a few drops of glacial acetic acid. The product formed was filtered, washed with methanol and dried *in vacuo*.



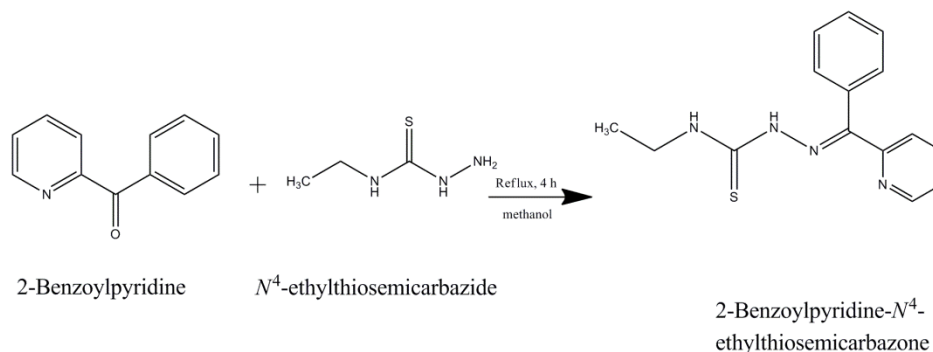
**Scheme 2.2**

Yield: 55%, M.P.: 160 °C, Elemental Anal. Found (Calcd) %: C, 39.35 (39.75); H, 4.85 (4.20); N, 13.52 (13.91); S, 10.13 (10.61)

### 2.2.2.3 2-Benzoylpyridine-*N*<sup>4</sup>-ethylthiosemicarbazone (*Hbpet*)

2-Benzoylpyridine-*N*<sup>4</sup>-ethylthiosemicarbazone was prepared by the condensation of 2-benzoylpyridine and *N*<sup>4</sup>-ethylthiosemicarbazide (Scheme 2.3). A few drops of glacial acetic acid is also added to the reaction mixture. A methanolic solution (20 mL) of *N*<sup>4</sup>-ethylthiosemicarbazide (0.119 g, 1 mmol) was added to a solution of 2-benzoylpyridine (0.183 g, 1 mmol) in 20 mL methanol and the reaction mixture is refluxed for 4 hours. The product formed was filtered, washed with methanol and dried *in vacuo*.



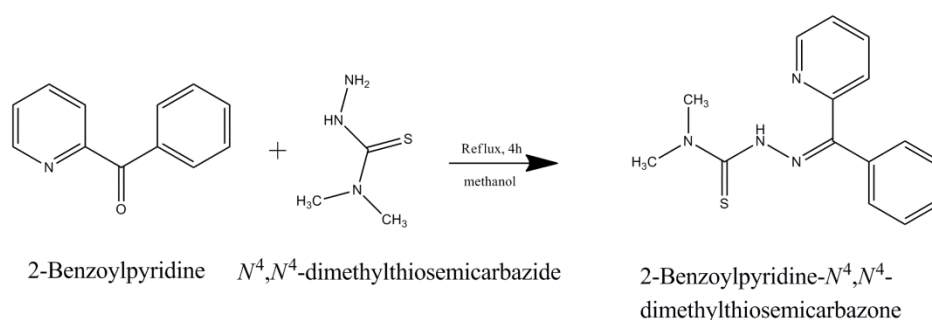


**Scheme 2.3**

Yield: 45%, M.P.: 160 °C, Elemental Anal. Found (Calcd) %: C, 63.00 (63.35); H, 5.50 (5.67); N, 19.50 (19.70); S, 10.90 (11.28)

#### 2.2.2.4 2-Benzoylpyridine- $N^4,N^4$ -dimethyl-3-thiosemicarbazone (Hbpd)

A methanolic solution of 2-benzoylpyridine (0.183 g, 1 mmol) was mixed with  $N^4,N^4$ -dimethyl-3-thiosemicarbazide (0.120 g, 1 mmol) in hot methanol and to this mixture 3 drops of glacial acetic acid was added. The reaction mixture was refluxed for 4 hours. On slow evaporation, yellow crystalline compound formed was filtered, washed with ether and recrystallized from methanol and dried over  $P_4O_{10}$  *in vacuo* (Scheme 2.4) [23].



**Scheme 2.4**

Yield: 45%, M.P.: 175 °C, Elemental Anal. Found (Calcd) %: C, 63.35 (63.85); H, 5.67 (5.86); N, 19.7 (20.01); S, 11.28 (11.00)

## **2.3 Characterization of thiosemicarbazones**

### **2.3.1 Elemental analysis**

C, H, N and S analysis results of thiosemicarbazones are given in Section 2.2.2.1-2.2.2.4 which shows that they are analytically pure.

### **2.3.2 Mass spectra**

The electrospray ionization (ESI) technique was used to measure the mass to charge ( $m/z$ ) ratio of charged particles. The organic molecules are bombarded with high energy electrons and the result is quantitatively recorded as a spectrum of positive ion fragments. The most abundant ion formed in the ionization chamber gives rise to the tallest peak in the spectrum called the base peak. The spectral intensities are normalized by setting the base peak to relative abundance 100 and the rest of the ions are recorded as percentages of the base peak intensity. Mass spectrum is a plot of  $m/z$  of positive ion fragments versus their relative abundance. In the present study, the molecular ion ( $M^+$ ) peaks at 376.2 and 285.2 amu for the thiosemicarbazones H<sub>2</sub>bspt and Hbpdt respectively indicate the molecular masses of the respective thiosemicarbazones synthesized. Mass spectra of H<sub>2</sub>bspt and Hbpdt are shown in Fig. 2.1.

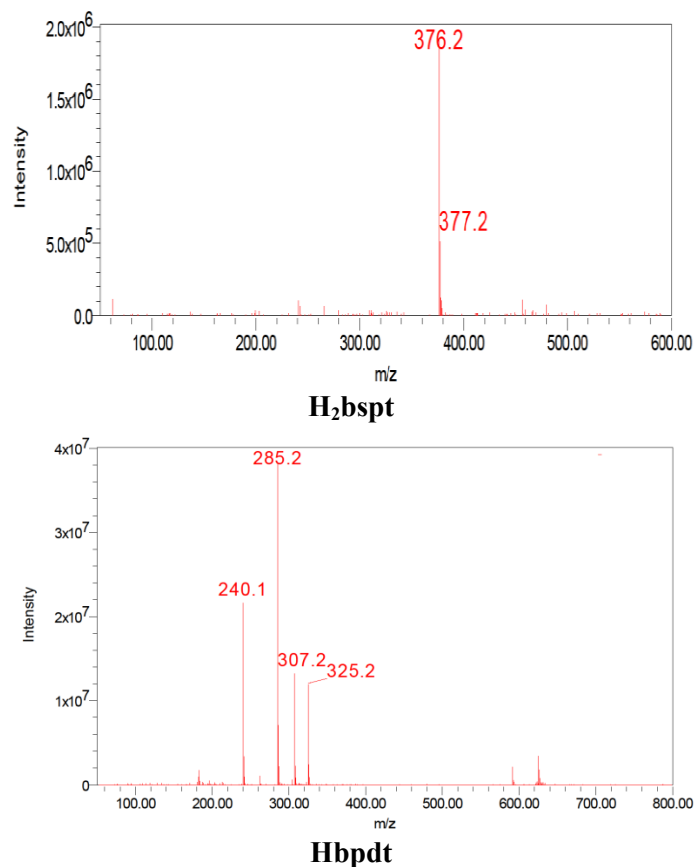


Fig. 2.1. Mass spectra of H<sub>2</sub>bspt and HbpdT showing molecular ion (M<sup>+</sup>) peak.

### 2.3.3 Infrared spectra

Infrared spectra of the thiosemicarbazones were recorded on a JASCO FT-IR-5300 spectrometer in the range 4000-400 cm<sup>-1</sup> using KBr pellets. The significant bands observed in the IR spectra of the thiosemicarbazones along with their relative assignments are presented in the Table 2.1. FT-IR spectral data of the compounds are in accordance with their molecular structure.

The characteristic IR bands of the thiosemicarbazone provide significant information regarding the various functional groups present in it. Since the thiosemicarbazones contain a thioamide functional group, they can exhibit thioamido-thioiminol tautomerism. A prominent band in the range 1540-1625  $\text{cm}^{-1}$  due to azomethine  $\nu(\text{C}=\text{N})$  linkage is observed in the spectrum indicating the condensation of thiosemicarbazide and the aldehyde moiety [90]. The  $\nu(\text{S}-\text{H})$  band at  $\sim 2600 \text{ cm}^{-1}$  is absent which indicates that the thiosemicarbazones exist as thioamido tautomer in the solid state [91,92]. This is further supported by a medium band in the range 3050-3150  $\text{cm}^{-1}$ , indicative of  $\nu(\text{N}-\text{H})$  vibration [93]. The IR spectral band observed in the range 1300-1390  $\text{cm}^{-1}$  corresponds to  $\nu(\text{C}=\text{S})$  and those in the range 802-832  $\text{cm}^{-1}$  corresponds to  $\delta(\text{C}=\text{S})$  vibration. Band at 3363 and 3299  $\text{cm}^{-1}$  in  $\text{H}_2\text{bspt}$  and  $\text{H}_2\text{brset}$  respectively are due to O–H stretching vibrations. Medium band observed at 1100-1112  $\text{cm}^{-1}$  is due to hydrazine N–N bond [94]. The IR spectra are shown in Fig. 2.2.

**Table 2.1. IR spectral data of the thiosemicarbazones**

Compound	$\nu(\text{O}-\text{H})$	$\nu(\text{N}-\text{H})$	$\nu(\text{C}=\text{N})$	$\nu(\text{C}=\text{S})$	$\nu(\text{N}-\text{N})$	$\delta(\text{C}=\text{S})$
<b><math>\text{H}_2\text{bspt}</math></b>	3366	3131	1625	1330	1112	832
<b><math>\text{H}_2\text{brset}</math></b>	3299	3142	1603	1319	1101	824
<b><math>\text{Hbpet}</math></b>	-	3056	1583	1306	1107	812
<b><math>\text{HbpdT}</math></b>	-	3042	1563	1309	1115	792

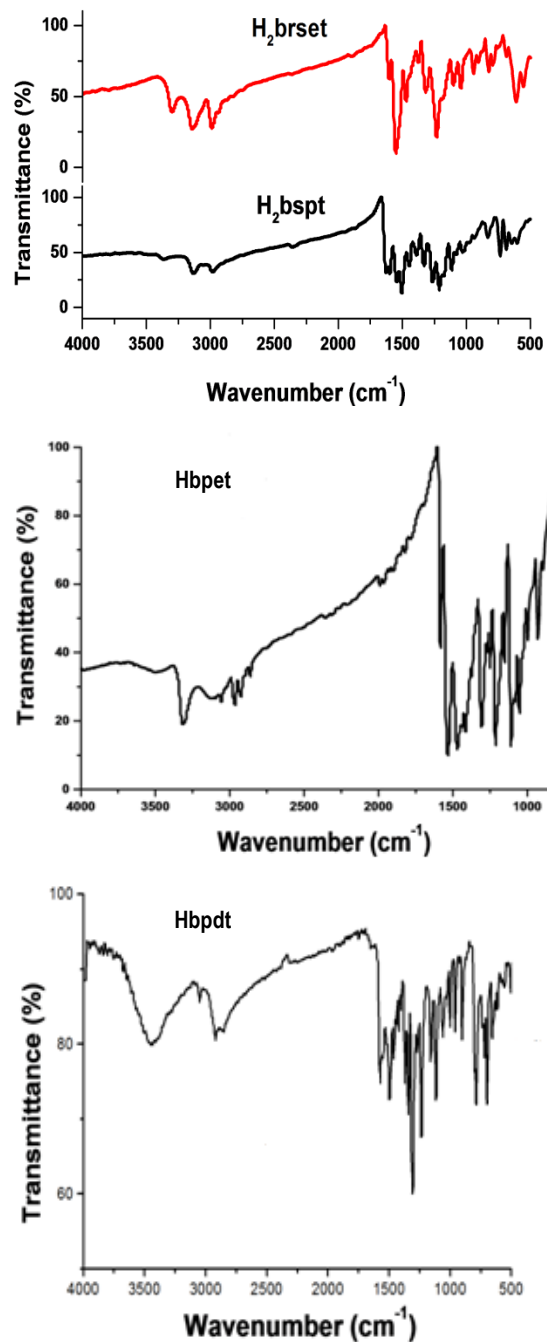


Fig. 2.2. IR spectra of the thiosemicarbazones.

### 2.3.4 Electronic spectra

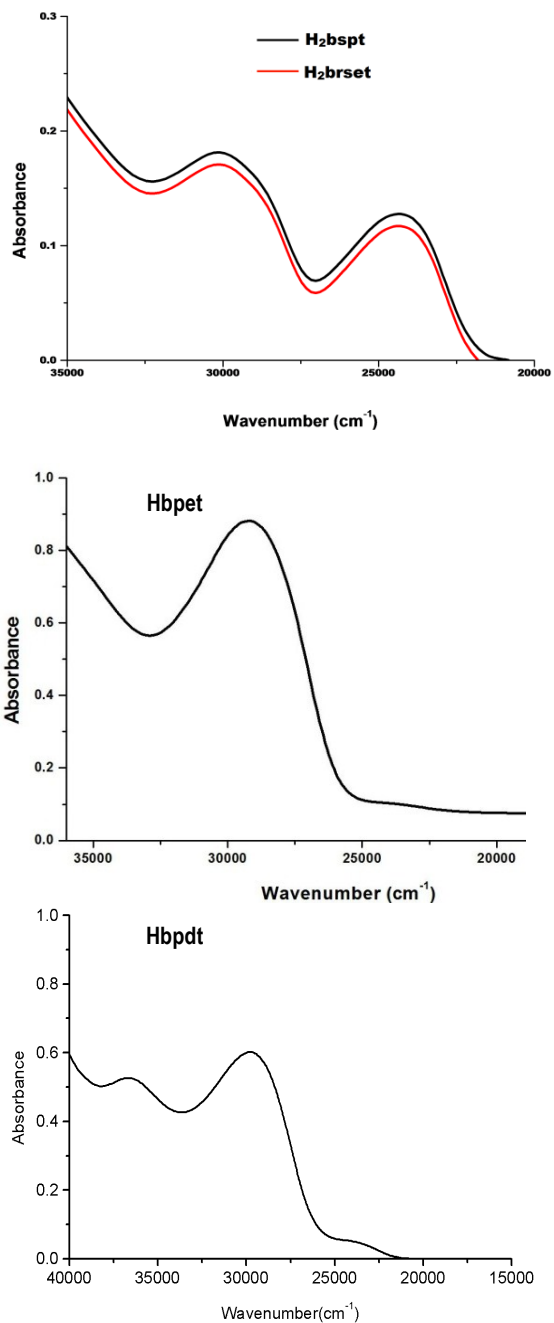


Fig. 2.3. Electronic spectra of the thiosemicarbazones.

The electronic spectra of the thiosemicarbazones were taken in DMF. Bands in the range 30100-24320  $\text{cm}^{-1}$  can be assigned to  $n \rightarrow \pi^*$  and  $\pi \rightarrow \pi^*$  transitions. This may be due to benzene ring, imine and thiocarbonyl groups present in the compounds. Fig. 2.3 represents the electronic spectra of the thiosemicarbazones and the spectral data are given in Table 2.2.

**Table 2.2. Electronic spectral data of the thiosemicarbazones**

Compound	$n \rightarrow \pi^*$ and $\pi \rightarrow \pi^*$ transitions
<b>H<sub>2</sub>bspt</b>	30100, 24320
<b>H<sub>2</sub>brset</b>	30100, 24310
<b>Hbpet</b>	29190
<b>Hbpdtd</b>	36580, 29820

### 2.3.5 NMR spectra

#### 2.3.5a. <sup>1</sup>H NMR spectrum-H<sub>2</sub>bspt

The <sup>1</sup>H NMR spectrum of the compound was recorded with deuterated dimethylsulphoxide (DMSO-d<sub>6</sub>) as solvent and trimethylsilane (TMS) as the internal standard and shown in Fig. 2.4.

A sharp singlet, which integrates as one hydrogen at 11.632 ppm is assigned to the -OH proton, while another similar singlet at 10.095 ppm is assigned to the N(2)H proton. The downfield shifts of these protons are assigned to their hydrogen bonding interactions. Hydrogen bonding decreases the electron density around the proton, and thus moves the proton absorption to a lower field. Absence of any coupling interactions by OH

and N(2)H protons due to the lack of availability of protons on neighboring atom render singlet peaks for them. These peaks are found to disappear in the  $\text{H}_2\text{bspt-D}_2\text{O}$   $^1\text{H}$  NMR spectrum, since those protons exchange with the deuterium in the  $\text{D}_2\text{O}$  (Fig. 2.5). The singlet at 8.404 ppm is assigned to  $-\text{CH}-\text{N}(1)$  proton. Another singlet at 9.971 ppm is assigned to N(3)H proton. Aromatic protons appear as a multiplet at 7.972-6.513 ppm range.

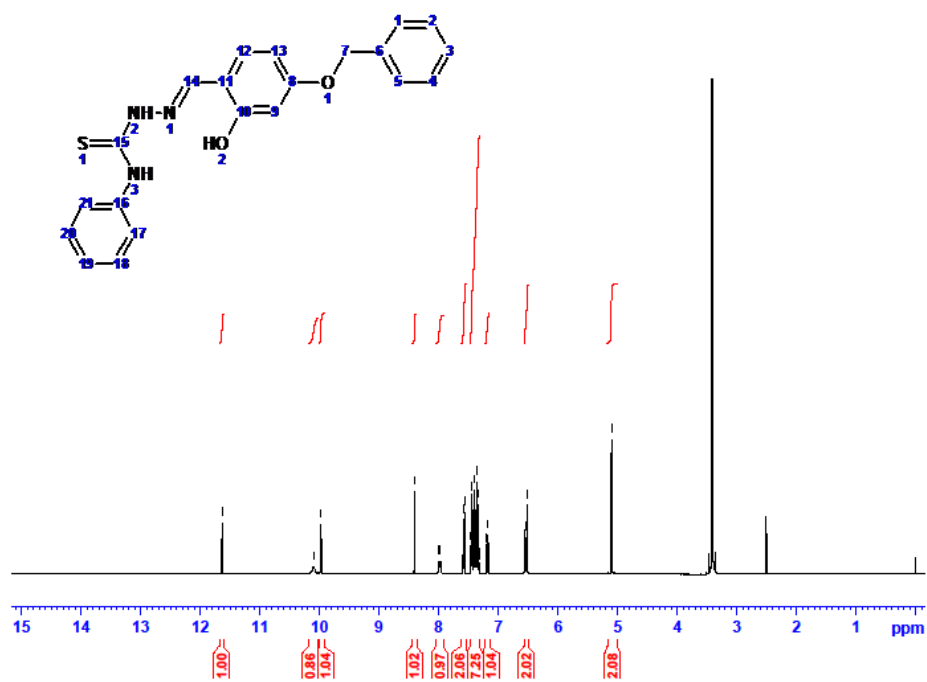


Fig. 2.4.  $^1\text{H}$  NMR spectrum of  $\text{H}_2\text{bspt}$ .



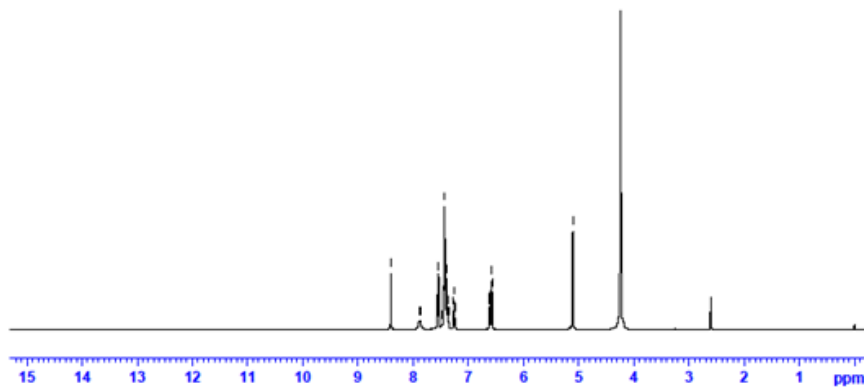


Fig. 2.5.  $^1\text{H}$  NMR spectrum of  $\text{H}_2\text{bspt-D}_2\text{O}$  exchange.

#### 2.3.5a.1 $^{13}\text{C}$ NMR spectrum

The proton decoupled  $^{13}\text{C}$  NMR spectrum provides direct information about the carbon skeleton of the molecule. The  $^{13}\text{C}$  NMR spectrum of the compound (Fig. 2.6) shows carbon signals supporting the  $^1\text{H}$  NMR assignments. There are 17 unique carbon atoms in the molecule which give a total of 17 different peaks in the spectrum. The non-protonated carbon atom C15 is shifted farthest downfield in the spectrum at 175.32 ppm due to the conjugative effect of the  $-\text{N}1-\text{N}2-\text{C}(\text{S})-\text{N}3-$  thiosemicarbazone skeleton. The peak at 136.74 ppm is assigned to the azomethine carbon C14. C8 and C10 carbon atoms also resonate at lower field values (C4, 161.11 ppm; C5, 158.01 ppm) due to a decreased electron density around carbon atoms resulting from the presence of electronegative oxygen atoms and  $\pi$  electron delocalization in the magnetic environment. The four different types of aromatic carbons on the N-substituted phenyl ring are clearly distinguishable in the  $^{13}\text{C}$  NMR spectrum. The peaks corresponding to the ortho positioned carbon atoms (C21 and C17) are observed rather downfield when compared to its *meta* (C20 and C18) and *para* (C19) counter parts.

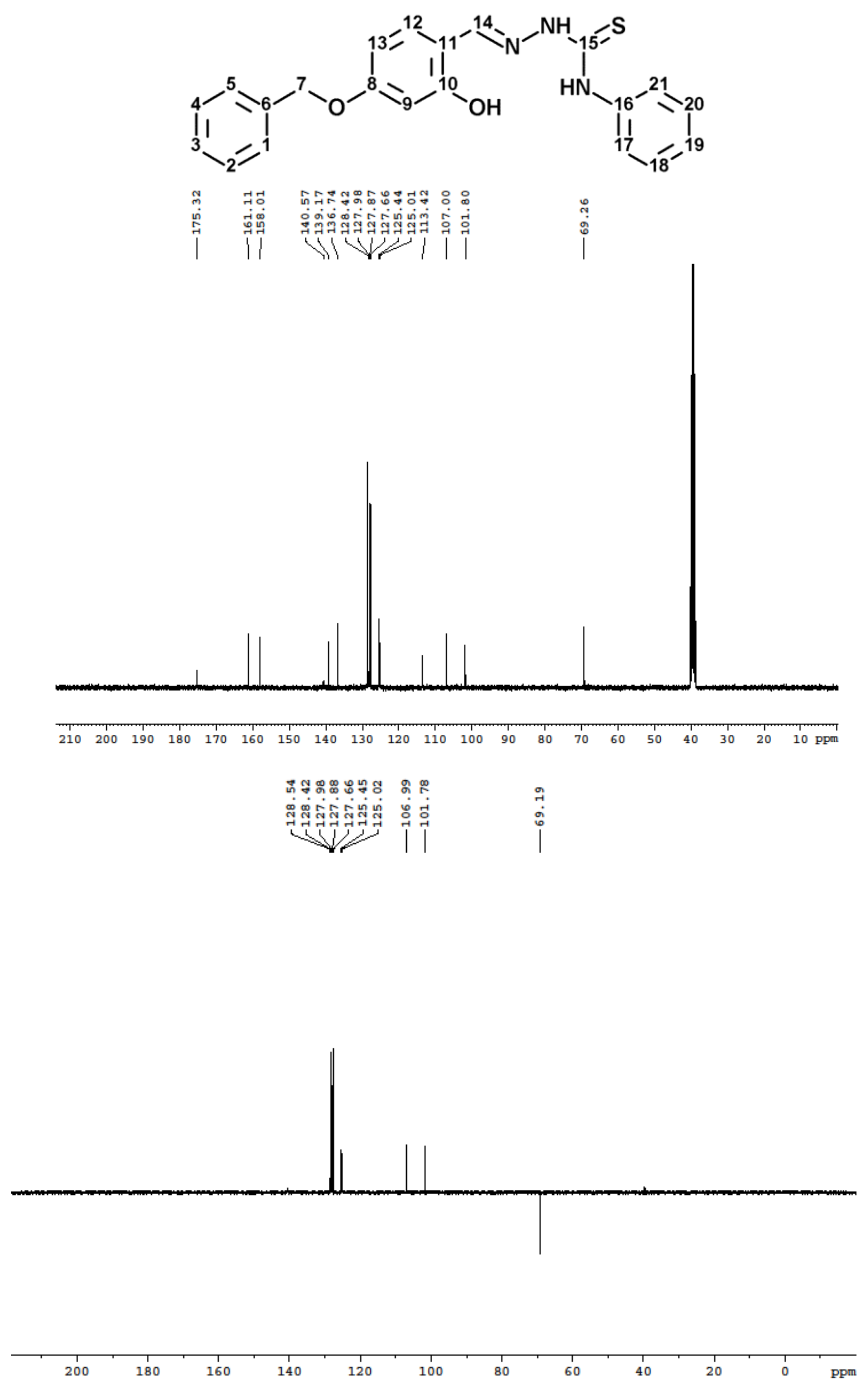


Fig. 2.6. <sup>13</sup>C NMR spectrum of H<sub>2</sub>bspt with DEPT.

The phenyl resonances are: C21 and C17, 127.98 ppm; C20 and C18, 127.87 ppm; C19, 113.42 ppm. The other  $^{13}\text{C}$  peaks can be assigned as follows: C16, 139.17 ppm; C12, 125.44 ppm; C13, 125.01; C9, 113.42 ppm; C1, 107.00 ppm; C7, 69.26 ppm.

In the DEPT-135 spectrum (Fig. 2.6), the signals due to C6, C8, C11, C10, C15 and C16 disappear whereas C1, C2, C3, C4, C5, C9, C12, C13, C14, C17, C18, C19 and C20 are retained positive. This shows that C1, C2, C3, C4, C5, C9, C12, C13, C14, C17, C18, C19 and C20 have odd number of hydrogens whereas the other carbons are without hydrogens. Signal due to C7 is inverted, it indicates the presence of carbon with even number of hydrogen atoms.

### **2.3.5b $^1\text{H}$ NMR spectrum- $\text{H}_2\text{brset}$**

A sharp singlet, which integrates as one hydrogen at 11.40 ppm is assigned to the –OH proton, while another similar singlet at 10.24 ppm is assigned to the N(2)H proton. The downfield shift of these protons is assigned to their hydrogen bonding interactions which is evident from the crystal structure. Hydrogen bonding decreases the electron density around the proton and thus moves the proton absorption to a lower field. Absence of any coupling interactions by OH and N(2)H protons due to the lack of availability of protons on neighboring atoms render singlet peaks for them (Fig. 2.7). These peaks are found to disappear in the  $\text{H}_2\text{brset-D}_2\text{O}$   $^1\text{H}$  NMR spectrum, since those protons exchange with the deuterium in the  $\text{D}_2\text{O}$  (Fig. 2.8). The singlet at 8.30 ppm is assigned to C(7)H proton and that at 8.05 ppm is assigned to N(3)H proton.

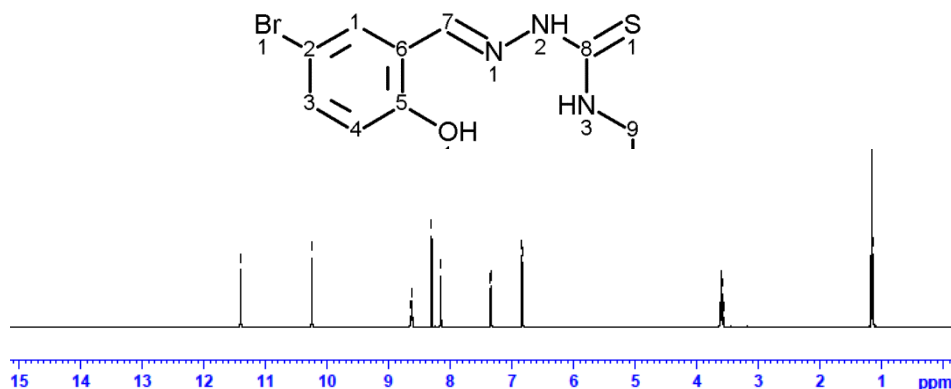


Fig. 2.7.  $^1\text{H}$  NMR spectrum of  $\text{H}_2\text{brset}$ .

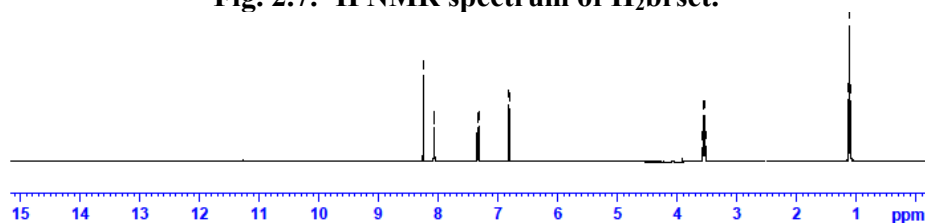


Fig. 2.8.  $^1\text{H}$  NMR spectrum of  $\text{H}_2\text{brset-D}_2\text{O}$  exchange.

### 2.3.5c. $^1\text{H}$ NMR spectrum-Hbpet

The  $^1\text{H}$  NMR spectrum of the compound was recorded with deuterated chloroform ( $\text{CDCl}_3$ ) as solvent. The proton NMR spectrum of the thiosemicarbazone is shown in Fig. 2.9.

A sharp singlet, which integrate as one hydrogen at 13.6 ppm for Hbpet is due to the existence of the compounds in thioamido-thioiminol form. On  $\text{D}_2\text{O}$  exchange the intensity of this signal is found to be considerably decreased (Fig. 2.10). Peak at 8.842 ppm is assigned to the N(4) proton. The aromatic protons appeared as multiplets at 7.78 -7.26 ppm range. A triplet at 1.291 ppm is assigned to  $-\text{CH}_3$  group and a doublet of quartets at around 3.8 ppm is assigned to  $-\text{CH}_2$  protons. The  $^1\text{H}$  NMR spectrum of the compound is shown in Fig. 2.9.

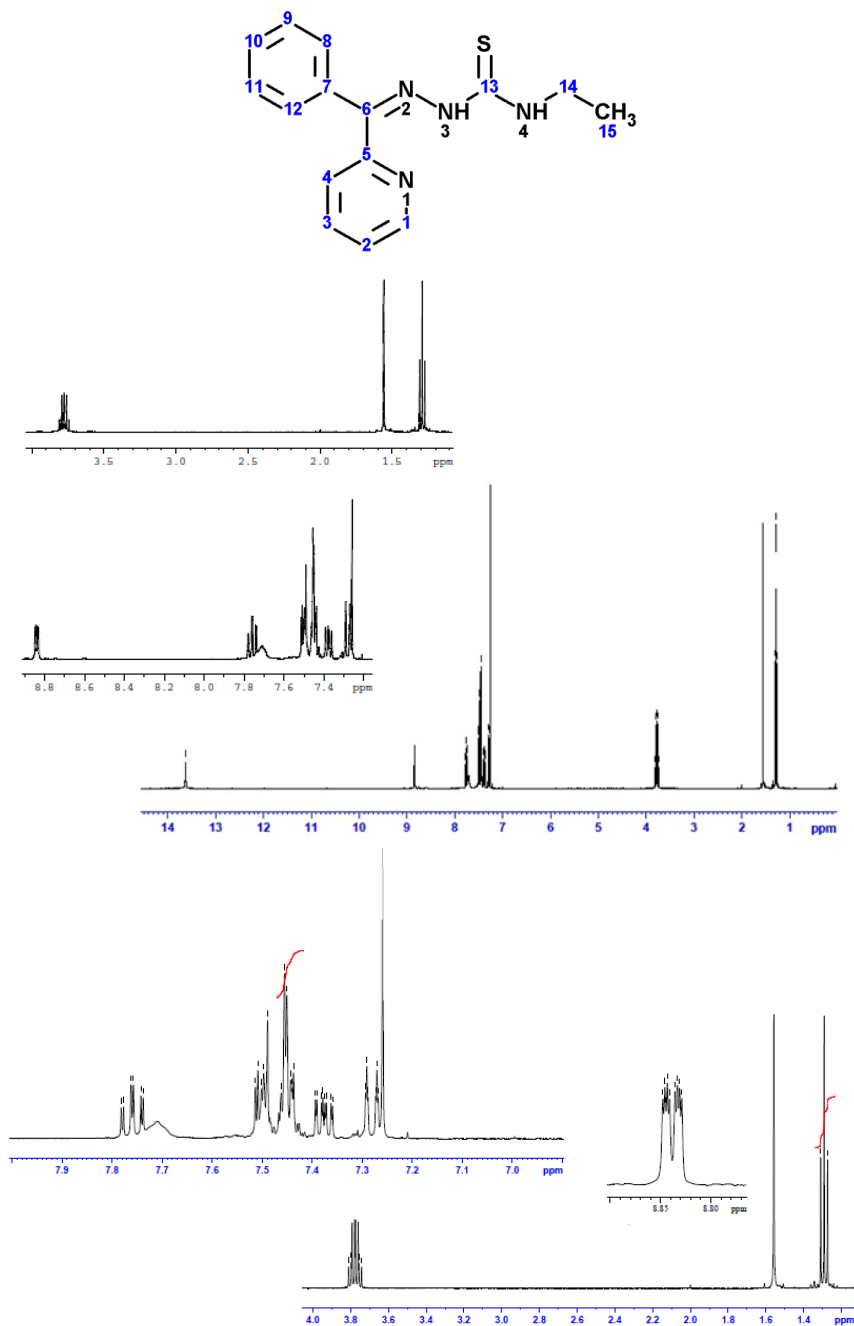


Fig. 2.9.  $^1\text{H}$  NMR spectrum of Hbpet.

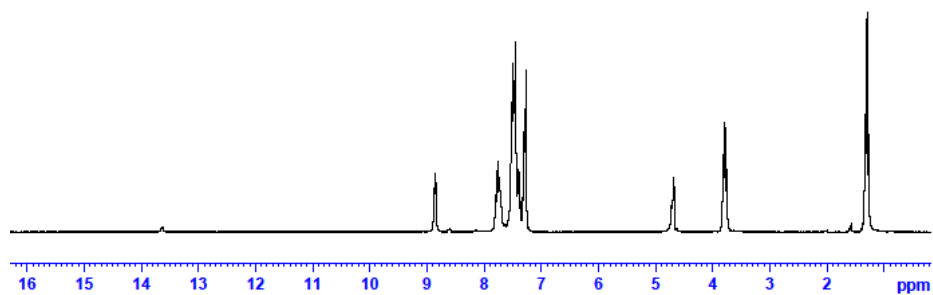


Fig. 2.10.  $^1\text{H}$  NMR spectrum of Hbpdt - $\text{D}_2\text{O}$  exchange.

### 2.3.5d $^1\text{H}$ NMR spectrum-Hbpdt

$^1\text{H}$  NMR spectrum of ligand Hbpdt along with spectral assignments are given in the Fig. 2.11. Hbpdt has a signal at 14.365 ppm which is due to N(3)H proton. This down field shift observation may be assigned to the deshielding of these protons as a result of the electron density after coordination.

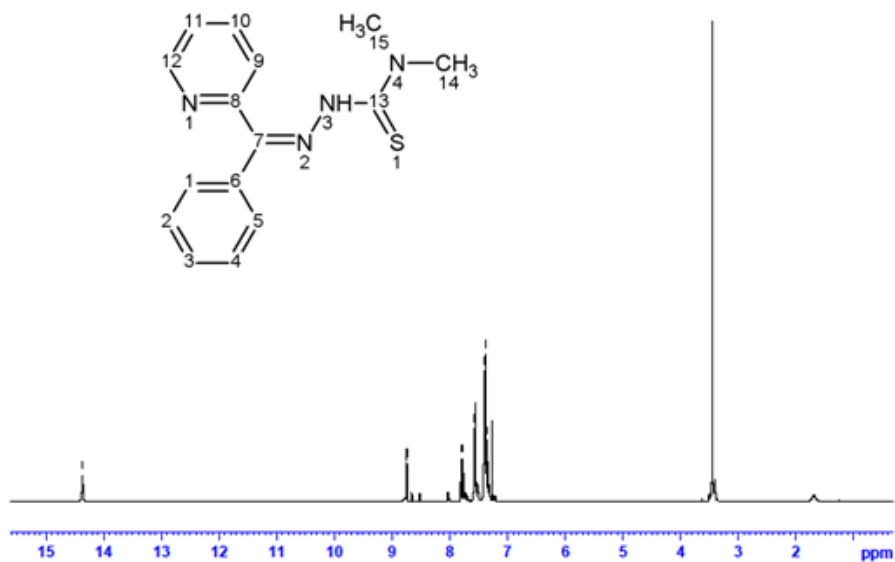


Fig. 2.11.  $^1\text{H}$  NMR spectrum of Hbpdt.

The thiosemicarbazone show hydrogen bonding by N(3)H proton based on the presence of a peak at 14.365 ppm in their spectra. The aromatic protons appear as multiplet at 8.753 to 7.347 ppm range. The sharp singlet at 3.452 ppm is due to two methyl groups.

### **2.3.6 X-ray crystallography**

Single crystal X-ray diffraction is an important technique in structural determination of crystalline materials for understanding their structure-property relationships. This powerful tool can be used to directly visualize the precise and detailed structural information of compounds. The data were collected using Bruker Kappa APEXII CCD diffractometer equipped with graphite monochromated MoK $\alpha$  ( $\lambda = 0.71073 \text{ \AA}$ ) radiation at the Sophisticated Analytical Instruments Facility, Cochin University of Science and Technology, Kochi-22, India. The intensity data were collected and absorption corrections were carried out using SADABS based on Laue symmetry using equivalent reflections [95]. The cell refinement was done using APEX2 and SAINT [95]. The data was reduced using SAINT and XPREP and the structure was solved by direct methods using SHELXS97 [65] and full-matrix least squares refinement on  $F^2$  using SHELXL97 [96] package. The graphics tool used was DIAMOND version 3.2g [66].

#### **2.3.6a Crystal structure-*H*<sub>2</sub>bspt**

Yellow block shaped crystals of 4-benzyloxysalicylaldehyde-*N*<sup>4</sup>-phenylthiosemicarbazone suitable for single crystal X-ray diffraction analysis were obtained by slow evaporation of its solution in methanol

over 3 days. A single crystal with approximate dimensions of  $0.30 \times 0.25 \times 0.25 \text{ mm}^3$  was selected for collecting the data. All H atoms on C were placed in calculated positions, guided by Fourier difference maps, with C–H bond distances  $0.93 \text{ \AA}$  (CH) or  $0.97 \text{ \AA}$  ( $\text{CH}_2$ ). H atoms were assigned as  $U_{\text{iso}}=1.2U_{\text{eq}}$ . H3A and H2B hydrogen atoms were located from Fourier difference maps and their distances were restrained using the DFIX instructions. H2A was located from a Fourier difference map and freely refined. The molecular structure of  $\text{H}_2\text{bspt}$  is given in Fig. 2.12.

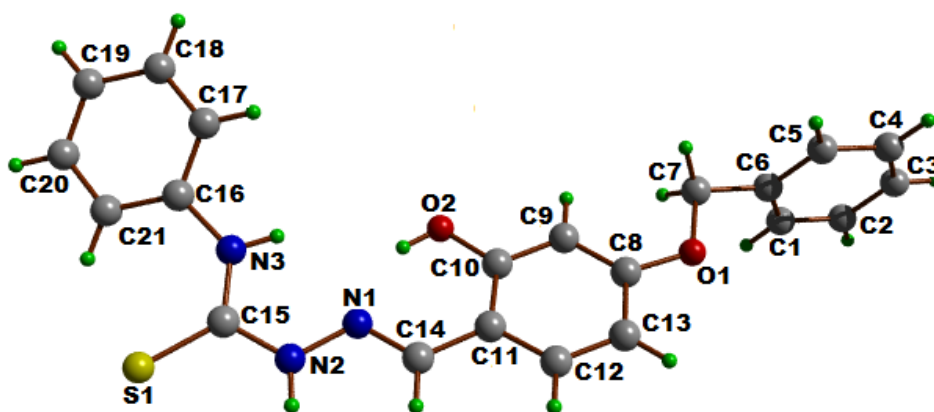


Fig. 2.12. Structure and labeling diagram for  $\text{H}_2\text{bspt}$ .

The crystallographic data and structure refinement parameters of the compound are given in Table 2.3 and the selected bond lengths and bond angles are given in Table 2.4 and torsion angles in Table 2.5.



**Table 2.3. Crystal data and structure refinement parameters for H<sub>2</sub>bspt**

Parameters	H <sub>2</sub> bspt
Empirical formula	C <sub>21</sub> H <sub>19</sub> N <sub>3</sub> O <sub>2</sub> S
Formula weight	377.45
Temperature (T) K	296(2)
Wavelength (Mo K $\alpha$ ) (Å)	0.71073
Crystal system	Monoclinic
Space group	C2/c
Cell parameters	
a	24.099(3) Å
b	16.173(2) Å
c	9.8370(11) Å
$\alpha$	90°
$\beta$	95.906(7)°
$\gamma$	90°
Volume V (Å <sup>3</sup> )	3813.5(8)
Z	8
Calculated density ( $\rho$ ) (Mg m <sup>-3</sup> )	1.315
Absorption coefficient, $\mu$ (mm <sup>-1</sup> )	0.191
F(000)	1584
Crystal size (mm <sup>3</sup> )	0.30 x 0.25 x 0.25
$\theta$ range for data collection	1.52 to 25.00°
Limiting indices	-28 ≤ h ≤ 28, -17 ≤ k ≤ 19, -11 ≤ l ≤ 11
Reflections collected	14247
Unique Reflections (R <sub>int</sub> )	3353 [R(int) = 0.0733]
Completeness to $\theta$	25 (99.9 %)
Absorption correction	Semi-empirical from equivalents
Refinement method	Full-matrix least-squares on F <sup>2</sup>
Data / restraints / parameters	3353 / 0 / 248
Goodness-of-fit on F <sup>2</sup>	1.005
Final R indices [I > 2 $\sigma$ (I)]	R <sub>1</sub> = 0.0505, wR <sub>2</sub> = 0.1324
R indices (all data)	R <sub>1</sub> = 0.1127, wR <sub>2</sub> = 0.1909
Largest difference peak and hole (e <sup>-</sup> Å <sup>-3</sup> )	0.237 and -0.292

$$R_1 = \sum ||F_o| - |F_c|| / \sum |F_o|, wR_2 = [\sum w(F_o^2 - F_c^2)^2 / \sum w(F_o^2)^2]^{1/2}$$

**Table 2.4. Selected bond lengths [Å] and angles [°] for H<sub>2</sub>bspt**

Bond lengths		Bond angles	
N(1)–C(14)	1.268(4)	C(14)–N(1)–N(2)	116.7(3)
S(1)–C(15)	1.668(3)	C(15)–N(2)–N(1)	121.3(3)
O(1)–C(8)	1.360(3)	C(16)–N(3)–C(15)	132.4(3)
N(1)–N(2)	1.373(3)	N(3)–C(15)–N(2)	114.4(3)
O(2)–C(10)	1.346(4)	N(3)–C(15)–S(1)	126.3(3)
N(2)–C(15)	1.341(4)	N(2)–C(15)–S(1)	119.3(3)
N(3)–C(16)	1.403(5)		
N(3)–C(15)	1.342(4)		

**Table 2.5. Selected torsion angles [°] for H<sub>2</sub>bspt**

Torsion angles	
O(2)–C(10)–C(11)–C(14)	-1.4(5)
N(2)–N(1)–C(14)–C(11)	-178.6(3)
N(1)–N(2)–C(15)–N(3)	0.5(5)
N(1)–N(2)–C(15)–S(1)	-178.3(2)

H<sub>2</sub>bspt crystallizes into a monoclinic space group, C2/c. According to the crystal structure, the compound exists in *E* configuration having N3 and N1 atoms *cis* to each other with respect to C(15)–N(2) bond [33,34]. The S(1)–C(15)–N(2)–N(1) torsion angle [-178.27(19)°] suggests that the thionyl atom S(1) is located *trans* to the azomethine nitrogen atom N(1). The closeness of the C(15)=S(1) bond distance [1.665(3) Å] to the expected distance of a C=S bond (1.60 Å) indicates that the compound exists in the thione form and it is further confirmed by the N(1)–N(2) and N(2)–C(15) bond distances. The

hydrazinecarbothioamide moiety, {N(1)–N(2)–N(3)–C(15)–S(1)–C(16)}, is nearly planar with a maximum deviation of 0.016(3) and -0.016(2) Å for atoms N(3) and N(2) from its least squares plane value. The three aromatic rings are twisted with a dihedral angle of 86.43(17)° between the least square plane of the rings C(1)–C(6) and C(8)–C(13), 67.99(19)° between rings C(1)–C(6) and C(16)–C(21) and 29.77(16)° between rings C(9)–C(13) and C(16)–C(21) respectively. An O(2)–H(2A)–N(1) intramolecular hydrogen bond, is observed which contributes to the planarity of the N(1)–C(14)–C(11)–C(10)–O(2) group with a maximum deviation of 0.146(2) Å for atom N(1). Weak N–H···S, C–H···O and C–H··· $\pi$  ring intermolecular interactions are also observed. Figs. 2.13 and 2.14 shows the packing diagram and the intra and inter molecular hydrogen bonding interactions in the ligand H<sub>2</sub>bspt.

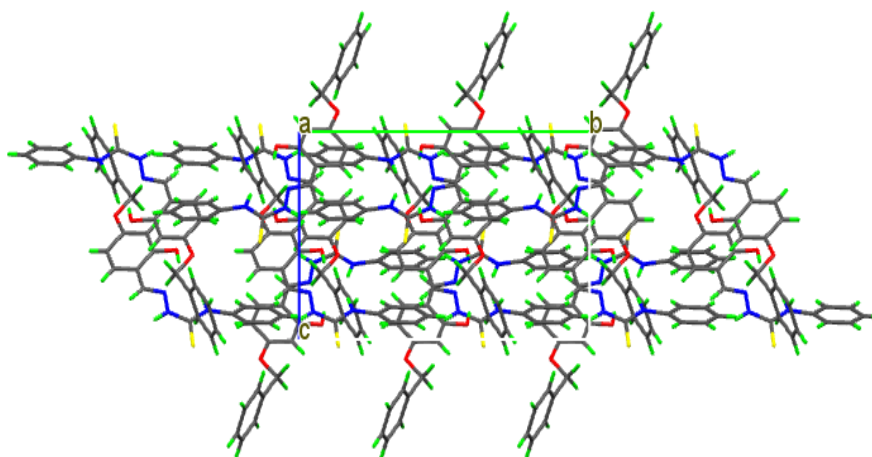


**Fig. 2.13. Packing diagram of H<sub>2</sub>bspt viewed along 'a' axis.**

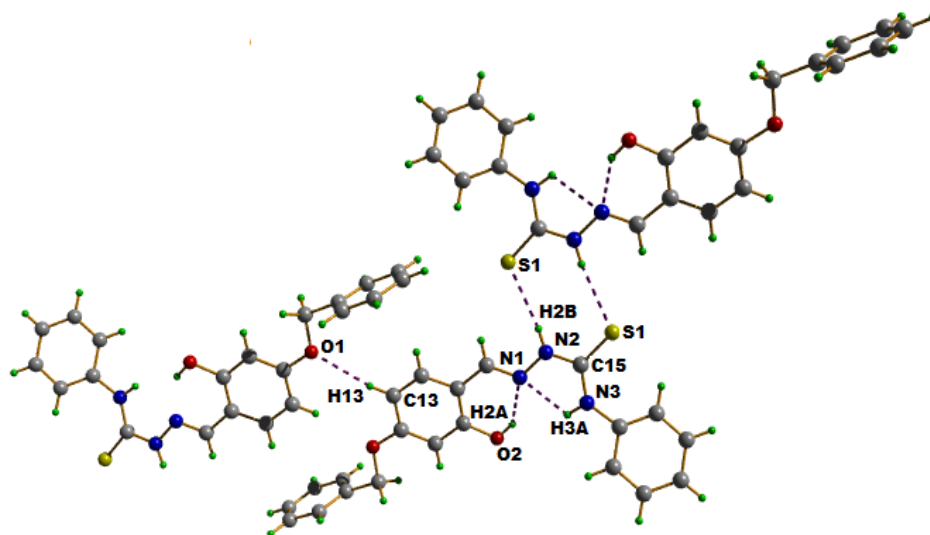


**Fig. 2.14.** Intra and intermolecular hydrogen bonding interactions of H<sub>2</sub>bspt.

Further stabilization is provided by C12–H12···Cg(1) and C5–H5···Cg(3) interactions (Fig. 2.15). The interaction parameters of H<sub>2</sub>bspt are given in Table 2.6.

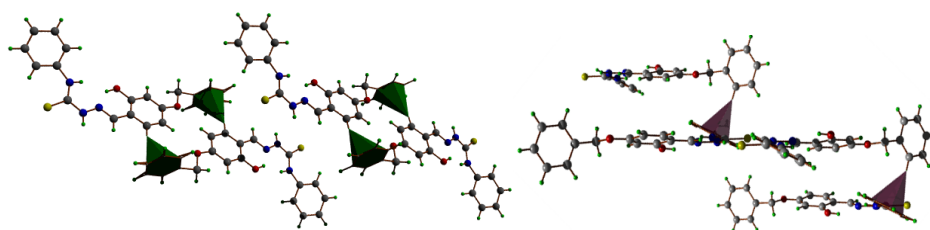


**Fig. 2.15.** C–H··· $\pi$  interactions in H<sub>2</sub>bspt.

Table 2.6. Interaction parameters of H<sub>2</sub>bspt

Hydrogen bonding				
D–H···A	D–H (Å)	H···A (Å)	D···A (Å)	∠D–H···A (°)
O(2)–H(2A)···N(1)	0.820	1.968	2.682	145.13
N(3)–H(3A)···N(1)	0.860	2.151	2.610	112.98
N(2)–H(2B)···S(1) <sup>a</sup>	0.868	2.534	3.392	170.20
C–H···π interactions				
C–H···Cg	C–H (Å)	H···Cg (Å)	C···Cg (Å)	∠C–H···Cg (°)
C(5)–H(5)···Cg(3) <sup>b</sup>	0.93	2.80	3.641(4)	152
C(12)–H(12)···Cg(1) <sup>c</sup>	0.93	2.87	3.743(4)	157

Equivalent position codes: a = -x+1, -y+1, -z+2; b = 3/2-x, -1/2+y, 3/2-z; c = 3/2-x, 1/2-y, 1-z

Cg(3) = C(16), C(17), C(18), C(19), C(20), C(21)

Cg(1) = C(1), C(2), C(3), C(4), C(5), C(6)

D = Donor, A = acceptor, Cg = Centroid of the ring

### 2.3.6b Crystal structure-H<sub>2</sub>brset

Colorless block shaped crystals of 5-bromo-N<sup>4</sup>-ethylthiosemicarbazone suitable for single crystal X-ray diffraction analysis were obtained by slow evaporation of its solution in 1:1 (v/v) mixture of DMF and methanol over 2 weeks. A single crystal with approximate dimensions of 0.30 × 0.25 × 0.20 mm<sup>3</sup> was selected for collecting the data. All H atoms on C were placed in calculated positions, guided by difference maps, with C–H bond distances 0.93–0.97 Å. H atoms were assigned as  $U_{\text{iso}}=1.2U_{\text{eq}}$  (1.5 for Me). O1–H1 H atom was located from

difference maps and their distances were restrained to  $0.82 \pm 0.01$  Å. The molecular structure of H<sub>2</sub>brset is given in Fig. 2.16.

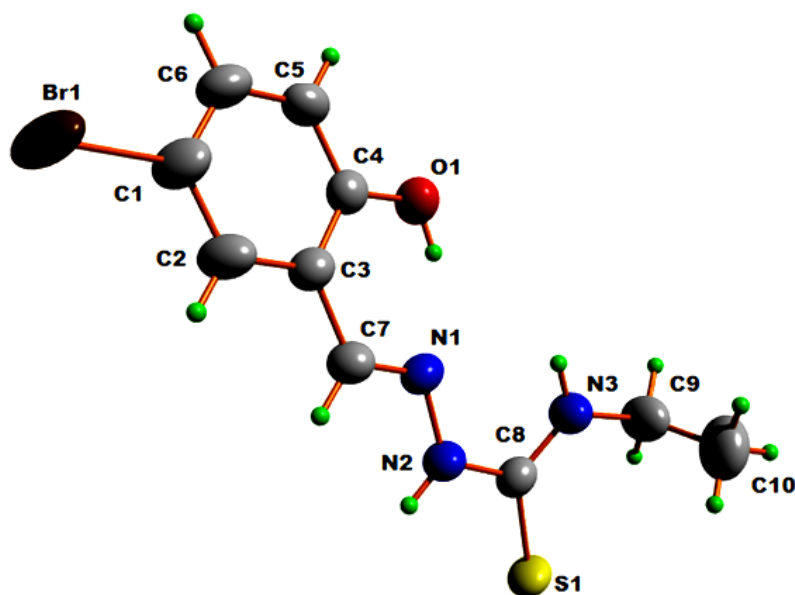


**Fig. 2.16. Structure and labeling diagram for H<sub>2</sub>brset.**

The crystallographic data and structure refinement parameters of the compound are given in Table 2.7 and the selected bond lengths and angles are given in Table 2.8 and torsion angles in Table 2.9.

**Table 2.7. Crystal data and structure refinement parameters for H<sub>2</sub>brset**

Parameters	H <sub>2</sub> brset
Empirical formula	C <sub>10</sub> H <sub>12</sub> BrN <sub>3</sub> OS
Formula weight	302.20
Color	Colorless
Temperature (T) K	293(2)
Wavelength (Mo K $\alpha$ ) (Å)	0.71073
Crystal system	Monoclinic
Space group	C2/c
Cell parameters	
a	22.3338(16) Å
b	11.9656(8) Å
c	9.5828(13) Å
$\alpha$	90°
$\beta$	102.796(5)°
$\gamma$	90°
Volume V (Å <sup>3</sup> )	2497.3(4)
Z	8
Calculated density ( $\rho$ ) (Mg m <sup>-3</sup> )	1.607
Absorption coefficient, $\mu$ (mm <sup>-1</sup> )	3.442
F(000)	1215.8
Crystal size (mm <sup>3</sup> )	0.30 x 0.25 x 0.20
$\theta$ range for data collection	2.76 to 28.22°
Limiting indices	-29 ≤ h ≤ 29, -15 ≤ k ≤ 15, -12 ≤ l ≤ 12
Reflections collected	18815
Unique Reflections (R <sub>int</sub> )	3055 [R(int) = 0.0734]
Completeness to $\theta$	28.22 (99.0 %)
Absorption correction	Semi-empirical from equivalents
Refinement method	Full-matrix least-squares on F <sup>2</sup>
Data / restraints / parameters	3055 / 29 / 186
Goodness-of-fit on F <sup>2</sup>	1.027
Final R indices [I > 2 $\sigma$ (I)]	R <sub>1</sub> = 0.0425, wR <sub>2</sub> = 0.0989
R indices (all data)	R <sub>1</sub> = 0.0789, wR <sub>2</sub> = 0.1163
Largest difference peak and hole (e <sup>-</sup> Å <sup>-3</sup> )	0.474 and -0.430

$$R_1 = \frac{\sum ||F_o| - |F_c||}{\sum |F_o|}, wR_2 = \left[ \frac{\sum w(F_o^2 - F_c^2)^2}{\sum w(F_o^2)^2} \right]^{1/2}$$

**Table 2.8. Selected bond lengths [Å] and angles [°] for H<sub>2</sub>brset**

Bond lengths		Bond angles	
N(1)–C(7)	1.274(3)	C(7)–N(1)–N(2)	115.9(2)
S(1)–C(8)	1.694(2)	C(8)–N(2)–N(1)	120.7(2)
O(1)–C(4)	1.348(3)	C(8)–N(3)–C(9)	126.1(8)
N(1)–N(2)	1.377(3)	N(3)–C(8)–N(2)	117.8(2)
O(2)–C(5)	1.351(4)	N(3)–C(8)–S(1)	124.26(19)
N(2)–C(8)	1.344(3)	N(2)–C(8)–S(1)	117.95(19)
N(3)–C(8)	1.313(3)		
N(3)–C(9)	1.459(5)		

**Table 2.9. Selected torsion angles [°] for H<sub>2</sub>brset**

Torsion angles	
O(1)–C(4)–C(3)–C(7)	-1.6(4)
N(2)–N(1)–C(7)–C(6)	-174.6(2)
N(1)–N(2)–C(8)–N(3)	9.2(4)
N(1)–N(2)–C(8)–S(1)	-171.49(17)

The compound crystallized into a monoclinic space group,  $P2_1/c$ . According to the molecular structure, the compound adopts an *E* configuration with respect to the C(8)–N(2) bond similar to H<sub>2</sub>bspt [99] and salicylaldehyde-*N*<sup>4</sup>-phenylthiosemicarbazone [98] but in contrast to 2-hydroxyacetophenone-*N*<sup>4</sup>-phenylthiosemicarbazone [100], where a *Z* configuration exists. This is confirmed by the N(1)–N(2)–C(8)–S(1) torsion angle of -171.49(17)°. Also *E* configuration is perceived about the azomethine bond [N(2)–N(1)–C(7)–C(6) = -174.6(2)°] [1]. The



C(8)–S(1) bond distance [1.694(2) Å] is closer to C=S bond length [1.60 Å] than to C–S bond length [1.81 Å] [1] which confirms the existence of the compound in the thioamido form in solid state. Also the C(7)–N(1) bond distance [1.274(3) Å] is appreciably close to that of a C=N double bond [1.28 Å], confirming the azomethine bond formation [101].

The mean plane deviation calculations show that the molecule as a whole is non-planar. But the central thiosemicarbazone moiety (C13–N3–N4–C14–S1) is almost planar with a maximum deviation from the mean plane of -0.002 Å for atom S(1). Fig. 2.17 shows the packing diagram of the compound.

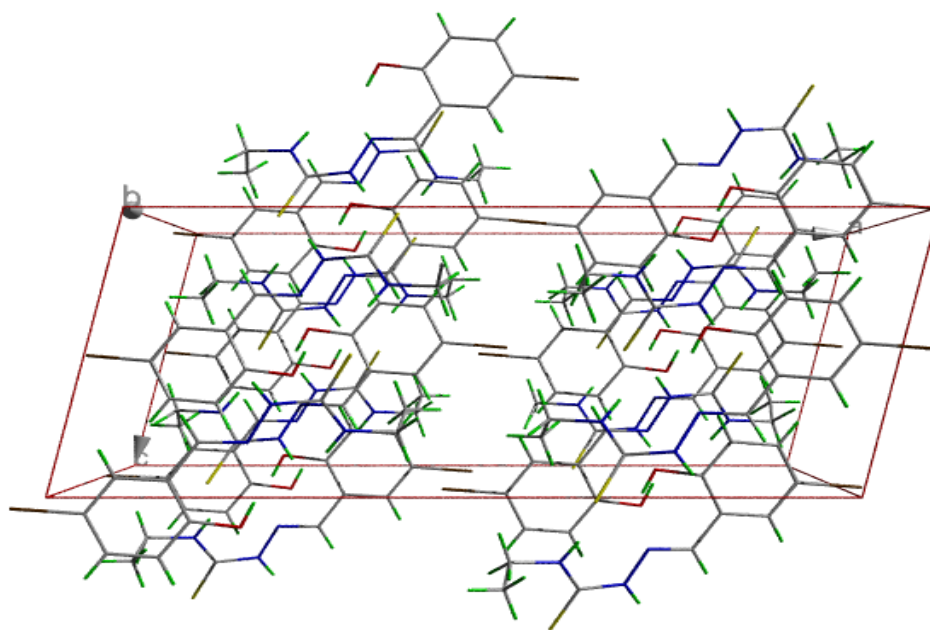


**Fig. 2.17. Packing diagram of H<sub>2</sub>brset viewed along 'a' axis.**

The crystal packing involves one intramolecular and two intermolecular hydrogen bonds (Table 2.10). The intramolecular hydrogen

bonding interaction, O(1)–H(1)···N(1) leads to the formation of a six membered ring comprising of atoms C(4), C(3), C(7), N(1), H(1) and O(1) and facilitates almost planar geometry in part of the molecule. The intermolecular hydrogen bonds N(2)–H(2N)···S(1) cause the pairing of molecules leading to the formation of centrosymmetric dimers in the crystal lattice (Fig. 2.18). Inversion dimers linked by pairs of N(2)–H(2N)···S(1) hydrogen bonds generate  $R^2_2(8)$ . Weak N(3)–H(3')···S(1) links connect the dimers into sheets.

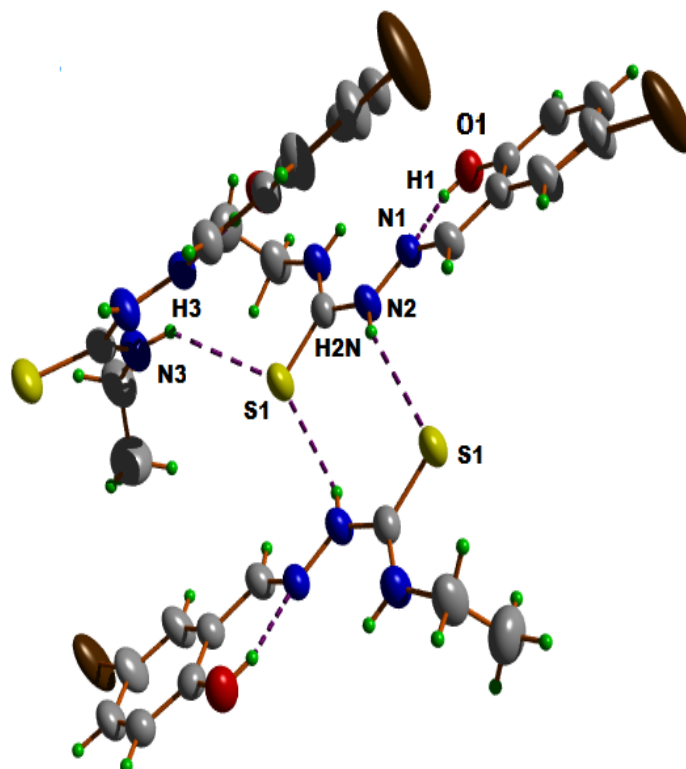


**Fig. 2.18.** Intra and intermolecular hydrogen bonding interactions of H<sub>2</sub>brset.

**Table 2.10. Interaction parameters of H<sub>2</sub>brset**

D–H···A	D–H	H···A	D···A	D–H···A
O(1)–H(1)···N(1)	0.824(19)	1.91(3)	2.658(3)	150(4)
N(2)–H(2N)···S(2) <sup>a</sup>	0.860	2.60	3.339(2)	144.7
N(3)–H(3)···S(2) <sup>b</sup>	0.86	2.90	3.539(2)	132.9

Equivalent position codes : a =  $-x+1/2, -y+1/2, -z+1$ , b =  $x, -y, z+1/2$

In the crystal packing, molecules are linked through intermolecular N(2)–H(2N)···S(1) hydrogen bonds forming *zig-zag* chains along ‘a’ axis. The dimers are further linked *via* hydrogen bonds N(3)–H(3')···S(1) forming 2D network. The packing diagram of H<sub>2</sub>brset shows the stacking of centrosymmetric dimers along ‘a’ axis (Fig. 2.19).

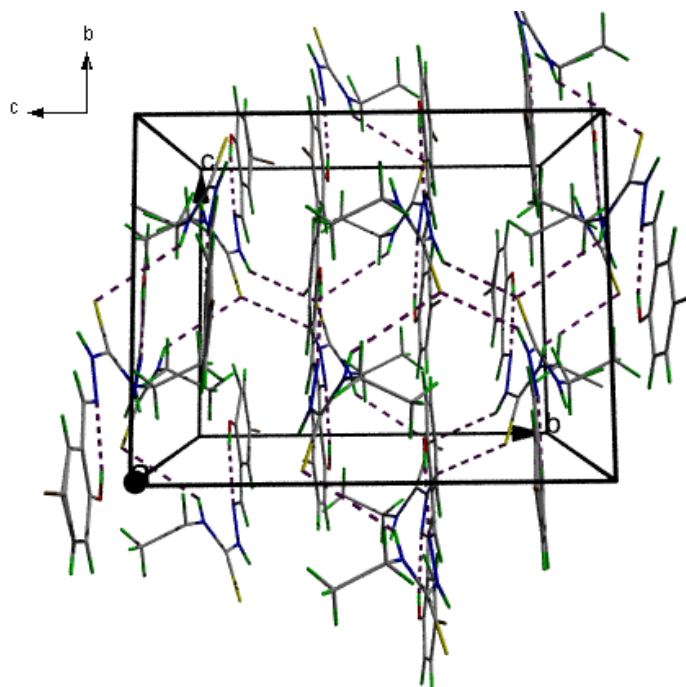


**Fig. 2.19. Packing diagram of H<sub>2</sub>brset showing the stacking of centrosymmetric dimers along ‘a’ axis.**

### 2.3.6c. Crystal structure-Hbpet

Colorless block shaped crystals of 2-benzoylpyridine- $N^4$ -ethylthiosemicarbazone suitable for single crystal X-ray diffraction analysis were obtained by slow evaporation of its solution in DMF over 2 weeks. A single crystal with approximate dimensions of  $0.30 \times 0.25 \times 0.20 \text{ mm}^3$  was selected for collecting the data. All H atoms on C were placed in calculated positions, guided by difference maps, with C–H bond distances 0.93–0.97 Å. H atoms were assigned as  $U_{\text{iso}}=1.2U_{\text{eq}}$  (1.5 for Me). N3–H3' and N4–H4' H atoms were located from difference maps and their distances were restrained to  $0.88 \pm 0.01 \text{ Å}$ . The molecular structure of Hbpet is given in Fig. 2.20.

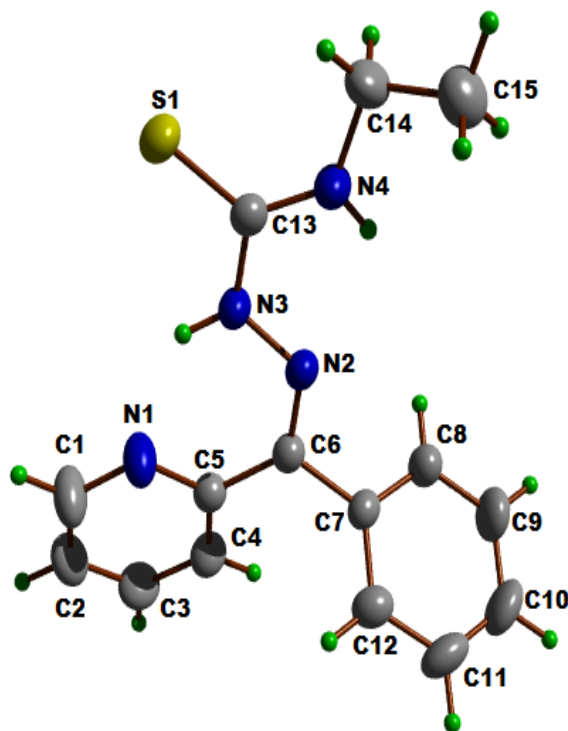


Fig. 2.20. Structure and labeling diagram for Hbpet.

The crystallographic data and structure refinement parameters of the compound are given in Table 2.11 and the selected bond lengths and angles are given in Table 2.12 and torsion angles in Table 2.13.

**Table 2.11. Crystal data and structure refinement parameters for Hbpet**

Parameters	Hbpet
Empirical formula	C <sub>15</sub> H <sub>16</sub> N <sub>4</sub> S
Formula weight	284.39
Color	Colorless
Temperature (T) K	293(2)
Wavelength (Mo K $\alpha$ ) (Å)	0.71073
Crystal system	Monoclinic
Space group	<i>P</i> 2 <sub>1</sub> / <i>c</i>
Cell parameters	
a	9.1840(9) Å
b	15.1956(14) Å
c	10.9860(9) Å
$\alpha$	90°
$\beta$	105.664(3)°
$\gamma$	90°
Volume V (Å <sup>3</sup> )	1476.2(2)
Z	4
Calculated density ( $\rho$ ) (Mg m <sup>-3</sup> )	1.280
Absorption coefficient, $\mu$ (mm <sup>-1</sup> )	0.215
F(000)	600
Crystal size (mm <sup>3</sup> )	0.30 x 0.25 x 0.20
$\theta$ range for data collection	2.35 to 26.99°
Limiting indices	-10 $\leq$ h $\leq$ 11, -19 $\leq$ k $\leq$ 19, -14 $\leq$ l $\leq$ 13
Reflections collected	11437
Unique Reflections (R <sub>int</sub> )	3224 [R(int) = 0.0209]
Completeness to $\theta$	26.99 (99.5 %)
Absorption correction	Semi-empirical from equivalents
Refinement method	Full-matrix least-squares on F <sup>2</sup>
Data / restraints / parameters	3208 / 2 / 189
Goodness-of-fit on F <sup>2</sup>	1.044
Final R indices [I > 2 $\sigma$ (I)]	R <sub>1</sub> = 0.0375, wR <sub>2</sub> = 0.0968
R indices (all data)	R <sub>1</sub> = 0.0510, wR <sub>2</sub> = 0.1079
Largest difference peak and hole (e Å <sup>-3</sup> )	0.206 and -0.202

$$R_1 = \frac{\sum ||F_o| - |F_c||}{\sum |F_o|}$$

$$wR_2 = \left[ \frac{\sum w(F_o^2 - F_c^2)^2}{\sum w(F_o^2)^2} \right]^{1/2}$$

**Table 2.12. Selected bond lengths [Å] and angles [°] for Hbpet**

Bond lengths		Bond angles	
N(2)–C(6)	1.2834(19)	C(6)–N(2)–N(3)	119.71(12)
S(1)–C(13)	1.6751(14)	C(13)–N(3)–N(2)	118.60(12)
N(3)–N(2)	1.3664(16)	C(13)–N(4)–C(14)	125.38(14)
N(3)–C(13)	1.355(2)	N(3)–C(13)–N(4)	115.84 (13)
		N(3)–C(13)–S(1)	118.75(11)
		N(4)–C(13)–S(1)	125.40(12)

**Table 2.13. Selected torsion angles [°] for Hbpet**

Torsion angles	
S(1)–C(13)–N(3)–N(2)	-171.23(11)
C(6)–N(2)–N(3)–C(13)	176.75(14)
N(3)–C(13)–N(4)–C(14)	-179.25(17)
S(1)–C(13)–N(4)–C(14)	1.7(3)
C(15)–C(14)–N(4)–C(13)	146.74(18)

The compound crystallized into a monoclinic space group  $P2_1/c$ . According to the molecular structure, the compound adopts an *E* configuration with respect to the C(13)–N(3) bond. This is confirmed by the S(1)–C(13)–N(3)–N(2) torsion angle of  $-171.23(11)^\circ$ . Also *Z* configuration is perceived about the azomethine bond [N(2)–N(3)–C(13)–S(1) =  $-171.23(2)^\circ$ ]. The C(13)–S(1) bond distance [1.6751(14) Å] is closer to C=S bond length [1.60 Å] than to C–S bond length [1.81 Å] [1] which confirms the existence of the compound in the thioamido form in solid state. Also the C(6)–N(2) bond distance [1.2834(19) Å] is appreciably close to that of a C=N double bond [1.28 Å], confirming the azomethine bond formation [101].

The compound exhibit one intramolecular and one intermolecular hydrogen bonds (Table 2.14). The hydrogen bonding interactions are shown in Fig. 2.21. The intramolecular hydrogen bonding interaction, N(3)–H(3')···N(1) leads to the formation of a six membered [S(5)] ring comprising of atoms N(3), N(2), C(6), C(5), N(1) and H(3') and facilitates almost planar geometry in part of the molecule. In the crystal molecules are linked through intermolecular N(4)–H(4')···S(1) hydrogen bonds forming *zig-zag* chains along *a* axis (Fig. 2.22).

**Table 2.14. Interaction parameters of Hbpet**

D–H···A	D–H	H···A	D···A	D–H···A
N(3)–H(3')···N(1)	0.879(9)	1.970(15)	2.6472(19)	132.8(16)
N(4)–H(4')···S(1) <sup>a</sup>	0.876(9)	2.931(15)	3.5757(16)	131.9(15)

Equivalent position codes: a =  $\bar{x}+1/2, -y+1/2, -z+1$ , b =  $x, -y, z+1/2$

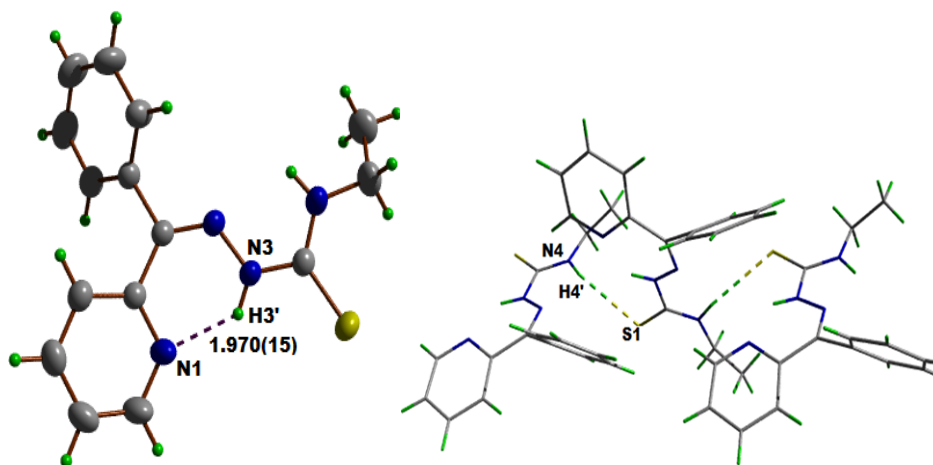


**Fig. 2.21. Intra and intermolecular hydrogen bonding interactions of Hbpet.**

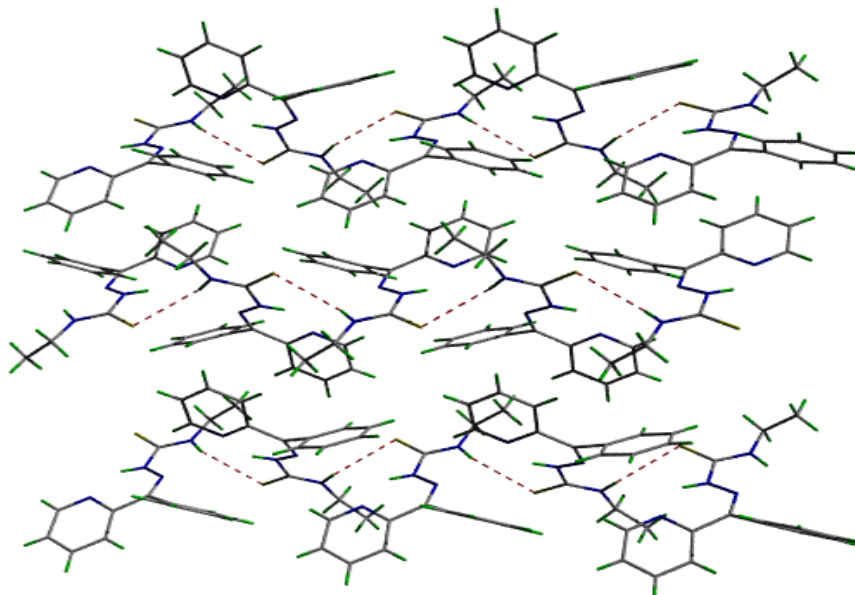


**Fig. 2.22.** Packing diagram of Hbpet showing the stacking of centrosymmetric dimers along 'a' axis.

#### 2.3.6d Crystal structure-Hbpd

Single crystals of thiosemicarbazone, Hbpd suitable for X-ray diffraction measurements were obtained from its methanol solution. Single crystals with approximate dimensions  $0.32 \times 0.28 \times 0.22 \text{ mm}^3$  of Hbpd was selected for collecting the data. The crystallographic data and structure refinement parameters of Hbpd are given in Table 2.15. The structure was solved by direct method and refined by least-square on  $F_0^2$  using SHELXL-97 [65]. All non-hydrogen atoms were refined anisotropically. All hydrogen atoms except those attached to nitrogen atoms were geometrically fixed at calculated positions. Those on nitrogen atoms were refined from Fourier map. Refinement of  $F^2$  was done against all reflections. All esds, except the esd in the dihedral angle between two least square planes, are estimated using the full covariance matrix. Flack  $x$



parameter is 0(2). As this value is 0, with standard uncertainty, the absolute structure given by structure refinement is likely correct [102].

**Table 2.15. Crystal data and structure refinement for Hbpd**

Parameters	Hbpd
Empirical formula	C <sub>15</sub> H <sub>16</sub> N <sub>4</sub> S
Formula weight	284.39
Color	Yellow
Temperature (T) K	296(2) K
Wavelength (Mo K $\alpha$ ) (Å)	0.71073
Crystal system	Monoclinic
Space group	<i>P</i> 2 <sub>1</sub> / <i>c</i>
Cell parameters	
a	10.011(2) Å
b	8.888(2) Å
c	16.256(4) Å
$\alpha$	90°
$\beta$	94.528(3)°
$\gamma$	90°
Volume V (Å <sup>3</sup> )	1441.9(6) Å <sup>3</sup>
Z	4
Calculated density ( $\rho$ ) (Mg m <sup>-3</sup> )	1.310
Absorption coefficient, $\mu$ (mm <sup>-1</sup> )	0.220
F(000)	600
Crystal size (mm <sup>3</sup> )	0.32 x 0.28 x 0.22
$\theta$ range for data collection	2.04 to 26.00°
Limiting indices	-12 $\leq$ h $\leq$ 12, -10 $\leq$ k $\leq$ 10, -19 $\leq$ l $\leq$ 19
Reflections collected	14231
Unique Reflections (R <sub>int</sub> )	2830 [R(int) = 0.0311]
Completeness to $\theta$	24.99 (99.9%)
Absorption correction	None
Refinement method	Full-matrix least-squares on F <sup>2</sup>
Data / restraints / parameters	2828 / 1 / 188
Goodness-of-fit on F <sup>2</sup>	1.048
Final R indices [I > 2 $\sigma$ (I)]	R <sub>1</sub> = 0.0603, wR <sub>2</sub> = 0.1826
R indices (all data)	R <sub>1</sub> = 0.0677, wR <sub>2</sub> = 0.1886
Largest difference peak and hole (eÅ <sup>-3</sup> )	0.592 and -0.543

$$R_1 = \frac{\sum ||F_o| - |F_c||}{\sum |F_o|}, wR_2 = \left[ \frac{\sum w(F_o^2 - F_c^2)^2}{\sum w(F_o^2)^2} \right]^{1/2}$$

The molecular structure of Hbpdtd along with the atom numbering scheme is given in Fig. 2.23. Selected bond lengths are given in Table 2.16. The compound crystallizes into a monoclinic space group,  $P2_1/c$ . The molecule is found to exist in *Z* configuration with respect to  $C7=N2$  bond. The  $S1=C13-N3-N2$  torsion-angle [ $14.4(2)^\circ$ ] indicates that thionyl atom S1 is positioned *cis* to azomethine nitrogen atom N2. The hydrazinecarbothioamide moiety adopts an extended conjugation, with electron delocalization throughout the  $N4/C13/S1/N3/N2$  group. The fact that the compound exists in the thioamido form is confirmed by the  $N3-N2$ ,  $N4-C13$  and  $C13=S1$  bond distances. The  $C13=S1$  bond distance is close to that expected for a  $C=S$  double bond of  $1.60 \text{ \AA}$  [1]. The  $N3-N2$  bond distance is very close to the reported similar substituted hydrazinecarbothioamide. The resonance form involving pyridine ring would account for the shortening of the  $N-N$  distance through extensive electron delocalization.

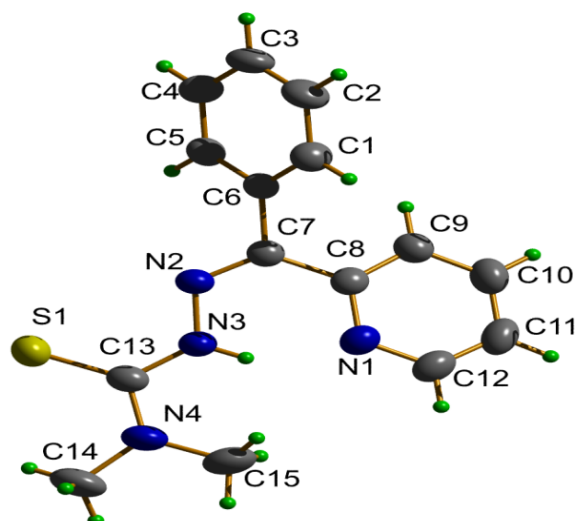
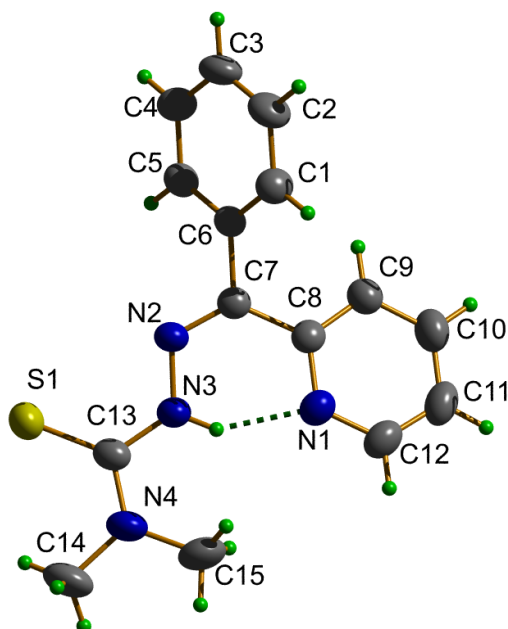


Fig. 2.23. Molecular structure of the Hbpdtd.

The hydrazinecarbothioamide moiety, comprising atoms N3, C13, S1 and N4, is almost planar with the maximum deviation of 0.013 (2) Å for atom N4. The pyridyl ring and phenyl ring are not in the same plane and the pyridyl ring is twisted significantly from the hydrazinecarbothioamide plane, with a torsional angle of -176.3(2)°.

Two types of intramolecular (classical and non-classical) hydrogen bond interactions are found in this molecule (Fig. 2.24). A classical hydrogen bonding interaction between the hydrogen attached to the N3 nitrogen and the N1 nitrogen with the D···A distance of 2.602(2) Å and the non-classical hydrogen bonding interaction between one of the hydrogen atom attached to the C14 atom and the S1 atom of the molecule with a D···A distance of 3.030(2) Å as described in Table 2.17. Fig. 2.25 shows the packing diagram of the title compound.



**Fig. 2.24.** Intramolecular hydrogen bonding in Hbpdtd.

**Table 2.16. Selected bond lengths [Å] for Hbpd**

bond lengths		bond angles	
S(1)–C(13)	1.675(3)	C(12)–N(1)–C(5)	119.3(3)
N(1)–C(1)	1.386(4)	C(6)–N(2)–N(3)	116.6(2)
N(1)–C(5)	1.397(4)	C(13)–N(3)–N(2)	122.2(2)
N(2)–C(6)	1.297(3)	C(13)–N(4)–C(14)	121.6(3)
N(2)–N(3)	1.364(3)	C(13)–N(4)–C(15)	122.2(2)
N(3)–C(13)	1.355(3)	C(14)–N(4)–C(15)	116.1(2)
N(4)–C(13)	1.348(3)	C(2)–C(1)–N(1)	120.5(3)
N(4)–C(14)	1.445(4)	C(3)–C(2)–C(1)	120.3(3)
N(4)–C(15)	1.464(4)	C(2)–C(3)–C(4)	120.1(3)
C(1)–C(2)	1.382(5)	C(5)–C(4)–C(3)	120.2(3)
C(2)–C(3)	1.362(5)	C(4)–C(5)–N(1)	119.7(2)
C(3)–C(4)	1.394(4)	C(4)–C(5)–C(6)	121.2(2)
C(4)–C(5)	1.379(4)	N(1)–C(5)–C(6)	119.1(2)
C(5)–C(6)	1.490(3)	N(2)–C(6)–C(7)	127.2(2)

**Table 2.17. Intramolecular hydrogen bonding interactions**

D–H···A	D–H (Å)	H···A (Å)	D···A (Å)	∠D–H···A (°)
N(3)–H(3')···N(1)	0.837(17)	1.869(17)	2.602(2)	145.4(15)
C(14)–H(14C)···S(1)	0.96	2.57(17)	3.030(2)	109.4

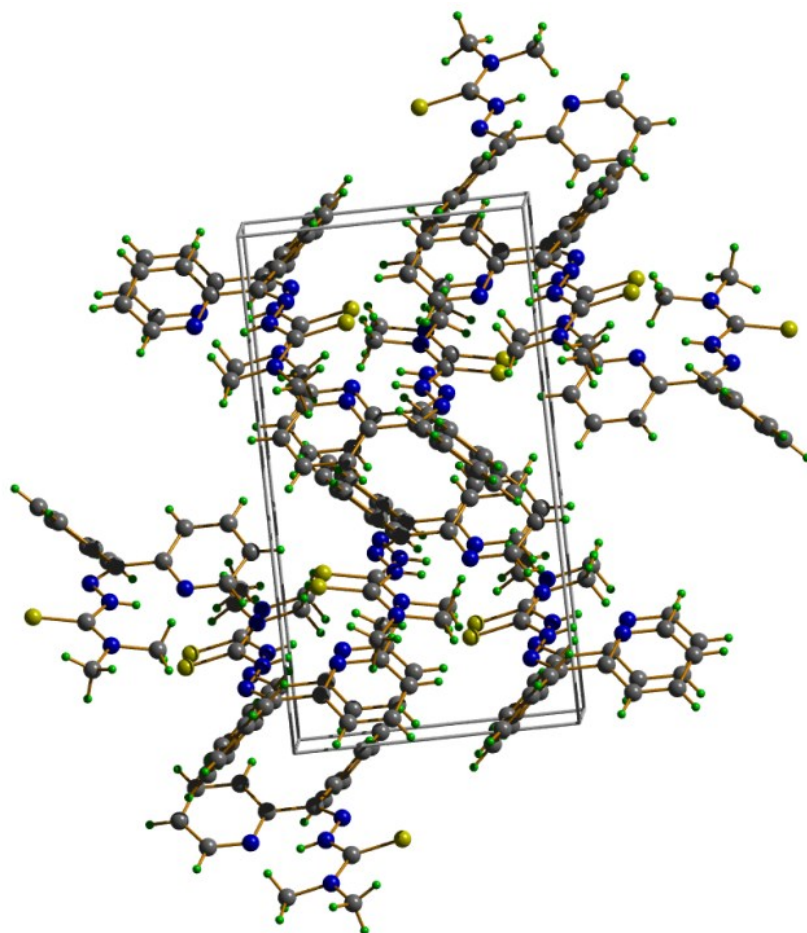


**Fig. 2.25.** Packing diagram of Hbpdt along 'a' axis.

.....*SC*.....



# Chapter 3

## SYNTHESES, SPECTRAL AND STRUCTURAL CHARACTERIZATION OF OXIDO/DIOXIDO VANADIUM (IV/V) COMPLEXES OF ONS AND NNS DONOR THIOSEMICARBAZONES

<i>Contents</i>	3.1 <i>Introduction</i>
	3.2 <i>Experimental</i>
	3.3 <i>Results and discussion</i>

### 3.1 Introduction

Vanadium is a rare, soft, ductile gray-white element found combined in certain minerals and used mainly to produce certain alloys. Vanadium was discovered in 1801 by the Spanish scientist Andres Manuel del Rio. Nothing more was heard of the element until 1830, when Nils Gabriel Sefström in Stockholm, Sweden, found a new metal in a Swedish iron ore. He called this new element vanadium after 'Vanadis' the Scandinavian goddess of beauty because of the beautiful multicolored compounds formed by the metal. Vanadium is found in the proteins known as vanabins. The coordination chemistry of vanadium is of great interest because of the discovery of its presence in abiotic as well as biotic systems. Some sea species of sea cucumbers and sea squirts have yellow

blood because of the vanabins in their blood [103]. The transition metal vanadium can easily expand its sphere beyond tetrahedral coordination, and switch between the oxidation states +5, +4 and +3 in a physiological environment. Vanadium is used for treating diabetes [104-106] low blood sugar, high cholesterol, heart disease, tuberculosis, syphilis, a form of “tired blood” (anemia), and water retention (edema); for improving athletic performance in weight training; and for preventing cancer. Macroalgae (seaweeds), fungi, lichens and *Streptomyces* bacteria have available haloperoxidases, and hence enzymes that enable the 2-electron oxidation of halide  $X^-$  with peroxide, catalyzed by a Lewis-acidic  $V^V$  center.

The coordination chemistry of both vanadium (IV/V) is relevant in bioinorganic chemistry. Nature has evolved several enzymatic systems utilizing vanadium as a central component for catalysis including vanadium-dependent haloperoxidases, nitrogenases, vanabins and non-enzymatic amavadin [107]. Complexes with ligands such as thiosemicarbazones may be used as models for an understanding of role of vanadium in biomolecules. They are of increasing interest due to their antibacterial, antifungal, antitumour as well as antiviral activities [108,109]. The literature survey revealed only few papers reporting the synthesis and characterization of oxidovanadium(IV) complexes with thiosemicarbazones. This chapter deals with the coordinaton chemistry of some oxidovanadium(IV) complexes derived from 4-benzyloxy-salicylaldehyde- $N^4$ -phenyl thiosemicarbazone and a dioxidovanadium (V) complex derived from 2-benzoylpyridine- $N^4, N^4$ -dimethyl thiosemicarbazone.



## **3.2 Experimental**

### **3.2.1 Materials**

Vanadyl sulphate monohydrate (Sigma-Aldrich), 1,10-phenanthroline (phen), 2,2'-bipyridine (bipy), 4,4'-dimethyl-2,2'-bipyridine (4,4'-dmbipy) and 5,5'-dimethyl-2,2'-bipyridine (5,5'-dmbipy) were of Analar grade and were used as received. Solvents used were methanol and DMF.

### **3.2.2 Syntheses of the thiosemicarbazones**

The syntheses of thiosemicarbazones H<sub>2</sub>bspt and Hbpd<sub>t</sub> are already discussed in Chapter 2.

### **3.2.3 Syntheses of the complexes**

#### **3.2.3.1 [VO(bspt)(bipy)] (1)**

Aqueous solution of vanadyl sulphate monohydrate (0.081 g, 0.5 mmol) was added to a stirred mixture of H<sub>2</sub>bspt (0.188 g, 0.5 mmol) in DMF and methanol (1:1 v/v) and 2,2'-bipyridine (0.078 g, 0.5 mmol) in methanol. The resultant solution was refluxed for three hours. The brown product obtained was filtered, washed with methanol and dried *in vacuo*.

Elemental Anal. Found (Calcd.) (%) : C, 62.11 (62.33); H, 4.85 (5.07); N, 11.26 (11.36); S, 5.31 (5.20). Yield: 80%.

#### **3.2.3.2 [VO(bspt)(phen)] (2)**

To a stirred mixture of H<sub>2</sub>bspt (0.188 g, 0.5 mmol) in DMF and methanol (1:1 v/v) and 1,10-phenanthroline (0.099 g, 0.5 mmol) in methanol, aqueous solution of vanadyl sulphate monohydrate (0.081 g,

0.5 mmol) was added. The resultant solution was refluxed for 3 hours and the brown product separated out was filtered, washed with methanol and dried *in vacuo*.

Elemental Anal. Found (Calcd.) (%) : C, 64.26 (63.66); H, 3.58 (4.05); N, 11.88 (11.25); S, 4.61 (5.15). Yield: 75%

### 3.2.3.3 [VO(bspt)(4,4'-dmbipy)] (3)

To a stirred mixture of H<sub>2</sub>bspt (0.188 g, 0.5 mmol) in DMF and methanol (1:1 v/v) was added aqueous solution of vanadyl sulphate monohydrate (0.081 g, 0.5 mmol) with constant stirring. This was followed by the addition of the base 4,4'-dimethyl-2,2'-bipyridine (0.092 g, 0.5 mmol) in the solid form. The resultant brown solution was refluxed for 3 hours and the brown product separated out was filtered, washed with methanol and dried *in vacuo*.

Elemental Anal. Found (Calcd.) (%) : C, 63.36 (63.25); H, 4.60 (4.66); N, 10.95 (11.08); S, 4.99 (5.12). Yield: 75%.

### 3.2.3.4 [VO(bspt)(5,5'-dmbipy)] (4)

To a stirred mixture of H<sub>2</sub>bspt (0.188 g, 0.5 mmol) in DMF and methanol (1:1 v/v) was added aqueous solution of vanadyl sulphate monohydrate (0.081 g, 0.5 mmol) with constant stirring. This was followed by the addition of the base 5,5'-dimethyl-2,2'-bipyridine (0.092 g, 0.5 mmol) in the solid form. The resultant brown solution was refluxed for 3 hours and the brown product separated out was filtered, washed with methanol and dried *in vacuo*.

Elemental Anal. Found (Calcd.) (%): C, 63.40 (63.25); H, 4.45 (4.66); N, 10.98 (11.08); S, 4.80 (5.12). Yield: 85%

### **3.2.3.5 [VO<sub>2</sub>(bpd<sub>t</sub>)] (5)**

A solution of ligand Hbpd<sub>t</sub> (0.135 g, 0.5 mmol) in methanol and a methanolic solution of vanadyl sulphate monohydrate (0.081 g, 0.5 mmol) were mixed and refluxed for 4 hours. On cooling brown colored crystals were filtered, washed with methanol and dried *in vacuo* over P<sub>4</sub>O<sub>10</sub>.

Elemental Anal. Found (Calcd.) (%) : C, 49.40 (49.18); H, 4.45 (4.13); N, 15.88 (15.29); S, 8.80 (8.75). Yield: 60%.

## **3.3 Results and discussion**

Four oxidovanadium complexes of ligand H<sub>2</sub>bspt and one dioxidovanadium complex of ligand Hbpd<sub>t</sub> were synthesized. The oxidovanadium complexes were synthesized by refluxing metal salt, corresponding heterocyclic bases and thiosemicarbazone in 1:1:1 ratio and the dioxidovanadium complex is synthesized by refluxing metal salt and the thiosemicarbazone in 1:1 ratio. All the complexes are brown in colour and are soluble in solvents like DMF and DMSO. In all the complexes except for the complex **5**, the thiosemicarbazone exists in the thioiminolate form and act as dideprotonated tridentate ligands coordinating through phenolate oxygen, thioiminolate sulfur and azomethine nitrogen. In complex **5** the ligand exists in the thioiminolate form, but monodeprotonated tridentate ligand coordinating through pyridyl nitrogen, thioiminolate sulfur and azomethine nitrogen.

Complexes **1-4** are monomeric mixed ligand metal chelates. However we could isolate single crystals of suitable quality for XRD studies for complex **5**. They are characterized by the following physico-chemical methods.

### 3.3.1 Elemental analyses

The analytical data indicate that the complexes are analytically pure. The elemental analyses data of complexes **1-4** are consistent with the general formula  $[\text{VOL}^1\text{B}]$ , where  $\text{L}^1$  is the doubly deprotonated thiosemicarbazone ligand and B is the bidentate heterocyclic bases *viz.* phen, bipy, 4,4'-dmbipy, 5,5'-dmbipy.

### 3.3.2 Molar conductivity and magnetic susceptibility measurements

The conductivity measurements were made in DMF ( $10^{-3}$  M) and all the complexes were found to be non-electrolytes [110]. The room temperature magnetic moments of the complexes **1-4** in the polycrystalline state are measured and the values are very close to the spin-only value for a  $d^1$  system (1.73 B.M.) [111].

All the complexes are EPR active due to this unpaired electron except for dioxidovanadium complex **5** which have no unpaired electrons. The magnetic moments and molar conductivity values of the complexes are listed in Table 3.1.

**Table 3.1. Molar conductivity and magnetic moments of V(IV/V) complexes**

Compound	$\lambda_m^a$	$\mu_{\text{eff}}$ (B.M.)
[VO(bspt)(bipy)] (1)	5.4	1.71
[VO(bspt)(phen)] (2)	8.8	1.68
[VO(bspt)(4,4'-dmbipy)] (3)	18.6	1.7
[VO(bspt)(5,5'-dmbipy)] (4)	25	1.8
[VO <sub>2</sub> (bpdt)] (5)	6.1	---

<sup>a</sup> = mho cm<sup>2</sup> mol<sup>-1</sup>

### 3.3.3 X-ray crystallography

Single crystals of compound [VO<sub>2</sub>(bpdt)] (5) suitable for X-ray diffraction studies were obtained by the slow evaporation of the mother liquor. Single crystals of dimensions 0.30 x 0.25 x 0.20 mm<sup>3</sup> of complex **5** were selected and mounted on a Bruker SMART APEXII CCD diffractometer, equipped with a graphite crystal, incident-beam monochromator and a fine focus sealed tube with Mo K $\alpha$  ( $\lambda = 0.71073$  Å) radiation as the X-ray source. The unit cell dimensions were measured and the data collection was performed at 296 K. Bruker SMART software was used for data acquisition and Bruker SAINT software for data integration [95]. Absorption corrections were carried out using SADABS based on Laue symmetry using equivalent reflections [95]. The structure was solved by direct methods using SHELXS97 [65] and refined by full-matrix least-squares calculations with SHELXL97 software package [96]. The molecular and crystal structures were plotted using DIAMOND version 3.2g [66]. All H atoms on C were placed in calculated positions, guided by difference maps, with C–H

bond distances 0.93–0.96 Å. H atoms were assigned as  $U_{\text{iso}}=1.2U_{\text{eq}}$  (1.5 for Me).

### 3.3.3.1 Crystal structure of [VO<sub>2</sub>(bpdt)] (5)

Crystal data and structure refinement for compound **5** are summarized in Table 3.2. The relevant bond lengths and bond angles for compound **5** are given in Table 3.3. The asymmetric unit consists of two independent molecules. Angular structural parameter  $\tau$  is used to propose an index of trigonality ( $\tau = \frac{\beta - \alpha}{60^\circ}$ ) [112]. The  $\tau$  value is found to be 0.06, hence vanadium atom in complex **5** shows the distorted square-pyramidal coordination. The tridentate thiosemicarbazone ligand is bonded to the vanadium atom through the pyridyl-nitrogen, imine-nitrogen and thiolato-sulphur atoms. The fourth and fifth coordination sites are occupied by two terminal oxo groups.

The vanadium atom is shifted for about 0.52 Å above the basal plane (base of the tetragonal pyramid), which is defined with O2, N1, S1 and N2, so that the five-membered chelate rings formed by chelation are not planar. The molecular structure of dioxidovanadium complex is shown in Fig. 3.1. The neighbouring molecules are interconnected by  $\pi \cdots \pi$  and CH $\cdots$  $\pi$  interactions (Fig. 3.2).

**Table 3.2. Crystal data and structure refinement parameters for complex 5**

Parameters	[VO <sub>2</sub> (bpd <sup>t</sup> )] (5)
Empirical formula	C <sub>15</sub> H <sub>15</sub> N <sub>4</sub> O <sub>2</sub> SV
Formula weight	366.31
Color	Brown
Temperature (T) K	296(2)
Wavelength (Mo K $\alpha$ ) (Å)	0.71073
Crystal system	Triclinic
Space group	$P\bar{1}$
Cell parameters	
a	10.9515(3) Å
b	11.0440(4) Å
c	13.8527(4) Å
$\alpha$	103.4990(10)°
$\beta$	93.9580(10)°
$\gamma$	97.7430(10)°
Volume V (Å <sup>3</sup> )	1605.52(9)
Z	4
Calculated density ( $\rho$ ) (Mg m <sup>-3</sup> )	1.515
Absorption coefficient, $\mu$ (mm <sup>-1</sup> )	0.762
F(000)	752
Crystal size (mm <sup>3</sup> )	0.30 x 0.25 x 0.20
$\theta$ range for data collection	1.52 to 25.00°
Limiting indices	-12 $\leq$ h $\leq$ 13, -9 $\leq$ k $\leq$ 13, -16 $\leq$ l $\leq$ 16
Reflections collected	9786
Unique Reflections (R <sub>int</sub> )	5581 [R(int) = 0.0579]
Completeness to $\theta$	25.00 (98.8%)
Absorption correction	Semi-empirical from equivalents
Maximum and minimum transmission	0.8626 and 0.8037
Refinement method	Full-matrix least-squares on F <sup>2</sup>
Data / restraints / parameters	5581 / 0 / 419
Goodness-of-fit on F <sup>2</sup>	1.043
Final R indices [I > 2 $\sigma$ (I)]	R <sub>1</sub> = 0.0977, wR <sub>2</sub> = 0.2586
R indices (all data)	R <sub>1</sub> = 0.1137, wR <sub>2</sub> = 0.2802
Largest difference peak and hole (e <sup>-</sup> Å <sup>-3</sup> )	3.634 and -1.681

**Table 3.3. Selected bond lengths and bond angles for complex 5**

Bond lengths		Bond angles	
V(1)–O(1)	1.609(5)	O(1)–V(1)–O(2)	109.6(3)
V(1)–O(2)	1.631(5)	N(5)–V(1)–N(1)	95.64(9)
V(1)–N(2)	2.151(5)	N(5)–V(1)–S(1)	93.45(7)
V(1)–S(1)	2.3520(19)	O(1)–V(1)–N(1)	100.2(2)
V(2)–O(4)	1.611(5)	O(2)–V(1)–N(1)	94.3(2)
V(2)–O(3)	1.617(6)	O(1)–V(1)–N(2)	107.6(2)
V(2)–N(6)	2.122(5)	O(2)–V(1)–N(2)	142.4(3)
V(2)–N(5)	2.163(6)	N(1)–V(1)–N(2)	73.92(19)
V(2)–S(2)	2.316(3)	O(1)–V(1)–S(1)	105.33(18)
S(1)–C(13)	1.741(7)	O(2)–V(1)–S(1)	97.5(2)
S(2)–C(28)	1.692(8)	N(1)–V(1)–S(1)	146.28(16)
V(1)–N(1)	2.091(5)	N(2)–V(1)–S(1)	77.57(14)
N(3)–C(13)	1.326(8)	O(4)–V(2)–N(6)	108.0(3)
N(7)–C(28)	1.333(9)	O(3)–V(2)–N(6)	141.2(3)
N(2)–N(3)	1.363(7)	O(4)–V(2)–N(5)	100.5(3)
N(6)–N(7)	1.427(8)	O(3)–V(2)–N(5)	93.8(3)
N(2)–C(6)	1.302(8)	N(6)–V(2)–N(5)	72.6(2)
		O(4)–V(2)–S(2)	104.2(3)
		O(3)–V(2)–S(2)	97.2(2)
		N(6)–V(2)–S(2)	79.82(17)
		N(5)–V(2)–S(2)	147.54(17)



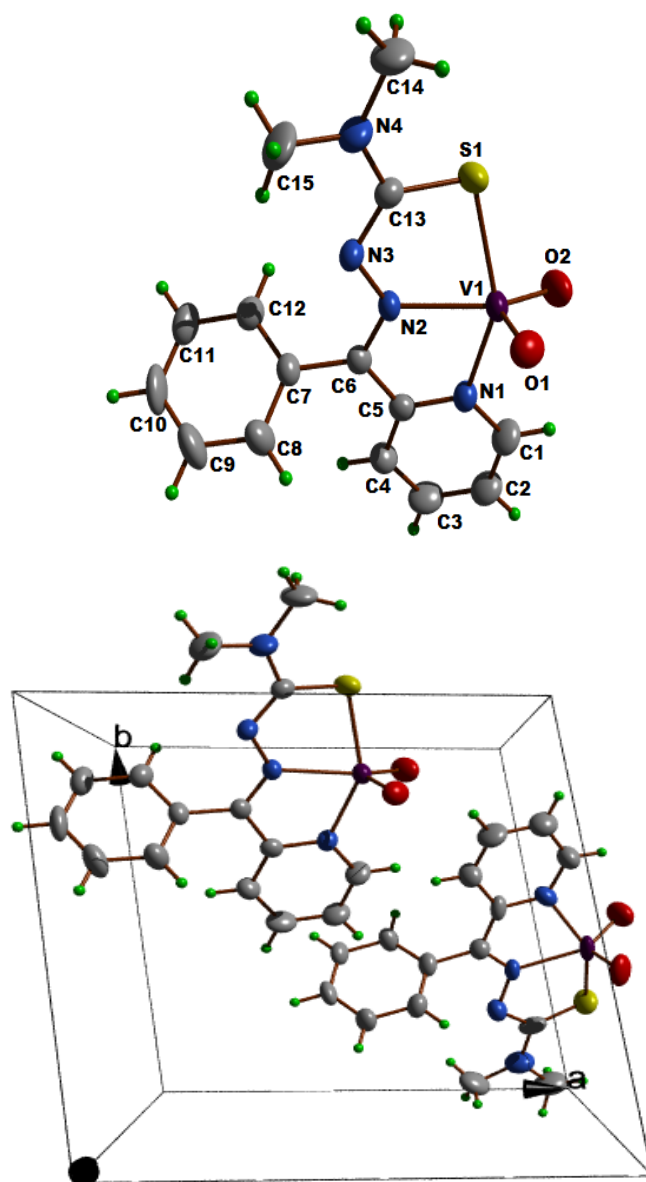


**Fig. 3.1.** Molecular structure of [VO<sub>2</sub>(bpdt)] (5).

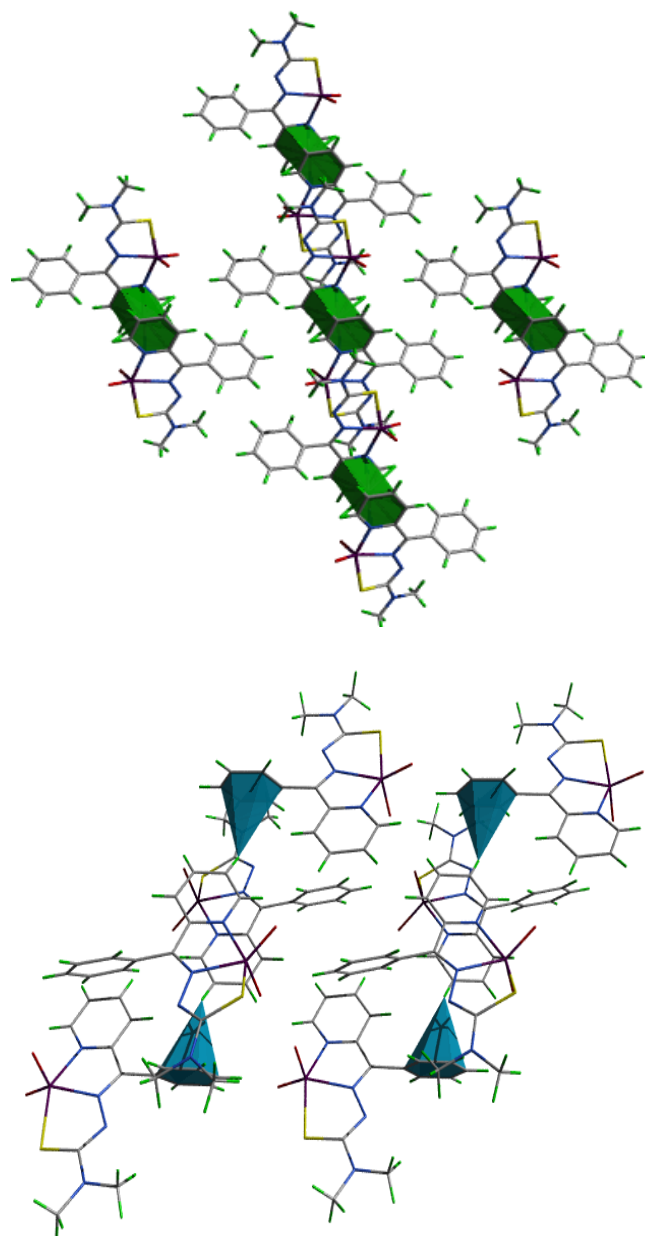


**Fig. 3.2.**  $\pi \cdots \pi$  and  $C-H \cdots \pi$  interactions of  $[VO_2(bpdt)]$  (5).

**Table 3.4.  $\pi \cdots \pi$  and C–H  $\cdots \pi$  interactions parameters for complex 5**

$\pi \cdots \pi$ interactions Cg(I) $\cdots$ Cg(J)	Cg $\cdots$ Cg (Å)	$\alpha$ (°)	$\beta$ (°)	$\gamma$ (°)
Cg(3) $\cdots$ Cg(3) <sup>a</sup>	3.597(4)	0	15.6	15.6
C–H $\cdots \pi$ interactions C–H(I) $\cdots$ Cg(J)	H $\cdots$ Cg (Å)	C–H $\cdots$ Cg (°)	C $\cdots$ Cg (Å)	
C(2)–H(2) $\cdots$ Cg(8) <sup>b</sup>	2.73	147	3.571(8)	

Equivalent position codes :  $a = 2 - x, -y, -z$ ;  $b = 1 + x, -1 + y, -1 + z$

Cg(3) = N(1), C(1), C(2), C(3), C(4), C(5)

Cg(8) = C(25), C(26), C(27), C(28), C(29), C(30)

$\alpha$  = dihedral angle between planes I and J

$\beta$  = angle between Cg(I)  $\cdots$  Cg(J) vector and Cg(J) perp

$\gamma$  = angle between Cg(I)  $\cdots$  Cg(J) vector and Cg(I) perp

### 3.3.4 Infrared spectra

A comparison of the IR spectra of H<sub>2</sub>bspt and the metal complexes shows that significant variations have occurred in the characteristic frequencies upon complexation. The tentative IR spectral assignments of the complexes are listed in Table 3.5. In all the complexes, the bands due to O–H and <sup>2</sup>N–H stretching vibrations are absent which is a clear evidence for the coordination of the thiosemicarbazone in the dideprotonated form. The band corresponding to azomethine bond,  $\nu(\text{C}=\text{N})$ , shifts to lower energy on coordination due to the combination of  $\nu(\text{C}=\text{N})$  with the newly formed C=N bond which results from the loss of the thioamide hydrogen from the thiosemicarbazone moiety [113-116,90]. The band at 1333 cm<sup>-1</sup> present in H<sub>2</sub>bspt shifts to lower wavenumbers in all the complexes and this can be assigned to the  $\nu(\text{C}-\text{S})$  vibration suggesting the change of bond order and strong electron-delocalization upon chelation. This shows that the H–N–C=S moiety in the ligand has transformed to N=C–S–H thereby coordinating to vanadium in the thioiminolate form. Coordination *via* thioiminolate

sulfur is also indicated by the negative shift of the band assigned to  $\delta(\text{C}=\text{S})$  vibration in the thiosemicarbazone [117]. The bands in the range  $416\text{-}513\text{ cm}^{-1}$  indicates the coordination of azomethine nitrogen to vanadium centre. The increase in frequency of  $\nu(\text{N}=\text{N})$  bands in complexes, due to the increase in double bond character is another proof for the coordination of the thiosemicarbazone through the azomethine nitrogen [118]. The broad absorption band at  $3366\text{ cm}^{-1}$  assigned to phenolic  $-\text{OH}$  of  $\text{H}_2\text{bspt}$  has disappeared in the complexes which indicate the coordination of the phenolic oxygen to the vanadium atom. The IR spectra of these complexes display bands characteristic of coordinated heterocyclic bases [119]. Further, the intense bands observed in the range  $961\text{-}964\text{ cm}^{-1}$  for all the complexes correspond to the terminal  $\text{V}=\text{O}$  stretching band [120]. Figs. 3.3 depict the infrared spectra of these complexes. Infrared spectrum of dioxidovanadium complex (**5**) is shown in Fig. 3.4.

**Table 3.5. IR spectral assignments ( $\text{cm}^{-1}$ ) of thiosemicarbazone and its oxido/dioxidovanadium (IV/V) complexes**

Compound	$\nu(\text{O}-\text{H})$	$\nu(\text{C}=\text{N})$	$\nu(\text{C}=\text{N})^a$	$\nu(\text{N}=\text{N})$	$\nu(\text{C}=\text{S})/\nu(\text{C}-\text{S}),$ $\delta(\text{C}=\text{S})/\delta(\text{C}-\text{S})$	$\nu(\text{C}-\text{O})$	$\nu(\text{V}-\text{N})$	$\nu(\text{V}=\text{O})$
$\text{H}_2\text{bspt}$	3366	1625	---	1112	1330, 832	1261	---	---
$[\text{VO}(\text{bspt})(\text{bipy})]$ ( <b>1</b> )	---	1600	1543	1118	1323, 835	1213	462	961
$[\text{VO}(\text{bspt})(\text{phen})]$ ( <b>2</b> )	---	1598	1545	1120	1331, 838	1209	464	964
$[\text{VO}(\text{bspt})(4,4'\text{-dmbipy})]$ ( <b>3</b> )		1607	1540	1130	1312, 835	1221	513	961
$[\text{VO}(\text{bspt})(5,5'\text{-dmbipy})]$ ( <b>4</b> )		1608	1555	1128	1324, 841	1225	476	965
$[\text{VO}_2(\text{bpdt})]$ ( <b>5</b> )		1535	1470	1110	1312, 818	----	481	950

<sup>a</sup> = newly formed  $\text{C}=\text{N}$  bond

In all the complexes, the thiosemicarbazone  $H_2bspt$  acts as a dianionic tridentate ligand coordinating to vanadium through O, N and S atoms and the two nitrogen atoms of heterocyclic bases occupy the fourth and fifth coordination positions of vanadium.

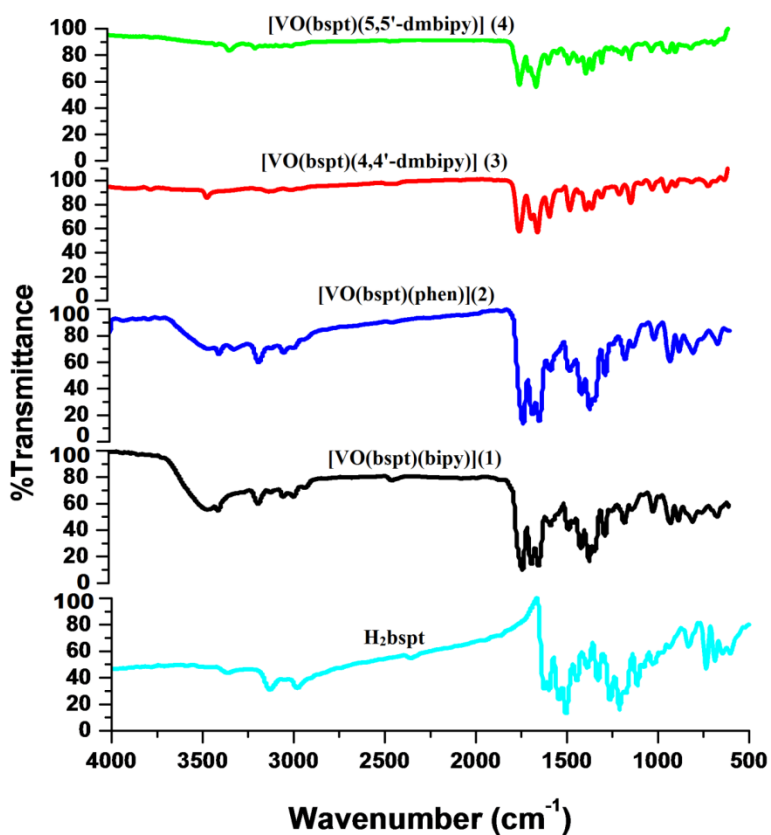


**Fig. 3.3.** Infrared spectra of oxidovanadium complexes.

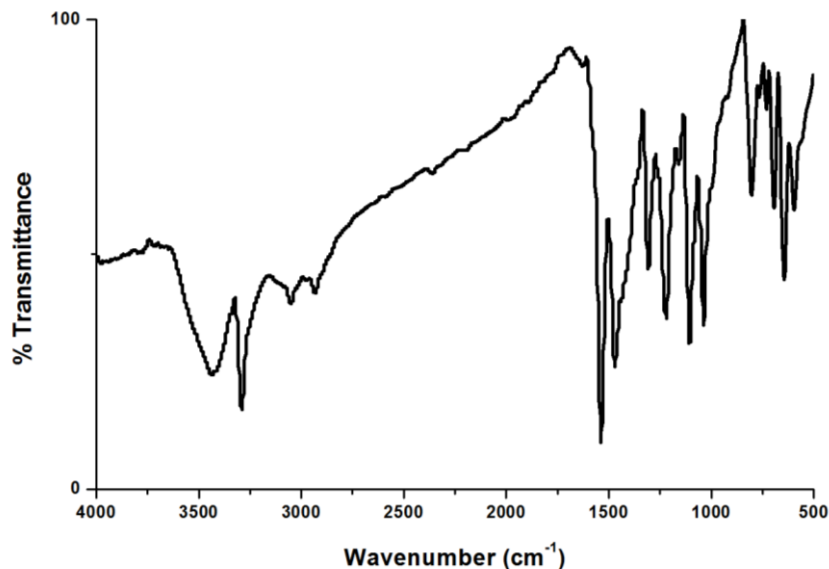


Fig. 3.4. Infrared spectrum of  $[\text{VO}_2(\text{bpdt})]$  (5).

### 3.3.5 Electronic spectra

The electronic spectra of all the complexes were taken in DMF. The significant electronic absorption bands in the spectra of  $\text{H}_2\text{bspt}$  and the oxidovanadium complexes are given in Table 3.6. The electronic transitions found in the free ligand due to imine function of thiosemicarbazone moiety were slightly shifted on complexation. The shift of the bands due to intraligand transitions is the result of the weakening of the C=S bond and the extension of conjugation upon complexation [121]. The shift occurs also due to coordination *via* phenolic oxygen and azomethine nitrogen [122] and is an indication of the enolization followed by the deprotonation of the thiosemicarbazone during complexation. The intraligand  $n \rightarrow \pi^*$  and  $\pi \rightarrow \pi^*$  transitions are assigned to bands in the range  $21770\text{--}35030\text{ cm}^{-1}$  for these complexes.

Fig. 3.5. represents the electronic spectra of the complexes. Fig. 3.6. represents the electronic spectrum of dioxidovanadium complex.

Ballhausen and Gray (BG scheme) have provided a convenient energy level scheme for VO(IV) type complexes [123]. In general, three absorptions are observed in the spectra of most of the oxidovanadium complexes, arising from the tetragonal compression caused by V=O bond, which results in further splitting of *d* orbitals and gives rise to three spin allowed transitions,  ${}^2E \leftarrow {}^2B_2$  ( $\nu_1$ ) ( $d_{xy} \rightarrow d_{xz}, d_{yz}$ ),  ${}^2B_1 \leftarrow {}^2B_2$  ( $\nu_2$ ) ( $d_{xy} \rightarrow d_{x^2-y^2}$ ),  ${}^2A_1 \leftarrow {}^2B_2$  ( $\nu_3$ ) ( $d_{xy} \rightarrow d_{z^2}$ ) [124]. Since the  ${}^2E$  and  ${}^2B_1$  levels are very close in energy, they may cross and result in a weak broad band. In all the complexes except for **1**(Fig. 3.7), the expected *d-d* bands are not observed and are probably obscured by the intense LMCT absorptions.

**Table 3.6. Electronic spectral assignments (cm<sup>-1</sup>) of thiosemicarbazone and its V(IV) complexes**

Compound	$n \rightarrow \pi^* / \pi \rightarrow \pi^*$	<i>d-d</i>
H <sub>2</sub> bspt	30100, 24320	....
[VO(bspt)(bipy)] ( <b>1</b> )	30990, 29170	14030
[VO(bspt)(phen)] ( <b>2</b> )	30760, 27571	....
[VO(bspt)(4,4'-dmbipy)] ( <b>3</b> )	35030, 25820	....
[VO(bspt)(5,5'-dmbipy)] ( <b>4</b> )	33230, 26200	....
[VO <sub>2</sub> (bpd <sub>t</sub> )] ( <b>5</b> )	30720, 21770	....

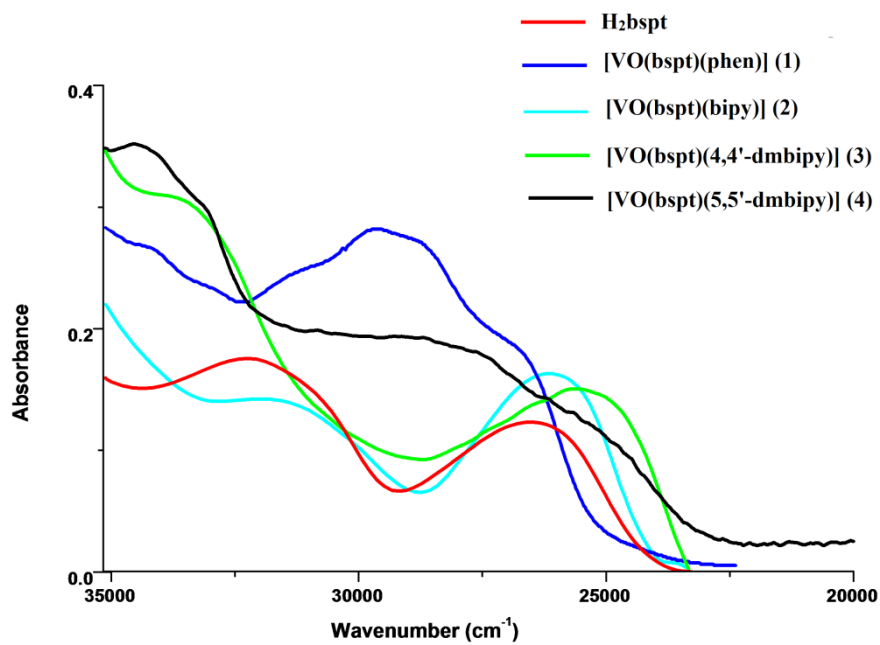


Fig. 3.5. Electronic spectra of H<sub>2</sub>bspt and its oxidovanadium complexes.

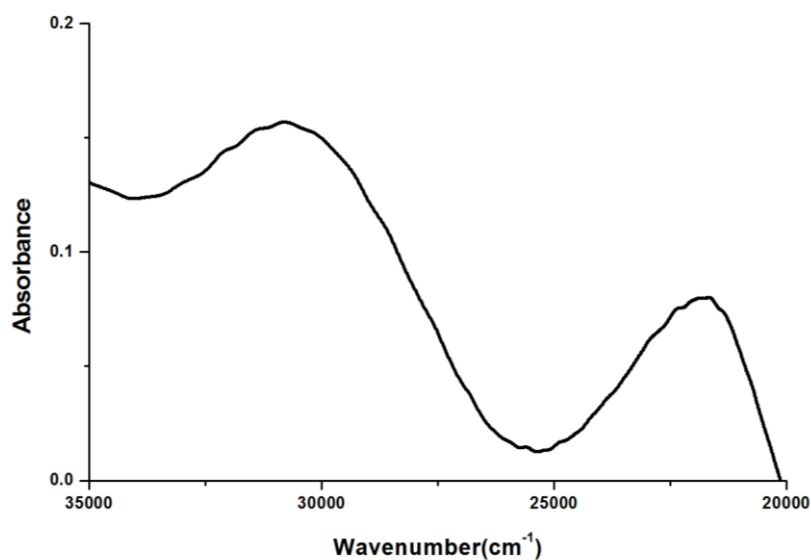
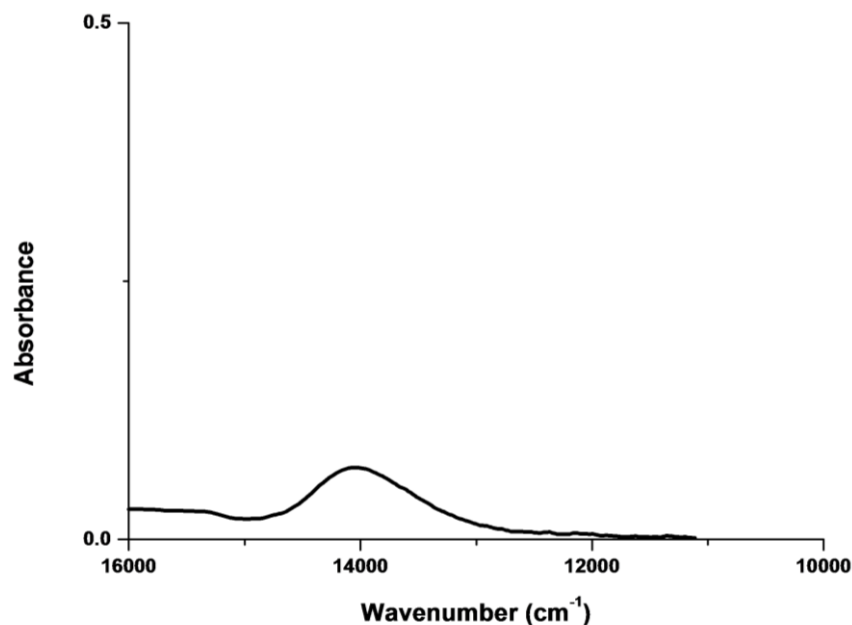


Fig. 3.6. Electronic spectrum of [VO<sub>2</sub>(bpdt)] (5).





**Fig. 3.7.** *d-d* band of [VO(bspt)(bipy)] (1).

### 3.3.6 EPR spectra

In Electron Paramagnetic Resonance spectroscopy, radiation of microwave frequency is absorbed by a molecule or ion having unpaired electron(s). Thus it is a convenient way to probe the electronic structure of paramagnetic compounds.

In vanadyl complexes, vanadium is in +4 oxidation state with  $d^1$  configuration and since the orbital angular momentum is quenched by the crystalline fields, the paramagnetism of the vanadyl ion arises from the single unpaired electron. In V(IV) complexes value of  $g$  is below the value for free electron. The spin of  $^{51}\text{V}$  nucleus is  $I = 7/2$ . In mononuclear V(IV) complexes, the EPR signals are split into eight and in binuclear complexes, fifteen hyperfine lines. Under the influence of

magnetic field, the electronic ground state ( $S = 1/2$ ) is split into two ( $m_s = +1/2$  and  $-1/2$ ) and additional splitting occurs through the different magnetic orientations of the nuclear spin ( $m_I$ ).

$\text{VO}^{2+}$  is one of the most stable diatomic cation and its paramagnetism is almost due to spin angular momentum and EPR absorptions are obtained over a wide range of temperature including room temperature [125].

EPR spectra of all the oxidovanadium(IV) complexes were recorded in polycrystalline state at 298 K and in DMF at 77 K and the spectral parameters are summarized in Table 3.7. Figs. 3.8-3.15 depict the EPR spectra of the oxidovanadium complexes.

The EPR spectra of all the complexes in the solid state at 298 K are isotropic in nature and hence only one  $g$  value, arising due to dipolar interactions and enhanced spin-lattice relaxation. In DMF at 77 K, all the complexes displayed well resolved axial anisotropy with two sets of eight line pattern which result from coupling of the electron spin with the spin of the  $^{51}\text{V}$  nucleus ( $I = 7/2$ ). They are found to exhibit  $g_{\parallel} < g_{\perp}$  and  $A_{\parallel} > A_{\perp}$  relationship, characteristic of an axially compressed  $d_{xy}^1$  configuration [126].

The absence of any superhyperfine lines in the spectrum is an explicit indication of the sole electron lying in the  $d_{xy}$  orbital ( ${}^2B_2$  ground state), localized on metal, thus excluding the possibility of its direct interaction with the azomethine nitrogen of the thiosemicarbazone [127,128]. The anisotropic parameters are related with isotropic parameters by the

equations,  $A_{\text{iso}} = 1/3(A_{\parallel} + 2A_{\perp})$  and  $g_{\text{iso}} = 1/3(g_{\parallel} + 2g_{\perp})$  [129]. In both compounds, the  $g_{\text{iso}}$  values calculated are near to the value obtained from the polycrystalline spectra which suggests that the molecules retain their structural identity in solution.

The EPR parameters  $g_{\parallel}$ ,  $g_{\perp}$ ,  $A_{\parallel}$  and  $A_{\perp}$  and energies of  $d-d$  transitions were used to evaluate the molecular orbital coefficients  $\alpha^2$  and  $\beta^2$  for the complexes by using the following equations:

$$\alpha^2 = \frac{(2.0023 - g_{\parallel})E_{d-d}}{8\lambda\beta^2}$$

$$\beta^2 = \frac{7}{6} \left[ \left( \frac{-A_{\parallel}}{P} \right) + \left( \frac{A_{\perp}}{P} \right) + \left( g_{\parallel} - \frac{5}{14}g_{\perp} \right) - \frac{9}{14}g_e \right]$$

where  $P = 128 \times 10^{-4} \text{ cm}^{-1}$ ,  $\lambda = 135 \text{ cm}^{-1}$  and  $E_{d-d}$  is the energy of  $d-d$  transition.

**Table 3.7. EPR spectral parameters of oxidovanadium(IV) complexes in the polycrystalline state at 298 K and in DMF at 77 K.**

Compound	Polycryst alline state at 298 K	DMF (77 K)							
	$g_{\text{iso}}$	$g_{\parallel}$	$g_{\perp}$	$g_{\text{av}}$	$A_{\parallel}^a$	$A_{\perp}^a$	$A_{\text{av}}^a$	$\alpha^2$	$\beta^2$
[VO(bspt)(bipy)] (1)	1.984	1.969	1.990	1.979	165	57	111	----	0.998
[VO(bspt)(phen)] (2)	1.973	1.955	1.969	1.964	165	54	91	0.753	1.03
[VO(bspt) (4,4'-dmbipy)] (3)	1.998	1.957	1.990	1.973	165	55	92	----	1.03
[VO(bspt) (5,5'-dmbipy)] (4)	1.967	1.957	1.975	1.969	164	51	89	----	1.05

<sup>a</sup>Expressed in units of  $\text{cm}^{-1}$  multiplied by a factor of  $10^{-4}$ .

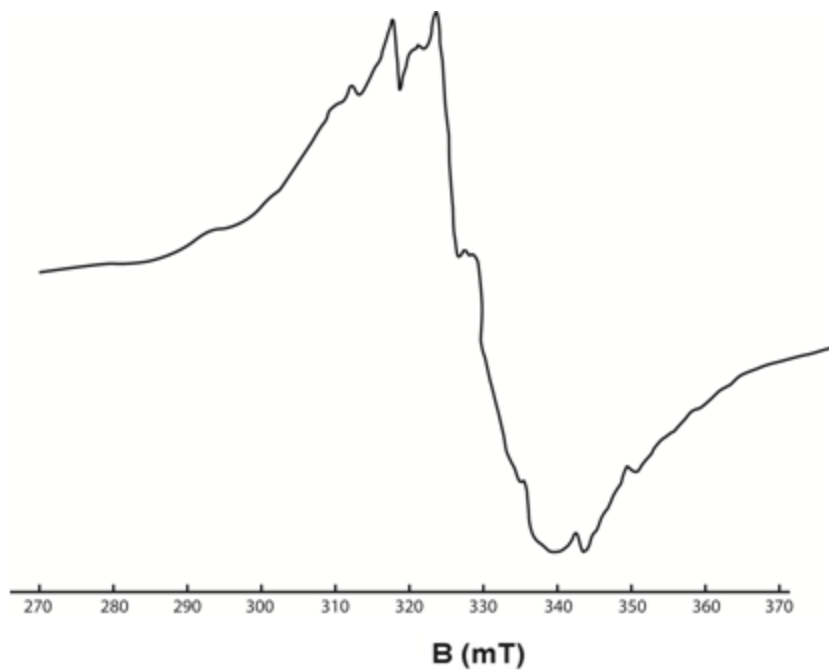


**Fig. 3.8.** EPR spectrum of [VO(bspt)(bipy)] (1) in polycrystalline state at 298 K.

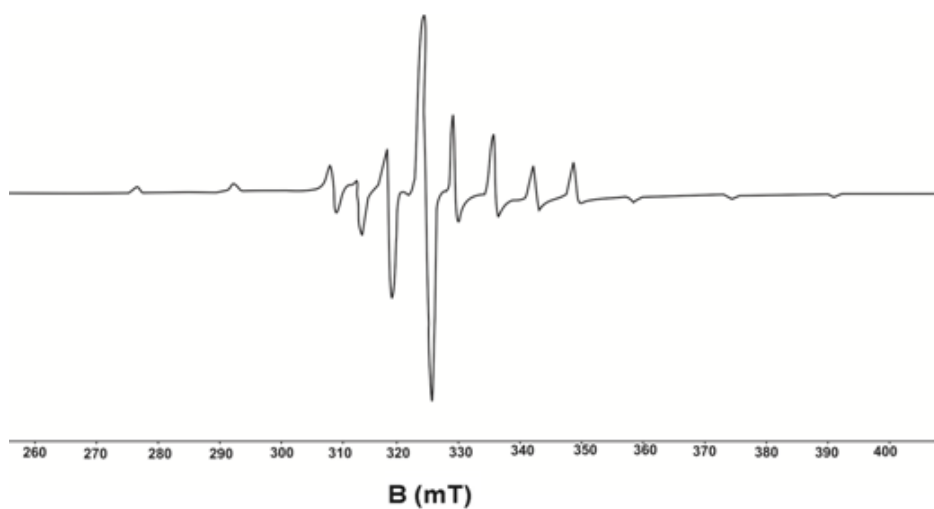


**Fig. 3.9.** EPR spectrum of [VO(bspt)(bipy)] (1) in DMF at 77 K.

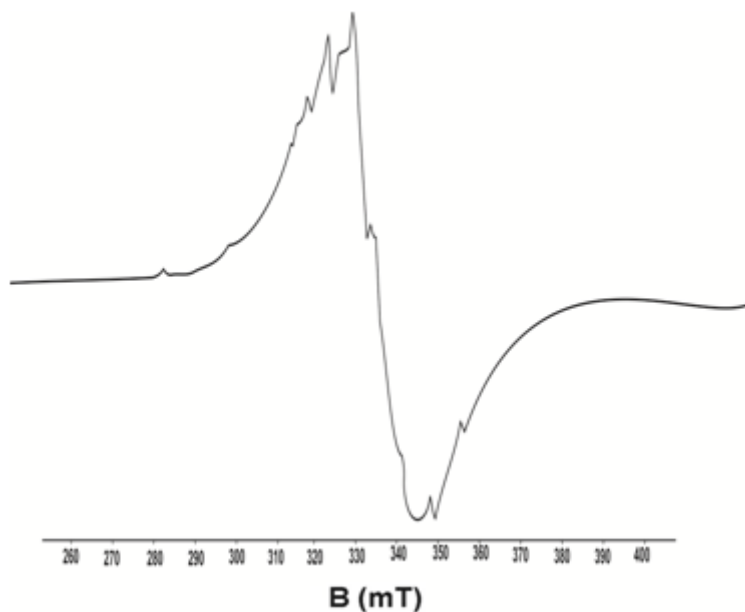


**Fig. 3.10.** EPR spectrum of [VO(bspt)(phen)] (2) in polycrystalline state at 298 K.

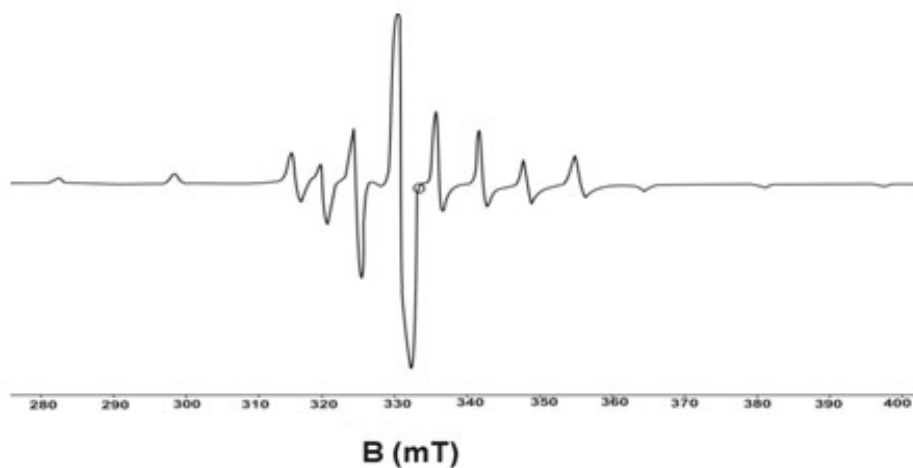


**Fig. 3.11.** EPR spectrum of [VO(bspt)(phen)] (2) in DMF at 77 K.

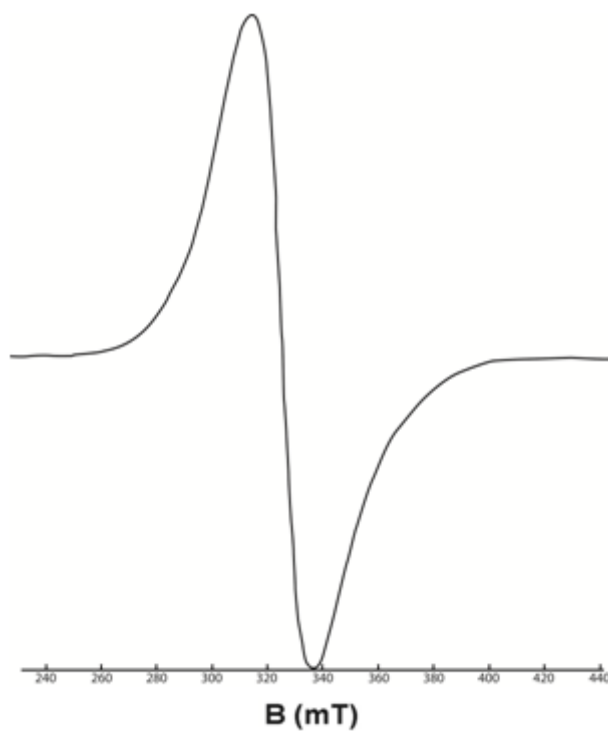


**Fig. 3.12.** EPR spectrum of [VO(bspt)(4,4'-dmbipy)] (3) in polycrystalline state at 298 K.

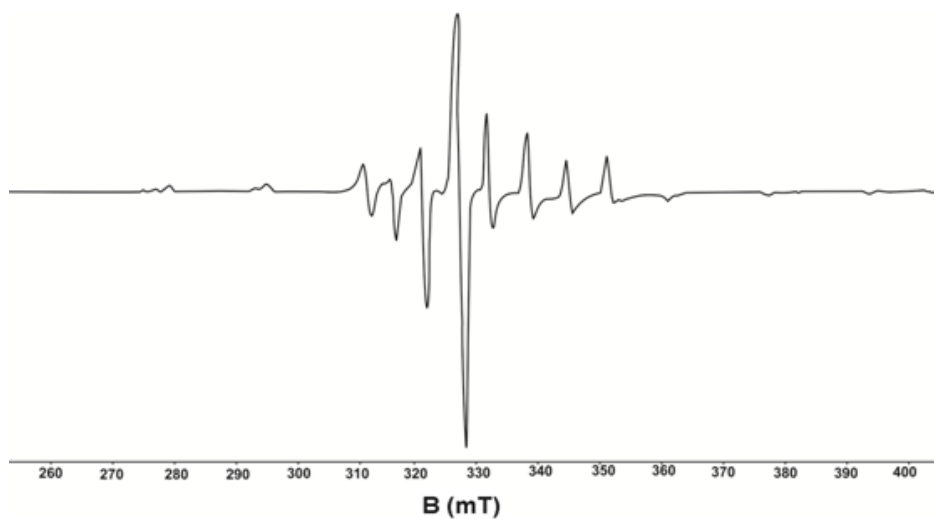


**Fig. 3.13.** EPR spectrum of [VO(bspt)(4,4'-dmbipy)] (3) in DMF at 77 K.

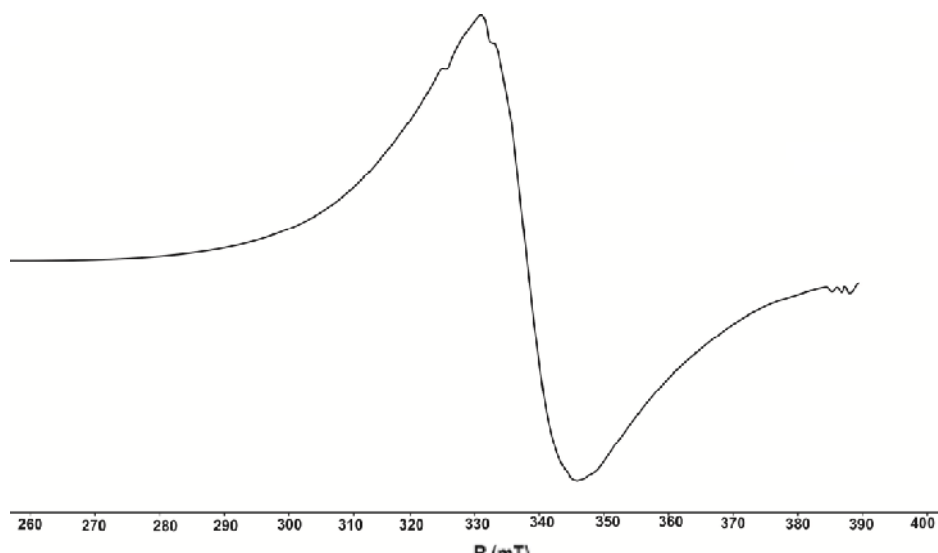


**Fig. 3.14.** EPR spectrum of [VO(bspt)(5,5'-dmbipy)] (4) in polycrystalline state at 298 K.

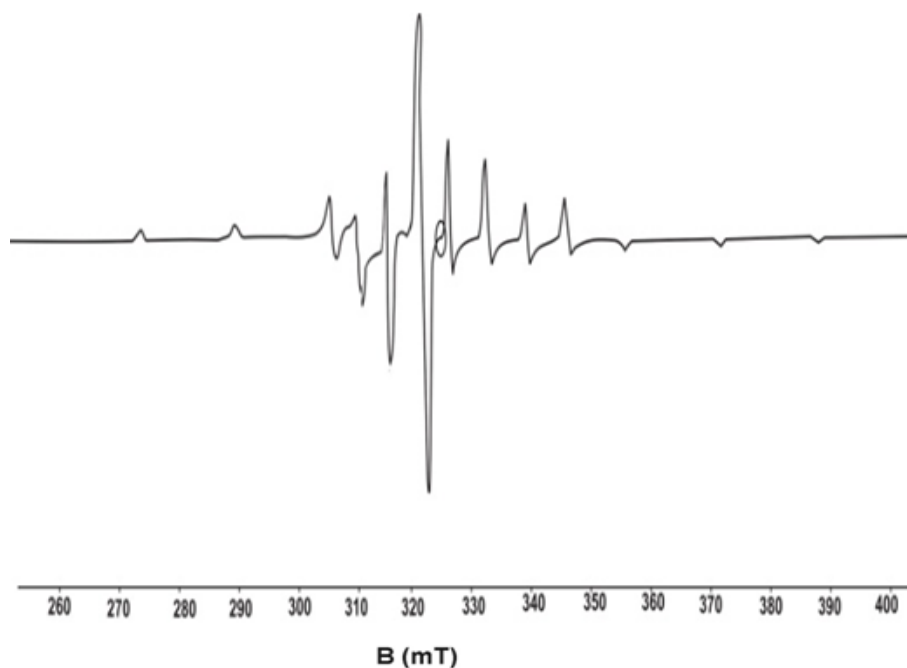


**Fig. 3.15.** EPR spectrum of [VO(bspt)(5,5'-dmbipy)] (4) in DMF at 77 K.

.....*SC*.....





## Chapter 4

# SYNTHESES, SPECTRAL AND STRUCTURAL CHARACTERIZATION OF NICKEL(II) COMPLEXES OF ONS AND NNS DONOR THIOSEMICARBAZONES

<i>Contents</i>	4.1 <i>Introduction</i>
	4.2 <i>Experimental</i>
	4.3 <i>Results and discussion</i>

### 4.1 Introduction

Nickel is a silvery white metal. It is a natural element that is found in the earth's crust (soil and rocks), air and water. Nickel was named in 1751 by a chemist named Cronstedt, but was in use for thousands of years before that year. Because of nickel's slow rate of oxidation at room temperature, it is considered corrosion-resistant. Historically, this has led to its use for plating metals such as iron and brass, coating chemistry equipment, and manufacturing certain alloys that retain a high silvery polish, such as German silver. About 6% of world nickel production is still used for corrosion-resistant pure-nickel plating. Nickel-plated items are noted for provoking nickel allergy. Nickel has been widely used in coins, though its rising price has led to some

replacement with cheaper metals in recent years. Nickel is one of four elements that are ferromagnetic around room temperature. Alnico permanent magnets based partly on nickel are of intermediate strength between iron-based permanent magnets and rare-earth magnets. The metal is chiefly valuable in the modern world for the alloys it forms, about 60% of world production is used in nickel-steels (particularly stainless steel). Other common alloys, as well as some new superalloys, make up most of the remainder of world nickel use, with chemical uses for nickel compounds consuming less than 3% of production [130]. As a compound, nickel has a number of niche chemical manufacturing uses, such as a catalyst for hydrogenation. Enzymes of some microorganisms and plants contain nickel as an active site, which makes the metal an essential nutrient for them. On earth, such native nickel is found in combination with iron, a reflection of those elements' origin as major end products of supernova nucleosynthesis. An iron-nickel mixture is thought to compose earth's inner core [131]. Naturally occurring nickel is composed of five stable isotopes;  $^{58}\text{Ni}$ ,  $^{60}\text{Ni}$ ,  $^{61}\text{Ni}$ ,  $^{62}\text{Ni}$  and  $^{64}\text{Ni}$  with  $^{58}\text{Ni}$  being the most abundant (68.077% natural abundance).  $^{62}\text{Ni}$  has the highest nuclear binding energy of any nuclide. Nickel has 31 total isotopes.

The biological activities of thiosemicarbazone can be modified or enhanced by the linkage to important metal ions such as Fe, Ni, Cu and Zn [132]. For example, nickel complexes of thiosemicarbazone have been shown to possess anti-proliferative activity in a few cancer cell lines [133-135]. Though the versatility binding modes of thiosemicarbazone to nickel ion have been reported, the biological effect of various  $\text{N}^4$ -

substituted groups is unknown. Nickel complexes of thiosemicarbazones were discovered a few decades ago and they are now attracting growing interest because of their pharmacological properties including antiviral, antibacterial, antimalarial [133,136] and anticancer effects [137]. Nickel is the twenty-second most abundant element by weight in the earth's crust. It is predominantly divalent and ionic in simple compounds, and exists as Ni(II) in most of its complexes. Nickel forms four, five and six coordinate complexes *viz*, square planar, tetrahedral, trigonal bipyramidal, square pyramidal and octahedral geometries.

In the 1970s, a specific physiological role for nickel was established when it was found to be a cofactor of the enzyme urease. Today, we have a substantial list of nickel enzymes, which covers a diverse array of chemical reactions and continues to grow. These enzymes are employed by many different organisms that inhabit all sorts of ecosystems around this planet, although a nickel enzyme has yet to be identified in animals. Researchers are interested in the coordination chemistry of nickel complexes as models for the active sites in nickel containing enzymes [138-140]. This is largely due to the discovery of nickel at the centers of many important enzymes [141-143]. There are six nickel enzymes discovered so far, they are: urease, NiFe hydrogenases, methyl coenzyme M reductase [144], carbon monoxide dehydrogenase [145], acetyl coenzyme A synthase [146] and more recently nickel superoxide dismutase (NiSOD) [147,148].

Nickel(II) Schiff base complexes containing sulfur donors have received attention due to identification of a sulfur-rich coordination

environment in biological nickel centres, such as the active sites of certain ureases, methyl-S-coenzyme-M-methyl reductase, and hydrogenases [149]. The known biological activity of nickel includes antiepileptics, anticonvulsant agents, antibacterial, antifungal, antimicrobial, and anticancer/antiproliferative activities. Several reports have described the reactivity of DNA with mononuclear nickel(II) complexes [150]. The chemistry of nickel complexes with multidentate Schiff base ligands has attracted attention because such complexes play an important role in bioinorganic chemistry and redox enzyme systems, and may provide the basis for models of the active sites of biological systems or act as catalysts [151].

## 4.2 Experimental

### 4.2.1 Materials

Nickel(II) acetate tetrahydrate (C.D.H. Chemicals), 1,10-phenanthroline (phen), 2,2'-bipyridine (bipy) and 4,4'-dimethylbipyridine (4,4'-dmbipy) were used as received. Solvents used are methanol and DMF.

### 4.2.2 Syntheses of thiosemicarbazones

The syntheses of thiosemicarbazones H<sub>2</sub>bspt and Hbpet are discussed already in Chapter 2.

### 4.2.3 Syntheses of nickel complexes

#### 4.2.3.1 [Ni<sub>2</sub>(bspt)<sub>2</sub>] (6)

This complex was synthesized by refluxing a solution of H<sub>2</sub>bspt (0.1885 g, 0.5 mmol) in 1:1 mixture of DMF and methanol with a methanolic solution of Ni(OAc)<sub>2</sub>·4H<sub>2</sub>O (0.124 g, 0.5 mmol) for 3 hours.

The complex formed was filtered, washed with methanol and dried *in vacuo*.

Elemental Anal. Found (Calcd.) (%) : C, 57.40 (58.10); H, 3.90 (3.95); N, 9.84 (9.68); S, 7.11 (7.39). Yield 60%.

#### **4.2.3.2 [Ni(bspt)(bipy)]·H<sub>2</sub>O (7)**

To a stirred mixture of H<sub>2</sub>bspt (0.1885 g, 0.5 mmol) in a mixture of DMF and methanol and 2,2'-bipyridine (0.078 g, 0.5 mmol) in methanol, nickel(II) acetate tetrahydrate (0.124 g, 0.5 mmol) was added. The brown solution was refluxed for 3 hours and brown product separated out was filtered, washed with methanol and dried *in vacuo*.

Elemental Anal. Found (Calcd.) (%) : C, 62.70 (62.86); H, 3.90 (4.59); N, 10.96 (11.82); S, 5.88 (5.41). Yield: 67%.

#### **4.2.3.3 [Ni(bspt)(phen)]·H<sub>2</sub>O (8)**

Methanolic solution of nickel(II) acetate tetrahydrate (0.124 g, 0.5 mmol) was added to a stirred mixture of H<sub>2</sub>bspt (0.1885 g, 0.5 mmol) in a mixture of DMF and methanol and the 1,10-phenanthroline (0.090 g, 0.5 mmol) in methanol was added to it. The resultant brown solution was refluxed for 3 hours. The product obtained was filtered, washed with methanol and dried *in vacuo*.

Elemental Anal. Found (Calcd.) (%): C, 64.96 (64.31); H, 3.97 (4.42); N, 10.61 (11.36); S, 5.68 (5.20). Yield: 65%.

#### **4.2.3.4 [Ni(bspt)(4,4'-dmbipy)]·CH<sub>3</sub>OH (9)**

To a stirred mixture of H<sub>2</sub>bspt (0.1885 g, 0.5 mmol) in a mixture of DMF and methanol and 4,4'-dimethylbipyridine (0.0920 g,

0.5 mmol) in methanol, nickel(II) acetate tetrahydrate (0.124 g, 0.5 mmol) was added. The brown solution was refluxed for 3 hours and brown product separated out was filtered, washed with methanol and dried *in vacuo*.

Elemental Anal. Found (Calcd.) (%): C, 61.69 (62.08); H, 4.56 (5.21); N, 11.07 (10.97); S, 4.83 (5.02). Yield: 55%.

#### 4.2.3.5 [Ni(*bpet*)(NCS)] (10)

To a stirred mixture of Hbpet (0.1421 g, 0.5 mmol) in a mixture of DMF and methanol (1:1 v/v) and aqueous solution of KCNS (0.097 g, 0.5 mmol), methanolic solution of nickel(II) acetate tetrahydrate (0.124 g, 0.5 mmol) was added. The resultant brown solution was refluxed for 3 hours and brown crystals separated out were washed with methanol and dried *in vacuo*.

Elemental Anal. Found (Calcd.) (%): C, 48.63 (48.03); H, 4.00 (3.78); N, 16.90 (17.50); S, 15.83 (16.03). Yield: 70%.

#### 4.2.3.6 [Ni(*bpet*)(NCO)] (11)

To a stirred mixture of Hbpet (0.1421 g, 0.5 mmol) in a mixture of DMF and methanol (1:1 v/v) and aqueous solution of sodium cyanate (0.0325 g, 0.5 mmol), methanolic solution of nickel(II) acetate tetrahydrate (0.124 g, 0.5 mmol) was added. The brown solution was refluxed for 3 hours and brown product separated out was filtered, washed with methanol and dried *in vacuo*.

Elemental Anal. Found (Calcd.) (%): C, 49.44 (50.03); H, 3.45 (3.94); N, 18.12 (18.23); S, 7.73 (8.35). Yield: 65%.

### **4.3 Results and discussion**

Six nickel complexes of the thiosemicarbazones were synthesized. The compound **6** is prepared by the reaction of equimolar mixture of the appropriate thiosemicarbazone and nickel acetate tetrahydrate. Complexes **7-9** were synthesized by refluxing metal salt, corresponding heterocyclic bases and thiosemicarbazones in 1:1:1 ratio. Complexes **10** and **11** were synthesized by refluxing metal salt, corresponding anions and thiosemicarbazones. All the complexes are brown in colour and are soluble in solvents like DMF and DMSO. In complexes **6-9**, thiosemicarbazones exist in the thioiminolate form and act as dideprotonated tridentate ligands coordinating through phenolate oxygen, thioiminolate sulfur and azomethine nitrogen. Compound **6** is dimeric in nature while others are monomeric mixed ligand metal chelates. They are characterized by the following physico-chemical methods.

#### **4.3.1 Elemental analyses**

The analytical data are consistent with the general formula  $[(NiL)_2]$  for complex **6** and  $[NiLB]$  for complexes **7-9** where L is the doubly deprotonated thiosemicarbazone ligand and B is the bidentate heterocyclic bases *viz.* phen, bipy and 4,4'-dmbipy. We could isolate single crystals with suitable quality for XRD studies for complex **10**.

#### **4.3.2 Molar conductivity and magnetic susceptibility measurements**

The conductivity measurements of nickel complexes were made in DMF ( $10^{-3}$  M) and it is observed that the values lie in the range 2-9  $\text{ohm}^{-1}\text{cm}^2\text{mol}^{-1}$ , which is well below the range (65-90  $\text{ohm}^{-1}\text{cm}^2\text{mol}^{-1}$ )

for uni-univalent electrolytes in the same solvent, indicating the non-electrolytic nature of the complexes [110]. The molar conductivity values are given in Table 4.1. The magnetic moments of the complexes were calculated from the magnetic susceptibility measurements at room temperature and suggest that the compounds **7-9** have magnetic moment values 2.9, 2.89 and 3.3 B.M. respectively. Normally five coordinate high spin Ni(II) complexes have magnetic moment values in the range of 3.0-3.4 B.M., which are expected for a triplet spin ground state ( $S=1$ ) of such complexes. But in complexes **7** and **8**, the lower values suggest the anomalous magnetic moment of the Ni(II) complexes. This behaviour is due to the quenching of the orbital contribution to the magnetic moment due to the distortion of  $D_{3h}$  symmetry [152]. Four coordinate complexes **6**, **10** and **11** show anomalous magnetic moments of 0.74, 0.24 and 0.79 B.M. respectively which may be due to deviation from a perfect square planar geometry or the presence of impurity [120]. Square planar Ni(II) complexes are diamagnetic but weakly paramagnetic systems with low spin have also been reported [153].

**Table 4.1. Molar conductivity and magnetic moments of Ni(II) complexes**

Compound	$\lambda_m^a$	$\mu_{\text{eff}}$ (B.M.)
[Ni <sub>2</sub> (bspt) <sub>2</sub> ] ( <b>6</b> )	2.9	0.74
[Ni(bspt)(bipy)]·H <sub>2</sub> O ( <b>7</b> )	4.0	2.9
[Ni(bspt)(phen)]·H <sub>2</sub> O ( <b>8</b> )	3.0	2.89
[Ni(bspt)(4,4'-dmbipy)]·CH <sub>3</sub> OH ( <b>9</b> )	4.0	3.3
[Ni(bpet)(NCS)] ( <b>10</b> )	8.9	0.24
[Ni(bpet)(NCO)] ( <b>11</b> )	1.7	0.79

<sup>a</sup> = mho cm<sup>2</sup> mol<sup>-1</sup>



### 4.3.3 X-ray crystallography

Single crystals of compound [Ni(bpet)(NCS)] (**10**) suitable for X-ray diffraction studies were obtained by the slow evaporation of the mother liquor. Single crystals of dimensions 0.30 x 0.25 x 0.20 mm<sup>3</sup> of the complex **10** is selected and mounted on a Bruker SMART APEXII CCD diffractometer, equipped with a graphite crystal, incident-beam monochromator and a fine focus sealed tube with Mo K $\alpha$  ( $\lambda = 0.71073 \text{ \AA}$ ) radiation as the X-ray source. The crystallographic data and structure refinement parameters for compound **10** are given in Table 4.2. The unit cell dimensions were measured and the data collection was performed at 296 (2) K. Bruker SMART software was used for data acquisition and Bruker SAINT software for data integration [62]. Absorption corrections were carried out using SADABS based on Laue symmetry using equivalent reflections [63]. The structure was solved by direct methods using SHELXS97 [64] and refined by full-matrix least-squares calculations with SHELXL97 software package [65]. The molecular and crystal structures were plotted using DIAMOND version 3.2g [66]. In [Ni(bpet)(NCS)] (**10**), all non-hydrogen atoms were refined anisotropically and all H atoms on C were placed in calculated positions, guided by difference Fourier maps, with C–H bond distances 0.93–0.96  $\text{\AA}$ . H atoms were assigned as  $U_{\text{iso}}=1.2U_{\text{eq}}$  (1.5 for Me). The N4–H4' H atom was located from difference maps and its distance is restrained to  $0.88 \pm 0.01 \text{ \AA}$ .

**Table 4.2. Crystal data and structure refinement parameters for complex 10**

Parameters	[Ni(bpet)(NCS)] (10)
Empirical formula	C <sub>16</sub> H <sub>15</sub> N <sub>5</sub> NiS <sub>2</sub>
Formula weight	400.16
Color	Brown
Temperature (T) K	296(2)
Wavelength (Mo K $\alpha$ ) (Å)	0.71073
Crystal system	Monoclinic
Space group	<i>P</i> 2 <sub>1</sub> / <i>n</i>
Cell parameters	
a	14.0577(9) Å
b	9.7437(4) Å
c	14.0665(8) Å
$\alpha$	90°
$\beta$	113.869(3)°
$\gamma$	90°
Volume V (Å <sup>3</sup> )	1761.96(17)
Z	4
Calculated density ( $\rho$ ) (Mg m <sup>-3</sup> )	1.509
Absorption coefficient, $\mu$ (mm <sup>-1</sup> )	1.345
F(000)	824
Crystal size (mm <sup>3</sup> )	0.30 x 0.25 x 0.20
$\theta$ range for data collection	2.62 to 28.34°
Limiting indices	-18 ≤ h ≤ 17, -12 ≤ k ≤ 12, -18 ≤ l ≤ 18
Reflections collected	13919
Unique Reflections (R <sub>int</sub> )	4338 [R(int) = 0.0579]
Completeness to $\theta$	28.34 (99.1%)
Absorption correction	Semi-empirical from equivalents
Maximum and minimum transmission	0.764 and 0.675
Refinement method	Full-matrix least-squares on F <sup>2</sup>
Data / restraints / parameters	4338 / 1 / 222
Goodness-of-fit on F <sup>2</sup>	1.021
Final R indices [I > 2 $\sigma$ (I)]	R <sub>1</sub> = 0.0343, wR <sub>2</sub> = 0.0788
R indices (all data)	R <sub>1</sub> = 0.0640, wR <sub>2</sub> = 0.0922
Largest difference peak and hole (e <sup>4</sup> Å <sup>-3</sup> )	0.309 and -0.292

#### 4.3.3.1 Crystal structure of [Ni(bpet)(NCS)] (10)

The compound crystallized in a monoclinic space group,  $P2_1/n$ . The molecular structure of complex **10** is shown in Fig. 4.1. Selected bond lengths and bond angles are given in Table 4.3. The nickel(II) atom has square-planar geometry surrounded by one sulfur atom and three nitrogen atoms. The uncomplexed thiosemicarbazone Hbpet shows *E* configuration about N(3)–C(13) bond. The organic molecule acts as a terdentate ligand with the NNS donor set placed on the same side. The third nitrogen atom is provided by the isothiocyanate anion. Coordination of the thiosemicarbazone results in the formation of two five-membered (NiSCNN and NiNCCN) chelate rings, all of them are planar within experimental error. A careful examination of bond length data shows that the Ni–N bonds involving the iminic and isothiocyanate nitrogens {1.8437(18) and 1.843(2) Å} are somewhat shorter than that involving the pyridine nitrogen {1.9030(19) Å}. This suggests that nickel(II) is small enough to perfectly fit in the ligand cavity and to bond effectively, by which the pyridine ring is required to flex inward towards the metal ion [154,155]. This results in a small distortion to the ligand structure easily quantified by a consideration of the bite angles N(1)–Ni–N(2) 84.07(8)°, N(1)–Ni–N(5) 95.64(9)°, N(2)–Ni–S(1) 86.99(6)°, and N(5)–Ni–S(1) 93.45(7)°. The Ni–S bond (2.137 Å) is comparable with those reported for other thiosemicarbazone nickel complexes [156,157] with strong coordination, attributable to the high basicity of the ligand.

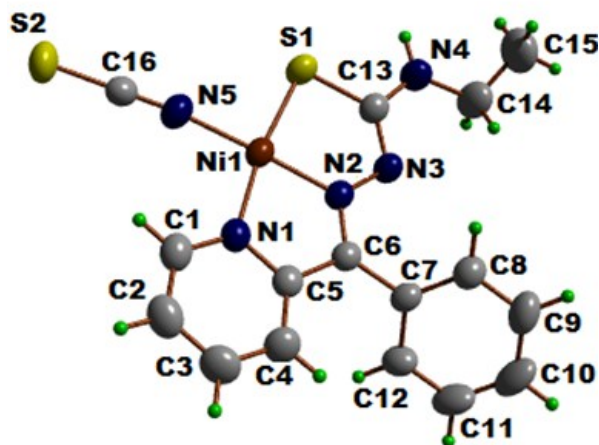


Fig. 4.1. Molecular structure of [Ni(bpet)(NCS)].

The environment around the Ni(II) ion is distorted square planar which is evident from the bond angles given in Table 4.3. The geometry index for four-coordinate complexes,  $\tau_4 = \frac{360^\circ - (\alpha + \beta)}{141^\circ}$  is found to be 0.084. The values of  $\tau_4$  will range from 1.00 for a perfect tetrahedral geometry to zero for a perfect square planar geometry [158]. The loss of the proton originally bound to N(3) produces a negative charge, which is delocalized on the N2–N3–C13 system, consistent with the bond distance C13–S1, 1.740 (2) Å compared to the normal C–S double bond (1.6 Å) in the range of single-bond character. The bond distances C(6)–N(2) 1.310(3) and N(3)–C(13) 1.314(3) Å, are intermediate between formal single and double bonds [159-161,23].

**Table 4.3. Bond lengths and bond angles of complex 10**

Bond lengths		Bond angles	
Ni(1)–N(5)	1.843(2)	N(5)–Ni(1)–N(2)	176.46(9)
Ni(1)–N(2)	1.8437(18)	N(5)–Ni(1)–N(1)	95.64(9)
Ni(1)–N(1)	1.9030(19)	N(2)–Ni(1)–N(1)	84.07(8)
Ni(1)–S(1)	2.1364(7)	N(5)–Ni(1)–S(1)	93.45(7)
S(1)–C(13)	1.740(2)	N(2)–Ni(1)–S(1)	86.99(6)
S(2)–C(16)	1.608(3)	N(1)–Ni(1)–S(1)	170.68(6)
N(3)–C(13)	1.314(3)		
N(2)–C(6)	1.310(3)		
N(2)–N(3)	1.363(3)		

The thiolate formation is also supported by the decrease in bond length of N3–C13, 1.314 Å from the normal N–C bond length, 1.47 Å. This substantiates the displacement of the tautomeric equilibrium to the thioiminol form. The ambidentate nature of SCN<sup>-</sup> may be interpreted in terms of sulfur being a “soft” base and nitrogen being a “hard” base [162,163]. When the thiocyanate ion is the only ligand present in a complex, its mode of bonding generally follows the hard (M–NCS) or soft (M–SCN) pattern throughout the periodic table. However, the nature of other ligands in a complex may determine whether the metal functions as a hard ion, and forms isothiocyanato complexes, or as a soft ion, and forms thiocyanato complexes. Steric factors in bulky ligands also may alter the nature of thiocyanate coordination [164]. Turco and Pecile [165] noted that the presence of other ligands in a complex apparently influenced whether the thiocyanate ion was N or S

bonded. They suggested that phosphines, arsines, and similar donor atoms withdraw electron density from the metal through  $d\pi-d\pi$  ( $M \rightarrow L$ ) back-bonding, thereby reducing the relative tendency for the sulfur atom of  $SCN^-$  to participate in  $\pi$  bonding. As a consequence, when a  $SCN^-$  group is coordinated to a metal, along with strong  $\pi$ -acceptor ligands, it may be expected to bond preferentially *via* the nitrogen atom.

The distances N(5)–C(16) 1.156(3) and C(16)–S(2) 1.608(3) Å in the thiocyanate group are in the double bond range in agreement with N-coordination of the isothiocyanate group. Single crystal XRD studies shows that nickel(II) complex exhibits distorted square planar arrangement consists of one nickel atom (Ni1), coordinated by nitrogen (N5) of terminal thiocyanate group, sulfur atom (S1) and two nitrogen atoms (N1, N2) from the principal ligand (Fig. 4.1). In the crystal packing three molecules are linked through hydrogen bonding i.e. two molecules are bridged by a third one (Fig. 4.2). Further, crystal packing is reinforced by very weak  $\pi \cdots \pi$  and metal  $\cdots \pi$  interactions (Fig. 4.3). Fig. 4.4 shows the packing diagram of the compound. The various interaction parameters are shown in Table 4.4.

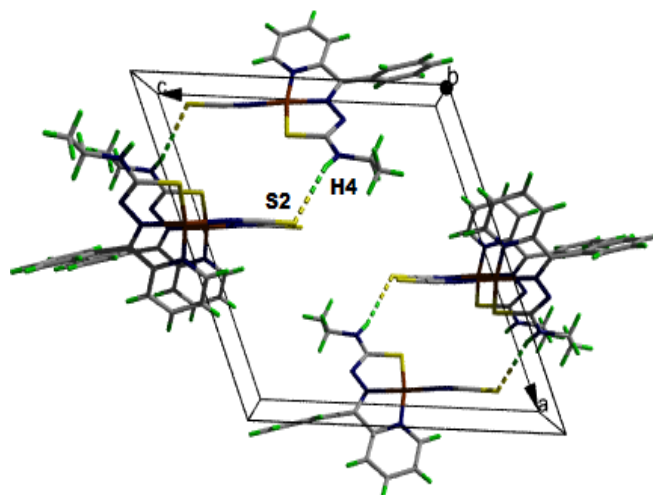


Fig. 4.2. Hydrogen bonding of [Ni(bpet)(NCS)].

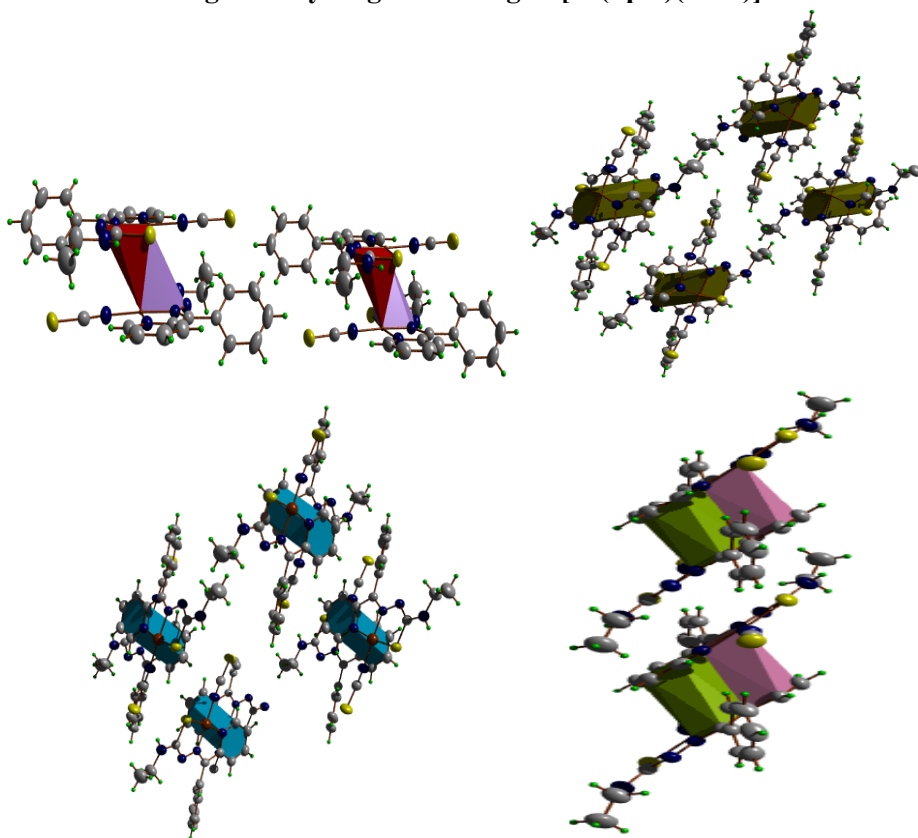


Fig. 4.3. Metal... $\pi$  and  $\pi$ ... $\pi$  interactions in the compound 10.

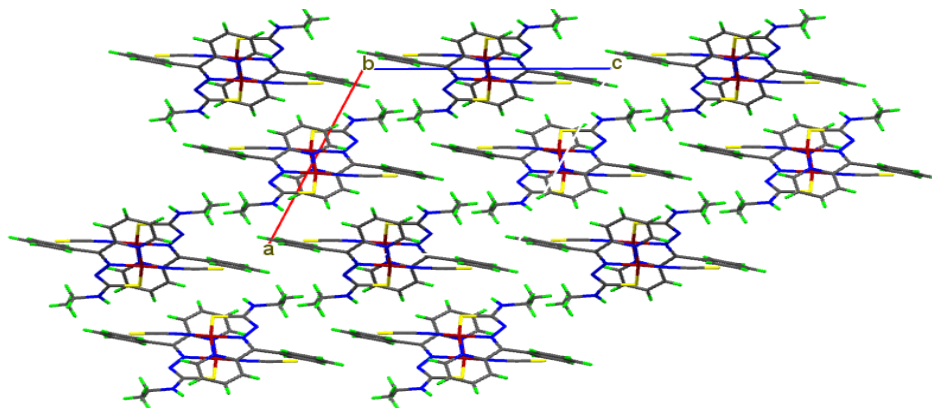


Fig. 4.4. Packing diagram viewed along 'b' axis

Table 4.4. Interaction parameters

H-bonding				
D-H...A	D-H (Å)	H...A (Å)	D...A (Å)	D-H...A (°)
N(4)-H(4')...S(2) <sup>a</sup>	0.867(10)	2.695(13)	3.522(2)	160(2)
$\pi \cdots \pi$ interactions				
Cg(I)...Cg(J)	Cg...Cg (Å)	$\alpha$ (°)	$\beta$ (°)	$\gamma$ (°)
Cg(1)...Cg(1) <sup>b</sup>	3.9992(12)	0	33.94	33.94
Cg(2)...Cg(3) <sup>c</sup>	3.9539(13)	3.66(12)	32.68	31.28
Cg(3)...Cg(2) <sup>c</sup>	3.9539(13)	3.66(12)	31.28	32.68
Cg(3)...Cg(3) <sup>c</sup>	3.6055(16)	0	22.72	22.72
Metal... $\pi$ interaction				
Cg(I)...Me(J)	Cg...Me (Å)	$\beta$ (°)		
Cg(1)...Ni(1) <sup>d</sup>	3.9992(12)	16.22		

Equivalent position codes :  $a = -x + \frac{3}{2}, y - \frac{1}{2}, -z + \frac{1}{2}$ ,  $b = \frac{5}{2} + x, \frac{1}{2} - y, \frac{3}{2} + z$ ,

$c = 2 - x, 1 - y, 1 - z$ ,  $d = 2 - x, -y, 1 - z$

Cg(1) = Ni(1), S(1), C(13), N(3), N(2);

Cg(2) = Ni(1), N(1), C(5), C(6), N(2); Cg(3) = N(1), C(1), C(2), C(3), C(4), C(5);

D = Donor, A = acceptor, Cg = Centroid

$\alpha$  = dihedral angle between planes I and J

$\beta$  = angle between Cg(I)...Cg(J) vector and Cg(J) perp

$\gamma$  = angle between Cg(I)...Cg(J) vector and Cg(I) perp



#### **4.3.4 Infrared spectra**

The characteristic IR bands (4000-400  $\text{cm}^{-1}$ ) of the Ni(II) complexes provide significant information regarding the bonding sites of the ligands. A comparison of the IR spectra of thiosemicarbazones and the Ni(II) complexes shows that significant variations have occurred in the characteristic frequencies upon complexation. The tentative IR spectral assignments of the thiosemicarbazones and Ni(II) complexes are listed in Table 4.5. In complexes **6-9**, the bands due to O-H and  $^2\text{N-H}$  stretching vibrations are absent which is a clear evidence for the coordination of the thiosemicarbazones in the dideprotonated form. The azomethine stretching vibrations are observed at 1600  $\text{cm}^{-1}$  in the thiosemicarbazones. However, in complexes these bands are shifted to lower wave numbers due to the combination of  $\nu(\text{C=N})$  with the newly formed C=N bond which results from the loss of the thioamide hydrogen from the thiosemicarbazone moiety [113-116,90]. It is learnt that the iminolization is thermodynamically most favored due to the additional stability conferred on the resulting complex upon complexation. Further proof for the coordination of azomethine nitrogen to nickel is the appearance of new bands in the range 429-445  $\text{cm}^{-1}$  assignable to  $\nu(\text{Ni-N})$  for the complexes [166-168]. The iminolization and the electron delocalization in the thiosemicarbazone moiety are supported by the increase in the stretching frequency of the N-N bond of the principal ligand [118]. The bands at 1330 and 1340  $\text{cm}^{-1}$  present in the thiosemicarbazones shift to lower wavenumbers in all the complexes and this can be assigned to the  $\nu(\text{C-S})$  vibration suggesting the change of bond order and strong electron delocalization upon chelation. This

shows that the H–N–C=S in the ligands has transformed to N=C–S–H thereby coordinating to nickel in the thioiminolate form. Coordination *via* thioiminolate sulfur is also indicated by the negative shift of the band assigned to  $\delta(\text{C}=\text{S})$  vibration in the ligands [169]. The broad band at  $3366\text{ cm}^{-1}$  is assigned to phenolic –OH of  $\text{H}_2\text{bspt}$  have disappeared in the complexes which indicates the coordination of the phenolic oxygen to the nickel atom [170]. The coordination of the heterocyclic bases to nickel is indicated by the presence of characteristic peaks of 1,10-phenanthroline, 2,2'-bipyridine and 5,5'-dimethyl-2,2'-bipyridine in the finger print region of  $600\text{--}1400\text{ cm}^{-1}$  in the complexes [171]. The SNNN mode of coordination is ascertained from the red shift of the  $\nu(\text{C}=\text{N})$  and pyridine (ring deformation out of plane and ring deformation in plane) vibrations and by the presence of a new band at  $2108\text{ cm}^{-1}$  indicating N-coordination of the thiocyanate group [172]. Fig. 4.5 depicts the infrared spectra of some of the nickel complexes of thiosemicarbazones.

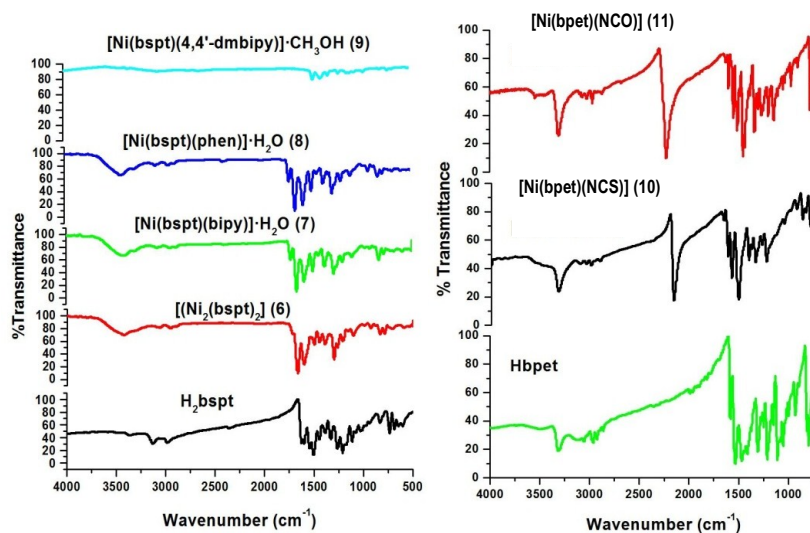


Fig. 4.5. Infrared spectra of some of the nickel (II) complexes.

It is observed that in all the complexes except **10** and **11**, the thiosemicarbazones act as dianionic tridentate ligands coordinating to nickel through O, N and S atoms. In the case of mixed ligand nickel chelates, the two nitrogen atoms of heterocyclic bases occupy the fourth and fifth coordination positions of nickel.

**Table 4.5. IR spectral assignments (cm<sup>-1</sup>) of thiosemicarbazones and their Ni(II) complexes**

Compound	$\nu(\text{O-H})$	$\nu(\text{C=N})$	$\nu(\text{C=N})^a$	$\nu(\text{N-N})$	$\nu(\text{C=S})/\nu(\text{C-S}),$ $\delta(\text{C=S})/\delta(\text{C-S})$	$\nu(\text{C-O})$	$\nu(\text{Ni-O})$	$\nu(\text{Ni-N})$	Bands due to heterocyclic base
H <sub>2</sub> bspt	3366	1625	----	1112	1330, 832	1261	----	----	----
[Ni <sub>2</sub> (bspt) <sub>2</sub> ] ( <b>6</b> )	----	1597	1522	1123	1313,839	1218	496	421	----
[Ni(bspt)bipy]·H <sub>2</sub> O ( <b>7</b> )	----	1597	1522	1123	1319,825	1211	496	438	1434,689
[Ni(bspt)phen]·H <sub>2</sub> O ( <b>8</b> )	----	1597	1516	1130	1313,825	1218	499	435	1428,737
[Ni(bspt) (4,4'-dmbipy)]·CH <sub>3</sub> OH ( <b>9</b> )	----	1602	1517	1162	1309,882	1201	515	435	1425,731

<sup>a</sup> = newly formed C=N bond

Compound	$\nu(\text{C=N})$	$\nu(\text{C=N})^a$	$\nu(\text{N-N})$	$\nu(\text{C=S})/\nu(\text{C-S}),$ $\delta(\text{C=S})/\delta(\text{C-S})$	$\nu(\text{CN})$	$\nu(\text{CS})/\nu(\text{CO})$	$\nu(\text{Ni-N})$	$\delta(\text{NCS})/\delta(\text{NCO})$
Hbpet	1583	----	1107	1340,814	----	----	----	----
[Ni(bpet)(NCS)] ( <b>10</b> )	1593	1545	1142	1329,836	2108	831	424	465
[Ni(bpet)(NCO)] ( <b>11</b> )	1599	1549	1145	1337,821	2218	1625	423	636

<sup>a</sup> = newly formed C=N bond

### 4.3.5 Electronic spectra

The electronic spectra give much insight into the coordination geometry around metal ion. The electronic spectra of all the Ni(II) complexes were taken in DMF. The electronic transitions found in thiosemicarbazones due to imine function were slightly shifted on complexation. The shift of the bands due to intraligand transitions is the result of the weakening of the C=S bond and the extension of conjugation upon complexation [121]. The shift occurs also due to coordination *via* phenolic oxygen and azomethine nitrogen [122] and is an indication of the iminolization followed by the deprotonation of the ligands during complexation. The intraligand  $n \rightarrow \pi^*$  and  $\pi \rightarrow \pi^*$  transitions are assigned to bands in the range 23500-30100  $\text{cm}^{-1}$  for the nickel complexes of H<sub>2</sub>bspt and 25060-32200  $\text{cm}^{-1}$  for the nickel complexes of Hbpet. In all the complexes, intense bands in the 24880-24250  $\text{cm}^{-1}$  range are assigned to ligand to metal charge transfer transitions and the broadness of these bands can be explained as due to the combination of  $\text{O} \rightarrow \text{Ni}^{\text{II}}$  and  $\text{S} \rightarrow \text{Ni}^{\text{II}}$  LMCT transitions [173,174]. Fig. 4.6 represents the electronic spectra of the Ni(II) complexes. The electronic spectral data of the thiosemicarbazones and their Ni(II) complexes are given in Table 4.6.

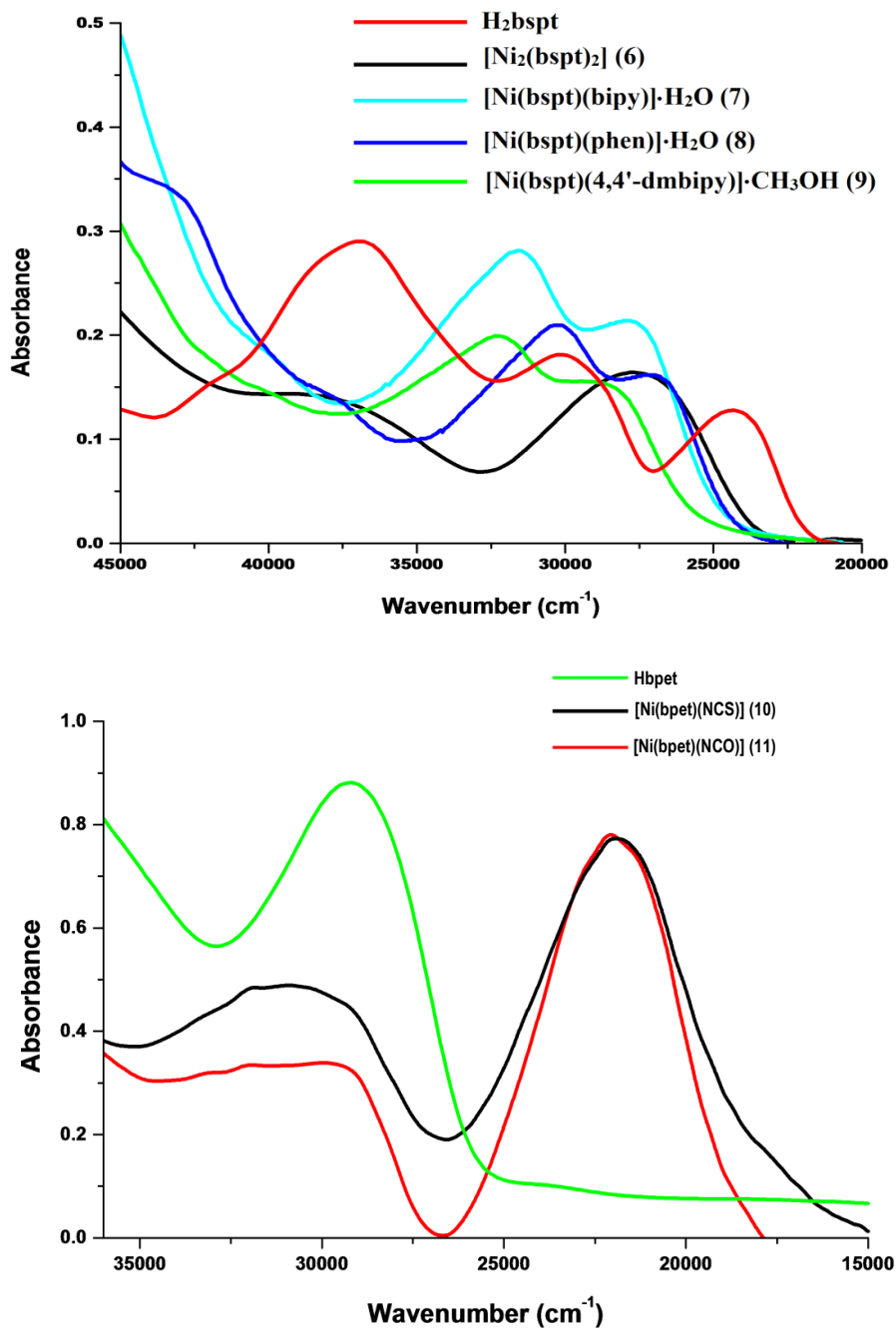


Fig. 4.6. Electronic spectra of nickel complexes.

For a diamagnetic Ni(II) complex, as a consequence of eight electrons being paired in the four low-lying  $d$  orbitals with the upper orbital being  $d_{x^2-y^2}$ , the four lower orbitals are often so close in energy that individual transitions from them to the upper  $d$  level cannot be distinguished, resulting in a single absorption band. The broad band at  $14020\text{ cm}^{-1}$  for  $[\text{Ni}_2(\text{bspt})_2]$  (**6**) may be attributed to  $d-d$  band of this type. However we could not locate any  $d-d$  bands for the other complexes, probably due to masking by the high intensity charge transfer bands. Visible spectrum of  $[\text{Ni}_2(\text{bspt})_2]$  (**6**) is shown in Fig. 4.7.

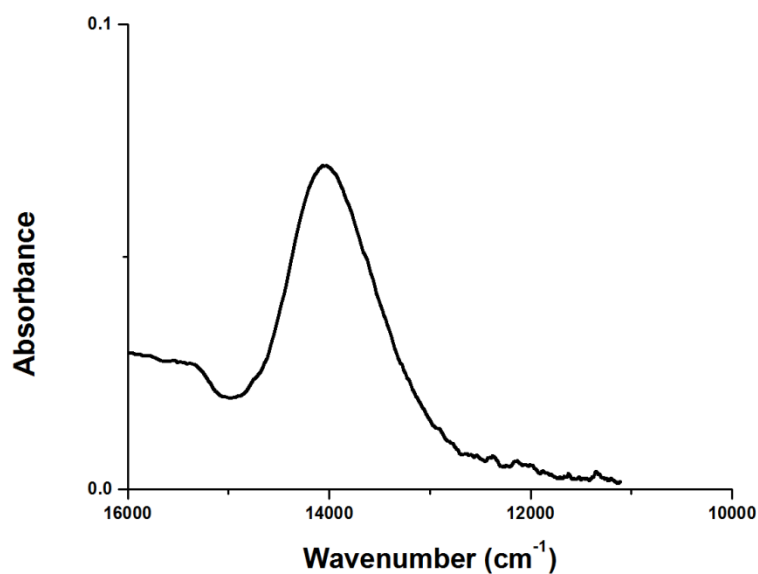


Fig. 4.7. Visible spectrum of  $[\text{Ni}_2(\text{bspt})_2]$  (**6**).

**Table 4.6. Electronic spectral assignments (cm<sup>-1</sup>) of thiosemicarbazones and their Ni(II) complexes**

Compound	n→π*/π→π*	LMCT	d-d
H <sub>2</sub> bspt	24230, 30110	----	----
[Ni <sub>2</sub> (bspt) <sub>2</sub> ] ( <b>6</b> )	26690, 31760	24490	14020
[Ni(bspt)(bipy)]·H <sub>2</sub> O ( <b>7</b> )	26520, 30150	24270	----
[Ni(bspt)(phen)]·H <sub>2</sub> O ( <b>8</b> )	26620, 31810	24360	----
[Nibspt(4,4'-dmbipy)]·CH <sub>3</sub> OH ( <b>9</b> )	26690, 31440	24250	
Hbpet	23500, 30800	----	----
[(Ni(bpet)(NCS)] ( <b>10</b> )	29970, 32220	24880	----
[(Ni(bpet)(NCO)] ( <b>11</b> )	25060, 30550	24530	----

#### 4.3.6 Thermogravimetric studies

Thermal analyses provide valuable information regarding the thermal stability and nature of water molecules in complexes. It helps us to distinguish the lattice water molecules and coordinated water molecules present in the compound. Reports show that the weight losses for lattice water are below 200 °C and due to coordinated water are in the range of 200-350 °C [175,176]. In complexes **7** and **8** there are weight losses in the region 100-180 °C indicating the presence of lattice water molecules. For the complex [Ni(bspt)(4,4'-dmbipy)]·CH<sub>3</sub>OH (**9**), a weight loss of 4.34% is observed due to the loss of a molecule of methanol in the temperature range 200-250 °C (calc. 4.91%). Fig. 4.8 shows the TG-DTG plot of complexes **7**, **8** and **9**.

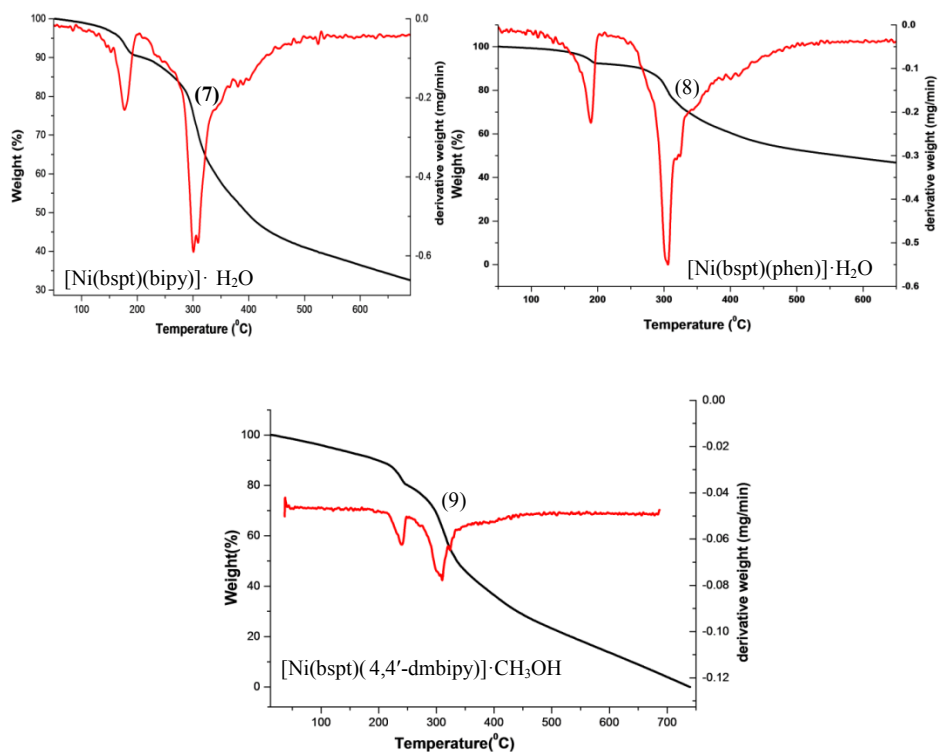


Fig. 4.8. TG-DTG plot of complexes 7, 8 & 9.

.....



# Chapter 5

## SYNTHESES, SPECTRAL AND STRUCTURAL CHARACTERIZATION OF COPPER(II) COMPLEXES OF ONS AND NNS DONOR THIOSEMICARBAZONES

<i>Contents</i>	5.1 <i>Introduction</i>
	5.2 <i>Experimental</i>
	5.3 <i>Results and discussion</i>

### 5.1 Introduction

Copper occupies the same family of the periodic table as silver and gold, since they each have one s-orbital electron on top of a filled electron shell which forms metallic bonds. This similarity in electron structure makes them similar in many characteristics. All of them have very high thermal and electrical conductivity, and all are malleable metals. Among pure metals at room temperature, copper has the second highest electrical and thermal conductivity, after silver.

The use of copper dates back far into history. Copper beads have been found in what is now modern Iraq, dating back to 9000 BC. The metal is relatively easy to mine and refine, contributing to its early and widespread use. Being soft, however, it is unsuitable for making reliable

tools and weapons. Early metal smiths as far back as 3000 BC learned to combine copper with other metals to produce more durable alloys. Brass (copper and zinc) and bronze (copper and tin) are two examples. The symbol and name for copper are from the Latin *cuprum*, which literally means "from the island of Cyprus", an early source of copper ore.

Copper forms a rich variety of coordination complexes with oxidation states Cu(II) and Cu(I), and very few examples of copper(III) compounds are reported [177]. The coordination chemistry of copper is dominated by Cu(II) derivatives with little but important examples of Cu(I) compounds. Since copper (I/II) complexes are (i) redox active, (ii) frequently labile, and (iii) typical in their preference for distorted coordination geometries, they are much less structurally predictable than other first-row transition metal complexes. Copper(I) strongly prefers ligands having soft donor atoms such as P, C, thioether S, and aromatic amines. Although two-coordinated linear and three-coordinated trigonal arrangements are known, Cu(I) complexes are mostly four-coordinated species adopting a tetrahedral geometry. In Cu(II) complexes the coordination number varies from four to six, including four-coordinate square-planar, five-coordinate trigonal bipyramidal, and six-coordinate octahedral geometries. The variety of accessible arrays allows for a great assortment in the choice of the ligands (from mono- to hexadentate chelates) and of the donor atoms (N, O, S, and halides) [178].

Thiosemicarbazones and their metal compounds exhibit a number of relevant biological properties. The studies developed during the last 30 years have yielded several conclusions. The biologically

active thiosemicarbazone compounds are planar and contain a pyridine ring or derivatives giving rise to NNS tridentate systems [179]. These ligands coordinate to metal ions inside the cell, forming complexes which supposedly act as the true active species. In this sense the behavior of the ligands can be modified by the linkage to metallic ions such as Cu(II) and Fe(II) enhancing their biological activity [180,181] as was found for other thiosemicarbazone complexes [182]. Copper bis(thiosemicarbazone) complexes have attracted more attention, because many of them displayed promising anticancer activity [183-189]. The mono (thiosemicarbazone) complexes of copper containing 1 or 2 equivalent of the ligand are well understood, and they manifest cytotoxicity mainly through ROS generation.

Copper(II) is a biologically active, essential ion; its chelating ability and positive redox potential allow participation in biological transport reactions [190]. Also, copper(II) forms the active centers of more than a dozen metalloproteins [191-196]. Further, copper complexes possess a wide range of biological activity and are among the most potent antiviral, antitumor and antiinflammatory agents. For example, a copper(II) complex of 2-formylpyridine thiosemicarbazone has been shown to inhibit the RNA-dependent DNA polymerases and the transforming ability of Rous sarcoma virus (RSV) [197]. In addition, copper complexes of 2-acetylpyridine thiosemicarbazones are active antimalarial agents [136]. They possess strong antineoplastic activity against a number of transplantable tumors, spontaneous murine tumors [198] and human tumors [199]. The mechanism of their antitumor action

is considered to involve either inhibition of the enzyme, ribonucleotide reductase, an obligatory enzyme in DNA synthesis [200-202] or creation of lesions in DNA strands [203]. Synthetically prepared copper(II) complexes have been successful in treating inflammatory diseases such as rheumatoid arthritis [204-206]. These biological activities have provided an impetus to the study of transition metal ion complexes of thiosemicarbazones in general, and have prompted us to update [207-209,115,181] the structural activity correlations of their copper(II) complexes. Liebermeister [210] demonstrated that the presence of copper ions enhances the antitubercular activity of p-acetamidobenzaldehyde thiosemicarbazone.

## 5.2 Experimental

### 5.2.1 Materials

Copper(II) acetate monohydrate (E-Merck), 1,10-phenanthroline (phen), 2,2'-bipyridine (bipy), 4,4'-dimethyl-2,2'-bipyridine (4,4'-dmbipy) and 5,5'-dimethyl-2,2'-bipyridine (5,5'-dmbipy) were used as received.

### 5.2.2 Syntheses of the thiosemicarbazones and complexes

The syntheses of thiosemicarbazones H<sub>2</sub>bspt, Hbpet and H<sub>2</sub>brset are discussed already in Chapter 2. All chemicals used for synthesis were reagent grade. The ligand Hbpet was formed *in situ* in the presence of metal salt. **Caution:** Azide compounds are potentially explosive and should be prepared only in small quantities and handled with care.

## **5.2.3 Syntheses of copper complexes**

### **5.2.3.1 [Cu<sub>2</sub>(bspt)<sub>2</sub>] (12)**

This complex was synthesized by refluxing a solution of H<sub>2</sub>bspt (0.188 g, 0.5 mmol) in a 1:1 mixture of DMF and methanol with a methanolic solution of Cu(OAc)<sub>2</sub>·H<sub>2</sub>O (0.099 g, 0.5 mmol) for 3 hours. The complex formed was filtered, washed with methanol and dried *in vacuo*. Elemental Anal. Found (Calcd.) (%) : C, 57.00 (57.46); H, 3.32 (3.90); N, 9.18 (9.57); S, 7.40 (7.30). Yield: 82%.

### **5.2.3.2 [Cu(bspt)(phen)] (13)**

Methanolic solution of copper(II) acetate monohydrate (0.099 g, 0.5 mmol) was added to a stirred mixture of H<sub>2</sub>bspt (0.188 g, 0.5 mmol) in DMF and methanol and 1, 10-phenanthroline (0.090 g, 0.5 mmol) in methanol. The resultant green solution was refluxed for 3 hours. The green product obtained was filtered, washed with methanol and dried *in vacuo*. Elemental Anal. Found (Calcd.) (%) : C, 63.76 (63.80); H, 4.54 (4.38); N, 11.80 (11.27); S, 5.30 (5.16). Yield: 78%.

### **5.2.3.3 [Cu(bspt)(bipy)] (14)**

To a stirred mixture of H<sub>2</sub>bspt (0.188 g, 0.5 mmol) in DMF and methanol and 2,2'-bipyridine (0.078 g, 0.5 mmol) in methanol, copper(II) acetate monohydrate (0.099 g, 0.5 mmol) was added. The green solution was refluxed for 3 hours and green product separated out was filtered, washed with methanol and dried *in vacuo*. Elemental Anal. Found (Calcd.) (%) : C, 62.90 (62.35); H, 5.14 (4.56); N, 11.16 (11.13); S, 5.09 (5.37). Yield: 80%.

#### 5.2.3.4 [Cu(bspt)(4,4'-dmbipy)] (15)

To a stirred mixture of H<sub>2</sub>bspt (0.188 g, 0.5 mmol) and 4,4'-dimethyl-2,2'-bipyridine (0.092 g, 0.5 mmol) in methanol, copper(II) acetate monohydrate (0.099 g, 0.5 mmol) was added. The solution was refluxed for 3 hours and green product separated out was filtered, washed with methanol and dried *in vacuo*.

Elemental Anal. Found (Calcd.) (%): C, 62.03 (61.81); H, 5.15 (4.87); N, 10.86 (10.92); S, 5.03 (5.00). Yield: 74%.

#### 5.2.3.5 [Cu(bspt)(5,5'-dmbipy)](16)

To a stirred mixture of H<sub>2</sub>bspt (0.188 g, 0.5 mmol) and 5,5'-dimethyl-2,2'-bipyridine (0.092 g, 0.5 mmol), copper(II) acetate monohydrate (0.099 g, 0.5 mmol) was added. The solution was refluxed for 3 hours and green product separated out was filtered, washed with methanol and dried *in vacuo*.

Elemental Anal. Found (Calcd.) (%): C, 63.29 (63.39); H, 4.77 (5.00); N, 11.02 (11.20); S, 4.72 (5.13). Yield: 80%.

#### 5.2.3.6 [Cu<sub>2</sub>(brset)<sub>2</sub>] (17)

To a stirred mixture of H<sub>2</sub>brset (0.5 mmol, 0.151g) in DMF and methanol, copper(II) acetate monohydrate (0.099 g, 0.5 mmol) was added. The bluish green solution was refluxed for 3 hours and the product separated out was filtered, washed with methanol and dried *in vacuo*.

Elemental Anal. Found (Calcd.) (%): C, 32.42 (33.02); H, 2.76 (2.77); N, 11.23 (11.55); S, 8.80 (8.82). Yield: 58%.

#### **5.2.3.7 [Cu(brset)(phen)] (18)**

Methanolic solution of copper(II) acetate monohydrate (0.099 g, 0.5 mmol) was added to a stirred mixture of H<sub>2</sub>brset (0.151 g, 0.5 mmol) in DMF and methanol and 1,10-phenanthroline (0.090 g, 0.5 mmol). The resultant solution was refluxed for 3 hours. The green product obtained was filtered, washed with methanol and dried *in vacuo*.

Elemental Anal. Found (Calcd.) (%) : C, 47.98 (48.58); H, 3.21 (3.34); N, 12.77 (12.88); S, 5.67 (5.90). Yield: 50%.

#### **5.2.3.8 [Cu(bpet)(I)] (19)**

2-Benzoylpyridine-4-ethylthiosemicarbazone (Hbpet) was prepared by heating 2-benzoylpyridine (0.183 g, 1 mmol) and N<sup>4</sup>-ethylthiosemicarbazide (0.119 g, 1 mmol) for 2 hours. Copper(I) iodide (0.190 g, 1 mmol) was added to the methanolic solution of ligand Hbpet and refluxed for another 4 hours. Green colored precipitate formed was filtered, washed and dried *in vacuo*.

Elemental Anal. Found (Calcd.) (%) : C, 37.42 (38.02); H, 2.77 (3.19); N, 11.76 (11.82); S, 6.17 (6.77). Yield: 82%.

#### **5.2.3.9 [Cu(bpet)(N<sub>3</sub>)] (20)**

2-Benzoylpyridine-N<sup>4</sup>-ethylthiosemicarbazone (Hbpet) was prepared by heating 2-benzoylpyridine (0.183 g, 1 mmol) and N<sup>4</sup>-ethylthiosemicarbazide (0.119 g, 1 mmol) for 2 hours. Copper(II) acetate monohydrate (0.199 g, 1 mmol) and NaN<sub>3</sub> (0.065 g, 1 mmol) were added to the solution and reflux was continued for another 4 hours.

Dark green colored precipitate was formed, filtered, washed and dried *in vacuo*. Dark green colored crystals were isolated from the cool solution. Elemental Anal. Found (Calcd.) (%) : C, 46.54 (46.32); H, 3.37 (3.89); N, 25.42 (25.21); S, 8.32 (8.24). Yield: 75%.

### 5.3 Results and discussion

Nine copper(II) complexes of the thiosemicarbazones were synthesized. The compounds **12** and **17** were prepared by the reaction of equimolar mixture of the appropriate thiosemicarbazone and copper acetate monohydrate. Complexes **13-16** and **18** were synthesized by refluxing metal salt, corresponding heterocyclic bases and thiosemicarbazones in 1:1:1 ratio. All the complexes are green in color which may be due to the sulfur to copper charge transfer bands dominating their visible spectra [211,212]. They are soluble in solvents like DMF and DMSO. In all the complexes except **19** and **20**, thiosemicarbazones exist in the thioiminolate form and act as dideprotonated tridentate ligands coordinating through phenolic oxygen, thioiminolate sulfur and azomethine nitrogen. Compounds **12** and **17** are dimeric in nature while others are monomeric mixed ligand metal chelates. They are characterized by the following physico-chemical methods.

#### 5.3.1 Elemental analyses

The analytical data indicate that the compounds are analytically pure. The elemental analyses data are consistent with the general formula [CuLB], for complexes **13-16** and **18** and [(CuL)<sub>2</sub>] for complexes **12** and **17**, where L is the doubly deprotonated thiosemicarbazone and B is the bidentate heterocyclic base.



### 5.3.2 Molar conductivity and magnetic susceptibility measurements

The conductivity measurements were made in DMF ( $10^{-3}$  M) and all the complexes were found to be non-electrolytes [110]. The room temperature magnetic susceptibility of the complexes **13-16** and **18-20** in the polycrystalline state fall in the range 1.61-1.87 B.M., which are very close to the spin-only value of 1.73 B.M. for a  $d^9$  copper system [213]. The magnetic moments of complexes **12** and **17** are found to be 0.99 and 0.96 B.M. respectively and this low magnetic moment may be attributed to considerable antiferromagnetic interaction between metal centres suggesting dimeric nature to these complexes [214].

**Table 5.1. Molar conductivity and magnetic moments of Cu(II) complexes**

Compound	$\lambda_m^a$	$\mu_{\text{eff}}$ (B.M.)
[Cu <sub>2</sub> (bspt) <sub>2</sub> ] ( <b>12</b> )	4.0	0.99
[Cu(bspt)(phen)] ( <b>13</b> )	2.6	1.83
[Cu(bspt)(bipy)] ( <b>14</b> )	3.1	1.62
[Cu(bspt)(4,4'-dmbipy)] ( <b>15</b> )	8.8	1.72
[Cu(bspt)(5,5'-dmbipy)] ( <b>16</b> )	4.9	1.79
[Cu <sub>2</sub> (brset) <sub>2</sub> ] ( <b>17</b> )	3.3	0.96
[Cu(brset)(phen)] ( <b>18</b> )	2.8	1.72
[Cu(bpet)(I)] ( <b>19</b> )	61	1.87
[Cu(bpet)(N <sub>3</sub> )] ( <b>20</b> )	3.6	1.83

<sup>a</sup> = mho cm<sup>2</sup> mol<sup>-1</sup>

### 5.3.3 Infrared spectra

The IR spectra of the copper complexes were recorded in the range 4000-400 cm<sup>-1</sup> with KBr pellets. A comparison of the IR spectra of thiosemicarbazones and the metal complexes shows that significant variations have occurred in the characteristic frequencies upon

complexation. The tentative assignments for the IR spectral bands useful for determining the ligand's mode of coordination are listed in Table 5.2. In the complexes **12-18**, the bands due to O–H and <sup>2</sup>N–H stretching vibrations are absent which is a clear evidence for the coordination of the thiosemicarbazones in the dideprotonated form. The band corresponding to azomethine bond,  $\nu(\text{C}=\text{N})$ , shifts to higher energy on coordination due to the combination of  $\nu(\text{C}=\text{N})$  with the newly formed  $\text{C}=\text{N}$  bond which results from the loss of the thioamide hydrogen from the thiosemicarbazone moiety [113-116,90].

The bands at 1333 and 1342  $\text{cm}^{-1}$  present in the thiosemicarbazones shift to lower wave numbers in all the complexes and this can be assigned to the  $\nu(\text{C}-\text{S})$  vibration suggesting the change of bond order and strong electron-delocalization upon chelation. This shows that the  $\text{H}-\text{N}-\text{C}=\text{S}$  in the ligands has transformed to  $\text{N}=\text{C}-\text{S}-\text{H}$  thereby coordinating to copper in the thioiminolate form. Coordination *via* thioiminolate sulfur is also indicated by the negative shift of the band assigned to  $\delta(\text{C}=\text{S})$  vibration in the thiosemicarbazones [117]. The bands in the range 473-513  $\text{cm}^{-1}$  indicate the coordination of azomethine nitrogen to copper centre. The increase in frequency of  $\nu(\text{N}-\text{N})$  bands in complexes, due to the increase in double bond character is another proof for the coordination of the ligands through the azomethine nitrogen [118]. The broad absorption bands at 3366 and 3299  $\text{cm}^{-1}$  assigned to phenolic –OH of thiosemicarbazones  $\text{H}_2\text{bspt}$  and  $\text{H}_2\text{brset}$  respectively have disappeared in the complexes which indicate the coordination of the phenolic oxygen to the copper atom. The IR

spectra of complexes **13-16** and **18** display bands characteristic of coordinating heterocyclic bases [119]. Fig. 5.1 depict the infrared spectra of some of the copper complexes of thiosemicarbazones. In compound **20** strong band at  $2060\text{ cm}^{-1}$  is assigned to the asymmetric stretching of azide.

It is observed that in all the complexes the thiosemicarbazones act as dianionic tridentate ligands coordinating to copper through O, N and S atoms. In the case of mixed ligand copper chelates, the two nitrogen atoms of heterocyclic bases occupy the fourth and fifth coordination positions of copper.

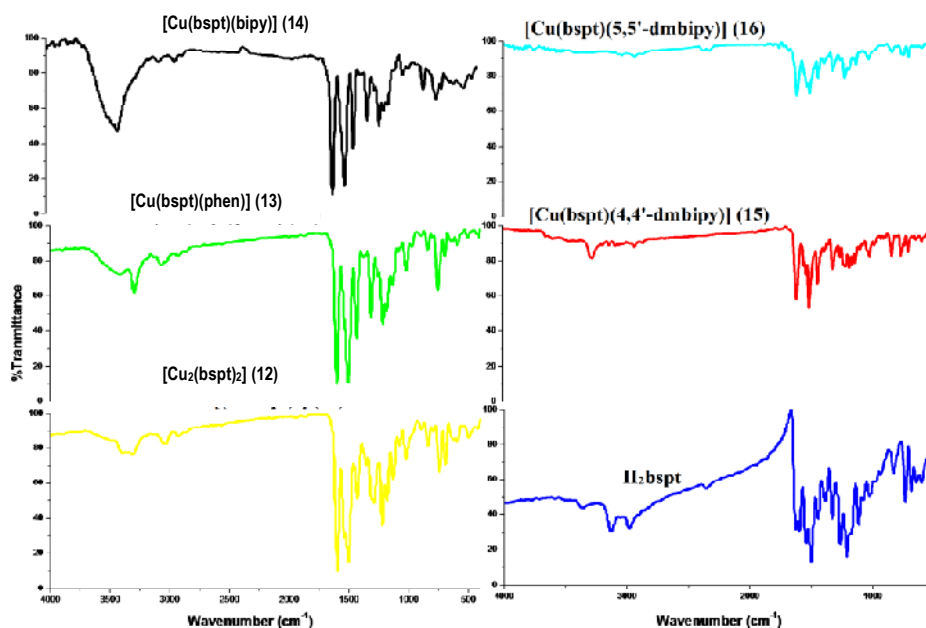


**Fig. 5.1.** IR spectra of thiosemicarbazone and its Cu(II) complexes.

Table 5.2. IR spectral assignments ( $\text{cm}^{-1}$ ) of thiosemicarbazones and their Cu(II) complexes

Compound	$\nu(\text{O-H})$	$\nu(\text{C=N})$	$\nu(\text{C=N})^a$	$\nu(\text{N-N})$	$\frac{\nu(\text{C=S})/\nu(\text{C-S})}{\delta(\text{C=S})/\delta(\text{C-S})}$	$\nu(\text{C-O})$	$\nu(\text{Cu-O})$	$\nu(\text{Cu-N})$
H <sub>2</sub> bspt	3366	1625	----	1112	1330, 832	1261	----	----
[Cu <sub>2</sub> (bspt) <sub>2</sub> ] ( <b>12</b> )	----	1597	1509	1130	1305, 839	1219	494	420
[Cu(bspt)(phen)] ( <b>13</b> )	----	1604	1516	1130	1313, 839	1211	502	415
[Cu(bspt)(bipy)] ( <b>14</b> )	----	1597	1496	1130	1313, 839	1210	505	435
[Cu(bspt)(4,4'-dmbipy)] ( <b>15</b> )	----	1608	1504	1181	1311, 749	1257	473	433
[Cu(bspt)(5,5'-dmbipy)] ( <b>16</b> )	----	1604	1499	1119	1311, 827	1256	513	427
H <sub>2</sub> brset	3290	1603	----	1101	1319, 824	1233	----	----
[Cu <sub>2</sub> (brset) <sub>2</sub> ] ( <b>17</b> )	----	1594	1510	1170	1309, 842	1240	506	420
[Cu(brset)(phen)] ( <b>18</b> )	----	1598	1521	1122	1301, 834	1298	497	426
Hbpet	----	1583	----	1107	1306, 812	----	----	----
[Cu(bpet)(I)] ( <b>19</b> )	----	1545	1494	1146	1296, 823	----	----	465
[Cu(bpet)(N <sub>3</sub> )] ( <b>20</b> )	----	1540	1446	1128	1273, 827	----	----	465

<sup>a</sup> = newly formed C=N bond

### 5.3.4 Electronic spectra

The electronic spectra give much insight into the coordination geometry around copper(II) ion. The electronic spectra of all the complexes were taken in DMF. The electronic transitions found in free ligands due to imine function of thiosemicarbazone moiety were slightly shifted on complexation. The shift of the bands due to intraligand transitions is the result of the weakening of the C=S bond and the extension of conjugation upon complexation [121]. The shift occurs also due to coordination *via* phenolic oxygen and azomethine nitrogen [122] and is an indication of the enolization followed by the deprotonation of the ligands during complexation. The intraligand  $n \rightarrow \pi^*$  and  $\pi \rightarrow \pi^*$  transitions are assigned to bands in the range 30530-30630  $\text{cm}^{-1}$  for the copper complexes of H<sub>2</sub>bspt, 30250, 30540  $\text{cm}^{-1}$  for the copper complexes of H<sub>2</sub>brset and 32450, 33090  $\text{cm}^{-1}$  for the complexes of Hbpet. In all the complexes, intense bands in the 22780-25490  $\text{cm}^{-1}$  range are assigned to ligand to metal charge transfer transitions and the broadness of these bands can be explained as due to the combination of O $\rightarrow$ Cu, N $\rightarrow$ Cu and S $\rightarrow$ Cu LMCT transitions [215]. Figs. 5.2-5.4 represent the electronic spectra of the complexes.

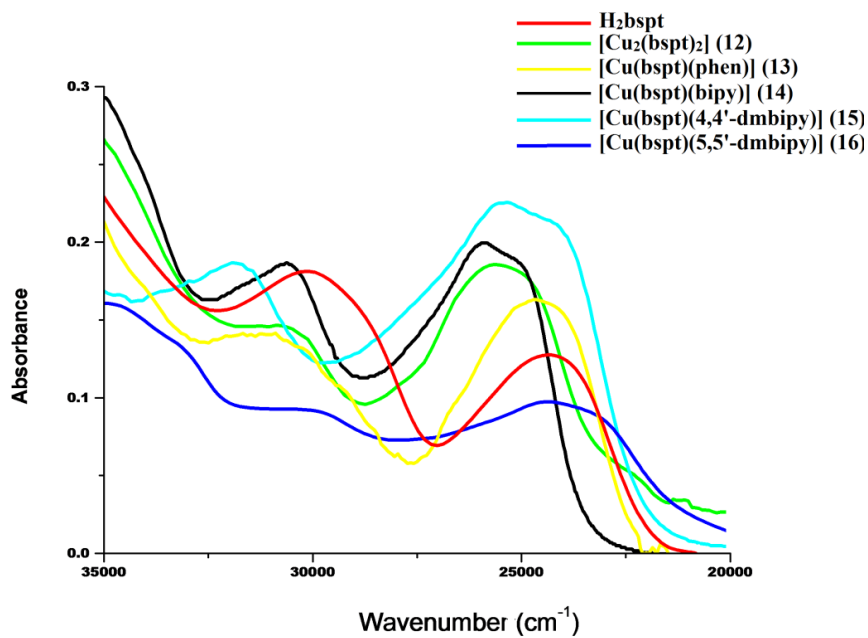


Fig. 5.2. Electronic spectra of H<sub>2</sub>bspt and its copper(II) complexes.

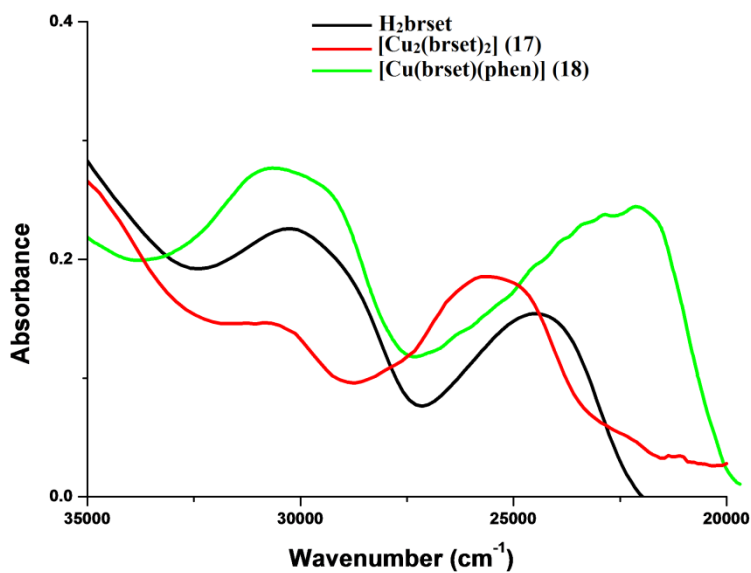


Fig. 5.3. Electronic spectra of H<sub>2</sub>brset and its copper(II) complexes.

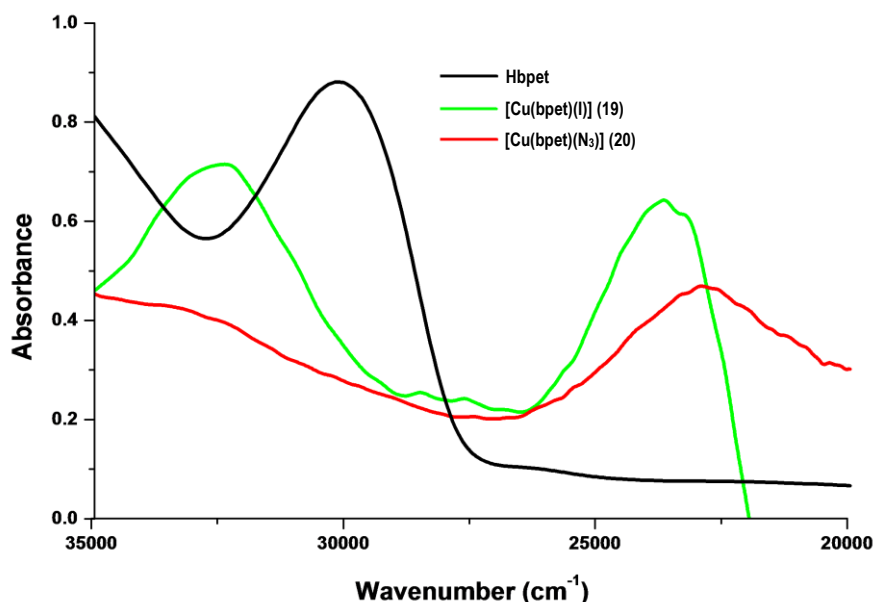


Fig. 5.4. Electronic spectra of Hbpet and its copper(II) complexes.

In an octahedral field, the ground state term  $^2D$  of copper(II) will be split into two levels,  $^2T_{2g}$  and  $^2E_g$ . However, the energy levels again split resulting in more transitions if the geometry around copper(II) complex is of lower symmetry. For square planar complexes with a  $d_{x^2-y^2}$  ground state [54], three transitions are possible viz,  $d_{x^2-y^2} \rightarrow d_{xy}$ ,  $d_{x^2-y^2} \rightarrow d_{z^2}$  and  $d_{x^2-y^2} \rightarrow d_{xz}$ ,  $d_{yz}$  ( $^2B_{2g} \leftarrow ^2B_{1g}$ ,  $^2A_{1g} \leftarrow ^2B_{1g}$  and  $^2E_g \leftarrow ^2B_{1g}$ ). Three transitions,  $d_{x^2-y^2} \rightarrow d_{z^2}$ ,  $d_{x^2-y^2} \rightarrow d_{xy}$  and  $d_{x^2-y^2} \rightarrow d_{xz}$ ,  $d_{yz}$  are possible for square pyramidal complexes with a  $d_{x^2-y^2}$  ground state [216,217]. Since the four  $d$  orbitals lie very close together, each transition cannot be distinguished by its energy and hence it is very difficult to resolve the three bands into separate components. The visible spectra of all the complexes were recorded in DMF and the  $d-d$  bands appeared as weak broad bands in the range 16940-17750  $\text{cm}^{-1}$

(Figs. 5.5-5.7) which can be assigned to  ${}^2T_{2g} \leftarrow {}^2E_g$  transitions [115]. The electronic spectral data of the copper(II) complexes are given in Table 5.3.

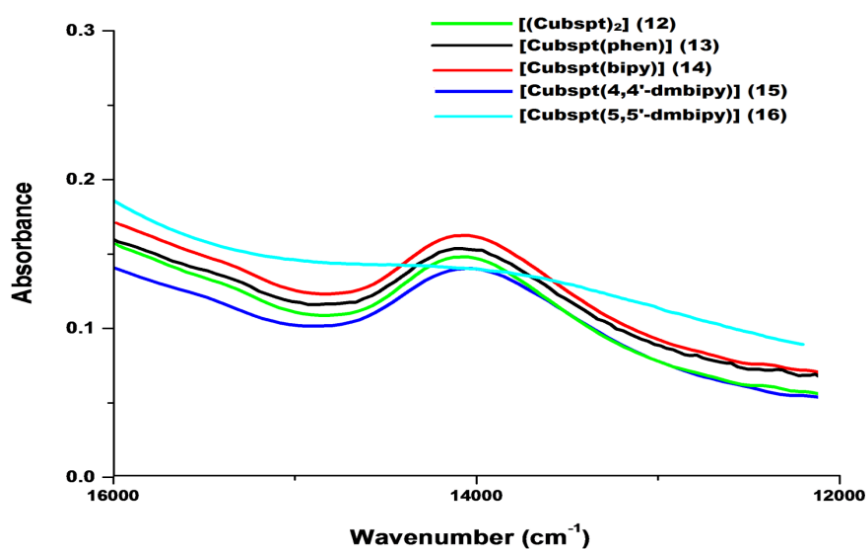


Fig. 5.5. Visible spectra of copper(II) complexes of H<sub>2</sub>bspt.

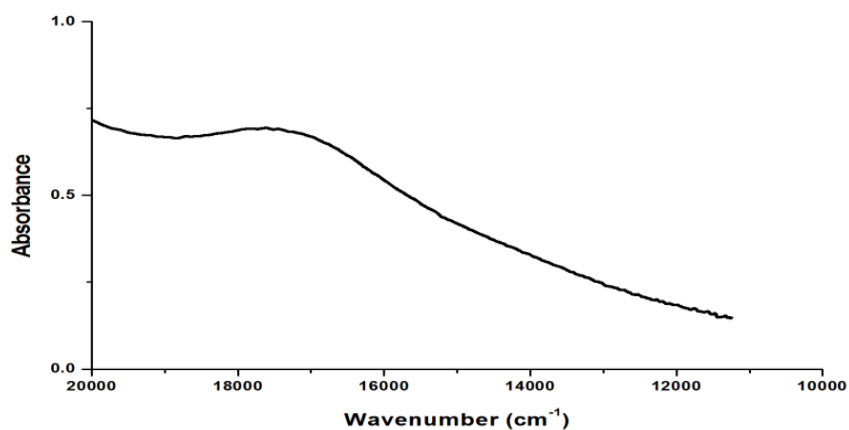


Fig. 5.6. Visible spectrum of [Cu<sub>2</sub>(brset)<sub>2</sub>] (17).



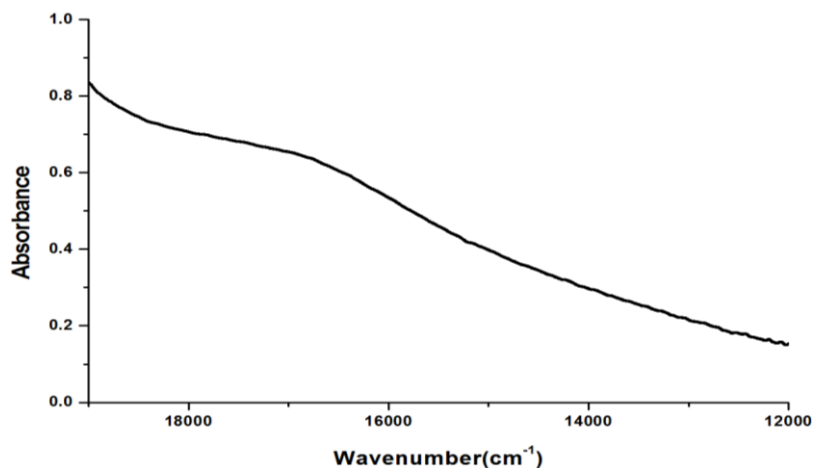


Fig. 5.7. Visible spectrum of [Cu(bpet)I] (19)

Table 5.3. Electronic spectral assignments ( $\text{cm}^{-1}$ ) of thiosemicarbazones and their Cu(II) complexes

Compound	$n \rightarrow \pi^* / \pi \rightarrow \pi^*$	LMCT	$d-d$
H <sub>2</sub> bspt	24230, 30110	----	----
[Cu <sub>2</sub> (bspt) <sub>2</sub> ] (12)	30530	25490	14050
[Cu(bspt)(phen)] (13)	30630	25430	14060
[Cu(bspt)(bipy)] (14)	30480	25390	14070
[Cu(bspt)(4,4'-dmbipy)] (15)	30530	25390	14030
[Cu(bspt)(5,5'-dmbipy)] (16)	30570	25430	17320
H <sub>2</sub> brset	24220, 29920	----	----
[Cu <sub>2</sub> (brset) <sub>2</sub> ] (17)	30250	24890	17450
[Cu(brset)(phen)] (18)	30540	25470	----
Hbpet	23500, 30800	----	----
[Cu(bpet)I] (19)	32450	23540	----
[Cu(bpet)(N <sub>3</sub> )] (20)	33090	22780	16800

### 5.3.5 EPR spectra

The electron paramagnetic resonance spectroscopy provides a wealth of information regarding the electronic structure of paramagnetic

compounds. The magnetic parameters measured in EPR study are related to the structure of the paramagnetic complex, the number of ligands, nature of bonding and spatial arrangements of the ligands around the central metal ion.

The copper(II) ion, with a  $d^9$  configuration, has an effective spin of  $S = \frac{1}{2}$  and associated spin angular momentum  $m_s = \pm\frac{1}{2}$ , which leads to a doubly degenerate spin state in the absence of magnetic field. In a magnetic field, this degeneracy is removed and the energy difference between these two states is given by  $E = h\nu = g\beta B$ , where  $h$  is Planck's constant,  $\nu$  is the frequency,  $g$  is the Lande splitting factor,  $\beta$  is the electronic Bohr magneton and  $B$  is the magnetic field. In the case of a  $3d^9$  copper(II) ion, the appropriate spin Hamiltonian assuming a  $B_{1g}$  ground state is given by

$$\hat{H} = \beta [g_{\parallel}B_zS_z + g_{\perp}(B_xS_x + B_yS_y)] + A_{\parallel}I_zS_z + A_{\perp}(I_xS_x + I_yS_y)$$

The copper(II) ion having a  $d^9$  configuration with an effective spin of  $S = \frac{1}{2}$  couples with nuclear spin of  $^{63}\text{Cu}$  ( $I = 3/2$ ) and gives rise to four ( $2nI+1=4$ ) hyperfine lines. The EPR spectra of all the complexes were recorded in polycrystalline state at 298 K and in DMF/DMSO at 77 K in the X- band frequency using TCNE as standard ( $g = 2.00277$ ) with 100 kHz modulation frequency and 9.1 GHz microwave frequency. In polycrystalline state, since it is magnetically concentrated the anisotropy may be lost. Dilution of the solid isolates the electron spin of the given complex from that of another paramagnetic molecule.

EPR spectra can be mainly of four types *viz.* isotropic, axial, rhombic and reverse axial. An isotropic spectrum with a single  $g$  value shows a cubic coordination environment. Sometimes broadening of signal can also occur which is attributable to enhanced spin lattice relaxation and dipolar interaction. For axial spectrum there will be atleast three fold axis of symmetry and  $g_{\parallel}$  is obtained when the magnetic field is aligned parallel to  $z$  axis. Signal due to  $g_{\perp}$  is obtained when the magnetic field is aligned perpendicular to  $z$  axis. A rhombic spectrum shows no axis of symmetry and hence three  $g$  values are obtained. Some of the EPR spectra are simulated using EasySpin 4.0.0 package [218] and the experimental (red) and simulated (blue) best fits are included.

The EPR parameters  $g_{\parallel}$ ,  $g_{\perp}$ ,  $A_{\parallel}$  and the energies of  $d-d$  transitions were used to evaluate the bonding parameters  $\alpha^2$ ,  $\beta^2$  and  $\gamma^2$  for the Cu(II) ion in various ligand field environments which may be regarded as measure of covalency in the in-plane  $\sigma$ -bonds ( $\alpha^2$ ), in-plane  $\pi$ -bonds ( $\beta^2$ ) and out-of-plane  $\pi$ -bonds ( $\gamma^2$ ) [219]. The orbital reduction factors  $K_{\parallel}$  and  $K_{\perp}$  were also calculated using these bonding parameters. The following expressions are used to calculate these parameters [112,220].

$$\alpha^2 = -(A_{\parallel}/0.036) + (g_{\parallel}-2.0023) + 3/7(g_{\perp}-2.0023) + 0.04$$

$$K_{\parallel}^2 = (g_{\parallel}-2.0023) E_{d-d}/8\lambda_0$$

$$K_{\perp}^2 = (g_{\perp}-2.0023) E_{d-d}/2\lambda_0$$

$$K_{\parallel} = \alpha^2 \beta^2$$

$$K_{\perp} = \alpha^2 \gamma^2$$

where  $\lambda_0$  is the spin-orbit coupling constant and has a value  $-828 \text{ cm}^{-1}$  for Cu(II)  $d^9$  system. The value of  $\alpha^2$  indicates the extent of covalent nature, where the value of 1.0 corresponds to a purely ionic nature.

According to Hathaway [221], for pure  $\sigma$ -bonding  $K_{\parallel} \approx K_{\perp} \approx 0.77$  and for in-plane  $\pi$ -bonding  $K_{\parallel} < K_{\perp}$ , while for out-of-plane  $\pi$ -bonding  $K_{\perp} < K_{\parallel}$ . The values of bonding parameters  $\alpha^2$ ,  $\beta^2$  and  $\gamma^2 < 1$  confirm the covalent nature of complexes.

The EPR spectrum of complex **12** is isotropic in nature, which is attributable to enhanced spin lattice relaxation and extensive exchange coupling through misalignment of the local molecular axes between different molecules in the unit cell (dipolar broadening) (Fig. 5.8). This type of spectrum unfortunately gives no information on the electronic ground state of copper(II) ions present in the complex. It showed a well-resolved axial spectrum with four hyperfine lines in the parallel region and perpendicular region (due to coupling of the electron spin with the spin of the  $^{63}\text{Cu}$  nucleus where  $I = 3/2$ ) in DMF at 77 K (Fig. 5.9) with  $g_{\parallel} > g_{\perp} > 2.0023$  relationship, consistent with a  $d_{x^2-y^2}$  ground state in a square planar geometry [222,223].

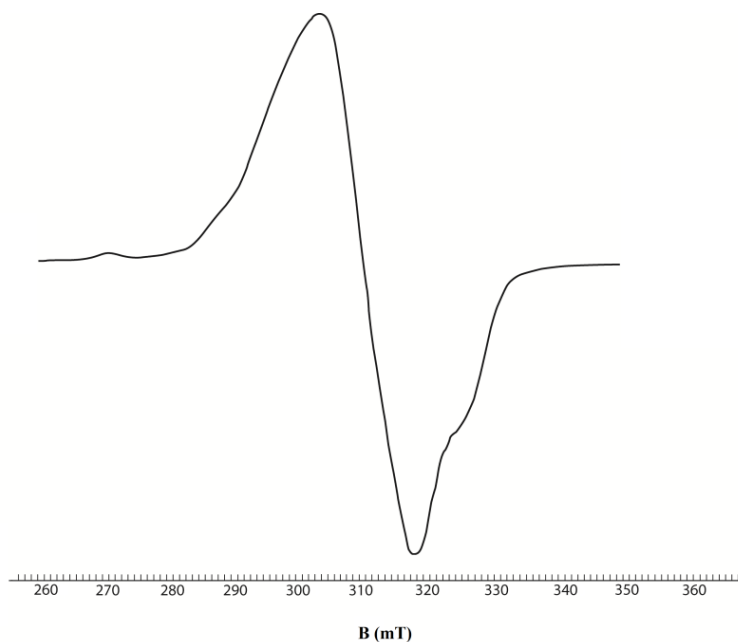


**Fig. 5.8.** EPR spectrum of  $[\text{Cu}_2(\text{bspt})_2]$  (12) in polycrystalline state at 298 K.

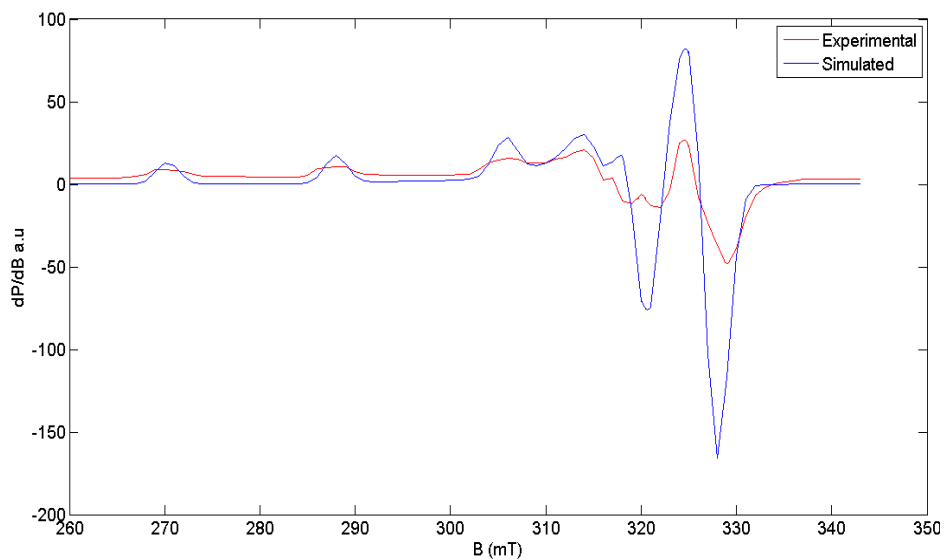


**Fig. 5.9.** EPR spectrum of  $[\text{Cu}_2(\text{bspt})_2]$  (12) in DMF at 77 K.

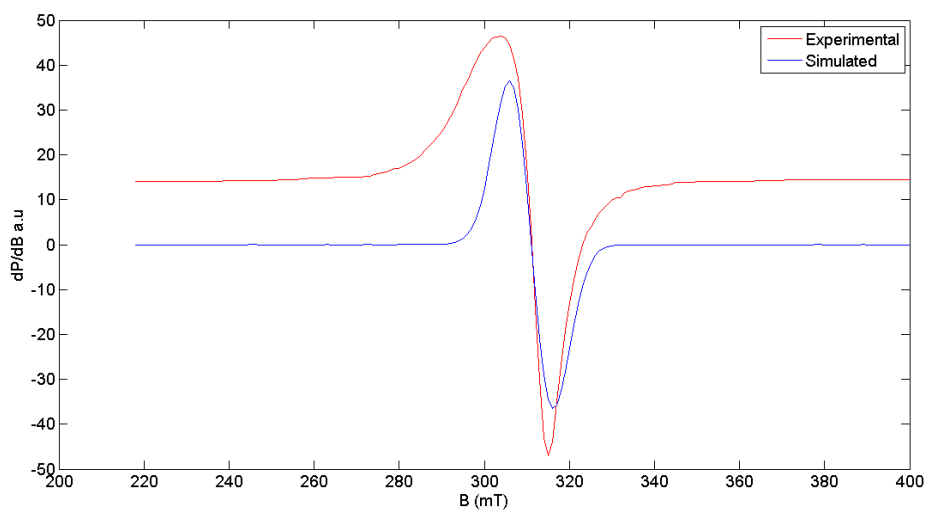


Fig. 5.10. EPR spectrum of [Cu(bspt)(phen)] (13) in polycrystalline state at 298 K.

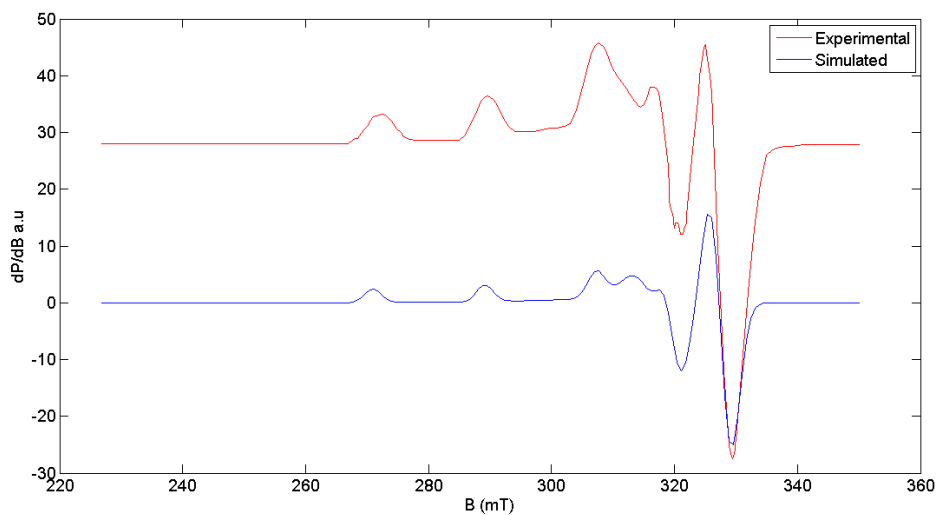
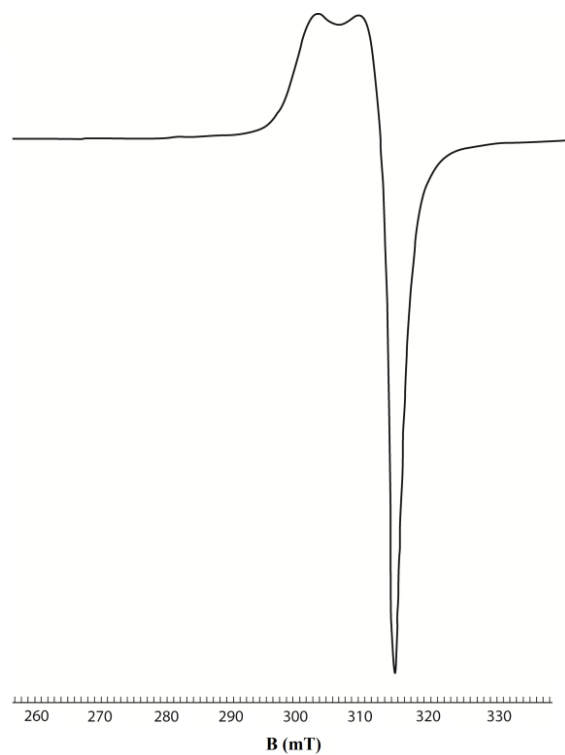
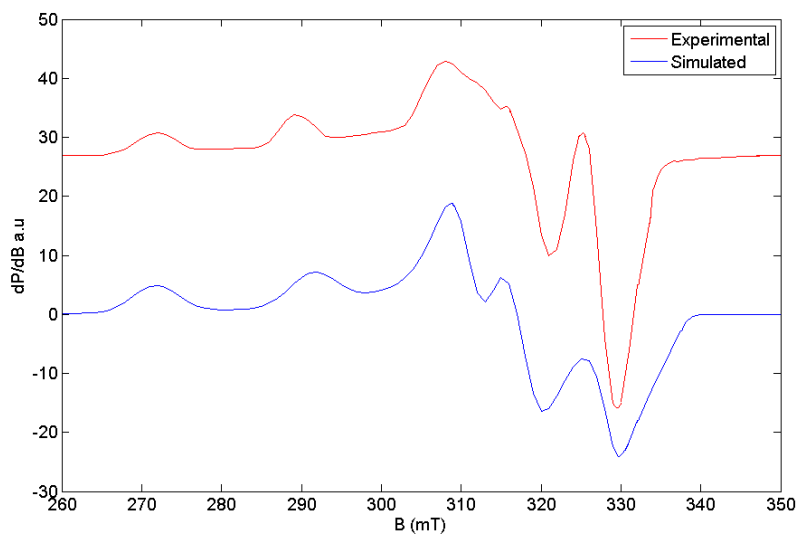


Fig. 5.11. EPR spectrum of [Cu(bspt)(phen)] (13) in DMF at 77 K.



**Fig. 5.12.** EPR spectrum of [Cu(bspt)(bipy)] (14) in polycrystalline state at 298 K.



**Fig. 5.13.** EPR spectrum of [Cu(bspt)(bipy)] (14) in DMF at 77 K.

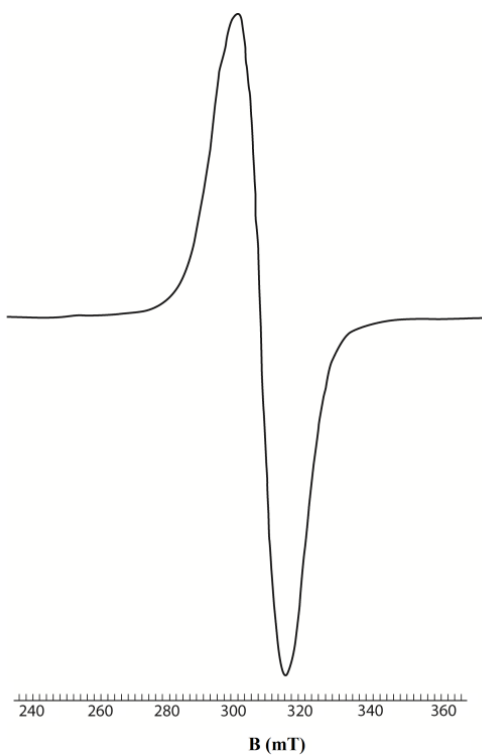


**Fig. 5.14.** EPR spectrum of [Cu(bspt)(4,4'-dmbipy)] (15) in polycrystalline state at 298 K.

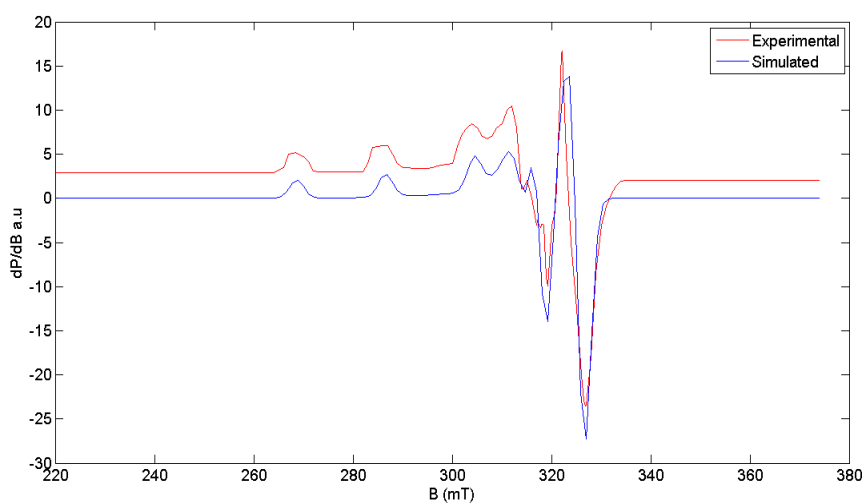


**Fig. 5.15.** EPR spectrum of [Cu(bspt)(4,4'-dmbipy)] (15) in DMF at 77 K.



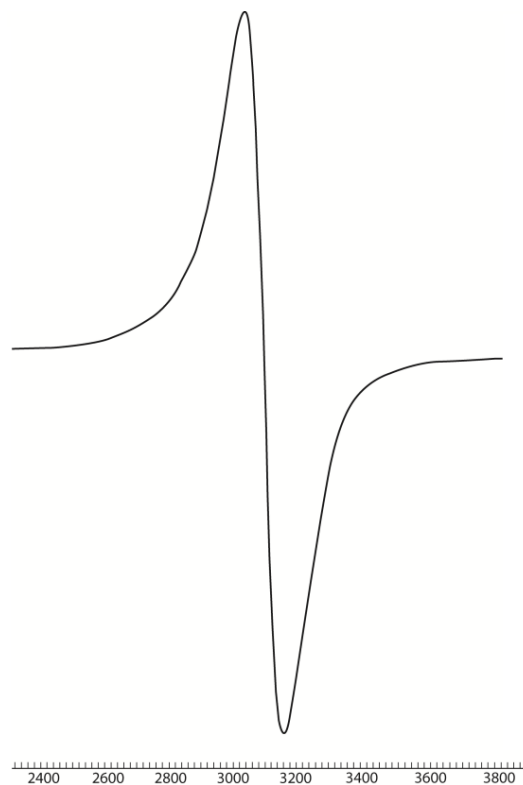


**Fig. 5.16.** EPR spectrum of [Cu(bspt)(5,5'-dmbipy)] (16) in polycrystalline state at 298 K.

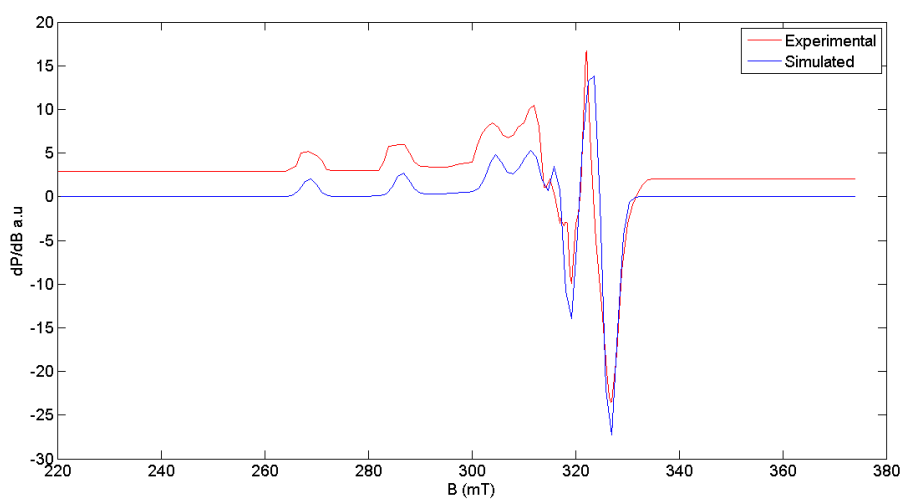


**Fig. 5.17.** EPR spectrum of [Cu(bspt)(5,5'-dmbipy)] (16) in DMF at 77 K.

In DMF at 77 K, all the compounds **13-16** showed four fairly resolved hyperfine lines [ $^{63,65}\text{Cu}$ ,  $I = 3/2$ ] corresponding to  $-3/2$ ,  $-1/2$ ,  $+1/2$  and  $+3/2$  transitions in parallel and perpendicular regions. In addition to this, three superhyperfine lines due to interaction with azomethine nitrogen are also observed. A square pyramidal geometry can be assigned to this complex since  $g_{\parallel} > g_{\perp}$  and rules out the possibility of a trigonal bipyramidal structure which is expected to have  $g_{\parallel} < g_{\perp}$ .

The  $\alpha^2$  values for the complexes were calculated and since the obtained values lie in between 0.5 and 1.0, it is inferred that the metal-ligand bonds in the complexes are partially ionic and partially covalent in nature. The EPR spectral parameters of the copper(II) complexes are presented in Table 5.4.

**Table 5.4. EPR spectral parameters of copper(II) complexes in the polycrystalline state at 298 K and in DMF at 77 K.**

	<b>12</b>	<b>13</b>	<b>14</b>	<b>15</b>	<b>16</b>
Polycrystalline (298 K)					
$g_{\text{iso}}$	2.09	2.09	2.09	2.09	2.09
DMF (77 K)					
$g_{\parallel}$	2.19	2.18	2.18	2.20	2.19
$g_{\perp}$	2.039	2.037	2.037	2.05	2.065
$g_{\text{av}}$	2.114	2.108	2.108	2.125	2.127
$A_{\parallel}^a$	198	201	201	202	201
$A_{\perp}^a$	190	218	218	220	221
$A_{\text{av}}^a$	105	108	108	109	109
$\alpha^2$	0.7944	0.7833	0.7833	0.8202	0.8141
$\beta^2$	0.7943	0.7841	0.7835	0.7896	0.8508
$\gamma^2$	0.7024	0.693	0.6925	0.7757	0.9834
$K_{\parallel}$	0.631	0.6142	0.6137	0.6476	0.6926
$K_{\perp}$	0.558	0.5428	0.5424	0.6362	0.8006

<sup>a</sup>Expressed in units of  $\text{cm}^{-1}$  multiplied by a factor of  $10^{-4}$ .

The geometric parameter  $G$ , which is a measure of the exchange interaction between the copper centers in the polycrystalline state is calculated using the equation,

$$G = g_{\parallel} - 2.0023 / g_{\perp} - 2.0023 \text{ for axial spectra.}$$

If  $G > 4.4$ , exchange interaction is negligible and if  $G < 4.4$  considerable exchange interaction is indicated in the solid state [224,225]. Since all spectra in polycrystalline state is isotropic in nature  $G$  value is not calculated.

From the EPR spectral data for these complexes it is clear that the  $g_{\parallel}$  values are nearly the same for all the complexes indicating that the bonding is dominated by the thiosemicarbazone moiety. Kivelson and Nieman have reported that  $g_{\parallel}$  values less than 2.3 indicate considerable covalent character to M–L bonds, while a value greater than 2.3 indicate ionic character. Here it is found that  $g_{\parallel} < 2.3$  showing significant covalent character to M–L bond [226,227]. The  $g_{av}$  values of all the complexes in the solution state are consistent with the  $g_{iso}$  values suggesting that they are not undergoing any kind of dissociation in the solution state.

The empirical factor,  $f = g_{\parallel}/A_{\parallel}$ , is an index of tetragonal distortion and it may be vary from 105 to 135. In compounds **12-16**,  $f$  falls in the range 105-135 which shows small to medium distortion from planarity [228].

.....✪.....



# Chapter 6

## SYNTHESES, SPECTRAL AND STRUCTURAL CHARACTERIZATION OF Zn(II) COMPLEXES OF ONS AND NNS DONOR THIOSEMICARBAZONES

Contents	6.1 Introduction
	6.2 Experimental
	6.3 Results and discussion

### 6.1 Introduction

Centuries before zinc was discovered in the metallic form, its ores were used for making brass and zinc compounds and also for healing wounds and sore eyes. Zinc is the second most prevalent trace element, after iron, and is involved in structure and function of over 300 enzymes. Use of zinc as a nutritional supplement has become common in many countries [229,230]. Zinc salts, primarily zinc citrate, are widely used as antimicrobials. Zinc exhibits activity against oral *Streptococci*, particularly *Streptococcus mutans* [231]. Zinc supplementation shows beneficial effects against infectious diseases, especially diarrhea, and it has been shown that zinc supplementation can improve mucosal innate immunity through induction of antimicrobial peptide secretion from intestinal epithelial cells [232]. Due to their interesting antibacterial [233], anti-convulsant [234] and antiproliferative-antitumor [235-237] activity, zinc(II)

complexes had attracted great attention in the recent years. As drugs for the treatment of Alzheimer disease [238], zinc(II) complexes had been structurally characterized. Zinc(II) complexes has also showed properties of DNA binding in the very recent research [239]. Moreover, zinc(II) complexes with appropriate ligands can be applied in optical devices, such as OLED [240] and light switching device [241].

Zinc metal has the significant role in bioinorganic chemistry, involving a large number of enzymatic and catalytic functions. So main interest is to observe metal ion coordination environment, using zinc metal because its  $d^{10}$  configuration, permits a wide range of symmetries and various coordination numbers, i.e. 4, 5 or 6 relatively, easily [242,243]. It is also the second most abundant transition-metal ion after iron in the human body and plays a pivotal role in the regulation of various metabolic processes, transcription factors, immune functions, ion channels, and neurotransmission [244,245].

Zinc atom has either a structural or analytical role in several proteins. It has been recognised as an important cofactor in biological molecules, either as a structural template in protein folding or as a Lewis acid catalyst that can readily adopt 4-, 5-, or 6- coordination [246]. Zinc is able to play a catalytic role in the activation of thiols as nucleophiles at physiological pH. Mononuclear zinc complexes serve as model compounds for zinc enzymes such as phospholipase C, bovine lens leucine aminopeptidase, ATPases, carbonic anhydrases and peptide deformylase. The zinc(II) ion is known to have a high affinity towards nitrogen and sulfur donor ligands.

This chapter consists of syntheses and characterization of eight Zn(II) complexes of 4-benzyloxysalicylaldehyde-*N*<sup>4</sup>-phenylthiosemicarbazone and 2-benzoylpyridine-*N*<sup>4</sup>-ethylthiosemicarbazone using infrared, electronic and <sup>1</sup>H NMR studies. It also describes the single crystal X-ray diffraction studies of [Zn(bpet)dca] (**26**) and [Zn(bpet)](NO<sub>3</sub>)<sub>2</sub>·H<sub>2</sub>O (**27**).

## **6.2 Experimental**

### **6.2.1 Materials**

Zinc(II) acetate dihydrate (E-Merck), 1,10-phenanthroline (phen), 2,2'-bipyridine (bipy), 4,4'-dimethyl-2,2'-bipyridine (4,4'-dmbipy), 5,5'-dimethyl-2,2'-bipyridine (5,5'-dmbipy), sodium dicyanamide (Sigma-Aldrich), zinc nitrate (E-Merck) were used as received.

### **6.2.2 Syntheses of the thiosemicarbazones**

The syntheses of thiosemicarbazones H<sub>2</sub>bspt and Hbpet are discussed already in Chapter 2.

### **6.2.3 Syntheses of the complexes**

#### **6.2.3.1 [Zn<sub>2</sub>(bspt)<sub>2</sub>] (**21**)**

This complex was synthesized by refluxing a solution of H<sub>2</sub>bspt (0.1885 g, 0.5 mmol) in 1:1 (v/v) mixture of DMF and methanol with a methanolic solution of Zn(OAc)<sub>2</sub>·2H<sub>2</sub>O (0.109 g, 0.5 mmol) for 3 hours. The complex formed was filtered, washed with methanol and dried *in vacuo*.

Elemental Anal. Found (Calcd.) (%) : C, 56.29 (57.21); H, 4.70 (3.89); N, 9.95 (9.53); S, 6.60 (7.27). Yield: 82%.

### 6.2.3.2 [Zn(bspt)(phen)] (22)

Methanolic solution of zinc(II) acetate dihydrate (0.109 g, 0.5 mmol) was added to a stirred mixture of H<sub>2</sub>bspt (0.1885 g, 0.5 mmol) in DMF and methanol (1:1 v/v) and 1,10-phenanthroline (0.099 g, 0.5 mmol) in methanol. The resultant homogenous yellow solution was refluxed for 3 hours. The yellow product obtained was filtered, washed with methanol and dried *in vacuo*.

Elemental Anal. Found (Calcd.) (%): C, 62.90 (63.61); H, 4.38 (4.37); N, 10.57 (11.24); S, 4.59 (5.15). Yield: 80%.

### 6.2.3.3 [Zn(bspt)(bipy)] (23)

To a stirred mixture of H<sub>2</sub>bspt (0.190 g, 0.5 mmol) in DMF and methanol (1:1 v/v) and 2,2'-bipyridine (0.078 g, 0.5 mmol) in methanol, zinc(II) acetate dihydrate (0.109 g, 0.5 mmol) was added. The resultant yellow solution was refluxed for 3 hours and the yellow product separated out was filtered, washed with methanol and dried *in vacuo*.

Elemental Anal. Found (Calcd.) (%): C, 61.39 (62.15); H, 4.09 (4.54); N, 11.31 (11.69); S, 5.04 (5.35). Yield: 83%.

### 6.2.3.4 [Zn(bspt)(4,4'-dmbipy)] (24)

To a stirred mixture of H<sub>2</sub>bspt (0.1885 g, 0.5 mmol) in DMF and methanol (1:1 v/v) and 4,4'-dimethyl-2,2'-bipyridine (0.092 g, 0.5 mmol) in methanol, methanolic solution of zinc(II) acetate dihydrate (0.109 g, 0.5 mmol) was added. The resultant yellow solution was refluxed for



3 hours. The yellow product obtained was filtered, washed with methanol and dried *in vacuo*.

Elemental Anal. Found (Calcd.) (%): C, 62.03 (62.14); H, 5.07 (5.06); N, 10.93 (10.66); S, 4.73 (4.88). Yield: 75%.

#### **6.2.3.5 [Zn(bspt)(5,5'-dmbipy)] (25)**

Methanolic solution of zinc(II) acetate dihydrate (0.109 g, 0.5 mmol) was added to a stirred mixture of H<sub>2</sub>bspt (0.1885 g, 0.5 mmol) in DMF and methanol (1:1 v/v) and 5,5'-dimethyl-2,2'-bipyridine (0.092 g, 0.5 mmol) in methanol. The resultant yellow solution was refluxed for 3 hours. The yellow product obtained was filtered, washed with methanol and dried *in vacuo*.

Elemental Anal. Found (Calcd.) (%): C, 60.22 (59.95); H, 4.84 (5.03); N, 10.78 (10.59); S, 4.41 (4.85). Yield: 72%.

#### **6.2.3.6 [Zn(bpet)(dca)]<sub>n</sub> (26)**

This complex was synthesized by refluxing a solution of Hbpet (0.1421 g, 0.5 mmol) in 1:1 (v/v) mixture of DMF and methanol with a methanolic solution of Zn(OAc)<sub>2</sub>·2H<sub>2</sub>O (0.109 g, 0.5 mmol) and sodium dicyanamide (0.0495 g, 0.5 mmol) for 3 hours. The complex formed was filtered, washed with methanol and dried *in vacuo*.

Elemental Anal. Found (Calcd.) (%): C, 49.25 (49.22); H, 3.88 (3.64); N, 23.68 (23.64); S, 7.86 (7.73). Yield: 60%.

#### 6.2.3.7 [Zn(Hbpet)<sub>2</sub>](NO<sub>3</sub>)<sub>2</sub>·H<sub>2</sub>O (27)

Methanolic solution of zinc(II) nitrate (0.1487 g, 0.5 mmol) was added to a solution of Hbpet (0.1421 g, 0.5 mmol) in DMF and methanol (1:1 v/v). The resultant homogenous yellow solution was refluxed for three hours. The yellow product obtained was filtered, washed with methanol and dried *in vacuo*.

Elemental Anal. Found (Calcd.) (%) : C, 36.14 (36.63); H, 3.36 (3.69); N, 17.55 (17.09); S, 6.36 (6.52). Yield: 64%.

#### 6.2.3.8 [Zn(bpet)(OAc)] (28)

A mixture of Hbpet (0.1421 g, 0.5 mmol) in DMF and methanol (1:1 v/v) and zinc(II) acetate dihydrate (0.109 g, 0.5 mmol) was refluxed for 3 hours and the yellow product separated out was filtered, washed with methanol and dried *in vacuo*.

Elemental Anal. Found (Calcd.) (%) : C, 49.84 (50.07); H, 4.35 (4.45); N, 13.71 (13.74); S, 7.53 (7.53). Yield: 62%.

### 6.3 Results and discussion

Equimolar ratios of the thiosemicarbazones and the metal acetate yielded the light yellow colored complex [Zn<sub>2</sub>(bspt)<sub>2</sub>] (**21**). The other compounds **22-25** were prepared by using the heterocyclic bases like 1,10-phenanthroline, 2,2'-bipyridine, 4,4'-dimethylbipyridine and 5,5'-dimethylbipyridine. Single crystals of compound **26** and **27** could be isolated and the structure was established by single crystal XRD studies. The complexes were characterized by the following physico-chemical methods.

### 6.3.1 Elemental analyses

From the observed C, H, N and S values, the above stoichiometry of the complexes were proposed.

### 6.3.2 Molar conductivity measurements

The molar conductivities of the complexes in DMF ( $10^{-3}$  M) were measured at 298 K with a Systronic model 303 direct reading conductivity bridge. The molar conductivity measurements showed that all the complexes except **27** are non-electrolytic in nature since the observed values are less than  $10 \text{ ohm}^{-1}\text{cm}^2\text{mol}^{-1}$  which are very much less than the value of  $65\text{-}90 \text{ ohm}^{-1}\text{cm}^2\text{mol}^{-1}$  reported for a 1:1 electrolyte in the same solvent [110].

**Table 6.1. Molar conductivity of Zn(II) complexes**

Compounds	$\lambda_m^a$
$[\text{Zn}_2(\text{bspt})_2]$ ( <b>21</b> )	4.0
$[\text{Zn}(\text{bspt})(\text{phen})]\cdot\text{H}_2\text{O}$ ( <b>22</b> )	2.9
$[\text{Zn}(\text{bspt})(\text{bipy})]$ ( <b>23</b> )	3.8
$[\text{Zn}(\text{bspt})(4,4'\text{-dmbipy})]$ ( <b>24</b> )	2.8
$[\text{Zn}(\text{bspt})(5,5'\text{-dmbipy})]$ ( <b>25</b> )	6.2
$[\text{Zn}(\text{bpet})(\text{dca})_n]$ ( <b>26</b> )	92.0
$[\text{Zn}(\text{Hbpet})_2](\text{NO}_3)_2\cdot\text{H}_2\text{O}$ ( <b>27</b> )	193.0
$[\text{Zn}(\text{bpet})(\text{OAc})]$ ( <b>28</b> )	5.7

<sup>a</sup> =  $\text{mho cm}^2 \text{mol}^{-1}$

### 6.3.3 Infrared spectra

To clarify the mode of bonding, the IR spectra of the thiosemicarbazones and their Zn(II) complexes were studied and assigned on the basis of a careful comparison of the latter with the thiosemicarbazones. The tentative IR spectral assignments are listed in Table 6.2. The IR spectrum of the thiosemicarbazone H<sub>2</sub>bspt exhibited a medium band at  $\sim 3366\text{ cm}^{-1}$  which is assigned to <sup>2</sup>NH vibration. It disappears in the spectra of complexes providing strong evidence for ligand coordination to the metal in the deprotonated thioiminolate form [247]. The band corresponding to azomethine bond,  $\nu(\text{C}=\text{N})$ , shifts to higher energy on coordination due to the combination of  $\nu(\text{C}=\text{N})$  with the newly formed C=N bond which results from the loss of the thioamide hydrogen from the thiosemicarbazone moiety [248,113-115,90]. The involvement of this nitrogen in bonding is also supported by a shift in  $\nu(\text{N}-\text{N})$  to higher frequencies. Coordination *via* the thioiminolate sulfur is indicated by the negative shift of the two bands assigned to  $\nu(\text{C}=\text{S})$  and  $\delta(\text{C}=\text{S})$  vibrations. Some of the IR spectra of the Zn(II) complexes are depicted in Figs. 6.1 and 6.2.

Table 6.2. IR spectral assignments (cm<sup>-1</sup>) of thiosemicarbazones and their Zn(II) complexes

Compound	v(O-H)	v(C=N)	v(C=N) <sup>a</sup>	v(N-N)	v(C=S)/ν(C-S), δ(C=S)/δ(C-S)	v(C-O)	v(Zn-N)
H <sub>2</sub> bspt	3366	1625	---	1112	1330, 832	1261	---
[Zn <sub>2</sub> (bspt) <sub>2</sub> ] ( <b>21</b> )	---	1598	1486	1130	1308, 834	1177	557
[Zn(bspt)(phen)]·H <sub>2</sub> O ( <b>22</b> )	---	1598	1497	1130	1302, 834	1177	498
[Zn(bspt)(bipy)] ( <b>23</b> )	---	1601	1497	1127	1308, 838	1172	499
[Zn(bspt)(4,4'-dmbipy)] ( <b>24</b> )	---	1602	1486	1128	1308, 838	1193	519
[Zn(bspt)(5,5'-dmbipy)] ( <b>25</b> )	---	1586	1486	1116	1301, 832	1178	616
Hbpet	---	1583	---	1107	1306, 812	---	---
[Zn(bpet)(dca)] <sub>n</sub> ( <b>26</b> )	---	1590	1548	1118	1298, 823	---	510
[Zn(Hbpet) <sub>2</sub> ](NO <sub>3</sub> ) <sub>2</sub> ·H <sub>2</sub> O ( <b>27</b> )	---	1560	1456	1091	1309, 792	---	466
[Zn(bpet)(OAc)] ( <b>28</b> )	---	1644	1580	1146	1319, 788	---	412

<sup>a</sup> = newly formed C=N bond

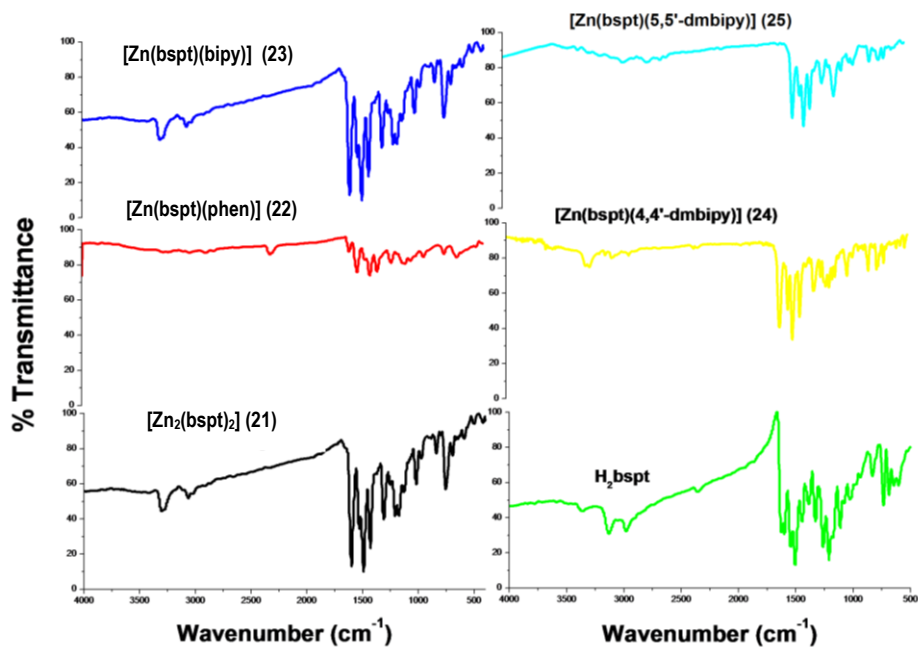


Fig. 6.1. Infrared spectra of thiosemicarbazone H<sub>2</sub>bspt and its Zn(II) complexes.

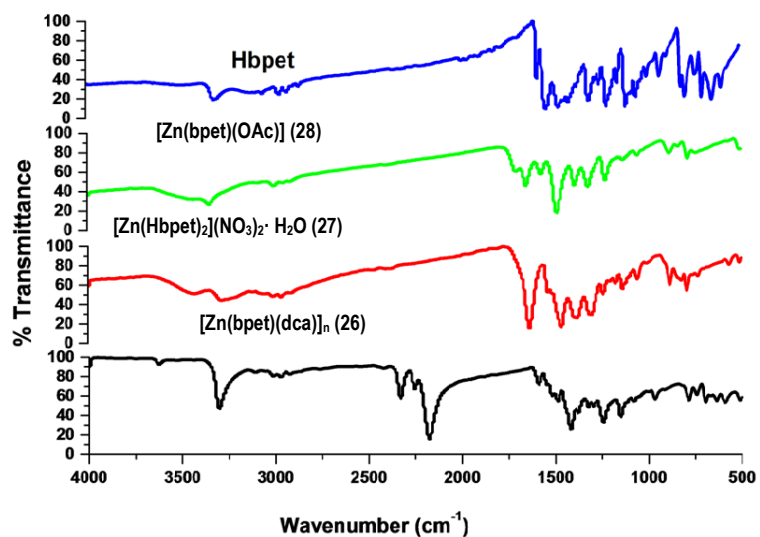


Fig. 6.2. Infrared spectra of thiosemicarbazone Hbpet and its Zn(II) complexes.

### 6.3.4 Electronic spectra

Electronic spectroscopy is an important and valuable tool for chemists to draw important information about the structural aspects of complexes. The UV-Vis spectra of the Zn(II) complexes were studied in DMF. The bands in the range 30000-31500 cm<sup>-1</sup> in the electronic spectra of thiosemicarbazones due to intraligand transitions suffered marginal shifts upon complexation. This may be due to the weakening of the C=S bond and the extensive conjugation upon complexation [121]. The shift occurs also due to coordination *via* phenolic oxygen and azomethine nitrogen [122] and is an indication of the enolization followed by the deprotonation of the ligands during complexation. In addition to this, a new band in the range 24290-25900 cm<sup>-1</sup> is observed in the spectra of complexes and this can be assigned to the Zn → O<sub>phenolate</sub>, Zn → N<sub>azomethine</sub> and Zn → S MLCT transitions [249,215]. The electronic spectral data of the Zn(II) complexes are given in Table 6.3. Figs. 6.3 and 6.4 represent the electronic spectra of the complexes.

**Table 6.3. Electronic spectral assignments (cm<sup>-1</sup>) of thiosemicarbazones and their Zn(II) complexes**

Compounds	n→π*/π→π*	MLCT
H <sub>2</sub> bspt	30100, 24320	----
[Zn(bspt) <sub>2</sub> ] ( <b>21</b> )	30420	25430
[Zn(bspt)(phen)]·H <sub>2</sub> O ( <b>22</b> )	31000	24460
[Zn(bspt)(bipy)] ( <b>23</b> )	31020	25650
[Zn(bspt)(4,4'-dmbipy)] ( <b>24</b> )	31130	25810
[Zn(bspt)(5,5'-dmbipy)] ( <b>25</b> )	30960	25700
Hbpet	30840, 23600	----
[Zn(bpet)(dca)] <sub>n</sub> ( <b>26</b> )	30010	24190
[Zn(Hbpet) <sub>2</sub> ](NO <sub>3</sub> ) <sub>2</sub> ·H <sub>2</sub> O ( <b>27</b> )	30020	24290
[Zn(bpet)(OAc)] ( <b>28</b> )	31410	24290

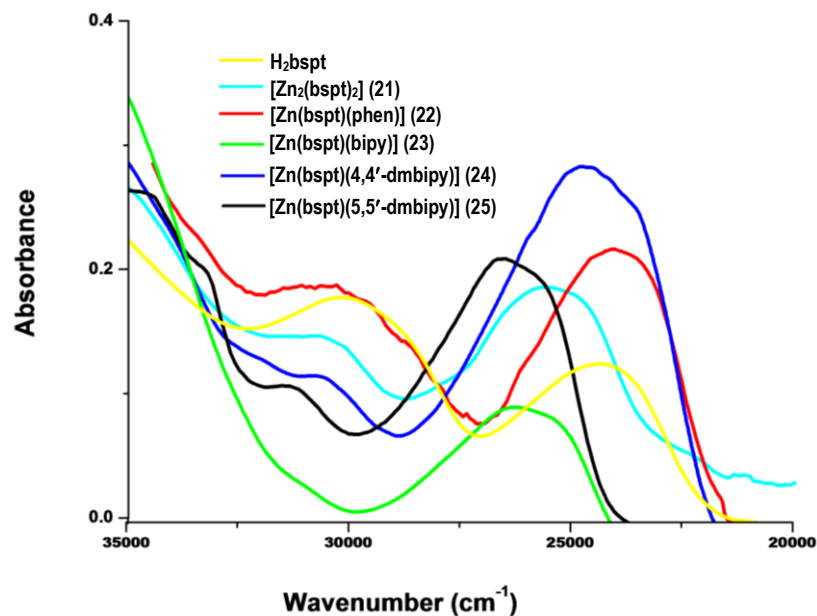
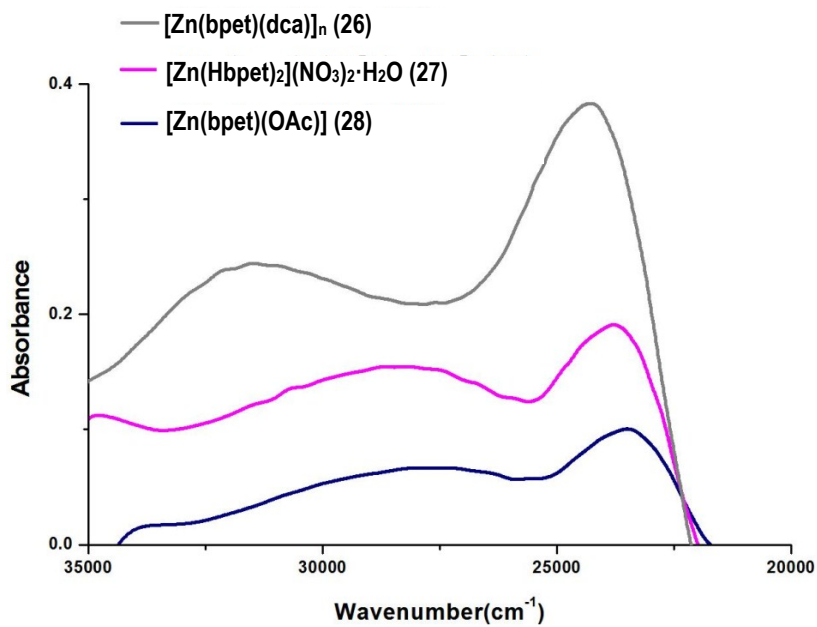
Fig. 6.3. Electronic spectra of Zn(II) complexes of H<sub>2</sub>bspt.

Fig. 6.4. Electronic spectra of Zn(II) complexes of Hbpet.



### 6.3.5. <sup>1</sup>H NMR spectra

Proton magnetic resonance spectroscopy is a powerful tool for the spectral studies of diamagnetic complexes. The <sup>1</sup>H NMR spectral data of the ligand Hbpet and its complex [Zn(Hbpet)](NO<sub>3</sub>)<sub>2</sub>·H<sub>2</sub>O (**27**) were recorded in DMSO-d<sub>6</sub> with tetramethylsilane as an internal standard.

In the case of [Zn(Hbpet)](NO<sub>3</sub>)<sub>2</sub>·H<sub>2</sub>O (**27**) complex (Fig. 6.5), the spectra are only slightly modified, with the same multiplicity of the signals and some slight changes in the chemical shifts with respect to the ligand. The singlet which integrate as a single hydrogen present in the spectrum of the ligand at 13.6 ppm is not disappeared in the spectrum of the complex. This provides an evidence for the existence of the neutral form of the thiosemicarbazone in the complex.

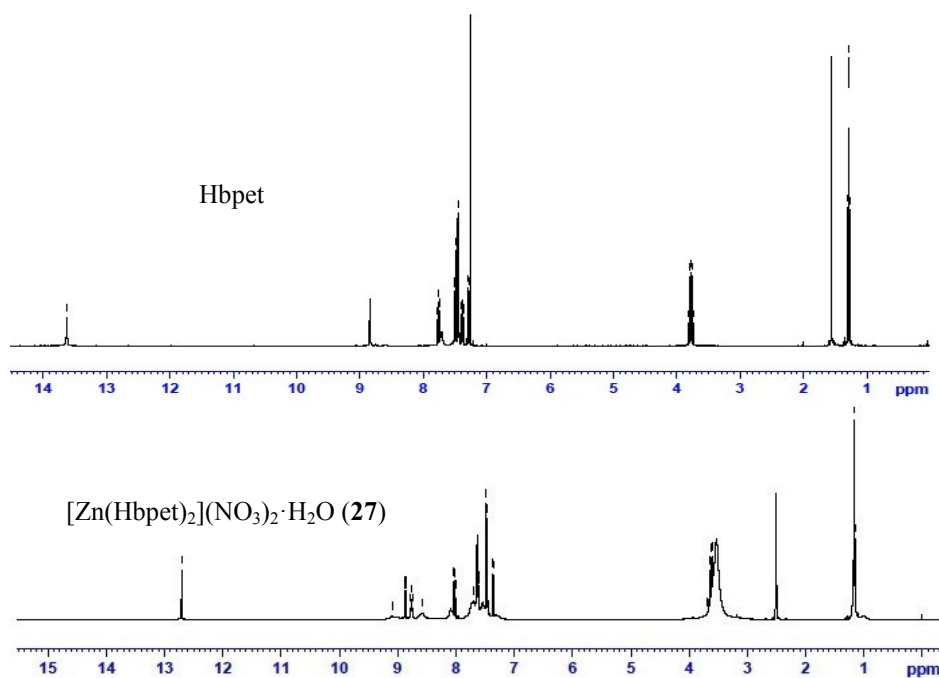


**Fig. 6.5.** <sup>1</sup>H NMR spectra of Zn(II) complex of Hbpet.

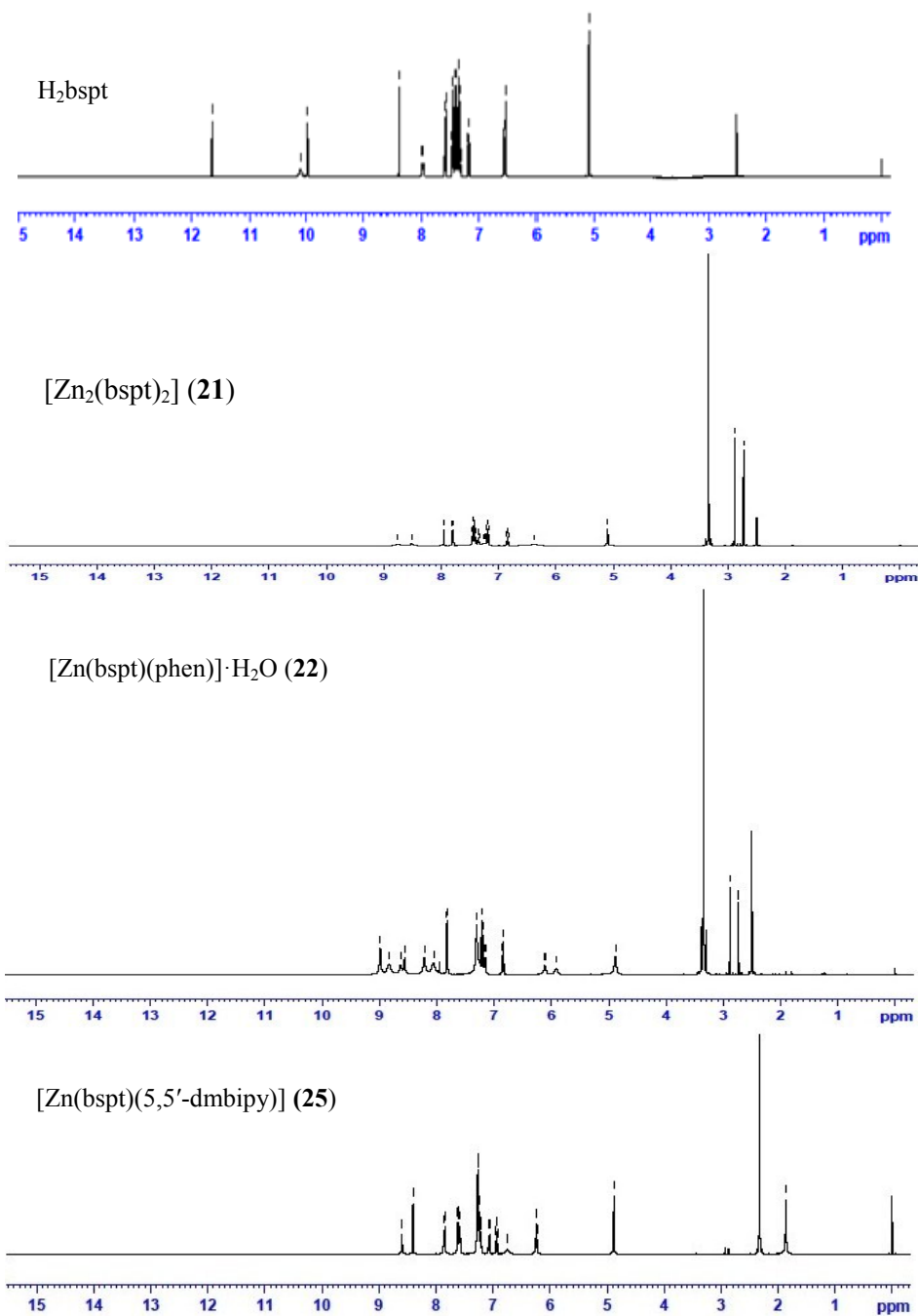


Fig. 6.6.  $^1\text{H}$  NMR spectra of  $\text{Zn}(\text{II})$  complexes of  $\text{H}_2\text{bspt}$ .

The <sup>1</sup>H NMR spectrum of the ligand H<sub>2</sub>bspt and its complexes **21**, **22** and **25** was recorded with deuterated dimethylsulfoxide (DMSO-d<sub>6</sub>) as solvent and trimethylsilane (TMS) as the internal standard. It is shown in Fig. 6.6.

A sharp singlet, which integrates as one hydrogen at 11.632 ppm is assigned to the –OH proton, and another similar singlet at 10.095 ppm is assigned to the N(2)H proton present in the spectrum of the ligand disappears in the spectra of the complexes because of the deprotonation on complex formation. This provides an evidence for the coordination of thiolato sulfur through iminolization followed by deprotonation.

### 6.3.6 X-ray crystallography

Single crystals of the complexes [Zn(bpet)(dca)]<sub>n</sub> (**26**) and [Zn(Hbpet)<sub>2</sub>](NO<sub>3</sub>)<sub>2</sub>·H<sub>2</sub>O (**27**) suitable for X-ray diffraction studies were obtained by slow evaporation of the mother liquor over 3 days. The crystallographic data and structure refinement parameters for the complexes are given in Table 6.4. All H atoms on C were placed in calculated positions, guided by difference maps, with C–H bond distances 0.93–0.96 Å and were included in the refinement in the riding model approximation, with *U*(H) set to 1.2 to 1.5 *U*(C,N). Nitrogen bound H-atoms were located from the difference Fourier map and its distance was restrained to 0.88±0.01 Å. H atoms were assigned as *U*<sub>iso</sub>=1.2*U*<sub>eq</sub> (1.5 for Me).

In the complex  $[\text{Zn}(\text{bpet})(\text{dca})]_n$  (**26**), N4–H4' hydrogen atom was located from difference maps and their distances were restrained using DFIX instructions. Orange block shaped crystal of the compound (**26**) having approximate dimensions of  $0.30 \times 0.25 \times 0.20 \text{ mm}^3$  was selected. In the complex  $[\text{Zn}(\text{Hbpet})_2](\text{NO}_3)_2 \cdot \text{H}_2\text{O}$  (**27**), N3–H3', N7–H7, O1S–H1A, O1S–H1B H atoms were located from difference maps and their distances were restrained using DFIX instructions. H1A–H1B hydrogen atom was located from difference maps and the distance was restrained using DFIX and DANG instructions. The unit cell parameters were determined and the data collections were performed on a Bruker SMART APEXII CCD diffractometer with graphite-monochromated Mo K $\alpha$  ( $\lambda = 0.71073 \text{ \AA}$ ) radiation at the Sophisticated Analytical Instruments Facility (SAIF), Cochin University of Science and Technology, Kochi-22, Kerala, India. The programs SAINT and XPREP were used for data reduction and APEX2 and SAINT were used for cell refinement [95]. The structure was solved by direct methods using SHELXS97 [64] and refined by full-matrix least-squares refinement on  $F^2$  using SHELXL97 [65]. The molecular and crystal structures were plotted using DIAMOND version 3.2g [66].

### 6.3.6a *Crystal structures of the compound $[\text{Zn}(\text{bpet})\text{dca}]_n$ (**26**) and $[\text{Zn}(\text{Hbpet})_2](\text{NO}_3)_2 \cdot \text{H}_2\text{O}$ (**27**)*

#### *$[\text{Zn}(\text{bpet})\text{dca}]_n$ (**26**)*

Orange crystals of  $[\text{Zn}(\text{bpet})(\text{dca})]_n$ , suitable for X-ray diffraction study were obtained by recrystallization of compound in methanol. Crystallographic data of complex **26** indicate that the Zn(II) ion is pentacoordinated in a distorted square-based pyramidal structure (Fig. 6.7).

**Table 6.4. Crystal data and structure refinement parameters for complex 26 and 27**

Parameters	[Zn(bpet)(dca)] <sub>n</sub> (26)	[Zn(Hbpet) <sub>2</sub> ](NO <sub>3</sub> ) <sub>2</sub> ·H <sub>2</sub> O (27)
Empirical formula	C <sub>17</sub> H <sub>15</sub> N <sub>7</sub> SZn	C <sub>30</sub> H <sub>34</sub> N <sub>10</sub> O <sub>7</sub> S <sub>2</sub> Zn
Formula weight	414.82	776.20
Color	Orange	Orange
Temperature (T) K	296(2)	296(2)
Wavelength (Mo Kα) (Å)	0.71073	0.71073
Crystal system	Monoclinic	Orthorhombic
Space group	<i>P</i> 2 <sub>1</sub> / <i>c</i>	<i>Pca</i> 2 <sub>1</sub>
Cell parameters		
a	10.0827(4) Å	38.612(6) Å
b	12.7099(5) Å	9.1358(13) Å
c	14.5117(6) Å	10.0943(15) Å
α	90°	90°
β	99.6060(10)°	90°
γ	90°	90°
Volume V (Å <sup>3</sup> )	1833.60(13)	3560.8(9)
Z	4	4
Calculated density (ρ) (mg m <sup>-3</sup> )	1.503	1.448
Absorption coefficient, μ(mm <sup>-1</sup> )	1.469	0.867
F(000)	848	1608
Crystal size (mm <sup>3</sup> )	0.30 × 0.25 × 0.20	0.30 × 0.25 × 0.20
θ range for data collection	2.60 to 28.27°	2.29 to 27.00°
Limiting indices	-13 ≤ h ≤ 12, -13 ≤ k ≤ 16, -18 ≤ l ≤ 19 -22 ≤ 1 ≤ 17	-47 ≤ h ≤ 49, -11 ≤ k ≤ 10, -11 ≤ l ≤ 12
Reflections collected	14669	17950
Unique Reflections (R <sub>int</sub> )	4555 [R(int) = 0.0307]	4043 [R(int) = 0.0579]
Completeness to θ	28.27 (99.4 %)	27.00 (98.1 %)
Absorption correction	Semi-empirical from equivalents	Semi-empirical from equivalents
Maximum and minimum transmission	0.745 and 0.650	0.764 and 0.675
Refinement method	0.745 and 0.650	Full-matrix least-squares on F <sup>2</sup>
Data / restraints / parameters	4527 / 1 / 240	4043 / 6 / 469
Goodness-of-fit on F <sup>2</sup>	1.048	1.300
Final R indices [I > 2σ (I)]	R <sub>1</sub> = 0.0328, wR <sub>2</sub> = 0.0858	R <sub>1</sub> = 0.0740, wR <sub>2</sub> = 0.1479
R indices (all data)	R <sub>1</sub> = 0.0502, wR <sub>2</sub> = 0.0929	R <sub>1</sub> = 0.0879, wR <sub>2</sub> = 0.1521
Largest difference peak and hole (e Å <sup>-3</sup> )	0.389 and -0.317	0.437 and -0.650

$$R_1 = \sum ||F_o| - |F_c|| / \sum |F_o|$$

$$wR_2 = [\sum w(F_o^2 - F_c^2)^2 / \sum w(F_o^2)]^{1/2}$$

The compound crystallized in monoclinic space group,  $P2_1/c$ . The crystal structure consist of Zn atom coordinated by deprotonated ligand and two bridged dicynamide ligand. The structure of  $[\text{Zn}(\text{bpet})(\text{dca})]_n$  is made up of  $[\text{Zn}(\text{bpet})(\text{dca})]$  units, which are connected by a  $\text{C}_2\text{N}_3^-$  group acting as bridge between two units, leading infinite 1D chains running along the  $b$  direction (Figure 6.8). The coordination geometry around Zn atom can be visualized as distorted square pyramid. In a five coordinate system, the angular structural parameter ( $\tau$ ) is used to propose an index of trigonality. The value of  $\tau$  is defined by an equation represented by  $\tau = (\beta - \alpha)/60$ , where  $\beta$  is the greatest basal angle (N1–Zn1–S1) and  $\alpha$  is the second greatest angle (N5–Zn1–N2). The value of the parameter  $\tau$  defined by Addison *et al.* is 0.0143 ( $\tau = 0$  for a regular square-based pyramid).

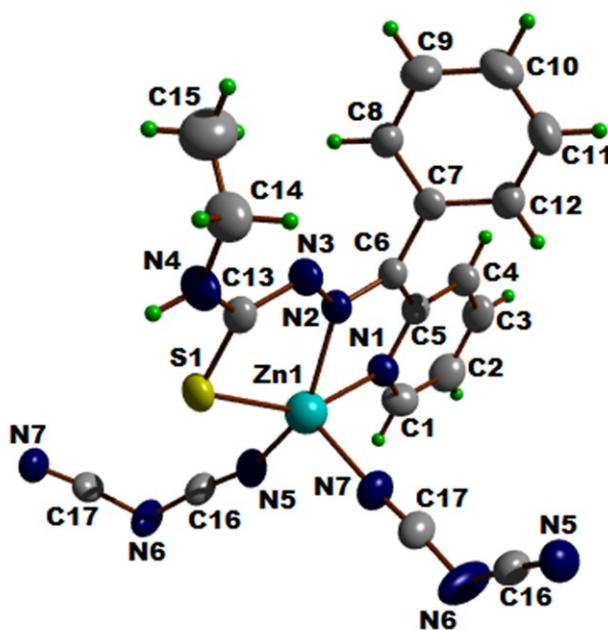
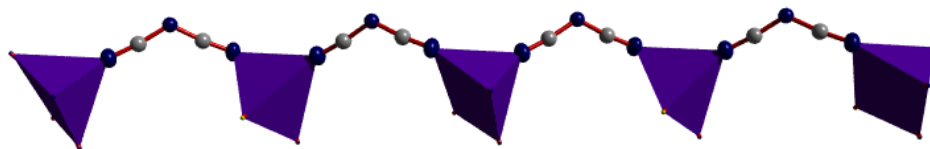
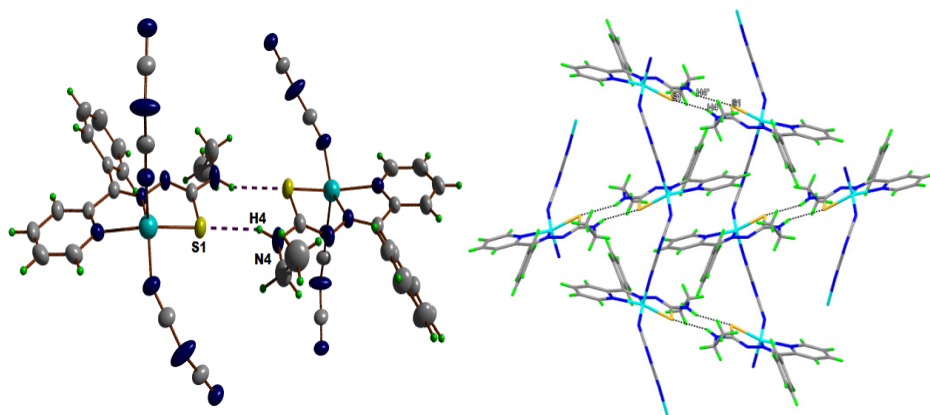


Fig. 6.7. Asymmetric unit of  $[\text{Zn}(\text{bpet})(\text{dca})]_n$  (26) along with atom numbering scheme.

Basal plane consist of azomethine N, pyridine N and S atom from ligand and N atom from dicynamide ligand and the axial site is occupied by a N atom of dicynamide ligand of the next monomeric unit. The dicynamide ligand employed the  $\mu_{1,5}$  bridge mode linking the adjacent Zn atom to produce one dimensional zig-zag chains (Fig. 6.8). Two parallel layers are interwoven to generate an interpenetrated two-dimensional sheet through intermolecular hydrogen bonding (Fig. 6.9). Selected bond distances and bond angles are given in Table 6.5 and interaction parameters are given in Table 6.6. C–H $\cdots\pi$  interactions of  $[\text{Zn}(\text{bpet})(\text{dca})]_n$  (26) is shown in Fig. 6.10.



**Fig. 6.8.** Coordination polyhedra of  $[\text{Zn}(\text{bpet})(\text{dca})]_n$  (26).



**Fig. 6.9.** Intermolecular hydrogen bonding interactions of  $[\text{Zn}(\text{bpet})(\text{dca})]_n$  (26).

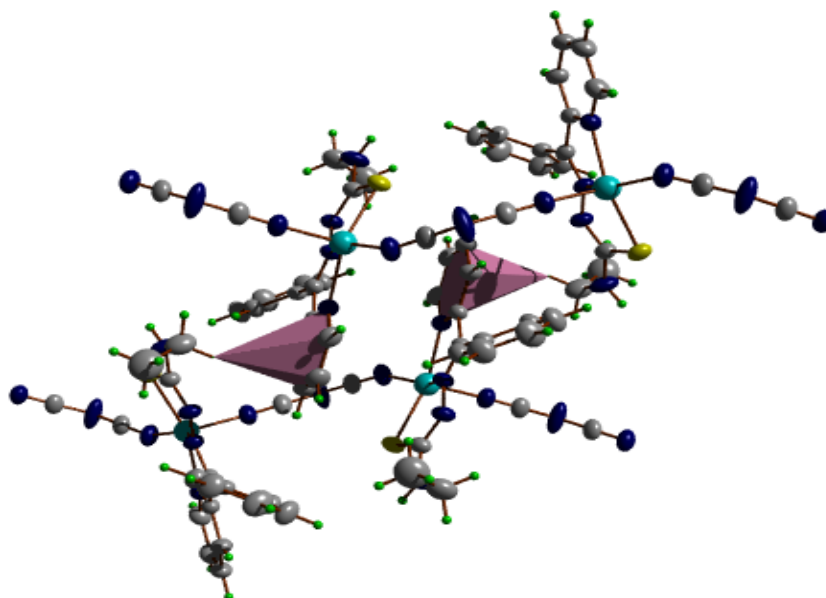


Fig. 6.10. C–H··· $\pi$  interactions of  $[\text{Zn}(\text{bpet})(\text{dca})]_n$  (26).

Table 6.5. Selected bond lengths and angles for complex 26

Bond lengths (Å)		Bond angles (°)	
Zn(1)–S(1)	2.373(6)	N(7)–Zn(1)–N(2)	105.45(7)
Zn(1)–N(2)	2.109(18)	N(5)–Zn(1)–N(2)	148.64(8)
Zn(1)–N(1)	2.143(17)	N(7)–Zn(1)–N(1)	97.18(7)
Zn(1)–N(5)	2.058(19)	N(5)–Zn(1)–N(1)	94.71(7)
Zn(1)–N(7)	2.026(19)	N(2)–Zn(1)–N(1)	75.76(6)
S(1)–C(13)	1.741(2)	N(7)–Zn(1)–S(1)	107.20(6)
N(2)–N(3)	1.357(2)	N(5)–Zn(1)–S(1)	96.17(6)
N(2)–C(6)	1.300(2)	N(2)–Zn(1)–S(1)	80.21(5)
N(3)–C(13)	1.324(3)	N(1)–Zn(1)–S(1)	149.50(5)



Table 6.6. Interaction parameters

Hydrogen bonding				
D–H···A	D–H (Å)	H···A (Å)	D···A (Å)	D–H···A (°)
N(4)–H(4')···S(1) <sup>a</sup>	0.870(16)	2.562(18)	3.385(2)	158(2)
C–H···π Interactions				
C–H···Cg	C–H (Å)	H···Cg (Å)	C···Cg (Å)	∠C–H···Cg(°)
C(14)–H(14A)···Cg(3) <sup>b</sup>	0.94	2.93	3.774	147

Equivalent position codes: a = -x+1, -y+1, -z+2, b = 1-x, -1/2+y, 3/2-z

Cg(3) = N(1), C(1), C(2), C(3), C(4), C(5)

A = acceptor, D = Donor, Cg = Centroid

#### [Zn(Hbpet)<sub>2</sub>](NO<sub>3</sub>)<sub>2</sub>·H<sub>2</sub>O (27)

Small orange needle crystals of **27** (0.30 × 0.25 × 0.20) cm<sup>3</sup> were obtained by slow evaporation from a methanol-DMF solution. The molecular structure of the Zn complex with atom numbering scheme is given in Fig. 6.11. Selected bond lengths and bond angles are represented in Table 6.7. Single crystal X-ray diffraction analysis reveals that this complex belongs to the orthorhombic, space group, *Pca*2<sub>1</sub>. This compound consists of cationic species [Zn(Hbpet)], two non-coordinating nitrate radical anions NO<sub>3</sub><sup>-</sup> and one water molecule in the asymmetric unit. In compound [Zn(Hbpet)](NO<sub>3</sub>)<sub>2</sub>·H<sub>2</sub>O (**27**), Zn centre displays a distorted octahedral geometry. The inter and intra molecular hydrogen bonding interactions of [Zn(Hbpet)](NO<sub>3</sub>)<sub>2</sub>·H<sub>2</sub>O (**27**) are shown in Fig. 6.12.

Table 6.7. Selected bond lengths and angles for complex 27

Bond lengths		Bond angles	
Zn(1)–S(1)	2.465(3)	N(5)–Zn(1)–N(2)	100.0(2)
Zn(1)–N(1)	2.200(7)	N(5)–Zn(1)–N(1)	91.9(3)
Zn(1)–N(5)	2.170(7)	N(2)–Zn(1)–N(1)	74.0(2)
Zn(1)–N(2)	2.170(6)	N(2)–Zn(1)–N(6)	172.2(3)
Zn(1)–N(6)	2.190(5)	N(1)–Zn(1)–N(6)	100.5(3)
Zn(1)–S(2)	2.433(3)	N(5)–Zn(1)–S(2)	153.74(19)
S(1)–C(13)	1.697(8)	N(2)–Zn(1)–S(2)	106.03(16)
S(2)–C(28)	1.684(8)	N(1)–Zn(1)–S(2)	92.30(18)
N(2)–C(6)	1.280(10)	N(6)–Zn(1)–S(2)	79.53(16)
N(2)–N(3)	1.343(9)	N(5)–Zn(1)–S(1)	90.5(2)
N(6)–C(21)	1.295(9)	N(2)–Zn(1)–S(1)	78.72(17)
N(6)–N(7)	1.342(9)	N(1)–Zn(1)–S(1)	152.66(18)
N(7)–C(28)	1.403(10)	N(6)–Zn(1)–S(1)	106.3(2)
		S(2)–Zn(1)–S(1)	97.48(11)

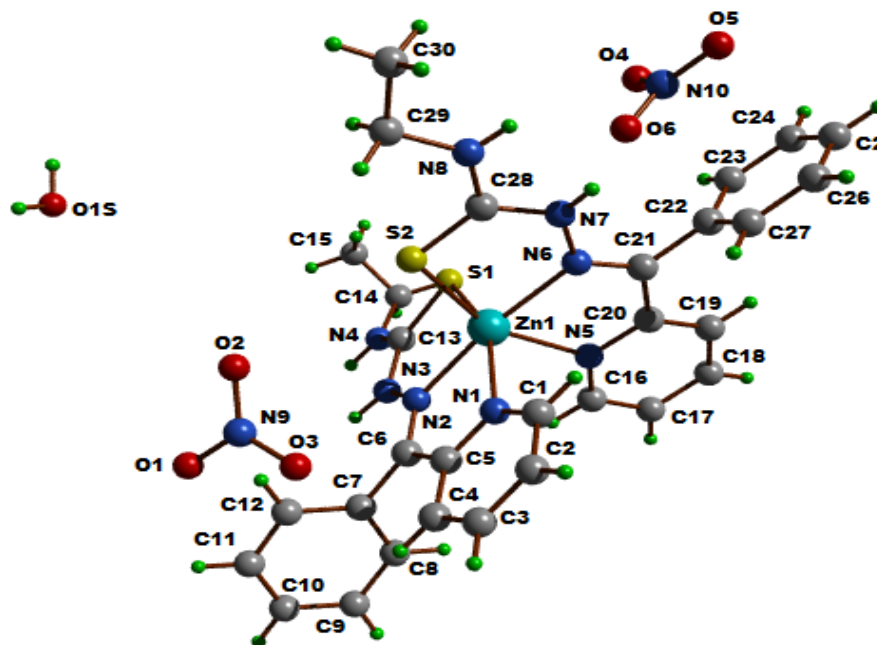


Fig. 6.11. Molecular structure of [Zn(Hbpet)<sub>2</sub>](NO<sub>3</sub>)<sub>2</sub>·H<sub>2</sub>O (27) along with atom numbering scheme.

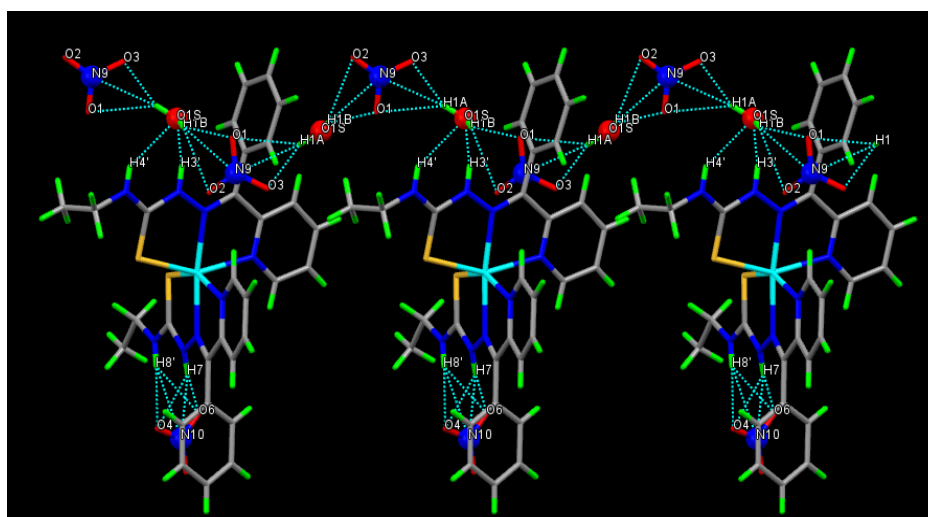


Fig. 6.12. Inter and intra molecular hydrogen bonding interactions of [Zn(Hbpet)<sub>2</sub>](NO<sub>3</sub>)<sub>2</sub>·H<sub>2</sub>O (27).

The zinc in the complex is hexacoordinated through two thioamide sulfur atoms, two azomethine nitrogen and two pyridyl nitrogen atoms. The basal plane consist of two pyridyl nitrogen and two thioamide sulfur atoms and the apical positions are occupied by azomethine nitrogen atoms which is evident from the *trans* angle of about  $172.2(3)^\circ$  (angle between N6–Zn1–N2). There are a large number of intra and intermolecular hydrogen bonding interactions in the crystal structure of the complex. Two oxygen atoms of nitrate anion are hydrogen bonded to two hydrogen atoms of water molecules. Every mononuclear unit is linked with other ones through this intermolecular hydrogen bond to form one-dimensional (1D) infinite chain of hydrogen bond system. Three-dimensional (3D) polymeric network arrangement was built *via* weak N–O $\cdots\pi$  and CH $\cdots\pi$  interactions between [Zn(Hbpet)] moieties (Fig. 6.14). Ring puckering analyses and least square plane calculations show that the Cg(4) ring comprising of atoms Zn(1), N(5), C(20), C(21) and N(5) adopts a half chair conformation twisted on Zn(1) and N(5) atoms. Cremer & Pople puckering parameter, Q(2) = 0.085(6) Å [250]. Packing diagram of [Zn(Hbpet)](NO<sub>3</sub>)<sub>2</sub>·H<sub>2</sub>O (27) viewed along ‘c’ axis is shown in Fig. 6.13.

**Table 6.8.** Inter and intra molecular hydrogen bonding interactions of [Zn(Hbpet)](NO<sub>3</sub>)<sub>2</sub>·H<sub>2</sub>O (27)

Intermolecular hydrogen bonding				
D–H···A	D–H	H···A	D···A	D–H···A
N(4)–H(4')···O(1S) <sup>a</sup>	0.86	2.34	3.070(12)	143.7
N(3)–H(3')···O(1S) <sup>a</sup>	0.880(11)	2.10(7)	2.844(11)	142(10)
O(1S)–H(1A)···O(3) <sup>b</sup>	0.859(11)	2.00(11)	2.811(13)	156(25)
O(1S)–H(1A)···O(1) <sup>b</sup>	0.859(11)	2.44(16)	3.180(12)	144(23)
O(1S)–H(1A)···N(9) <sup>b</sup>	0.859(11)	2.57(4)	3.419(14)	169(14)
O(1S)–H(1B)···O(1) <sup>c</sup>	0.861(11)	2.27(5)	3.018(13)	145(8)
O(1S)–H(1B)···O(2) <sup>c</sup>	0.861(11)	2.56(7)	3.188(16)	131(7)
Intramolecular hydrogen bonding				
N(8)–H(8')···O(6)	0.86	2.20	2.917(15)	140.9
N(8)–H(8')···O(4)	0.86	2.36	3.138(11)	150.4
N(8)–H(8')···N(10)	0.86	2.63	3.462(11)	161.7
N(7)–H(7)···O(4)	0.881(11)	2.25(7)	3.000(11)	142(9)
N(7)–H(7)···O(6)	0.881(11)	2.35(5)	3.161(12)	153(9)
N(7)–H(7)···N(10)	0.881(11)	2.64(3)	3.501(11)	165(9)

Equivalent position codes :  $a = -x, -y + 1, z + \frac{1}{2}$ ,  $b = x, y, z - 1$ ,  $c = -x, -y = 2, z - \frac{1}{2}$

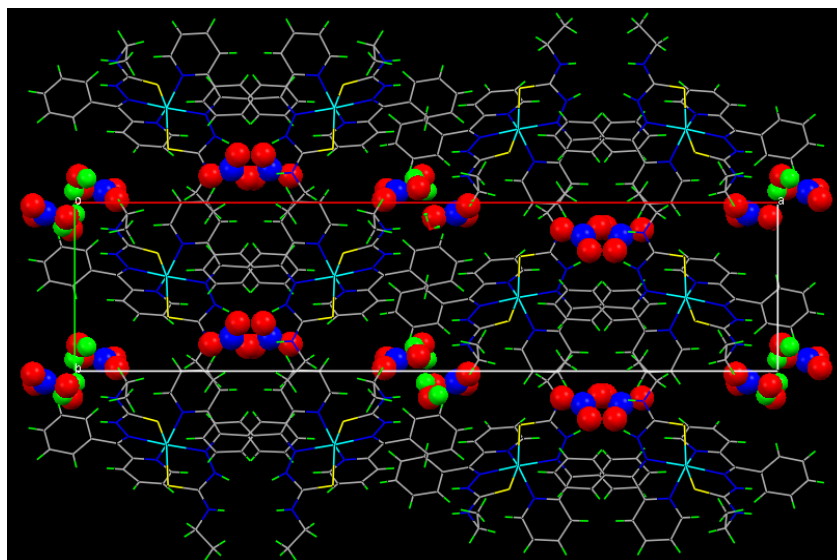


**Fig. 6.13.** Packing diagram of [Zn(Hbpet)<sub>2</sub>](NO<sub>3</sub>)<sub>2</sub>·H<sub>2</sub>O (27) viewed along *c* axis.

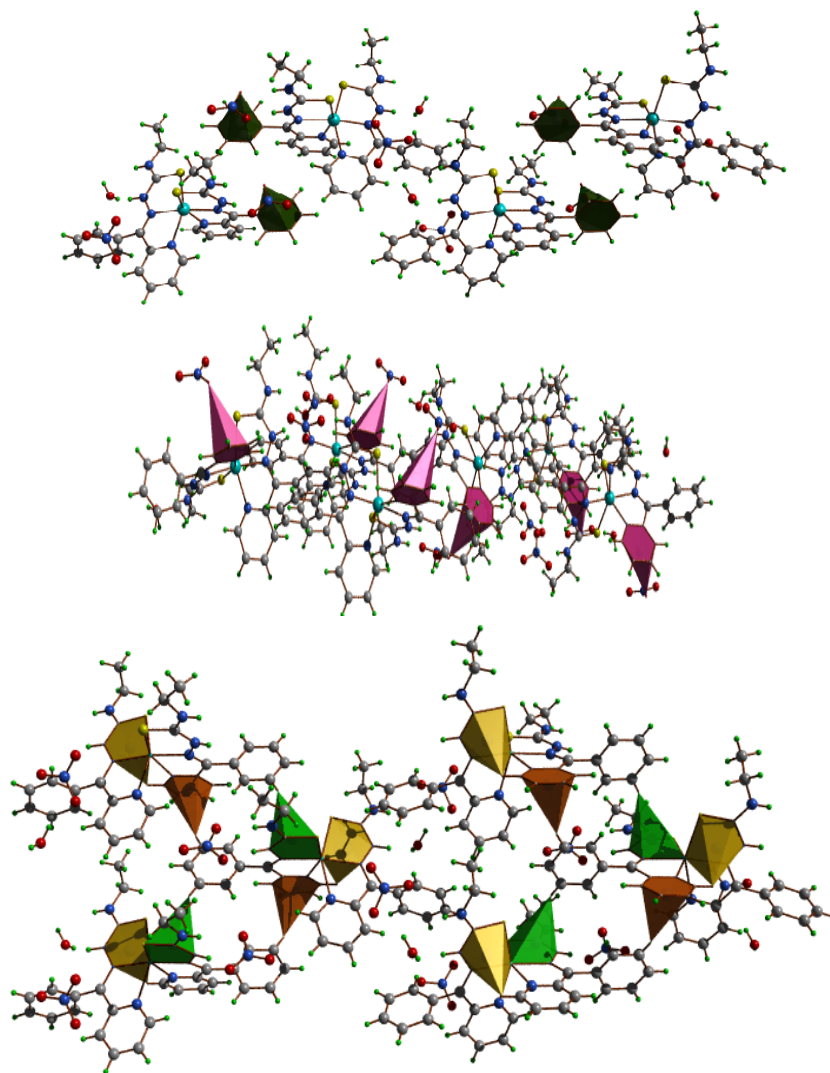


**Fig. 6.14.** N–O··· $\pi$  and C–H··· $\pi$  interactions in Zn(Hbpet)<sub>2</sub>(NO<sub>3</sub>)<sub>2</sub>·H<sub>2</sub>O (27).

**Table 6.9. Interaction parameters**

<b>C–H⋯π Interactions</b>				
<b>C–H⋯Cg</b>	<b>C–H (Å)</b>	<b>H⋯Cg (Å)</b>	<b>C⋯Cg (Å)</b>	<b>∠C–H⋯Cg(°)</b>
C16–H16⋯Cg(1) <sup>a</sup>	0.93	2.92	3.316(11)	107
C24–H24⋯Cg(6) <sup>b</sup>	0.93	2.98	3.845(11)	156
C26–H26⋯Cg(2) <sup>c</sup>	0.93	2.94	3.740(11)	145
<b>N–O⋯π Interactions</b>				
<b>N–O⋯Cg</b>	<b>N–O (Å)</b>	<b>O⋯Cg (Å)</b>	<b>N⋯Cg (Å)</b>	<b>∠N–O⋯Cg(°)</b>
N10–O4⋯Cg(8) <sup>d</sup>	1.173	3.481(11)	3.849(11)	99(7)
N9–O3⋯Cg(5) <sup>d</sup>	1.216	3.619(10)	4.292(10)	115.2(7)

Equivalent position codes: a = x,y,z; b = 1/2-x, y, -1/2+z; c = 1/2-x, y, 1/2+z; d = x, y, z

Cg(1) = Zn(1), S(1), C(13), N(3), N(2)

Cg(6) = N(5), C(16), C(17), C(18), C(19), C(20)

Cg(2) = Zn(1), S(2), C(28), N(7), N(6)

Cg(8) = C(22), C(23), C(24), C(25), C(26), C(27)

Cg(5) = N(1), C(1), C(2), C(3), C(4), C(5)

A = acceptor, D = Donor, Cg = Centroid of the ring

..........





# Chapter 7

## SYNTHESES, SPECTRAL AND STRUCTURAL CHARACTERIZATION OF Cd(II) COMPLEXES OF ONS AND NNS DONOR THIOSEMICARBAZONES

Contents	7.1 <i>Introduction</i>
	7.2 <i>Experimental</i>
	7.3 <i>Results and discussion</i>

### 7.1 Introduction

Cadmium is a lustrous, silver-white, ductile, very malleable metal. Its surface has a bluish tinge and the metal is soft enough to be cut with a knife, but it tarnishes in air. It is soluble in acids but not in alkalis. It is similar in many respects to zinc but it forms more complex compounds. Cadmium (Latin *cadmia*, meaning "calamine", a cadmium-bearing mixture of minerals, which was named after the Greek mythological character, Cadmus, the founder of Thebes) was discovered simultaneously in 1817 by Friedrich Stromeyer and Karl Samuel Leberecht Hermann, both in Germany, as an impurity in zinc carbonate. Stromeyer found the new element as an impurity in zinc carbonate (calamine), and, for 100 years, Germany remained the only important producer of the metal.

The metal was named after the Latin word for calamine, because it was found in this zinc compound. Cadmium is a minor metallic element, one of the naturally occurring components in the earth's crust and water, and present everywhere in our environment. Naturally-occurring cadmium-sulfide based pigments were used as early as 1850 because of their brilliant red, orange and yellow colors, and appeared prominently in the paintings of Vincent Van Gogh in the late 1800s.

Cadmium(II) complexes have been extensively studied from a chemical and structural point of view, mainly due to the capability of cadmium(II) to adopt different modes of coordination (shared by most  $d^{10}$  metal ions) determined by consideration of size, as well as electrostatic and bonding forces [251]. Amongst these complexes are thiosemicarbazides, a class of metal complexes that have been shown to exhibit a wide range of biological activities, which is considered to be related to their ability to chelate metals [252]. Some complexes of thiosemicarbazide derivatives are potential anti-tumor and hypertensive agents and others are active against influenza and protozoa [253]. A number of complexes of transition metals with thiosemicarbazide-based ligands have found extensive application in medicine, technology and analytical chemistry [254]. Interest in the crystal engineering of metal complexes has stimulated investigation of means of thiosemicarbazide-based metal complexes in supramolecular structures [255]. The relatively rigid structure of metal thiosemicarbazide chelate rings and the capacity of the ligand for hydrogen bonding make these molecules potentially important for stabilization of supramolecular structures. In its

complexes, thiosemicarbazide behaves as a chelating bidentate ligand coordinated through the terminal hydrazine N atom and S atom. Complexes of the  $d^{10}$  metal ions of mixed diimine and thiolate ligands have also been shown to exhibit an interesting type of intra-ligand charge transfer transition in the visible region without the involvement of the metal ion [256]. These kinds of non-linear optical (NLO) complexes are characterized with a central metal ion surrounded by a number of organic and/or inorganic ligands [257,258]. The organic ligand is usually more dominant in the NLO effect. Much focus has been on the 11B (Zn, Cd, Hg) group metal complexes, as these metals have a high transparency in the UV region because of their closed  $d^{10}$  shell. This has stimulated research on the excited state electronic properties of thiolato- complexes of these metal ions.

## **7.2 Experimental**

### **7.2.1 Materials**

Cadmium(II) acetate dihydrate (E-Merck), cadmium chloride (anhydrous) (CDH), potassium thiocyanate (E-Merck), 1,10-phenanthroline (phen), 2,2'-bipyridine (bipy), 4,4'-dimethyl-2,2'-bipyridine (4,4'-dmbipy), 5,5'-dimethyl-2,2'-bipyridine (5,5'- dmbipy), sodium dicyanamide (Sigma-Aldrich) were used as received.

### **7.2.2 Syntheses of thiosemicarbazones**

The syntheses of thiosemicarbazones H<sub>2</sub>bspt and Hbpet are discussed already in Chapter 2.

## 7.2.3 Syntheses of cadmium complexes

### 7.2.3.1 [ $Cd_2(bspt)_2$ ] (29)

This complex was synthesized by refluxing a solution of  $H_2bspt$  (0.1885 g, 0.5 mmol) in 1:1 mixture of DMF and methanol with a methanolic solution of  $Cd(OAc)_2 \cdot 2H_2O$  (0.1332 g, 0.5 mmol) for 3 hours. The complex formed was filtered, washed with methanol and dried *in vacuo*.

Elemental Anal. Found (Calcd.) (%): C, 51.51(51.70); H, 3.10(3.51); N, 8.51(8.61); S, 6.25(6.57). Yield: 60%.

### 7.2.3.2 [ $Cd(bspt)(phen)$ ] (30)

Methanolic solution of cadmium(II) acetate dihydrate (0.1332 g, 0.5 mmol) was added to a stirred mixture of  $H_2bspt$  (0.1885 g, 0.5 mmol) in DMF and methanol and 1,10-phenanthroline (0.090 g, 0.5 mmol) in methanol. The resultant solution was refluxed for 3 hours. The orange product obtained was filtered, washed with methanol and dried *in vacuo*.

Elemental Anal. Found (Calcd.) (%): C, 58.72(59.33); H, 3.67(3.77); N, 9.77(9.46); S, 4.62(4.82). Yield: 68%.

### 7.2.3.3 [ $Cd(bspt)(bipy)$ ] (31)

To a stirred mixture of  $H_2bspt$  (0.5 mmol, 0.1885 g) in DMF and methanol and 2,2'-bipyridine (0.078 g, 0.5 mmol) in methanol, cadmium(II) acetate dihydrate (0.1332 g, 0.5 mmol) was added. The solution was refluxed for 3 hours and orange crystalline product separated out was filtered, washed with methanol and dried *in vacuo*.

Elemental Anal. Found (Calcd.) (%): C, 54.87 (55.17); H, 5.35 (5.04); N, 10.31(10.48); S, 5.02 (4.33). Yield: 62%.

#### **7.2.3.4 [Cd(bspt)(4,4'-dmbipy)] (32)**

To a stirred mixture of H<sub>2</sub>bspt (0.1885 g, 0.5 mmol) in DMF and methanol and 4,4'-dimethylbipyridine (0.0920 g, 0.5 mmol) in methanol, cadmium(II) acetate dihydrate (0.1332 g, 0.5 mmol) was added. The solution was refluxed for 3 hours and orange crystalline product separated out was filtered, washed with methanol and dried *in vacuo*.

Elemental Anal. Found (Calcd.) (%) : C, 56.72 (57.27); H, 3.07 (4.81); N, 9.89 (10.12); S, 4.62 (4.6). Yield: 73%.

#### **7.2.3.5 [Cd(bspt)(5,5'-dmbipy)] (33)**

To a stirred mixture of H<sub>2</sub>bspt (0.5 mmol, 0.1885 g) in DMF and methanol and 5,5'-dimethylbipyridine (0.0920 g, 0.5 mmol) in methanol, cadmium(II) acetate monohydrate (0.1332 g, 0.5 mmol) was added. The solution was refluxed for 3 hours and orange crystalline product separated out was filtered, washed with methanol and dried *in vacuo*.

Elemental Anal. Found (Calcd.) (%): C, 56.72(57.27); H, 3.07(4.81); N, 9.89(10.12); S, 4.62(4.6). Yield: 60%.

#### **7.2.3.6 [Cd(bpet)(NCS)] (34)**

A solution of the ligand Hbpet (0.1421 g, 0.5 mmol) in methanol was treated with a methanolic solution of Cd(OAc)<sub>2</sub>·2H<sub>2</sub>O (0.133 g, 0.5 mmol). The solution was heated under reflux and potassium thiocyanate was added to the solution and further refluxed for 4 hours. The resulting solution was allowed to stand at room temperature and

upon slow evaporation gave yellow crystals. The product then separated out was collected, washed and dried over  $P_4O_{10}$  *in vacuo*.

Elemental Anal. Found (Calcd.) (%) : C, 42.11(42.34); H, 3.80 (3.33); N, 15.71(15.43); S, 14.53 (14.13). Yield: 55%.

#### 7.2.3.7 [*Cd(bpet)(N<sub>3</sub>)*] (35)

A solution of the ligand Hbpet (0.1421 g, 0.5 mmol) in methanol was treated with a methanolic solution of cadmium acetate dihydrate (0.133 g, 0.5 mmol). The solution was heated under reflux and sodium azide was added to the solution and further refluxed for 4 hours. The resulting solution was allowed to stand at room temperature and upon slow evaporation gave yellow crystals. The product then separated out was collected, washed and dried over  $P_4O_{10}$  *in vacuo*.

Elemental Anal. Found (Calcd.) (%): C, 41.27 (41.15); H, 2.97 (3.45); N, 22.63 (22.40); S, 7.42 (7.32). Yield: 52%.

#### 7.2.3.8 [*Cd<sub>2</sub>(bpet)<sub>2</sub>(Cl)<sub>2</sub>*] (36)

A solution of the ligand Hbpet (0.142 g, 0.5 mmol) in methanol was treated with a methanolic solution of  $CdCl_2 \cdot 2H_2O$  (0.114 g, 0.5 mmol). The solution was refluxed for 4 hours. The resulting solution was allowed to stand at room temperature and upon slow evaporation gave yellow crystals. The crystals then separated out was collected washed and dried over  $P_4O_{10}$  *in vacuo*.

Elemental Anal. Found (Calcd.) (%): C, 42.08 (41.78); H, 3.71 (3.51); N, 13.02 (12.99); S, 7.84 (7.44). Yield: 62%.

### **7.3 Results and discussion**

Equimolar ratios of the thiosemicarbazones, metal acetate yielded yellow colored complexes. In complexes **30-33**, 1,10-phenanthroline, 2,2'-bipyridine, 4,4'-dimethyl-2,2'-bipyridine, 5,5'-dimethyl-2,2'-bipyridine are used as coligands and in complexes **34-36**, azide, chloride and thiocyanate were used as anions. Single crystal of compound [Cd<sub>2</sub>(bpet)<sub>2</sub>Cl<sub>2</sub>] (**36**) could be isolated and the structure was established by single crystal XRD studies. The complexes were characterized by the following physico-chemical methods.

#### **7.3.1 Elemental analyses**

From the observed C, H, N and S values, the above stoichiometry of the complexes were proposed.

#### **7.3.2 Molar conductivity measurements**

The molar conductivities of the complexes in DMF (10<sup>-3</sup> M) was measured at 298 K with a Systronic model 303 direct reading conductivity bridge. The molar conductivity measurements showed that all the complexes are non-electrolytic in nature since the observed values are less than 10 ohm<sup>-1</sup>cm<sup>2</sup>mol<sup>-1</sup> which are very much less than the value of 65-90 ohm<sup>-1</sup>cm<sup>2</sup>mol<sup>-1</sup> reported for a 1:1 electrolyte in the same solvent [110]. The molar conductivity values are given in Table 7.1.

**Table 7.1. Molar conductivity of Cd(II) complexes**

Compound	$\lambda_m^a$
[Cd <sub>2</sub> (bspt) <sub>2</sub> ] ( <b>29</b> )	4.0
[Cd(bspt)(phen)] ( <b>30</b> )	2.4
[Cd(bspt)(bipy)] ( <b>31</b> )	3.6
[Cd(bspt)(4,4'-dmbipy)] ( <b>32</b> )	6.2
[Cd(bspt)(5,5'-dmbipy)] ( <b>33</b> )	5.2
[Cd(bpet)(NCS)] ( <b>34</b> )	52.0
[Cd(bpet)(N <sub>3</sub> )] ( <b>35</b> )	13.0
[Cd <sub>2</sub> (bpet) <sub>2</sub> (Cl) <sub>2</sub> ] ( <b>36</b> )	4.8

<sup>a</sup> = mho cm<sup>2</sup> mol<sup>-1</sup>

### 7.3.3 X-ray crystallography

Single crystals of compound [Cd<sub>2</sub>(bpet)<sub>2</sub>(Cl)<sub>2</sub>] (**36**) suitable for X-ray diffraction studies were obtained by the slow evaporation of the mother liquor. Single crystals of dimensions 0.50 x 0.45 x 0.40 mm<sup>3</sup> of the complex **36** is selected and mounted on a Bruker SMART APEXII CCD diffractometer, equipped with a graphite crystal, incident-beam monochromator and a fine focus sealed tube with Mo K $\alpha$  ( $\lambda = 0.71073 \text{ \AA}$ ) radiation as the X-ray source. The crystallographic data and structure refinement parameters for compound **36** are given in Table 7.2. The unit cell dimensions were measured and the data collection was performed at 296 (2) K. Bruker SMART software was used for data acquisition and Bruker SAINT software for data integration [62]. Absorption corrections were carried out using SADABS based on Laue symmetry using equivalent reflections [63]. The structure was solved by direct methods using SHELXS97 [64] and refined by full-matrix least-squares calculations with SHELXL97 software package [65]. The



molecular and crystal structures were plotted using DIAMOND version 3.2g [66]. In  $[\text{Cd}_2(\text{bpet})_2(\text{Cl})_2]$  (**36**), all non-hydrogen atoms were refined anisotropically and all H atoms on C were placed in calculated positions, guided by difference Fourier maps, with C–H bond distances 0.93–0.96 Å. H atoms were assigned as  $U_{\text{iso}}=1.2U_{\text{eq}}$  (1.5 for Me). The N4–H4' H atom was located from difference maps and its distance is restrained to  $0.88 \pm 0.01$  Å.

### 7.3.3 Crystal structure of $[\text{Cd}_2(\text{bpet})_2(\text{Cl})_2]$ (**36**)

Crystal data and structure refinement for compound **36** are summarized in Table 7.2. The relevant bond lengths and angles for compound **36** are given in Table 7.3. The compound crystallized in a monoclinic space group  $C2/c$ . This compound is a sulfur-bridged cadmium box-dimer in which the environment of each Cd(II) atom can be described as distorted pentagonal pyramidal. Each cadmium(II) ion is pentacoordinated with four positions occupied by the two imine nitrogen atoms and sulfur atom from a thiosemicarbazone ligand while the fifth position is occupied by the sulfur atom of the adjacent  $[\text{Cd}(\text{bpet})]$  entity, acting as a bridge. This complex could be alternatively described as two cadmium monomer complexes connected through one of the sulfur atoms. S-bridged dimeric cadmium complexes are unusual for thiosemicarbazone ligands. The molecular structure of the compound **36** is shown in Fig. 7.1.

**Table 7.2. Crystal data and structure refinement parameters of [Cd<sub>2</sub>(bpet)<sub>2</sub>(Cl)<sub>2</sub>] (36)**

Parameters	[Cd <sub>2</sub> (bpet) <sub>2</sub> (Cl) <sub>2</sub> ] (36)
Empirical formula	C <sub>30</sub> H <sub>30</sub> Cd <sub>2</sub> Cl <sub>2</sub> N <sub>8</sub> S <sub>2</sub>
Formula weight	862.48
Color	Yellow
Temperature (T) K	296(2)
Wavelength (Mo K $\alpha$ ) (Å)	0.71073
Crystal system	Monoclinic
Space group	C2/c
Cell parameters	
a	20.9473(8)Å
b	12.3048(8)Å
c	16.1750(9)Å
$\alpha$	90°
$\beta$	125.339(3)°
$\gamma$	90°
Volume V (Å <sup>3</sup> )	3401.0(3)
Z	4
Calculated density ( $\rho$ ) (mg m <sup>-3</sup> )	1.684
Absorption coefficient, $\mu$ (mm <sup>-1</sup> )	1.564
F(000)	1712
Crystal size (mm <sup>3</sup> )	0.50 x 0.45 x 0.40
$\theta$ range for data collection	2.59 to 28.00°
Limiting indices	-27 $\leq$ h $\leq$ 23, -16 $\leq$ k $\leq$ 16, -20 $\leq$ l $\leq$ 20
Reflections collected	12530
Unique Reflections (R <sub>int</sub> )	4044 [R(int) = 0.0351]
Completeness to $\theta$	28.00 (98.6%)
Absorption correction	Semi-empirical from equivalents
Maximum and minimum transmission	0.535 and 0.462
Refinement method	Full-matrix least-squares on F <sup>2</sup>
Data / restraints / parameters	4100 / 1 / 204
Goodness-of-fit on F <sup>2</sup>	1.161
Final R indices [I > 2 $\sigma$ (I)]	R <sub>1</sub> = 0.0299, wR <sub>2</sub> = 0.0702
R indices (all data)	R <sub>1</sub> = 0.0375, wR <sub>2</sub> = 0.0772
Largest difference peak and hole (e Å <sup>-3</sup> )	0.916 and -0.796

The Cd<sub>2</sub>S<sub>2</sub> angles [S(1)–Cd(1)<sup>#1</sup>–S(1)#1 ] and [S(1)–Cd(1)–S(1)#1] are slightly deviated from a square planar arrangement, which can be attributed to the restricted bite angle of the donor atoms in the thiosemicarbazone ligand. The deprotonation of the ligand can be confirmed with the C–S distances, because they are longer than the typical thione double bond distance (around 1.6 Å). The [Cd(bpet)Cl]<sub>2</sub> dimer unit permits the establishment of intermolecular hydrogen bond [N(4)–H(4')···Cl(1) 2.513(17) Å] between the thioamide nitrogen proton and the chloride atom (Fig. 7.2). This interaction links two dimer units in the crystal cell giving rise to a 2D laminar packed structure (Fig. 7.3).

**Table 7.3. Selected bond lengths ad bond angles of [Cd<sub>2</sub>(bpet)<sub>2</sub>(Cl)<sub>2</sub>] (36)**

Bond lengths		Bond angles	
Cd(1)–N(1)	2.319(2)	N(1) Cd(1)–N(2)	70.28(8)
Cd(1)–N(2)	2.343(2)	N(1)–Cd(1)–Cl(1)	98.97(6)
Cd(1)–Cl(1)	2.151(5)	N(2)–Cd(1)–Cl(1)	142.92(6)
Cd(1)–S(1)	2.6162(7)	N(1)–Cd(1)–S(1)	144.18(6)
Cd(1)–S(1) <sup>#1</sup>	2.6225(8)	N(2)–Cd(1)–S(1)	74.02(6)
S(1)–C(13)	1.770(3)	Cl(1)–Cd(1)–S(1)	107.86(3)
S(1)–Cd(1) <sup>#1</sup>	2.6225(8)	N(1)–Cd(1)–S(1) <sup>#1</sup>	98.30(7)
N(2)–N(3)	1.369(3)	N(2)–Cd(1)–S(1) <sup>#1</sup>	107.96(6)
N(3)–C(13)	1.308(3)	Cl(1)–Cd(1)–S(1) <sup>#1</sup>	108.69(3)
		S(1)–Cd(1)–S(1) <sup>#1</sup>	95.16(2)
		C(13)–S(1)–Cd(1)	97.53(9)
		C(13)–S(1)–Cd(1) <sup>#1</sup>	96.39(9)
		Cd(1)–S(1)–Cd(1) <sup>#1</sup>	84.05(2)

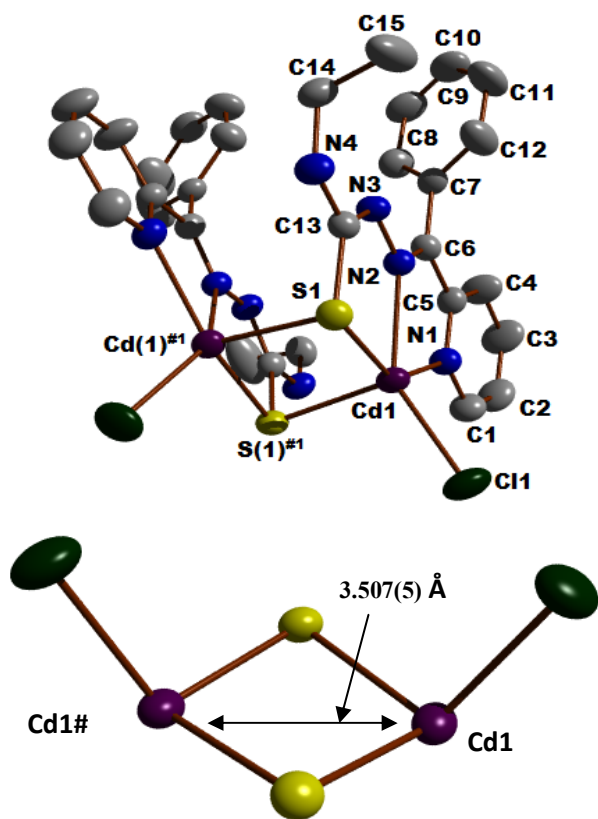


Fig. 7.1. Molecular structure of  $[\text{Cd}_2(\text{bpet})_2(\text{Cl})_2]$  (36).

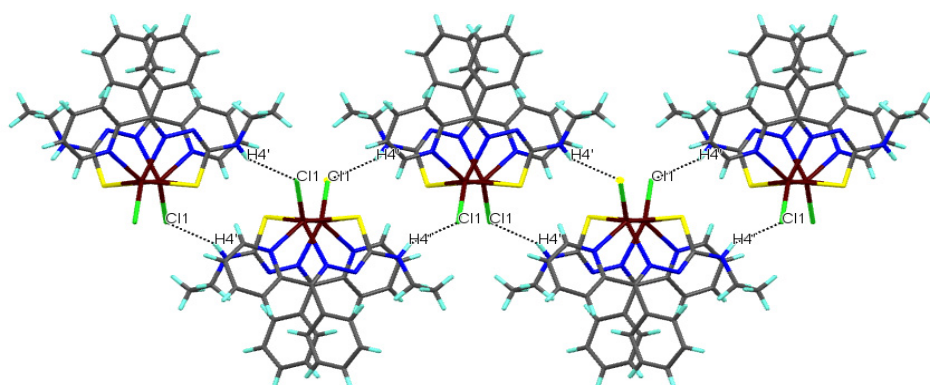
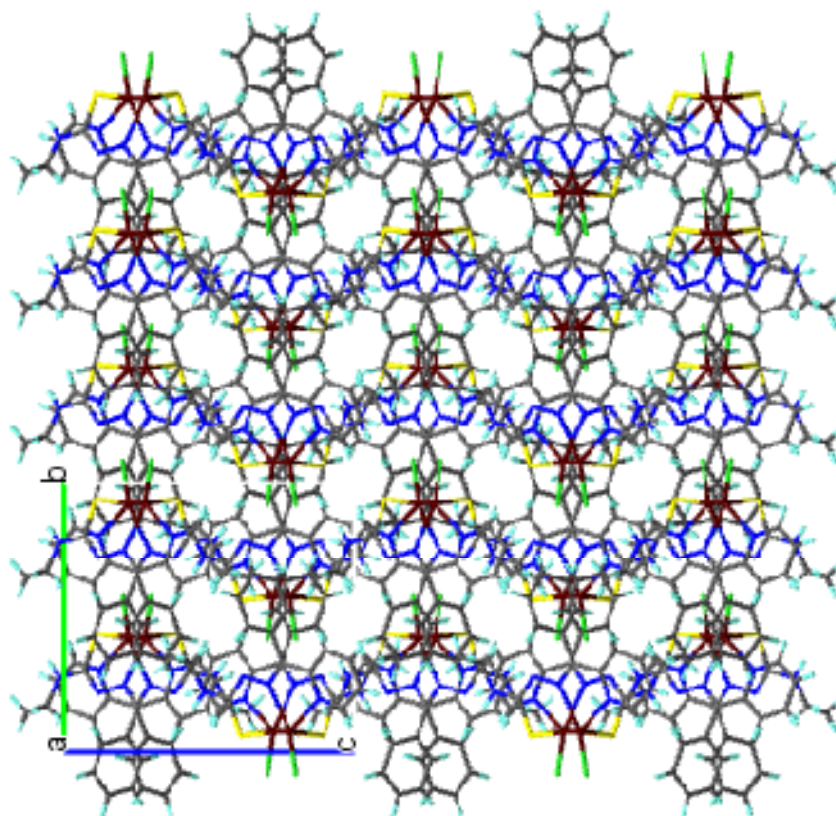
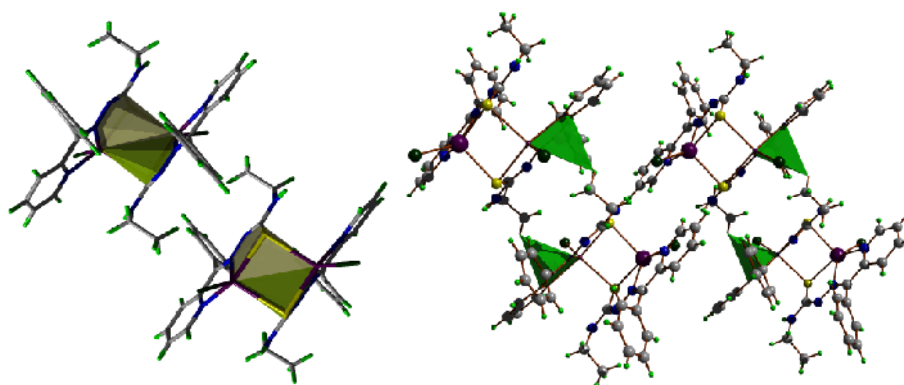


Fig. 7.2. Intermolecular hydrogen bonding interactions.



**Fig. 7.3.** Packing diagram of [Cd<sub>2</sub>(bpet)<sub>2</sub>(Cl)<sub>2</sub>] (36) viewed along 'a' axis.



**Fig. 7.4.** Metal... $\pi$  interaction and C-H... $\pi$  interactions.

Further, crystal packing is reinforced by very weak C–H··· $\pi$  and metal··· $\pi$  interactions (Fig. 7.4). Fig. 7.3 shows the packing diagram of the compound. The various interaction parameters are shown in Table 7.4.

**Table 7.4. Interaction parameters**

<b>H-bonding</b>				
<b>D–H···A</b>	<b>D–H (Å)</b>	<b>H···A (Å)</b>	<b>D···A (Å)</b>	<b>D–H···A (°)</b>
N(4)–H(4')···Cl(1) <sup>a</sup>	0.879(10)	2.513(17)	3.324(3)	154(3)
<b>C–H···<math>\pi</math> interactions</b>				
<b>C–H(I)···Cg(J)</b>	<b>C–H (Å)</b>	<b>H···Cg (Å)</b>	<b>C···Cg (Å)</b>	<b><math>\angle</math>C–H···Cg (°)</b>
C15–H15C---Cg(3)		2.86	3.440(7)	120
<b>Metal···<math>\pi</math> interaction</b>				
<b>Cg(I)···Me(J)</b>	<b>Cg···Me (Å)</b>		<b><math>\beta</math> (°)</b>	
Cg(2)–Cd(1)	3.155		35.29	

Equivalent position codes : a = x, –y + 1, z + 1/2

Cg(2)–Cd(1)–S(1)–C(13)–N(3)–N(2); Cg3–Cd(1)–N(1)–C(5)–C(6)–N(2)

D = Donor, A = acceptor, Cg = Centroid of the ring

$\beta$  = angle between Cg(I)···Cg(J) vector and Cg(J) perp

### 7.3.4 Infrared spectra

The IR spectra of the thiosemicarbazones when compared with the Cd(II) complexes confirm the coordination of the thiosemicarbazone to the metal. The significant bands observed in the IR spectra of the thiosemicarbazones and their complexes are summarized in Table 7.5.

The band corresponding to azomethine bond,  $\nu(\text{C}=\text{N})$ , shifts to higher energy on complexation due to the combination of  $\nu(\text{C}=\text{N})$  with the newly formed C=N bond which results from the loss of the

thioamide hydrogen from the thiosemicarbazone moiety [113-116,90]. Strong bands found at 1112 and 1107 cm<sup>-1</sup> in the thiosemicarbazones are assigned to the  $\nu(\text{N-N})$  band. The increase in frequency of this band in the spectra of complexes is due to the increase in the bond strength, again confirming the coordination *via* the azomethine nitrogen. Coordination *via* thioiminolate sulfur is indicated by the downward shift of frequencies of  $\delta/\nu$  CS bands in the complexes [259]. Some of the IR spectra of complexes are given in Fig. 7.5.

**Table 7.5. IR spectral assignments (cm<sup>-1</sup>) of thiosemicarbazones and their Cd(II) complexes**

Compound	$\nu(\text{O-H})$	$\nu(\text{C=N})$	$\nu(\text{C=N})^a$	$\nu(\text{N-N})$	$\nu(\text{C=S})/\nu(\text{C-S}),$ $\delta(\text{C=S})/\delta(\text{C-S})$	$\nu(\text{C-O})$
H <sub>2</sub> bspt	3366	1625	----	1112	1330, 832	1261
[Cd <sub>2</sub> (bspt) <sub>2</sub> ] ( <b>29</b> )	----	1607	1555	1215	1369, 840	1214
[Cd(bspt)(phen)] ( <b>30</b> )	----	1595	1536	1295	1425, 847	1256
[Cd(bspt)(bipy)] ( <b>31</b> )	----	1590	1535	1286	1384, 831	1249
[Cd(bspt)(4,4'-dmbipy)] ( <b>32</b> )	----	1597	1539	1293	1328,833	1253
[Cd(bspt)(5,5'-dmbipy)] ( <b>33</b> )	----	1605	1540	1293	1328,833	1256
Hbpet	—	1583	----	1107	1306,812	—
[Cd(bpet)(NCS)] ( <b>34</b> )	----	1587	1545	1155	1315,819	—
[Cd(bpet)(N <sub>3</sub> )] ( <b>35</b> )	----	1586	1545	1138	1311,892	—
[Cd <sub>2</sub> (bpet) <sub>2</sub> (Cl) <sub>2</sub> ] ( <b>36</b> )	----	1592	1506	1111	1322,854	—

<sup>a</sup> = newly formed C=N bond

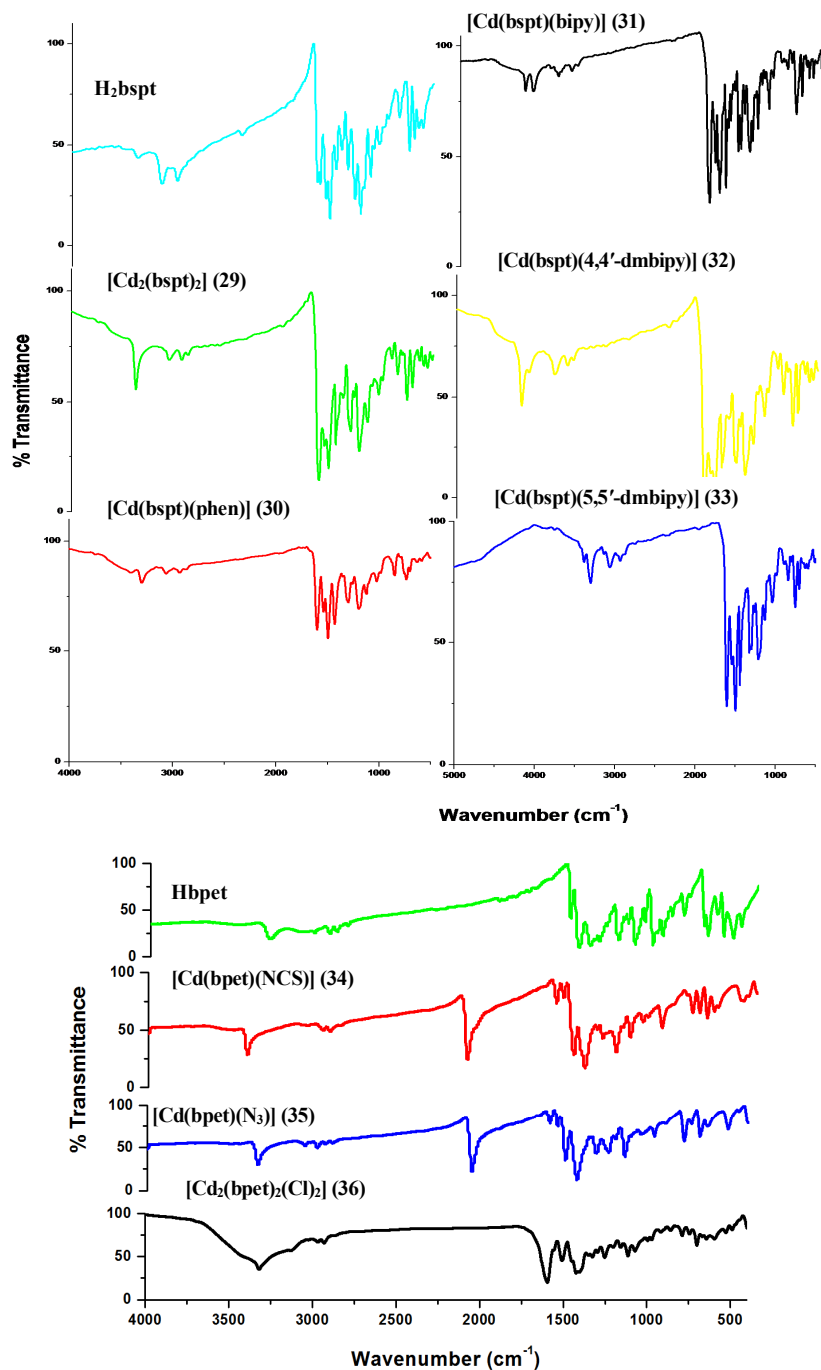


Fig. 7.5. Infrared spectra of cadmium(II) complexes.



### 7.3.5 Electronic spectra

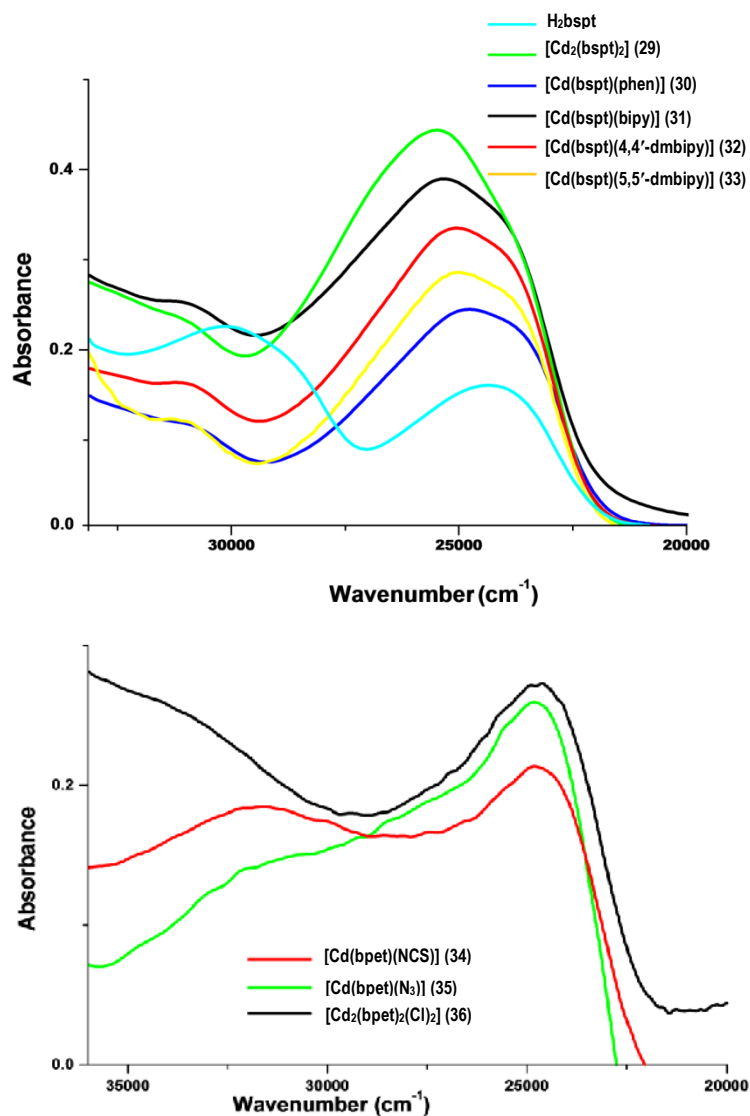


Fig. 7.6. Electronic spectra of cadmium(II) complexes.

The electronic spectral assignments for the thiosemicarbazones and their Cd(II) complexes recorded in DMF are summarized in Table 7.6. The electronic spectra of the thiosemicarbazones showed bands in the range

24200-30850  $\text{cm}^{-1}$  which are assignable to azomethine bond and the thiosemicarbazone moiety [260]. These bands are slightly shifted on complexation. In addition to these bands due to intraligand transitions, new bands around 23000-26200  $\text{cm}^{-1}$  range are observed in the spectra of complexes. These bands can be assigned to metal to ligand charge transfer transitions. No appreciable absorptions occurred below 20000  $\text{cm}^{-1}$ , indicating the absence of  $d-d$  bands, which is in accordance with the  $d^{10}$  configuration of Cd(II) ion [261]. The electronic spectra of complexes are given in Fig. 7.6.

**Table 7.6. Electronic spectral assignments ( $\text{cm}^{-1}$ ) of thiosemicarbazones and their Cd(II) complexes**

Compound	$n \rightarrow \pi^*/\pi \rightarrow \pi^*$	MLCT
H <sub>2</sub> bspt	30110, 24238	----
[Cd <sub>2</sub> (bspt) <sub>2</sub> ] ( <b>29</b> )	31077	26000
[Cd(bspt)(phen)] ( <b>30</b> )	31077	25800
[Cd(bspt)(bipy)] ( <b>31</b> )	31077	26200
[Cd(bspt)(4,4'-dmbipy)] ( <b>32</b> )	31043	26022
[Cd(bspt)(5,5'-dmbipy)] ( <b>33</b> )	31164	25850
Hbpet	30840	23600
[Cd(bpet)(NCS)] ( <b>34</b> )	31655	24710
[Cd(bpet)(N <sub>3</sub> )] ( <b>35</b> )	31960	24790
[Cd <sub>2</sub> (bpet) <sub>2</sub> (Cl) <sub>2</sub> ] ( <b>36</b> )	33131	24636

### 7.3.6 <sup>1</sup>H NMR spectra

Proton Magnetic resonance Spectroscopy is a powerful tool for the spectral studies of diamagnetic complexes like zinc. The <sup>1</sup>H NMR spectral data of the ligand Hbpet and the complex [Cd(bpet)NCS] (**34**) was recorded in DMSO-d<sub>6</sub> with tetramethylsilane as an internal standard.

A sharp singlet, which integrates as one hydrogen at 13.62 ppm is assigned to the –N(3)H proton, present in the spectrum of the ligand disappeared in the spectrum of the complex because of the deprotonation on complex formation. This provides an evidence for the coordination of thiolato sulphur through enolization followed by deprotonation. The nmr spectra of Hbpet and its complex **34** are given in Fig. 7.7.

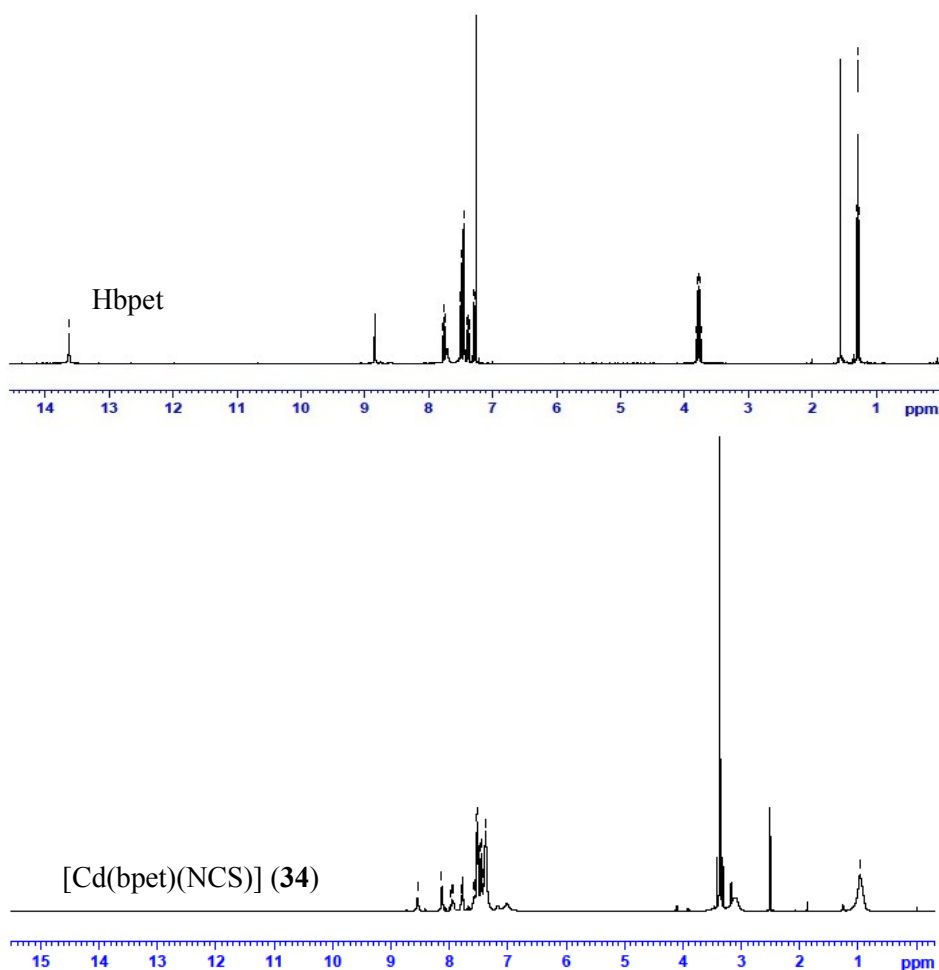


**Fig. 7.7.** The nmr spectra of Hbpet and [Cd(bpet)(NCS)] (**34**).

.....SCS.....



## SUMMARY AND CONCLUSION

---

---

The chemistry of transition metal complexes of thiosemicarbazones has been receiving considerable attention largely because of their pharmacological properties. Due to their interesting biological activities, such as antibacterial, anti-convulsant and antiproliferative-antitumor, thiosemicarbazones have attracted great attention in the recent years. The biological activity and the medicinal properties of thiosemicarbazones depend upon the chemical nature of the moiety attached to the C=S carbon atom. The structure diversity of thiosemicarbazide based compounds is considerably increased not only due to the condensation of the different carbonyls but also due to the alkylation of the different part of the thiosemicarbazide. Thiosemicarbazone usually act as chelating ligands with transition metal ion, bonding through the sulfur and hydrazine nitrogen atom. Thiosemicarbazones can coordinate to metal as neutral molecules or after deprotonation, as anionic ligands and can adopt variety different coordination modes. The possibility of their being able to transmit electronic effects between a reduce unit and metal centre is suggested by the delocalization of the  $\pi$  bonds in the thiosemicarbazone chain.

Thiosemicarbazones ( $R^1R^2C^2=N^3-N^2(H)-C^1(=S)N^1R^3R^4$ ) constitute an important class of N, S-donor ligands, and their coordination chemistry

was initially explored during the early sixties. The synthesis of thiosemicarbazones involves condensation of a ketone, or an aldehyde with a thiosemicarbazide under ambient conditions. They are represented by the general formula  $R^1R^2C=N-NH-C(S)-NH_2$ . In the solid state, these thiosemicarbazones exist in the thione form. In solution, however, they are known to tautomerize into the thiol form. Complexation usually takes place *via* dissociation of the acidic proton, resulting in the formation of a five membered chelate ring. When an additional donor site D is incorporated in such ligands, linked to the carbonylic carbon *via* one or two intervening atoms, D,N,S tricoordination usually takes place.

### **Objectives of the present work**

Thiosemicarbazones have emerged as an important class of ligands over a period of time, for a variety of reasons, such as variable donor properties, structural diversity and biological applications. In order to pursue the interesting coordinating properties of thiosemicarbazones, complexes with different types of ligand environments are essential. With this knowledge taken from the literature, we undertook the present study by taking two different NNS and ONS donor types thiosemicarbazones as principal ligands. Introduction of heterocyclic bases like 1,10-phenanthroline, 2,2'-bipyridine, 4,4'-dimethyl-2,2'-bipyridine and 5,5'-dimethyl-2,2'-bipyridine, and anions like azide, chloride, dicyanamide, thiocyanate etc., the classical *N,N* donor ligands leads to the syntheses of mixed-ligand complexes which can cause different bonding, spectral properties and geometries in coordination compounds.

We have synthesized the following two new and two earlier reported ligands using 4-benzyloxysalicylaldehyde, 5-bromosalicylaldehyde, 2-benzoylpyridine 4-phenylthiosemicarbazide, 4-ethylthiosemicarbazide, 4-methylthiosemicarbazide and *N,N*-dimethylthiosemicarbazide.

- 4-Benzyloxysalicylaldehyde-*N*<sup>4</sup>-phenylthiosemicarbazone (H<sub>2</sub>bspt)
- 5-Bromosalicylaldehyde -*N*<sup>4</sup>-ethylthiosemicarbazone (H<sub>2</sub>brset)
- 2-Benzoylpyridine -*N*<sup>4</sup>-ethylthiosemicarbazone (Hbpet)
- 2-Benzoylpyridine -*N*<sup>4</sup>,*N*<sup>4</sup>-dimethylthiosemicarbazone (Hbpdtd)

### Summary of the thesis:

The thesis is divided into seven chapters.

#### Chapter 1

Chapter 1 involves a brief overview to thiosemicarbazones and their metal complexes, bonding and coordination nature of thiosemicarbazones and their various applications. The objectives of the present work and the various physicochemical methods adopted for the characterization of the thiosemicarbazones and their complexes are also discussed in this chapter.

#### Chapter 2

Chapter 2 describes the syntheses of four tridentate thiosemicarbazones and their characterization by elemental analyses, mass, FT-IR, UV-Vis and <sup>1</sup>H NMR spectral studies. Among the four ligands two are ONS and remaining are NNS ligands. X-ray quality single crystals of these two ligands were grown and their molecular structures were established by single crystal X-ray diffraction studies.

The thiosemicarbazones synthesized are

- 4-Benzyloxysalicylaldehyde- $N^4$ -phenylthiosemicarbazone (H<sub>2</sub>bspt)
- 5-Bromosalicylaldehyde - $N^4$ -ethylthiosemicarbazone (H<sub>2</sub>brset)
- 2-Benzoylpyridine - $N^4$ -ethylthiosemicarbazone (Hbpet)
- 2-Benzoylpyridine - $N^4, N^4$ -dimethylthiosemicarbazone (Hbpdtd)

### **Chapter 3**

This chapter deals with the coordination chemistry of four oxidovanadium(IV) complexes derived from 4-benzyloxysalicylaldehyde- $N^4$ -phenyl thiosemicarbazone and a dioxidovanadium(V) complex derived from 2-benzoylpyridine- $N^4, N^4$ -dimethyl thiosemicarbazone.

All complexes except the dioxidovanadium complex are mononuclear with heterocyclic bases 1,10-phenanthroline, 2,2'-bipyridine, 4,4'-dimethyl-2,2'-bipyridine and 5,5'-dimethyl-2,2'-bipyridine as coligands. All the complexes are characterized by various techniques such as elemental analyses, molar conductivity and magnetic susceptibility measurements, FTIR, UV-vis and EPR spectral studies. The observed molar conductivity values in  $10^{-3}$  M DMF solution confirm that all the complexes are non-electrolytic in nature. Magnetic susceptibility measurements clearly indicate that all the complexes except the dioxidovanadium complex are paramagnetic in nature with vanadium in +4 oxidation state. In all the complexes except the dioxidovanadium complex, thiosemicarbazones are coordinated to the metal centre in the thioiminolate form and act as dideprotonated tridentate ligands. In the EPR spectra, *g* values are found to be less than the free electron value



and in DMF at 77 K, they displayed well resolved axial anisotropy with two sets of eight line pattern with  $g_{\parallel} < g_{\perp}$  and  $A_{\parallel} > A_{\perp}$  relationship characteristic of an axially compressed  $d^1_{xy}$  configuration. We could isolate X-ray quality single crystals for the dioxidovanadium complex by the slow evaporation of the mother liquor. The molecule exhibited distorted square pyramidal geometry with N, N and S atoms of the principal ligand and one of the oxo group occupying the square plane and the other oxo group occupying the axial position. There are no intra and intermolecular hydrogen bonds in the molecule. The neighbouring molecules are interconnected by  $\pi \cdots \pi$  and C–H $\cdots\pi$  interactions.

#### Chapter 4

Chapter 4 deals with the syntheses and characterization of six nickel complexes of the thiosemicarbazones by CHNS analyses, conductivity and magnetic susceptibility measurements, infrared and electronic spectral studies. All the complexes are found to be non-electrolytic in nature. The five-coordinate complexes are found to be paramagnetic with two unpaired electrons. In all of them, thiosemicarbazone moiety coordinates to the metal in the thioiminolate form as evidenced from the infrared spectra. We could isolate X-ray quality single crystal for one of the nickel complex by the slow evaporation of the mother liquor. The nickel(II) atom has square-planar geometry surrounded by one sulfur atom and three nitrogen atoms. In the crystal packing three molecules are linked through hydrogen bonding i.e., two molecules are bridged by a third one. Further, crystal packing is reinforced by very weak  $\pi \cdots \pi$  and metal $\cdots\pi$  interactions.

## **Chapter 5**

This chapter describes the syntheses and characterization of nine copper(II) complexes. The characterization techniques include elemental analyses, molar conductivity studies and magnetic susceptibility measurements, FTIR, UV-Vis and EPR spectral studies. Heterocyclic bases like 1,10-phenanthroline, 2,2'-bipyridine, 4,4'-dimethyl-2,2'-bipyridine and 5,5'-dimethyl-2,2'-bipyridine were used as coligands and iodide and azide as anions. In all the complexes, the ONS donor thiosemicarbazones (H<sub>2</sub>bspt and H<sub>2</sub>brset) exist in thioiminolate form and coordinates to the metal through azomethine nitrogen, thioiminolate sulfur and phenolate oxygen. For NNS donor thiosemicarbazones, the ligands coordinate to the metal through azomethine nitrogen, thioiminolate sulfur and pyridyl nitrogen. The molar conductivity values obtained for all the complexes confirmed their non-electrolytic nature. The magnetic susceptibility measurements reveal that all the complexes are paramagnetic and for mononuclear complexes the effective magnetic moment values are found to be close to the spin only value which corresponds to a single unpaired electron. The low magnetic moment values for two complexes may be due to considerable antiferromagnetic interaction between the metal centers. EPR spectra in polycrystalline state at 298 K show that some of the compounds are isotropic and some are axial. In DMF at 77 K, some complexes are found to be axial with hyperfine lines in the parallel and perpendicular regions. Superhyperfine splittings give clear evidence for the coordination of azomethine nitrogen and that of heterocyclic bases to the metal. The *g* values calculated indicate that in most of the complexes the unpaired electron in

Cu(II) resides in the  $d_{x^2-y^2}$  orbital. The complexes in which  $g_{\parallel} > g_{\perp} > 2.0023$  suggest a distorted square pyramidal structure and rules out the possibility of a trigonal bipyramidal structure which would be expected to have  $g_{\parallel} < g_{\perp}$ .

## Chapter 6

Chapter 6 explains the syntheses and characterization of eight zinc complexes of the thiosemicarbazones by CHNS analyses, conductivity and magnetic susceptibility measurements, infrared and electronic spectral studies. The observed molar conductivity values in  $10^{-3}$  M DMF solution confirm that all the complexes are non-electrolytes. The tridentate character of the thiosemicarbazones is inferred from IR spectra. The structure of two of the complexes  $[\text{Zn}(\text{bpet})(\text{dca})]_n$  and  $[\text{Zn}(\text{Hbpet})](\text{NO}_3)_2 \cdot \text{H}_2\text{O}$  has been resolved using single crystal X-ray diffraction studies. The crystal structure revealed a monoclinic space group  $P2_1$  for complex  $[\text{Zn}(\text{bpet})(\text{dca})]_n$  and orthorhombic space group  $Pca2_1$  for  $[\text{Zn}(\text{Hbpet})](\text{NO}_3)_2 \cdot \text{H}_2\text{O}$ . The compound  $[\text{Zn}(\text{bpet})(\text{dca})]_n$  adopts a distorted square pyramidal geometry. Basal plane consist of azomethine N, pyridine N and S atom from ligand and N atom from dicynamide ligand and the axial site is occupied by a N atom of dicynamide ligand of the next unit. The dicynamide ligand employed the  $\mu_{1,5}$  bridge mode linking the adjacent Zn atom to produce one dimensional zig-zag chains. In compound  $[\text{Zn}(\text{Hbpet})](\text{NO}_3)_2 \cdot \text{H}_2\text{O}$ , Zn centre displays a distorted octahedral geometry and the ligand is coordinated in the neutral form. The zinc in the complex is hexacoordinated through two thioamide sulfur atoms, two azomethine nitrogen and two pyridyl nitrogen atoms.

The basal plane consist of two pyridyl nitrogen and two thioamide sulfur atoms and the apical positions are occupied by azomethine nitrogen atoms. Three-dimensional (3D) polymeric network arrangement was built *via* weak N–O $\cdots\pi$  and CH $\cdots\pi$  interactions between [Zn(Hbpet)] moieties.

The  $^1\text{H}$  NMR spectral data of the ligand Hbpet and its complex [Zn(Hbpet)](NO<sub>3</sub>)<sub>2</sub>·H<sub>2</sub>O were recorded in DMSO-d<sub>6</sub> with tetramethylsilane as an internal standard. In the case of [Zn(Hbpet)](NO<sub>3</sub>)<sub>2</sub>·H<sub>2</sub>O complex, the spectrum is only slightly modified, with the same multiplicity of the signals and some slight changes in the chemical shifts with respect to the ligand. The singlet which integrate as a single hydrogen present in the spectra of the ligand at 13.6 ppm is not disappeared in the spectra of the complex. This provides an evidence for the coordination of the ligand in the thioiminol form.

## **Chapter 7**

Eight cadmium complexes have been synthesized and physico-chemically characterized by CHNS analyses, conductivity and magnetic susceptibility measurements, infrared and electronic spectral studies. Heterocyclic bases like 1,10-phenanthroline, 2,2'-bipyridine, 4,4'-dimethyl-2,2'-bipyridine, 5,5'-dimethyl-2,2'-bipyridine and anions like thiocyanate, azide and chloride act as coligands. The molar conductivity measurements in DMF (10<sup>-3</sup> M) indicate that all the complexes are non-electrolytes. The IR spectral studies show that the thiosemicarbazones coordinate in thioiminolate form in all the complexes and act as dideprotonated tridentate ligands. We could isolate X-ray quality single

crystals for one of the cadmium complex by the slow evaporation of the mother liquor. This compound is a sulfur-bridged cadmium box-dimer in which the environment of each Cd(II) atom can be described as distorted square pyramidal. The intermolecular hydrogen bonding interaction links two dimer units in the crystal cell giving rise to a 2D laminar packed structure. Further, crystal packing is reinforced by very weak C–H $\cdots\pi$  and metal $\cdots\pi$  interactions.

.....✪.....



## References

- [1] J.E. Huheey, E.A. Keiter, R.L. Keiter, *Inorganic Chemistry, Principles of Structure and Reactivity*, 4<sup>th</sup> ed., Harper Collins College Publishers, New York, 1993.
- [2] D. Sakthilatha, A. Deepa, R. Rajavel, *Synth. React. Inorg. Met.-Org. Chem.* 45.2 (2015) 286.
- [3] K.P. Balasubramanian, R. Karvembu, R. Prabhakaran, V. Chinnusamy, K. Natarajan, *Spectrochim. Acta* 68A (2007) 50.
- [4] G.F. de Sousa, C.A.L. Filgueiras, M.Y. Darensbourg, J.H. Reibenspies, *Inorg. Chem.* 31 (1992) 3044.
- [5] R. Prabhakaran, R. Karvembu, T. Hashimoto, K. Shimizu, K. Natarajan, *Inorg. Chim. Acta* 358 (2005) 2093.
- [6] K.P. Balasubramanian, R. Karvembu, R. Prabhakaran, V. Chinnusamy, K. Natarajan, *Spectrochim. Acta* 68A (2007) 50.
- [7] D.X. West, G.A. Bain, R.J. Butcher, J.P. Jasinski, R.Y. Pozdniakiv, *Polyhedron* 15 (1996) 665.
- [8] E.K. John, M.A. Green, *J. Med. Chem.* 33 (1990) 1764.
- [9] I.G. Santos, A. Hagenbach, U. Abram, *Dalton Trans.* (2004) 677.
- [10] A.V. Ablov, N.V. Gerbeleu, *Russ. J. Inorg. Chem.* 9 (1964) 1260.
- [11] P. Domiano, G.G. Fava, M. Nardelli, P. Sgarabotto, *Acta Crystallogr.* 25B (1969) 343.
- [12] K.L. Williamson, *Macroscale and microscale organic experiments*, 3rd edn. Houghto-Mifflin, Boston, 1999.

- [13] T.S. Lobana, R.J. Butcher, *Transit. Met. Chem.* 29 (2004) 291.
- [14] T.S. Lobana, R.J. Butcher, A. Castineiras, E. Bermejo, P.V. Bharatam, *Inorg. Chem.* 45 (2006) 1535.
- [15] T.S. Lobana, S. Khanna, R.J. Butcher, A.D. Hunter, M. Zeller, *Inorg. Chem.* 46 (2007) 5826.
- [16] T.S. Lobana, S. Khanna, R.J. Butcher, *Z. Anorg. Allg. Chem.* 633 (2007) 1820.
- [17] T.S. Lobana, P. Kumari, R.J. Butcher, *Inorg. Chem. Commun.* 11 (2008) 11.
- [18] E.M. Jouad, A. Riou, M. Allain, M.A. Khan, G.M. Bouet, *Polyhedron* 20 (2001) 67.
- [19] S. Lhuachan, S. Siripaisarnpipat, N. Chaichit, *Eur. J. Inorg. Chem.* 2 (2003) 263.
- [20] E. Bermejo, R. Carballo, A. Castineiras, R. Dominguez, C. Maichle-Mossmer, J. Strahle, D.X. West, *Polyhedron* 18 (1999) 3695.
- [21] P. Gomez-Saiz, J. Garcia-Tojal, M.A. Maestro, J. Mahia, F.J. Arniaz, L. Lezama, T. Rojo, *Eur. J. Inorg. Chem.* 14 (2003) 2639.
- [22] E. Labisbal, K.D. Haslow, A. Sousa-Pedrares, J. Valdes-Martinez, S. Hernandez-Ortega, D.X. West, *Polyhedron* 22 (2003) 2831.
- [23] D. Kovala-Demertzi, A. Domopoulou, M.A. Demertzis, J. Valdes-Martinez, S. Hernandez-Ortega, G. Espinosa-Perez, D.X. West, M.M. Salberg, G.A. Bain, P.D. Bloom, *Polyhedron* 15 (1996) 2587.
- [24] J.S. Casas, E.E. Castellano, M.C. Rodriguez-Arguellas, A. Sanchez, J. Sordo, J. Zukerman-Schpector, *Inorg. Chim. Acta* 260 (1997) 183.



- [25] J. Garcia-Tojal, J.L. Pizarro, A. Garcia-Orad, A.R. Perez-Sanz, M. Ugalde, A.A. Diaz, J.L. Serra, M.I. Arriortua, T. Rojo, J. Inorg. Biochem. 86 (2001) 627.
- [26] J.S. Casas, M.V. Castano, M.C. Cifuentes, A. Sanchez, J. Sordo, Polyhedron 21 (2002) 1651.
- [27] T.S. Lobana, G. Bawa, A. Castineiras, R.J. Butcher, Inorg. Chem. Comm. 10 (2007) 505.
- [28] S. Halder, S.-M. Peng, G.-H. Lee, T. Chatterjee, A. Mukherjee, S. Dutta, U. Sanyal, S. Bhattacharya, New J. Chem. 32 (2008) 105.
- [29] D. Kovala-Demertzi, N. Kourkoumelis, M.A. Demertzis, J.R. Miller, C.S. Frampton, J.K. Swearingen, D.X. West, Eur. J. Inorg. Chem. (2000) 727.
- [30] T.S. Lobana, G. Bawa, R.J. Butcher, B.-J. Liaw, C.W. Liu, Polyhedron 25 (2006) 2897.
- [31] L.J. Ashfield, A.R. Cowley, J.R. Dilworth, P.S. Donnelly, Inorg. Chem. 43 (2004) 4121.
- [32] I. Pal, F. Basuli, T.C.W. Mak, S. Bhattacharya, Angew. Chem. Int. Ed. 40 (2001) 2923.
- [33] M. Gil, E. Bermejo, A. Castineiras, H. Beraldo, D.X. West, Z. Anorg. Allg. Chem. 626 (2000) 2353.
- [34] R. Pedrido, M.R. Bermejo, M.J. Romero, M. Vazquez, A.M. Gonzalez-Noya, M. Maneiro, M.J. Rodriguez, M.I. Fernandez, J. Chem. Soc., Dalton Trans. (2005) 572.
- [35] J.S. Casas, E.E. Castellano, J. Ellena, M.S. Garcia-Tasende, A. Sanchez, J. Sordo, E.M. Vazquez-Lopez, M.J. Vidarte, Z. Anorg. Allg. Chem. 629 (2003) 261.

- [36] D.X. West, J.K. Swearingen, J. Valdes-Martinez, S. Hernandez-Ortega, A.K. El-Sawaf, F. V. Meurs, *Polyhedron* 18 (1999) 2919.
- [37] S. Arora, S. Agarwal, S. Singhal, *Int. J. Pharm. Sci.* 6 (2014) 34.
- [38] S.E. Ghazy, M.A. Kabil, A.A. El-Asmy, Y.A. Sherief, *Anal. Lett.* 29 (1996) 1215.
- [39] J.R. Dilworth, A.H. Cowley, P.S. Donnelly, A.D. Gee, J.M. Heslop, *J. Chem. Soc., Dalton Trans.* (2004) 2404.
- [40] A.A. Abou-Hussen, N.M. El-Metwally, E.M. Saad, A.A. El-Asmy, *J. Coord. Chem.* 58 (2005) 1735.
- [41] T.S. Lobana, R. Sharma, G. Bawa, S. Khanna, *Coord. Chem. Rev.* 253 (2009) 977.
- [42] I.C. Mendes, F.B. Costa, G.M. de Lima, J.D. Ardisson, I. Garcia-Santos, A. Castineiras, *Polyhedron* 28 (2009) 1179.
- [43] J. Rivadeneira, D.A. Barrio, G. Arrambide, D. Gambino, L. Bruzzzone, S.B. Etcheverry, *J. Inorg. Biochem.* 103 (2009) 633.
- [44] D. Kovala-Demertzi, A. Papageorgiou, L. Papathanasis, A. Alexandratos, P. Dalezis, J.R. Miller, *Eur. J. Med. Chem.* 44 (2009) 1296.
- [45] M. Belicchi-Ferrari, F. Bisceglie, A. Buschini, S. Franzoni, G. Pelosi, S. Pinelli, *J. Inorg. Biochem.* 104 (2010) 199.
- [46] V. Vrdoljak, I. Đilović, M. Rubčić, S.K. Pavelić, M. Kralj, D. Matković-Čalogović, *Eur. J. Med. Chem.* 45 (2010) 38.
- [47] U. El-Ayaan, M.M. Youssef, S. Al-Shihry, *J. Mol. Stru.* 936 (2009) 213.

- [48] A.A. El-Asmy, O.A. Al-Gammal, D.A. Saad, S.E. Ghazy, *J. Mol. Stru.* 934 (2009) 9.
- [49] M. Li, J. Zhou, H. Zhao, C. Chen, J. Wang. *J. Coord. Chem.* 62 (2009) 1423.
- [50] C Marzano, M Pellei, F Tisato, C Santini. *Anticancer Agents Med. Chem.* 9 (2009) 185.
- [51] D.X. West, A.C. Whyte, F.D. Sharif, H. Gebremedhin A.E. Liberta, *Transit. Met. Chem.* 18 (1993) 238.
- [52] M.C. Rodríguez-Argüelles, P. Tourón-Touceda, R. Cao, A.M. García-Deibe, P Pelagatti, C. Pelizzi, F. Zani, *J. Inorg. Biochem.* 103 (2009) 35.
- [53] D.B. Lovejoy, D.M. Sharp, N. Seebacher, P. Obeidy, T. Prichard, C. Stefani, M.T. Basha, P.C. Sharpe, P.J. Jansson, D.S. Kalinowski, P.V. Bernhardt, D.R. Richardson, *J. Med. Chem.* 55 (2012) 7230.
- [54] T.K. Yeh, Z. Lu, M.G. Wientjes, J.L. Au, *Pharm. Res.* 22 (2005) 867.
- [55] J. Rodriquez, A.G. De Torres, J. M. Cano Pavon, *Talanta* 28 (1981) 131.
- [56] J.R. Koduru, L.K. Duk, *Food Chemistry* 150 (2014) 1.
- [57] S. Reddy, Adi Narayana, *J. Saudi Chem. Soc.* 2012.
- [58] K.M.M.S. Prakash, L.D. Prabhakar, D.V. Reddy, *Analyst* 111 (1986) 1301.
- [59] J.R. Dimmock, R.N. Puthucode, J.M. Smith, M. Hetherington, J.W. Quail, U. Pugazhenthii, J. Lechler, J.P. Stables, *J. Med. Chem.* 39 (1996) 3984.
- [60] A.C.F. Caires, *Anticancer Agents Med. Chem.* 7 (2007) 484.

*References*

---

- [61] H.P. Ebrahimi, J.S. Hadi, T.A. Alsalim, T.S. Ghalib, Z. Bolandnazar, *Spectrochim. Acta A* 137 (2015) 1067.
- [62] SMART and SAINT, Area Detector Software Package and SAX Area Detector Integration Program, Bruker Analytical X-ray; Madison, WI, USA, 1997.
- [63] SADABS, Area Detector Absorption Correction Program; Bruker Analytical X-ray; Madison, WI, 1997.
- [64] G.M. Sheldrick, *Acta Cryst. A* 64 (2008) 112.
- [65] G.M. Sheldrick, SHELXL97 and SHELXS97, University of Göttingen, Germany, 1997.
- [66] K. Brandenburg, Diamond Version 3.2g, Crystal Impact GbR, Bonn, Germany, 2010.
- [67] T.S. Lobana, R. Sharma, G. Bawa, S. Khanna, *Coord. Chem. Rev.* 253 (2009) 977.
- [68] V.K. Lekshmi, R.G. Nath, *Indian J. Res. Found.* 1 (2015) 23.
- [69] K. Jayakumar, M. Sithambaresan., N. Aiswarya, M.R.P. Kurup, *Spectrochim. Acta A* 139 (2015) 28.
- [70] D.X. West, A.E. Liberta, S.B. Padhye, R.C. Chikate, P.B. Sonawane, A.S. Kumbhar, R.G. Yerande, *Coord. Chem. Rev.* 123 (1993) 49.
- [71] H.P. Ebrahimi, J.S. Hadi, T.A. Alsalim, T.S. Ghali, Z. Bolandnazar, *Spectrochim. Acta A* 137 (2015) 1067.
- [72] D.R. Smith, *Coord. Chem. Rev.* 164 (1997) 575.
- [73] T.S. Lobana, S. Khanna, R. Sharma, G. Hundal, R. Sultana, M. Chaudhary, R.J. Butcher, A. Castineiras, *Cryst. Growth Design* 8 (2008) 1203.

- [74] R.K. Mahajan, I. Kaur, T.S. Lobana, *Talanta* 59 (2003) 101.
- [75] R.K. Mahajan, I. Kaur, T.S. Lobana, *Ind. J. Chem.* 45A (2006) 639.
- [76] R.K. Mahajan, T.P.S. Walia, Sumanjit, T.S. Lobana, *Talanta* 67 (2005) 755.
- [77] D. Udhayakumari, S. Velmathi, *Sensors and Actuators B: Chemical* 209 (2015) 462.
- [78] K.J. Reddy, J.R. Kumar, C. Ramachandraiah, T. Thriveni, A.V. Reddy, *Food. Chem.* 101 (2007) 585.
- [79] M.A. Ali, M.E. Khalifa, S.E. Ghazy, M.M. Hassanien, *Anal. Sci.* 18 (2002) 1235.
- [80] F. Bacher, O. Dömötör, M. Kaltenbrunner, M. Mojović, A. Popović-Bijelić, A. Gräslund, V. B. Arion, *Inorg. Chem.* 23 (2014) 12595.
- [81] K. Nomiya, K. Sekino, M. Ishiawa, A. Honda, M. Yokoyama, N.C. Kasuga, H. Yokoyama, S. Nakano, K. Onodera, *J. Inorg. Biochem.* 98 (2004) 601.
- [82] M.B. Ferrari, F. Bisceglie, G. Pelosi, P. Tarasconi, R. Albertini, A. Bonati, P. Lunghi, S. Pinelli, *J. Inorg. Biochem.* 83 (2001) 169.
- [83] A.P. Ingale, *J. Chem. Pharm. Res.* 6(11) (2014) 460.
- [84] J. Garcia-Tojal, L. Lezama, J.L. Pizarro, M. Insausti, M.I. Arriortua, T. Rojo, *Polyhedron* 18 (1999) 37.
- [85] K. Jayakumar, M. Sithambaresan, A.A. Aravindakshan, M.R.P. Kurup, *Polyhedron* 75 (2014) 50.
- [86] N.A. Mohamed, R.R. Mohamed, R.S. Seoudi, *Int. J. Biol. Macromol.* 63 (2014) 163.
- [87] E.M. Jouad, G. Larcher, M. Allain, A. Riou, G.M. Bouet, M.A. Khan, X.D. Thanh, *J. Inorg. Biochem.* 86 (2001) 565.

## References

---

- [88] K. Jayakumar, M. Sithambaresan, M.R.P. Kurup, *Acta Cryst.* E67 (2011) o3195.
- [89] D.X. West, J.S. Ives, J. Krejci, M.M. Salberg, T.L. Zumbahlen, G.A. Bain, A. E. Liberta, *Polyhedron* 14 (1995) 2189.
- [90] B.S. Garg, M.R.P. Kurup, S.K. Jain, *Transition Met. Chem.* 13 (1988) 247.
- [91] Y.-P. Tian, W.-T. Yu, C.-Y. Zhao, M.-H. Jiang, Z.-G. Gai, H.-K. Fun, *Polyhedron* 21 (2002) 1219.
- [92] R.P. John, A. Sreekanth, M.R.P. Kurup, H.-K. Fun, *Polyhedron* 24 (2005) 601.
- [93] A.K. El-Sawaf, D.X. West, F.A. El-Saied, R.M. El-Bahnasawy, *Transit. Met. Chem.* 23 (1998) 649.
- [94] M. Joseph, M. Kuriakose, M.R.P. Kurup, E. Suresh, A. Kishore, S.G. Bhatt, *Polyhedron* 25 (2006) 61.
- [95] Bruker, *SADABS*, *APEX2*, *XPREP* and *SAINT*, Bruker AXS Inc., Madison, Wisconsin, USA, 2004.
- [96] G.M. Sheldrick, *Acta. Cryst.* A64 (2008) 112.
- [97] E.B. Seená, M.R.P. Kurup, E. Suresh, *J. Chem. Crystallogr.* 38 (2008) 93.
- [98] J.M. Jacob, M.R.P. Kurup, *Acta Cryst.* E68 (2012) o836.
- [99] K. Nisha, M. Sithambaresan, M.R.P. Kurup, *Acta Cryst.* E67 (2011) o3420.
- [100] E.B. Seená, M.R.P. Kurup, E. Suresh, *J. Chem. Crystallogr.* 36 (2006) 189.
- [101] J. March, *Advanced Organic Chemistry, Reactions, Mechanisms and Structure*, 4<sup>th</sup> ed. New York: Wiley, 1992.

- [102] H.D. Flack, G. Bernardinelli, *J. Appl. Cryst.* 33 (2000) 114.
- [103] M. Nomura, M. Nakamura, R. Soeda, Y. Kikawada, M. Fukushima, T. Oi *Isot. Environ. Health Stud.* 48 (2012) 434.
- [104] T.A. Clark, J.F. Deniset, C.E. Heyliger, G.N. Pierce, *Heart Fail Rev.* 19 (2014) 123.
- [105] D. Sanna, M. Serra, G. Micera, E. Garribba, *Inorg. Chem.* 53 (2014) 1449.
- [106] M. Xie, D. Chen, F. Zhang, G.R. Willsky, D.C. Crans, W. Ding, *J. Inorg. Biochem.* 136 (2014) 47.
- [107] S.R. Akabayov, B. Akabayov, *Inorg. Chim. Acta* 420 (2014) 16.
- [108] P. Ying, X. Tian, P. Zeng, J. Lu, H. Chen, M. Xiao, *Med. Chem.* 4 (2014) 549.
- [109] R.C. Maurya, D. Sutradhar, M.H. Martin, S. Roy, J. Chourasia, A.K. Sharma, P. Vishwakarma, *Arabian J. Chem.* 8 (2015) 78.
- [110] W.J. Geary, *Coord. Chem. Rev.* 7 (1971) 81.
- [111] R.I. Dutta, G.P. Sengupta, *J. Ind. Chem. Soc.* 49 (1972) 919.
- [112] A.W. Addison, T.N. Rao, R. Reedijk, J.V. Rigin, G.C. Verschoor, *J. Chem. Soc., Dalton Trans.* (1984) 1349.
- [113] M. Joseph, V. Suni, M.R.P. Kurup, M. Nethaji, A. Kishore, S.G. Bhat, *Polyhedron* 23 (2004) 3069.
- [114] M.A. Ali, M.T.H. Tarafdar, *J. Inorg. Nucl. Chem.* 39 (1977) 1785.
- [115] M.J.M. Campbell, *Coord. Chem. Rev.* 15 (1975) 279.
- [116] B.S. Garg, M.R.P. Kurup, S.K. Jain, Y.K. Bhoon, *Transit. Met. Chem.* 16 (1991) 111.

- [117] R. Mayer, *Organosulfur Chemistry*, M.J. Janssen, Ed.; Wiley-Interscience: New York (1967) 219.
- [118] B.S. Garg, M.R.P. Kurup, S.K. Jain, Y.K. Bhoon, *Transit. Met. Chem.* 13 (1988) 309.
- [119] P. Bindu, M.R.P. Kurup, T.R. Satyakeerty, *Polyhedron* 18 (1999) 321.
- [120] E. Manoj, M.R.P. Kurup, *Polyhedron* 27 (2008) 275.
- [121] I.-X. Li, H.-A. Tang, Y.-Z. Li, M. Wang, L.-F. Wang, C.-G. Xia, *J. Inorg. Biochem* 78 (2000) 167.
- [122] R.P. John, A. Sreekanth, M.R.P. Kurup, A. Usman, I.A. Razak, H.-K. Fun, *Spectrochim. Acta* 59A (2003) 1349.
- [123] C.J. Ballhausen, H.B. Gray, *Inorg. Chem.* 1 (1962) 111.
- [124] E. Garriba, G. Micerra, A. Panzanelli, *Inorg. Chem.* 42 (2003) 3981.
- [125] D. Mustafí, M.W. Makinen, *Inorg. Chem.* 44 (2005) 5580.
- [126] S. Bhattacharya, T. Ghosh, *Indian J. Chem.* A38 (1999) 601.
- [127] H. Kon, E. Sharpless, *J. Chem. Phys.* 42 (1965) 906.
- [128] D. Kivelson, S.K. Lee, *J. Chem. Phys.* 41 (1964) 1896.
- [129] D. Rehder, *Bioinorganic Vanadium Chemistry*, Wiley, Chichester (2008).
- [130] D.G.E. Kerfoot, "Nickel", *Ullmann's Encyclopedia of Industrial Chemistry*, Weinheim: Wiley-VCH. (2005).
- [131] S. Lars, W. Evgeny, C. Ronald, *J. Geophys. Res.* 102 (1997) 24729.
- [132] A. Sankaraperumal, J. Karthikeyan, A.N. Shetty, R. Lakshmisundaram, *Polyhedron* 50 (2013) 264.



- [133] G. Pelosi, *The Open Crystallography Journal*. 3 (2010) 16.
- [134] Z. Afrasiabi, E. Sinn, W. Lin, Y. Ma, C. Campana, *J. Inorg. Biochem.* 99 (2005) 1526.
- [135] M.B. Ferrari, F. Bisceglie, G. Pelosi, M. Sassi, P. Tarasconi, *J. Inorg. Biochem.* 90 (2002) 113.
- [136] D.L. Klayman, J.F. Bartosevich, T.S. Griffin, C.J. Mason, J.P. Scovill, *J. Med. Chem.* 22 (1979) 855.
- [137] I. Đilovic, M. Rubcic, V. Vrdoljak, S.K. Pavelic, M. Kralj, *Bioorg. Med. Chem.* 16 (2008) 5189.
- [138] M.A. Halcrow, G. Christou, *Chem. Rev.* 94 (1994) 2421.
- [139] P. Stavropoulos, M.C. Muetterties, M. Carrié, R.H. Holm, *J. Am. Chem. Soc.* 113 (1991) 8485.
- [140] G.C. Tucci, R.H. Holm, *J. Am. Chem. Soc.* 117 (1995) 6489.
- [141] I. Tommasi, M. Aresta, P. Giannoccaro, E. Quaranta, C. Fragale, *Inorg. Chim. Acta* 38 (1998) 272.
- [142] U. Ermler, W. Grabarse, S. Shima, M. Goubeaud, R.K. Thau, *Curr. Op. Struct. Biol.* 8 (1998) 749.
- [143] F. Dole, M. Medina, C. More, R. Cammack, P. Bertrand, B. Guigliarelli, *Biochemistry* 35 (1996) 16399.
- [144] J. Telser, *Struct. Bonding* 31 (1998) 91.
- [145] C.Y. Ralston, H. Wang, S.W. Ragsdale, M. Kumar, N.J. Spangler, P.W. Ludden, W. Gu, R.M. Jones, D.S. Patil, S.P. Cramer, *J. Am. Chem. Soc.* 122 (2000) 10553.
- [146] S.W. Ragsdale, M. Kumar, *Chem. Rev.* 96 (1998) 2515.

*References*

---

- [147] H.-D. Youn, E.-H. Kim, J.-H. Roe, S.-O. Kang, *Biochemistry* 318 (1996) 889.
- [148] S.B. Choudhury, J. -W. Lee, G. Davidson, Y.-I . Yim, K. Bose, M.L. Sharma, S.-O. Kang, D.E. Cabelli, M.J. Maroney, *Biochemistry* 38 (1999) 3744.
- [149] O.B. Ibrahim, M.A. Mohamed, M.S. Refat. *Can. Chem. Trans.* 2 (2014) 108.
- [150] N. Selvakumaran, N.S.P. Bhuvanesh, A. Endo, R. Karvembu, *Polyhedron* 75 (2014) 95.
- [151] B. Shafaatian, A. Soleymanpour, N.K. Oskouei, B. Notash, S.A. Rezvani, *Spectrochim. Acta A*128 (2014) 363.
- [152] R.D. Bereman, G.D. Shields, *Inorg. Chem.* 18 (1979) 946.
- [153] M. Mathew, G.J. Palenik, G.R. Clark, *J. Inorg. Chem.* 12 (1973) 446.
- [154] E.C. Constable, S.M. Elder, D.A. Tocher, *Polyhedron* 11 (1992) 2599.
- [155] E.C. Constable, S.M. Elder, D.A. Tocher, *Polyhedron* 11 (1992) 1337.
- [156] E.C. Constable, S.M. Elder, M.J. Hannon, A. Martin, P.R. Raithby, D.A. Tocher, *J. Chem. Soc., Dalton Trans.* 2423 (1996).
- [157] V.M. Leovac, V.I. Cesljevic, G. Argay, A. KaÂlmaÂn, B. RibÂar, *J. Coord. Chem.* 34 (1995) 357.
- [158] L. Yang, D.R. Powell, R.P. Houser, *Dalton Trans.* 955 (2007) 955.
- [159] P. Souza, A. Arquero, A. Garcia-Onrubia, V. Fernandez, A.M. Leiva, U. Miiller, *Z. Naturforsch. Teil B* 44 (1989) 946.
- [160] C. Collins, R.E. Dans, *Acta Crystallogr.* B34 (1978) 283.
- [161] P. Arjuan, V. Ramamurthy, K. Ventakesan, *Acta Cryst.* C40 (1984) 556.

- [162] R.G. Pearson, *J. Am. Chem. Soc.* 85 (1963) 3533.
- [163] R.G. Pearson, *Science* 151 (1966) 172.
- [164] M.F. Farona, A. Wojcicki, *ibid.* 4 (1965) 1402.
- [165] A. Turco, C. Pecile, *Nature* 191 (1961) 66.
- [166] K. Nakamoto, *Infrared and Raman Spectra of Coordination Compounds*, 3<sup>rd</sup> edn, John Wiley and Sons, NY 1978.
- [167] V. Suni, M.R.P. Kurup, M. Nethaji, *Polyhedron* 26 (2007) 3097.
- [168] D.X. West, A.A. Nassar, F.A. El-Saied, M.I. Ayad, *Transit. Met. Chem.* 23 (1998) 423.
- [169] R. Mayer, *Organosulfur Chemistry*, M.J. Janssen, Ed.; Wiley-Interscience: New York (1967) 219.
- [170] P. Bindu, M.R.P. Kurup, *Ind. J. Chem.* 36A (1997) 1094.
- [171] P.B. Sreeja, M.R.P. Kurup, *Spectrochim. Acta A61* (2005) 331.
- [172] L.J. Bellamy, *Advances in Infrared Group Frequencies* (Chapman and Hall, London, (1975).
- [173] V. Philip, V. Suni, M.R.P. Kurup, M. Nethaji, *Polyhedron* 23 (2004) 1225.
- [174] L. Latheef, M.R.P. Kurup, *Polyhedron* 27 (2008) 35.
- [175] S. Kavlak, H. Kaplan Can, Z.M.O. Rzaev, A. Guner, *J. Appl. Polym. Sci.* 100 (2006) 3926.
- [176] G.A. Nazri, C. Julien, *Solid State Ionics* 80 (1995) 271.
- [177] R. Mukherjee, In *Comprehensive Coordination Chemistry II-From Biology to Nanotechnology*; J.A. McCleverty, T.J. Meyer, Eds., Elsevier Ltd. Oxford, U.K., 6 (2004).

- [178] K.C. Agrawal, A.C. Sartorelli, in: G.P. Ellis, G.B. West (Eds.), *Progress in Medicinal Chemistry*, vol. 15, Elsevier, Amsterdam, (1987) 321.
- [179] W.E. Antholine, J.M. Knight, D.H. Petering, *J. Med. Chem.* 19 (1976) 339.
- [180] L.A. Saryan, E. Ankel, C. Krishnamurthi, D.H. Petering, *J. Med. Chem.* 22 (1979) 1218.
- [181] D.X. West, S.B. Padhye, P.B. Sonawane, *Struct. Bonding* 76 (1991) 1.
- [182] A. Price, A. Caragounis, B.M. Paterson, G. Filiz, I. Volitakis, C.L. Masters, K.J. Barnham, P.S. Donnelly, P.J. Crouch, A.R. White, *J. Med. Chem.* 52 (2009) 6606.
- [183] Z. Xiao, P.S. Donnelly, M. Zimmermann, A.G. Wedd, *Inorg. Chem.* 47 (2008) 4338.
- [184] B. Sharma, R. Kothari, *Int J. Pharm. Bio. Sci.* 6 (2015) 1154.
- [185] B.A. Booth, A.C. Sartorelli, *Nature* 210 (1966) 104.
- [186] S.I. Pascu, P.A. Waghorn, B.W.C. Kennedy, R.L. Arrowsmith, S.R. Bayly, J.R. Dilworth, M. Christlieb, R.M. Tyrrell, J. Zhong, R.M. Kowalczyk, D. Collison, P.K. Aley, G.C. Churchill, F.I. Aigbirhio, *Chem. Asian J.* 5 (2010) 506.
- [187] C.R. Kowol, P. Heffeter, W. Miklos, L. Gille, R. Trondl, L. Cappellacci, W. Berger, B.K. Keppler, *J. Biol. Inorg. Chem.* 17 (2012) 409.
- [188] D.B. Lovejoy, P.J. Jansson, U.T. Brunk, J. Wong, P. Ponka, D.R. Richardson, *Cancer Res.* 7 (2011) 5871.
- [189] P.J. Jansson, P.C. Sharpe, P.V. Bernhardt, D.R. Richardson, *J. Med. Chem.* 53 (2010) 5759.

- [190] J. Peisach, P. Aisen, W. Blumberg, (Eds.), *The Biochemistry of Copper*, Academic Press, New York, 1966.
- [191] T.G. Spiro (Ed.), *Copper Proteins*, Wiley International, New York, 1981.
- [192] E. Ochiai, *Bioinorganic Chemistry: An Introduction*, Allyn and Bacon, Boston, 1977.
- [193] A.S. Brill, *Transition Metals in Biochemistry*, Springer Verlag, Berlin, 1977.
- [194] M.N. Hughes, *Inorganic Chemistry of Biological Systems*, Wiley, Chichester, 2nd edn., 1981.
- [195] H. Sigel (Ed.), *Metal Ions in Biological Systems*, Vol. 13, Dekker, New York, 1981.
- [196] K.D. Karlin, J. Zubieta, (Eds.), *Copper Coordination Chemistry: Biochemical and Inorganic Perspectives*, Adenine Press, New York, 1983; *Biological and Inorganic Copper Chemistry*, Adenine Press, New York, 1986.
- [197] W.C. Kaska, C. Carrans, J. Michalowski, J. Jackson, W. Levinson, *Bioinorg. Chem.* 8 (1978) 225.
- [198] M. Ligo, A. Hoshi, K. Kuretani, M. Natsume, M. Wada, *Jpn. J. Cancer Res.* 68 (1977) 221.
- [199] A. Sartorelli, K.C. Agrawal, *ACS Symp. Ser. No. 301*, 1976.
- [200] C. Chan-Stier, D.T. Minkel, D.H. Petering, *Bioinorg. Chem.* 6 (1976) 203.
- [201] W.E. Antholine, J.M. Knight, D.H. Petering, *J. Med. Chem.* 19 (1976) 339.

*References*

---

- [202] L.A. Saryan, E. Ankel, C. Krishnamurti, D.H. Petering, H. Elford, *J. Med. Chem.* 22 (1979) 1218.
- [203] M. Karon, W.F. Benedict, *Science* 178 (1972) 62
- [204] E. Fenz, *Muench. Med. Wochenschr.* 41 (1951) 1101.
- [205] J. Forestier, A. Certonciny, *Presse Med.* 64 (1946) 884.
- [206] W.S. Hangarter, in J.R.J. Sorensen (Ed.), *Inflammatory Disease and Copper*, Humana Press, Clifton, NJ, 1982, p. 439.
- [207] S.E. Livingstone, *Q. Rev. Chem. Soc.* 19 (1965) 386
- [208] K.C. Agrawal, A.C. Sartorelli, in G.P. Ellis and G.B. West (Eds.), *Progress in Medicinal Chemistry*, Vol. 15, Elsevier, Amsterdam, 1978, p. 321.
- [209] S. Padhye, G.B. Kauffman, *Coord. Chem. Rev.* 63 (1985) 127.
- [210] K. Liebermeister, *Z. Naturforsch. Teil B*, 5 (1950) 79.
- [211] H. Beraldo, L.P. Boyd, D.X. West, *Transit. Met. Chem.* 23 (1998) 67.
- [212] H. Beraldo, S.B. Kaisner, J.D. Turner, I.S. Billeh, J.S. Ives, D.X. West, *Transit. Met. Chem.* 22 (1997) 459.
- [213] P.S. Mane, S.G. Shirodkar, B.R. Arbad, T.K. Chondhekar, *Indian J. Chem.* 40A (2001) 648.
- [214] G. Plesch, C. Friebel, *Polyhedron* 14 (1995) 1185.
- [215] V. Philip, V. Suni, M.R.P. Kurup, M. Nethaji, *Polyhedron* 24 (2005) 1133.
- [216] A.B.P. Lever, *Inorganic Electronic Spectroscopy*, 2<sup>nd</sup> ed., Elsevier, Amsterdam, 1984.

- [217] B.J. Hathaway, A.A.G. Tomlinson, *Coord. Chem. Rev.* 5 (1970) 24.
- [218] S. Stoll, *Spectral Simulations in Solid-State Electron Paramagnetic Resonance*, Ph.D. thesis, ETH, Zurich, 2003.
- [219] U.L. Kala, S. Suma, S. Krishnan, M.R.P. Kurup, R.P. John, *Polyhedron* 26 (2007) 1427.
- [220] M. Antosik, N.M.D. Brown, A.A. McConnell, A.L. Porte, *J. Chem. Soc. A* (1969) 545.
- [221] B.J. Hathaway, *J. Chem. Soc., Dalton Trans.* (1972) 1196.
- [222] S. Thakurta, P. Roy, G. Rosair, C.J.G. –Garcia, E. Garriba, S. Mitra, *Polyhedron* 28 (2009) 695.
- [223] V.P. Singh, *Spectrochim. Acta A* 71 (2008) 17.
- [224] A.H. Maki, B.R. McGarvey, *J. Chem. Phys.* 29 (1958) 35.
- [225] B.J. Hathaway, D.E. Billing, *Coord. Chem. Rev.* 5 (1970) 1949.
- [226] D. Kivelson, R. Nieman, *J. Chem. Soc., Dalton Trans.* 35 (1961) 149.
- [227] J.R. Wasson, C. Trapp, *J. Phys. Chem.* 73 (1969) 3763.
- [228] S.I. Findone, K.W.H. Stevens, *Proc. Phys. Soc.* 73 (1959) 116.
- [229] J.G. Da Silva, C.H.C. Perdigao, N.L. Speziali, H. Beraldo, *J. Coord. Chem.* 66 (2013) 385.
- [230] J. Sheng, P.T.M. Nguyen, R.E. Marquis, *Arch. Oral Biol.* 50 (2005) 747.
- [231] Y. Oyama, H. Matsui, M. Morimoto, Y. Sakanashi, Y. Nishimura, Y. Okano, *Toxicol. Lett.* 171 (2007) 138.

- [232] P. Talukder, T. Satho, K. Irie, T. Sharmin, D. Hamady, Y. Nakashima, F. Miake, *Int. Immunopharmacol.* 11 (2011) 141.
- [233] Z.Q. Li, F.J. Wu, Y. Gong, C.W. Hu, Y.H. Zhang, M.Y. Gan, *Chin. J. Chem.* 25 (2007) 1809.
- [234] J. d'Angelo, G. Morgant, N.E. Ghermani, D. Desmaele, B. Fraisse, F. Bonhomme, E. Dichi, M. Sghaier, Y. Li, Y. Journaux, J.R.J. Sorenson, *Polyhedron* 27 (2008) 537.
- [235] D. Kovala-Demertzi, P.N. Yadav, J. Wiecek, S. Skoulika, T. Varadinova, M.A. Demertzis, *J. Inorg. Biochem.* 100 (2006) 1558.
- [236] Z. Travnicek, V. Krystof, M. Sipl, *J. Inorg. Biochem.* 100 (2006) 214.
- [237] J.S. Casas, E.E. Castellano, M.D. Couce, J. Ellena, A. Sanchez, J. Sordo, C. Taboada, *J. Inorg. Biochem.* 100 (2006) 124.
- [238] M. Di Vaira, C. Bazzicalupi, P. Orioli, L. Messori, B. Bruni, P. Zatta, *Inorg. Chem.* 43 (2004) 3795.
- [239] N.J. Pace, E. Weerapana, *Biomolecules* 4 (2014) 419.
- [240] L. Chen, J. Qiao, J.F. Xie, L. Duan, D.Q. Zhang, L.D. Wang, Y. Qiu, *Inorg. Chim. Acta* 362 (2009) 2327.
- [241] T.W. Ngan, C.C. Ko, N.Y. Zhu, W.W. Yam, *Inorg. Chem.* 46 (2007) 1144.
- [242] R. Ghosh, S.H. Rahaman, C.N. Lin, T.H. Lu, B.K. Ghosh, *Polyhedron* 25 (2006) 3104.
- [243] S. Sen, S. Mitra, P. Kundu, M.K. Saha, C. Kruger, J. Bruckmann, *Polyhedron* 16 (1997) 2481.
- [244] D. Palanimuthu, S. V. Shinde, D. Dayal, K. Somasundaram, A.G. Samuelson, *Eur. J. Inorg. Chem.* 3542 (2013) 3549.



- [245] a) J. E. Coleman, *Annu.Rev. Biochem.* 61 (1992) 897.  
b) B. L. Vallee, K. H. Falchuk, *Physiol. Rev.* 73 (1993) 79.  
c) T. Fukada, S. Yamasaki, K. Nishida, M. Murakami, T. Hirano, *J. Biol. Inorg. Chem.* 16 (2011) 1123.
- [246] K. Peariso, C. W. Goulding, S. Huang, R.G. Matthews, J.E. Penner-Hahn, *J. Am. Chem. Soc.* 120 (1998) 8410.
- [247] V. Philip, V. Suni, M.R.P. Kurup, M. Nethaji, *Spectrochim. Acta Part A* 64 (2006) 171.
- [248] G. Plesch, C. Friebel, *Polyhedron* 14 (1995) 1185.
- [249] M.A. Ali, D.A. Chowdhary, M. Nazimuddin, *Polyhedron* 3 (1984) 595.
- [250] D. Cremer, J.A. Pople, *J. Am. Chem. Soc.* 97 (1975) 1354.
- [251] X. Wang, J. Yang, *Inorg. Chim. Acta* 409 (2014) 208.
- [252] Y. Tian, W. Yu, M. Jiang, S.S.S. Raj, P. Yang, H.-K. Fun, *Acta Cryst.* 55 (1999) 1639.
- [253] S. Arora, S. Agarwal, S. Singhal, *Int. J. Pharm. Pharm. Sci.* 6 (2014) 34.
- [254] S.B. Novacovic, Z.D. Tomic, V. Jetovic, V.M. Leovac, *Acta Cryst.* (2002) m358.
- [255] R. Takjoo, M. Hakimi, M. Seyyedin, *J. Sulfur Chem.* 31 (2010) 415.
- [256] M.A. Ali, M. Nazimuddin, H. Rahman, R.J. Butcher, *Transit. Met. Chem.* (2002) 268.
- [257] Y. Tian, C. Duan, C. Zhao, X. You, T.C.W. Mak, Z. Zhang, *Inorg. Chem.* 36 (1997) 1247.
- [258] M. Jiang, Q. Fang, *Adv. Mater.* 11 (1999) 1147.

*References*

---

- [259] P.F. Rapheal, E. Manoj, M.R.P. Kurup, E. Suresh, *Polyhedron* 26 (2007) 607.
- [260] A. Castineiras, E. Bermejo, D.X. West, L.J. Ackerman, J.V. Martinez, S.H. Ortega, *Polyhedron* 18 (1999) 1469.
- [261] V. Philip, V. Suni, M.R.P. Kurup, *Polyhedron* 25 (2006) 1931.

........

## Curriculum Vitae

### **Nisha, K.**

Pankipurath  
Kuppady P.O.  
Sulthan Bathery  
Wayanad-673592  
Kerala, India

Email: nichuanil@gmail.com  
nishak@cusat.ac.in



**Areas of Interest:** Teaching and Research

### **Academic Profile**

Pursuing Ph.D. (Inorganic Chemistry)  
(2010-present)  
Area of research – Coordination Chemistry  
Supervising guide – Prof. M.R. Prathapachandra Kurup  
Department of Applied Chemistry.  
Cochin University of Science & Technology, Kochi.

M.Sc. (2003-2005)  
Department of Applied Chemistry  
Cochin University of Science and Technology, Kerala  
Percentage of marks – 67%

B.Sc. (2001-2003)  
St. Mary's College, Sulthan Bathery  
Calicut University, Kerala.  
Percentage of marks – 81.4%

Pre Degree (1998-2000)  
St. Mary's College, Sulthan Bathery  
Calicut University, Kerala.  
Percentage of marks – 74.8%

S.S.L.C (2007)  
St. Joseph's English High School (1997), Sulthan Bathery  
Kerala.  
Percentage of marks – 87%

### **Achievements**

1. Qualified CSIR-JRF - 2008 December
2. Qualified State Eligibility Test (SET) - 2006 May

### **Research Experience**

- Nearly four years of research experience in the field of coordination chemistry

### **Professional Skills**

- Familiar with MS Office
- Familiar with chemistry software packages like Chemsketch, Origin, EPR simulation packages
- Familiar with crystallographic softwares
- Experienced in using instruments like UV-Vis spectrometer, FTIR spectrometer, Thermogravimetric analyzer, Gouy balance etc.

### **Personal Profile**

Father's name : C.K. Kuttappan  
Date of Birth : 27<sup>th</sup> July 1981  
Nationality : Indian  
Gender : Female  
Marital Status : Married

### **Papers published**

1. (E)-2-(4-Benzyloxy-2-hydroxybenzylidene)-N-phenylhydrazinecarbothioamide, K. Nisha, M. Sithambaresan, M.R.P. Kurup, Acta Cryst. (2011) E67, o3420.
2. Syntheses, Spectral and Structural studies of Zinc(II) complexes of Di-2-pyridyl ketone N<sup>4</sup>-methylthiosemicarbazone, S. Renjusha, **K. Nisha** and M. R. P. Kurup. 23rd Swadeshi Science Congress – 2013, 209-212.

### **Papers presented in symposia**

1. Participated and presented a poster in the National Conference "Current Trends in Chemistry" (CTriC-2012) held at the Department of Applied Chemistry, Cochin University of Science and Technology, Kochi during 20-21 January 2012.

2. Participated and presented a poster in the National Conference “Current Trends in Chemistry” (CTriC-2013) held at the Department of Applied Chemistry, Cochin University of Science and Technology, Kochi during 22-23 March 2013.
3. Participated and presented a poster in the National Conference “Current Trends in Chemistry” (CTriC-2013) held at the Department of Applied Chemistry, Cochin University of Science and Technology, Kochi during 17-18 January 2014.
4. Participated and presented a paper in the 23<sup>rd</sup> “Swadeshi Science Congress” held at Mahatma Gandhi University, Kottayam during 6-8 November 2013.
5. Participated and presented a poster in the International Conference on “Emerging Frontiers and challenges in Chemistry” held at the Department of Chemistry, All Saints’ College, Thiruvananthapuram 2014.
6. Participated in International Conference on Materials for the Millennium (MATCON-2016) held at the Department of Applied Chemistry, Cochin University of Science and Technology, Kochi during 13-16 January 2016.

.....✍.....